UNIVERSITY OF LIVERPOOL

An examination of the endoplasmic reticulum stress response in the filamentous fungus, *Aspergillus nidulans*.

Thesis submitted in accordance with the requirements to the University of Liverpool for the degree of Doctor of Philosophy.

Ewan S M Young

December 2017

Abstract

Filamentous fungi are used throughout the biotechnology industry for the production of both native and recombinant proteins. There is a marked difference in the level of recombinant protein production compared to native, with yields decreasing from grams to milligrams per litre. The endoplasmic reticulum stress response (ERSR) has been identified as a potential bottleneck for recombinant protein production. In higher eukaryotes the ERSR has three known sensors, *ire1*, *perk* and *atf6*. Through these sensors, ER stress is attenuated by upregulation of ERSR target genes, global translational repression and degradation of transcripts targeted to the ER. Fungi have only one confirmed sensor of the higher eukaryotic ERSR, coordinated by the functional homologue of *ire1* (*ireA*) which induces the ERSR through activation of the transcription factor HacA. In this study, I examine the ERSR of the filamentous fungi *Aspergillus nidulans*, a model organism for *Aspergillus* spp, to elucidate the fungal ERSR in an attempt to identify targets for increased recombinant protein production (RPP) yields. In this thesis I show that IreA is required for viability outwith its role in HacA activation as overexpression of the TF did not recover a *ΔireA* strain's lethal phenotype. Also, that during ER stress, IreA is required for degradation of two transcripts encoding ER processed proteases as is observed in higher eukaryotes. I provide evidence for a second transcriptional pathway regulating gene expression during ER stress in *A. nidulans*. Further to this, polysome profiling has shown global translational repression during ER stress similar to that observed in higher eukaryotes. The findings of this research project are that the fungal ERSR is more conserved with that of higher eukaryotes than previously assumed, providing several new targets to potentially increase recombinant protein production (RPP).

Acknowledgements

I would firstly like to thank Professor Mark X. Caddick for both his supervision, good humour and endless patience during my masters and the PhD.

I'd like to thank Davey and Ghadbags for making my time in Liverpool as fun as it's been and for generally looking after me!

Jade, for all her happiness and optimism which perks me up even on the worst days. Richard for the inane, distracting yet most interesting conversations anyone could hope to have. Stefany for her positivity and always having a smile, you've helped me along these last few years! To Christina for always being a phone call away and to pour out encouragement whenever it's needed!

And of course a big shout out to StAnge, for never letting me think anything was beyond my abilities and always encouraging me to be at my best, you two supporting me are the reason I've gotten to where I am today.

Lastly, I'd like to thank the BBSRC and University of Liverpool for the funding and opportunity to carry out this PhD.

Abbreviation list

Amino acids	AA
Cetrimonium bromide	CTAB
Diethyl pyrocarbonate	DEPC
Dithiothreitol	DTT
Ethylenediaminetetraacetic acid	EDTA
Endoplasmic reticulum	ER
Endoplasmic reticulum associated degradation	ERAD
Endoplasmic reticulum stress response	ERSR
Global translational repression	GTR
Inner nuclear membrane	INM
Inter-nuclear space	INS
Linker of nucleoskeleton and cytoskeleton	LINC
3-(N-morpholino) propanesulfonic acid	MOPS
Nuclear envelope	NE
Nucleotide	nt
Outer nuclear membrane	ONM
Rate of translation	RT
Recombinant protein production	RPP
Regulated ire1-dependent decay	RIDD
Repression under secretion stress	RESS
Rough endoplasmic reticulum	RER
Transcription factor	TF
Trisaminomethane	Tris

Saline-sodium citrate	SSC
Sodium dodecyl sulfate	SDS
Signal recognition particle	SRP
Signal sequence	SS
Smooth endoplasmic reticulum	SER
Ubiquitin-Proteasome pathway	UPP
Unconventionally secreted protein	USP
Unfolded protein response	UPR
4 – phenylbutyric acid	4-PBA

Contents

List of Figures

List of Tables

Table 1. Genes modified in *A. nidulans* for this study and their homologues in various spp.

Aspergillus nidulans	*Aspergillus niger*	*Aspergilluse oryzae*	*Saccharomyces cerevisiae*	*Homo sapiens*
ireA[1] (AN0235)	*ireA*[2]	*ireA*[3]	*ire1*[18]	*ern1/ire1*[25]
hacA[4] (AN9397)	*hacA*[5]	*hacA*[6]	*hac1*[19]	*xbp1*[26]
gcn2[1] (AN2246)	Uncharacterised (An17g00860)	Uncharacterised (AO090701000211)	*gcn2*[20]	*eif2αK4*[27]
hriA[1] (AN7321)	Uncharacterised (An04g08580)	Uncharacterised (AO090102000172)	*Absent*	eif2α1[28]
eif2α (AN3156)	Uncharacterised (An02g09370)	Uncharacterised (AO090012000783)	*sui2*[21]	*eif2α*[29]

Table 2. Q-PCR gene targets examined in this study in *A. nidulans* and various spp.

Aspergillus nidulans	*Aspergillus niger*	*Aspergilluse oryzae*	*Saccharomyces cerevisiae*	*Homo sapiens*
bipA[7] (AN2062)	*bipA*[5]	*bipA*[8]	*kar2*[23]	*grp78*[30]
hrdC[7] (AN0810)	*hrdC*[9]	Uncharacterised (AO090003000492)	*hrd3*[22]	*syvn1*[31]
ireA[1] (AN0235)	*ireA*[2]	*ireA*[3]	*ire1*[18]	*ire1*[26]
pepJ[10] (AN7962)	Uncharacterised/Absent	Uncharacterised (AO090001000135)	*Absent*	*Absent*
prtA[11] (AN5558)	*pepD*[12]	*alpA*[13]	*prb1*[24]	*Absent*
actA[14] (AN6542)	*actA*[15]	*actA*[16]	act1[17]	actg2[32]

See appendix 1.F for table specific references

1. Introduction

The endoplasmic reticulum (ER) is composed of a single continuous bilayer membrane containing a lumenal area and displays structurally different but connected domains. The ER has been found to constitute >10% of total cell volume and thus is the largest eukaryotic organelle (Prinz *et al.*, 2000; Anderson and Hetzer, 2008). Utilizing electron microscopy the ER was first identified in 1945 and with increased understanding of ribosomes was hailed as the site of secretory and intramembrane protein synthesis (Porter, Claude and Fullam, 1945). Over the years through numerous studies the perceived responsibilities of the ER have been expanded with new evidence of a more complex role. The expanded role of the ER has been shown to range across vesicular transport, glycosylation, lipid and steroid biogenesis, ca^{2+} storage as well as concurrent protein synthesis (Bell and Coleman, 1981; Milner, Famulski and Michalak, 1992; Rexach and Biology, 1994; Yamaguchi *et al.*, 2004; Mooradian and Haas, 2011; Flis, 2013). Having several significant roles for cell health the ER has evolved a means of regulating its homeostasis in accordance with internal and external pressures; initially termed the unfolded protein response (UPR) and more recently -and aptly- the ER stress response (ERSR). The ERSR has been identified as a bottleneck for the recombinant protein production (RPP) industry where there is large scale use of filamentous fungi due to their secretion capacity (Mattanovich *et al.*, 2004; Guillemette *et al.*, 2011). In this study, I examine the model organism *Aspergillus nidulans* and sought to elucidate the ERSR which hitherto has been found to be less complex in fungi than in other eukaryotic species. Higher and lower eukaryotes are terms used to delineate between eukaryotes based on organism complexity. For the purpose of this project higher eukaryote will refer to multicellular, tissue containing organisms. Lower eukaryotes refers to unicellular or multicellular organisms without tissue specialisation.

1.1.ER structure

The structure and organisation of the ER has been studied extensively, revealing the presence of a variety of contiguous domains and interacting transmembrane surfaces (Wooding, 1967; Staehelin, 1997; Voeltz, Rolls and Rapoport, 2002; Schwarz and Blower, 2016). The terms Rough endoplasmic reticulum (RER) and Smooth endoplasmic reticulum (SER) refer to portions of the ER with ribosomes embedded on the cytosolic surface (rough) and little to no ribosomal presence (smooth) (Palade, 1956; Chanat *et al.*, 2016). Despite these two commonly characterised aspects of the ER there is also the nuclear envelope (NE) connecting the two structures (Subramanian and Meyer, 1997; Shibata, Voeltz and Rapoport, 2006; Schwarz and Blower, 2016). The peripheral ER is a term encompassing both the RER and SER but excluding the NE. The peripheral ER can be found throughout animal cells whereas in fungi and plants it is primarily located under the plasma membrane (Pichler *et al.*, 2001; West *et al.*, 2011). The dynamic nature of the peripheral ER allows for rearrangement of its structure according to the need of the cell however this is yet to be fully understood (Du, Ferro-novick and Novick, 2004; Griffing, 2010). Depending on cell function and organism, there are morphological differences observed for the organelle; between organisms for example, tubules of the ER are 60nm in mammalian cells and 30nm in fungi (Shibata, Voeltz and Rapoport, 2006). Differences within multicellular organisms include the heightened presence of RER in pancreatic cells, which have a high secretory load and increased tubules in adrenal glands where there are high levels of steroids produced (Carrasco and Meyer, 2011).

1.1.1. Nuclear envelope

The NE is the most visible aspect of the ER and is composed of two lipid bilayers, the inner and outer nuclear membrane (INM and ONM respectively). The stacking of the INM and ONM create the inter-nuclear space (INS). The INS is maintained at a width of ~50nm, coordinated by the LINC complex (Tzur, Wilson and Gruenbaum, 2006; Sosa *et al.*, 2012). The LINC complex has been shown to be active in many roles including nuclear relocation, centromere attachment to the nucleus as well as nuclear pore formation (Tapley and Starr, 2013). The NE shares the common lumenal domain found throughout the ER structure. Nuclear pores across both the INM and ONM allow for transport of molecules including RNAs and proteins though the use of diffusion or active transport depending on the molecule (Suntharalingam, Wente and South, 2003). The structure of the INM is believed to be dependent on the INM proteins binding to laminin and chromatin (Burke and Ellenberg, 2002; Hetzer, Walther and Mattaj, 2005).The NE is then connected to the cisternae which constitute the RER (Lavoie *et al.*, 1996). See Figure 1.

1.1.2. Cisternae

Cisternae (the RER) constitute a significant part of the peripheral ER and is primarily found localised to the NE and have a high density of embedded ribosomes (Savitz and Meyer, 1990; Lavoie *et al.*, 1996). This structure consists of two lipid bilayers with an internal lumen and whilst flat, display curved structure at the edges of the membranes. Despite varying in size throughout and between cells the lumenal area is maintained with a size of 50nm and 30nm in mammals and fungi respectively (Mcdonald and Walter, 2006). Cisternae are usually seen stacked upon one another and are connected by membrane structures which display helical edges (Terasaki *et al.*, 2013).

1.1.3. Tubules

Tubules (SER) form a network which is subject to rearranging and display three way junctions connecting separate tubules whilst having very few ribosomes associated with their surface (West *et al.*, 2011). Tubules and cisternae display different structures but maintain similar lumenal size. Tubules are more common in cells such as liver and muscle due to the functional roles such as lipid synthesis and Ca^{2+} signalling (Papa and Walter, 2006).

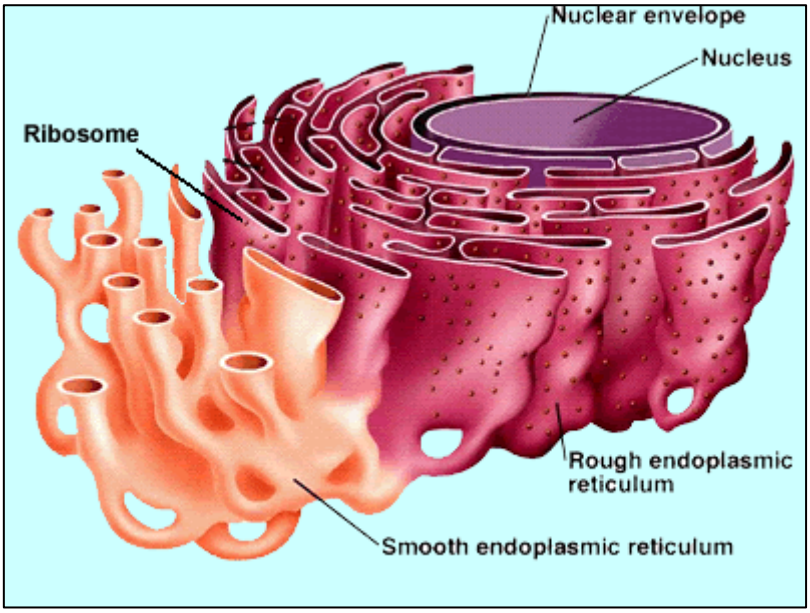

Figure 1. 1 Model of the nucleus, nuclear envelope, rough endoplasmic reticulum and smooth endoplasmic reticulum. (DynamicScience, 2012)

1.2. Roles of the ER

Whilst the ER has been implicated in a variety of roles, I will look at several of the more prominent ones that have a large impact on the ERSR, either by virtue of being involved in protein quality control or membrane structural regulation.

1.2.1. Protein synthesis and the ER secretory pathway

The most noted role for the ER is nascent peptide synthesis, specifically proteins destined for secretion or membrane localisation (Wiertz *et al.*, 1996; Freedman, Dunn and Ruddock, 1998; Pavio *et al.*, 2003). Entry into the ER is the beginning step of the secretory pathway, this pathway also includes the Golgi apparatus and intracellular transport mediated by vesicles, see Fig 2 (Trucco *et al.*, 2004; Koreishi *et al.*, 2013). Proteins entering the ER account for approximately one third of a cells proteome, although with recent findings of cytosol resident peptides being translated within the ER, this number is undoubtedly higher (Chen *et al.*, 2012; Zhou *et al.*, 2014). The ER lumen maintains specific redox and pH levels, houses a host of chaperones, foldases, lipids, glycans and a variety of other molecules and enzymes. These all function in the production of nascent peptides and their subsequent modification. To achieve a fully functional and correctly situated protein requires several steps; including initial synthesis, modification, quality control and subsequent transport to the appropriate site. (Caldwell, Hill and Cooper, 2001). Figure 1. 2 depicts the pathway of ER processed secreted proteins.

Whilst the majority of secreted proteins are processed via the secretory pathway (Babitha, Soccol and Pandey, 2007; Miura and Ueda, 2018; Nickel and Rabouille, 2009) it should be noted that there are exceptions throughout eukaryotes. Secreted proteins that are processed outside the secretory pathway are generally termed unconventionally secreted proteins (USP).

Predominantly these USPs are found in higher eukaryotes and play important physiological roles including angiogenesis, cell growth and the immune response. Interleukin 1β (I1β), a pro-inflammatory cytokine is a well known example of a USP and is primarily produced by neutrophils as part of the immune response. Despite extensive literature on I1β function, the exact mechanism of secretion is still not understood (Iula et al., 2018; Piccioli and Rubartelli, 2013). There are at least two types of unconventional protein transport, firstly proteins that are targeted to the ER via the signal recognition particle (SRP) (see Synthesis and translocation) yet are localised to the cell membrane in a golgi-independent manner. Bypassing of the Golgi can be achieved via transport in a coat protein complex (COPII) which travels directly to the cell membrane. Examples of USPs which utilize this pathway are lst2 in yeast or the mammalian cystic fibrosis transmembrane conductance regulator (CFTR) (Jüschke et al., 2004; Yoo et al., 2002). The second type of unconventional protein transport regards cytoplasmic or nuclear proteins, without an SRP, being secreted in a non-ER or Golgi related manner. These include the aforementioned I1β, mammalian fibroblast growth factor 2 and the AcbA protein identified in *Dictyostelium discoideum* (Engling, 2002; Kinseth et al., 2007). USPs identified in lower eukaryotes include heat shock protein 70 (hsp70p), a molecular chaperone, and enolase, an enzyme integral to glycolysis; these have both been identified as USPs in *Candida albicans* and *Saccharomyces cerevisiae* (Gil-Bona et al., 2014; Oliveira et al., 2010). *Aspergillus oryzae* was recently found to secrete a non SRP containing peptide termed Acyl-CoA 2 (AoAcb2). Acyl-CoA-binding protein is involved in lipid metabolism. AoAcb2 is functionally similar to AcbA in *D. discoideum* and AcbAp in *S. cerevisae*, all three fungal spp produce this USP (Duran et al., 2010; Engling, 2002; Kwon et al., 2017).

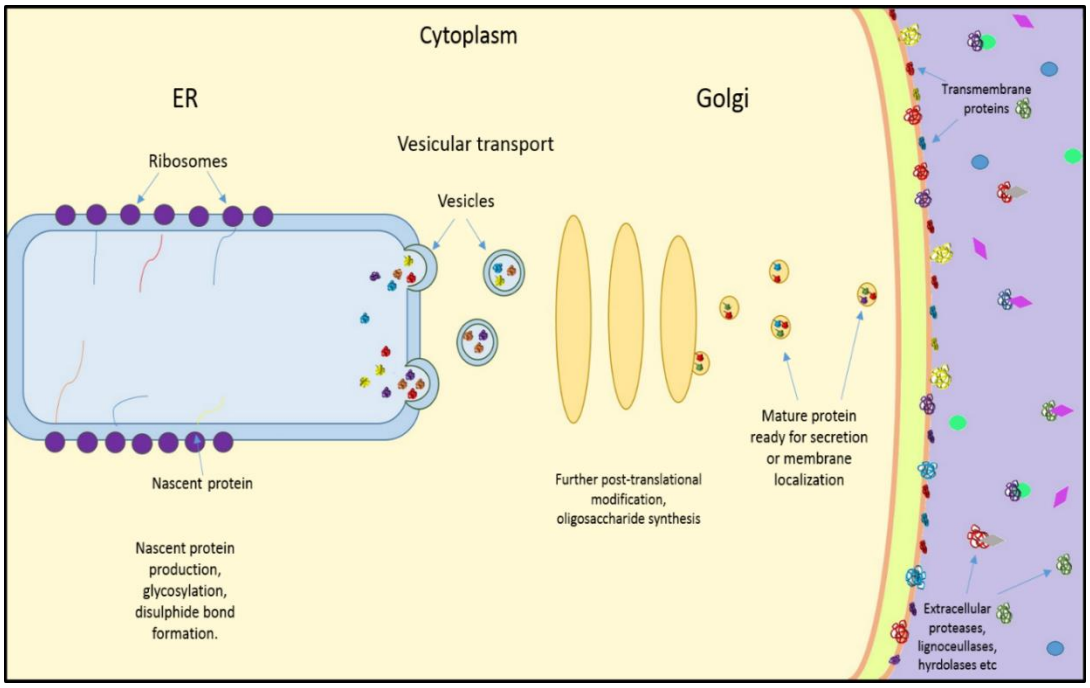

Figure 1. 2 An overview of the secretory pathway. Ribosomes synthesising nascent peptides are localised to the ER membrane for co-translational modification. Once appropriately structured and ER post-translational modifications are complete the peptides are transported via vesicles to their final destination or for further modification within the Golgi body. Upon maturation the proteins are transported via vesicle to their final destination.

1.2.2. Synthesis and translocation

mRNA destined for ER processing encode a signal peptide, this is a short sequence within the N-terminus of protein product, once translation has begun on a free ribosome a protein termed the Signal Recognition Particle (SRP) binds the ribosome/protein complex and localises to the ER to facilitate translation of the peptide directly into the ER lumen (Blobel and Dobberstein, 1975; Katt, Sarge and Bundesanstalt, 1998; Batey, 2000) The term "translocon" refers to the pore structure that facilitates entry of nascent peptide into the lumen. This is regulated by the protein Sec61 (Alder *et al.*, 2005; Hessa *et al.*, 2007) which specifically allows entry of ER targeted proteins via recognition of the signal peptide. Due to pore size proteins entering the lumen must do so in an unfolded state. Regulation of protein translational rate and the translocation of correct peptides is vital to minimize ERSR induction.

1.2.3. Co and Post-translational modification

Modifications to peptides include both structural and chemical, these modifications can occur during synthesis (co-translational) and/or after (post-translational) synthesis. Chemical modifications can include glycosylation, phosphorylation, ubiquitination, methylation, acetylation, lipidation and numerous others (Gruss *et al.*, 1999; Aebi and Hennet, 2001; Velickovska and van Breukelen, 2007; Pehar *et al.*, 2012). Structural modifications to the nascent peptide include disulphide bond formation, proteolysis and even the conjugation of proteins. Each of these modifications are performed to tailor and target a protein to a specific function and location (Appenzeller-Herzog *et al.*, 2010). Each modification, glycosylation, acetylation etc, requires a tailored set of proteins and enzymes to facilitate the specific modification which increases the complexity of the ER's proteome and thus potential for ER stress. The benefits provided however, far outweigh the drawbacks as one gene can encode numerous different proteins.

Once translocated into the ER, secondary structure is achieved through formation of disulphide bonds between cysteine residues (Wang *et al.*, 2006). These bond formations are mediated by a host of resident foldases and chaperones (Gilbert, 1994; Wynn *et al.*, 1994). Foldases are responsible for the correct folding of new peptides, one well characterised foldase is *protein disulphide-isomerase* (Pdi) and as the name suggests is a key effector in forming disulphide bonds. Chaperones act as escorts for new peptides but also as inhibitors of incorrect folding as this could lead to terminally-misfolded proteins; i.e. a protein has attained an irreversible incorrect conformation. An example chaperone is the classic ERSR target *binding immunoglobulin protein* (Bip) (Grp78 in mammals) responsible for binding to new unfolded proteins and supporting subsequent folding. Bip accomplishes this through binding of

hydrophobic domains to inhibit incorrect folding. Bip is also noteworthy for its role as a regulator of the ERSR through interactions with the ERSR sensors lumenal domains. Chaperones inhibiting incorrect folding saves energy for the cell as misfolded proteins need to be unfolded and refolded correctly or targeted for degradation. Proteins targeted for degradation are done so when terminally misfolded. When this occurs the misfolded product has to be removed otherwise ERSR initiation can occur.

1.2.4. Quality control and ERAD

To ensure proteins are correctly formed requires quality control over nascent protein production and a means of recycling misfolded proteins. ER associated degradation (ERAD) is the recycling of misfolded proteins that have accumulated within the ER lumen and occurs as a response to ER stress, ERAD is also a target for upregulation during ER stress (Travers *et al*., 2000). ERAD requires the ubiquitin-proteasome pathway for proteolysis, this occurs within the cytosol and not the ER. Therefore misfolded proteins need to be identified, then transported across the ER membrane, as well as being poly-ubiquinated before degradation can occur. The ubiquitin-proteasome pathway (UPP) is the means via which ERAD recycles misfolded proteins. Targeting proteins to the proteasome begins with ubiquitin-activating enzyme (E1). E1 binds to ubiquitin, the ubiquitin is then transferred to E2, referred to as ubiquitin carrier. E2 facilitates binding of E3, also referred to as ubiquitin protein ligase. (Fueller *et al.*, 2008; Baldridge and Rapoport, 2016; Rock et al., 1994). The proteasome is then able to recognise the target for proteolytic activity, recycling proteins into their AA constituents.

Identifying unfolded proteins relies on sensing of physical structures within the nascent peptide such as exposed hydrophobic regions, improperly formed glycan additions as well as unpaired cysteine residues (Ruddock and Molinari, 2006. Weids et al., 2016). Whilst numerous components of the ERAD system have been identified and their functions elucidated, there is

still much to be understood in regards to the identification of misfolded proteins (Fueller *et al.*, 2008). In *S. cerevisiae* there are three modes of ERAD depending on where the misfolded protein resides; within the ER lumen, embedded in the membrane or exposed to the cytosol. These three situations illict similar but varied ERAD response. These have been termed ERAD-L, ERAD-M and ERAD-C respectively (Carvalho, Goder and Rapoport, 2006; Taxis et al., 2003). ERAD-L requires the heterotetrameric membrane protein complex Hrd1p, this is composed of Hrd1p, as well as Hrd3p, Usa1p, and Der1p (Carvalho, Goder and Rapoport, 2006; Knop et al., 1996). ERAD-M utilizes a subset of this complex where as ERAD-C requires Doa10p to act as an ubiquitin ligase in place of Hrd3p (Swanson, 2001).

1.2.5. Vesicular Transport

Vesicles are small structures consisting of a lipid bilayer surrounding a fluid filled core which contains macromolecules for transport. Typically vesicles transport proteins and lipids from the ER to other organelles such as the Golgi for final protein maturation. They are self-assembled from the ER or Golgi membranes via "pinching", similar to exocytosis (Bonifacino and Glick, 2004). Vesicles therefore inherently contain transmembrane proteins, the composition of which determines cargo and destination. Vesicular transport does not function in a linear manner; for instance, retrograde transfer of proteins from the Golgi back to the ER (Pfeffer, 1996; Patil and Walter, 2001). This can occur when ER resident proteins need final maturation via sugar moiety addition in the Golgi.

1.2.6. Glycosylation

Acknowledged as a major post-translational modification as it impacts on folding, localisation, stability and function of a protein, glycosylation is the enzymatic addition of glycan groups to nascent peptides. These glycans then undergo a process of "trimming" to attain the correct final structure. There are several types of glycosylation but the two most common are N-linked and

O-linked glycosylation. N-linked refers to glycosylation of nitrogen atoms from asparagine/arginine residues while O-linked occurs on an oxygen atom in variety of amino acids and fats (Wang, Groenendyk and Michalak, 2015). Processing of N-linked glycans has been identified as a part of the quality control of protein production within the ER. Synthesis of N-linked glycans occurs on the cytosolic face of the ER before being transferred into the lumen for protein binding and trimming. Synthesis of glycans and subsequent modification upon addition to nascent proteins is a highly regulated process (see Fig1.3) dependent on the ER.

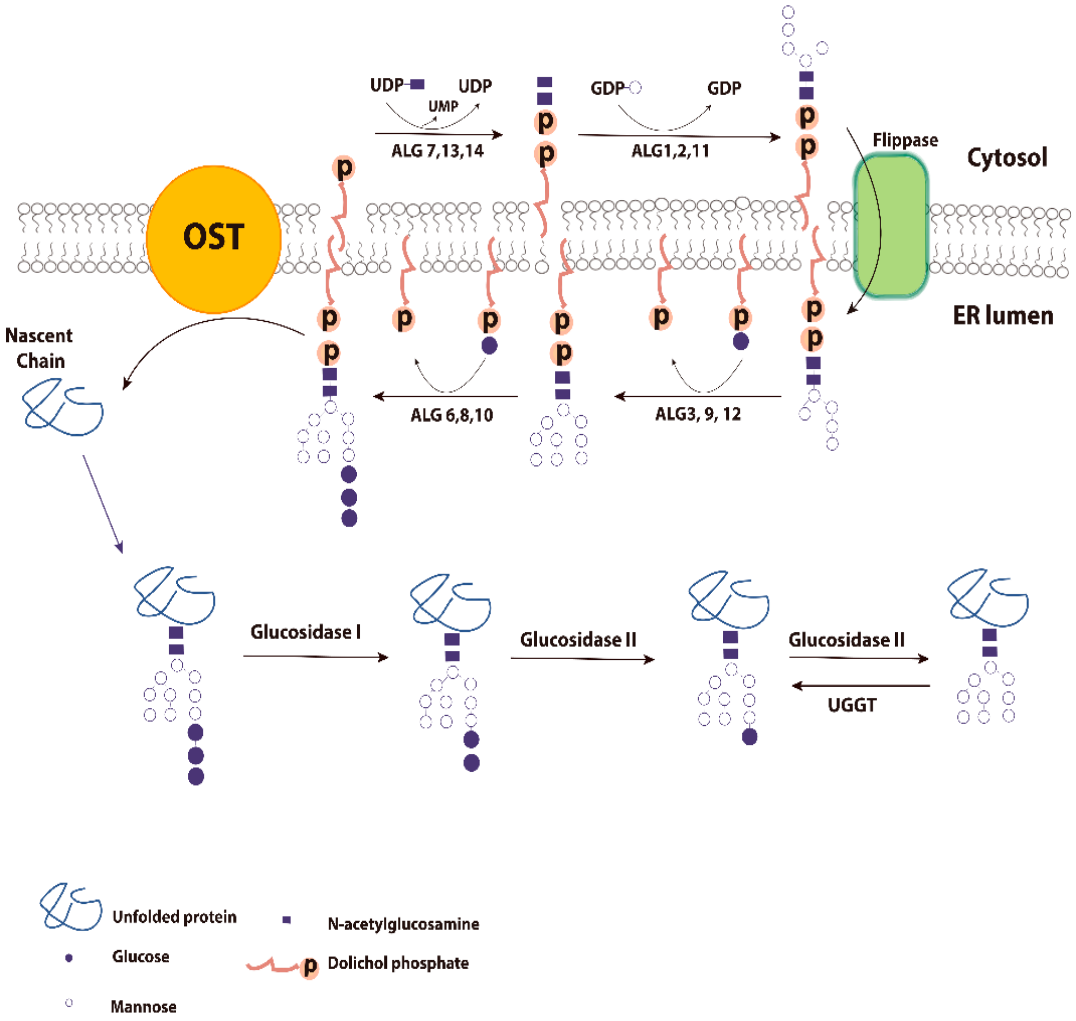

Figure 1. 3 Depiction of N-Glycan synthesis and subsequent modification after binding to nascent peptides within the ER within a mammalian system. N-glycans biosynthesis begins on the cystolic ER membrane and is catalysed by the ALG genes. GlcNAc-P is attached to the membrane-bound dolichol phosphate has from UDP-GlcNAc via GlcNAc-1-phosphotransferase (ALG 7). UMP then released. ALG13/14, ALG1, 2 and then 11 catalyse the addition of GlcNAc with mannose residues. The ATP-independent flippase coordinates the transfer of the partially synthesized N-glycan (GlcNAc2Man5) into the ER lumenal domain. The final N-glycan is formed by the addition of three glucose and four mannose residues. Oligosaccharyltransferase (OST) then transfers the mature N-glycan to a nascent peptide. The glucoses located at the terminal end of the N-glycan can be removed via glucosidase I and II. The remaining glucose monomer can be removed by glucosidase II and can be re-attached by UGGT. Figure (Wang, Groenendyk and Michalak, 2015).

1.2.7. Ca^{2+} storage

Ca^{2+} is a ubiquitous eukaryotic secondary messenger involved in various signalling pathways, muscle contraction and regulating transcription of specific genes. The ER acts as a reservoir for intracellular Ca^{2+}which must be tightly controlled; unregulated levels leads to initiation of signalling pathways including apoptosis (Berridge, Lipp and Bootman, 2000; Delucinge-vivier *et al.*, 2009). Calcium storage within the ER has been measured as 100-800 µM while as low

as 5-10 nM in the cytosol, this large disparity highlights the degree of Ca^{2+} regulation and storage (Demaurex and Frieden, 2003; Liebert *et al.*, 2006). The majority of ER chaperones and foldases have a high Ca^{2+} binding capacity and have an active role in Ca^{2+} storage (Wetmore and Hardman, 1996). Alterations in ER lumenal levels of Ca^{2+} leads to disruption of chaperone function and conversely ESRS activity impacts on Ca^{2+} levels (Ou, 1995; Corbett *et al.*, 1999). Ca^{2+} regulation is therefore another key role for the ER.

1.2.8. Lipid biogenesis

Lipids are a diverse family of water insoluble compounds including sterols, fats, phospholipids and waxes and have significant importance to cell health for a variety of aspects. Lipids provide building blocks for larger macromolecules, they also act as molecular chaperones, act as modifiers of membrane associations, serve as an energy source and are a key component of biological membranes (Beckert and Lester, 1980; Menon and Stevens, 1992; Fankhausers *et al.*, 1993; Kaback and Dowhan, 1996; Bogdanov and Dowhan, 1998). Membranes are used for a variety of functions within cells; compartmentalising, storage, phagocytosis and cell to cell interactions (Volmer and Ron, 2015). Disruption to lipid composition and/or synthesis induces aspects of the ERSR in mammalian cells (Biology, 2003; Devries-seimon *et al.*, 2005; Szpigel *et al.*, 2017). This is true for *Saccharomyces cerevisiae* where deletion of lipid biosynthetic genes upregulated ERSR target genes (Jonikas *et al.*, 2009). Correct lipid maintenance is complex but vital and another aspect of the ER's dynamic role.

1.3. Higher eukaryotic ER stress response

As the ER plays numerous roles for maintaining cell health, perturbations to any of these aspects can lead to misfolded proteins accumulating and thus the ERSR. The ERSR in higher eukaryotes is regulated via three ER transmembrane proteins, inositol requiring enzyme 1

(IRE1) and activating transcription factor 6 (ATF6) which act to modulate transcription and PKR-like ER resident kinase (PERK) which lowers global translation across the cell. IRE1 in higher eukaryotes is capable of degrading transcripts encoding secreted and transmembrane proteins as well as modifying the transcriptome (Mishiba *et al.*, 2013).

Upon ERSR induction there is increased transcription of genes involved in all aspects of the ER such as lipid biosynthesis, intracellular transport, chaperones, foldases and ERAD associated genes (Guillemette *et al.*, 2007; Iwata *et al.*, 2010, Travers *et al*., 2000). This influx of ERSR genes mitigates stress by boosting rates of folding (foldases), limiting further accumulation of misfolded proteins (chaperones), increasing removal of correctly formed products (intracellular transport and lipid biosynthesis) as well as increased ERAD capacities. PERK and IRE1 attenuate stress by limiting the volume of nascent peptides entering the lumen, through global translational attenuation and degradation of ER bound transcripts. PERK also biases translational machinery to translate specific transcripts upregulated by the ERSR, see Fig 1.4. The ERSR, if unable to resolve protein accumulation related stress, will initiate cell apoptosis via regulation of caspases (Nakagawa *et al.*, 2000).

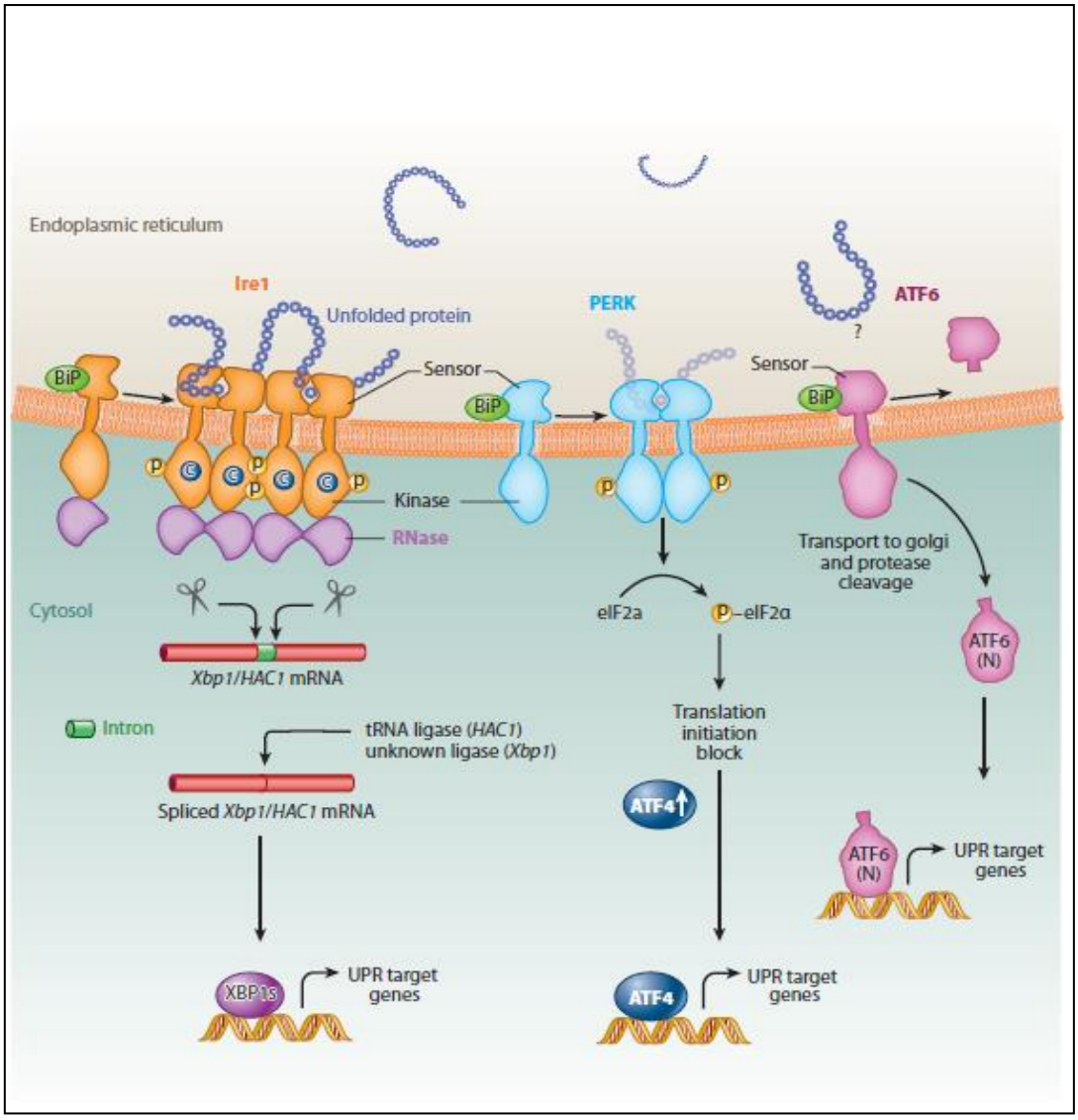

Figure 1. 4 Depiction of the eukaryotic ERSR. IRE1 (inositol requiring enzyme 1) is responsible for cleaving a transcript in order to remove an intron allowing for the translation of XBP-1/HacA, a transcription factor which targets ERSR genes. PERK is responsible for attenuating translation of specific transcripts to lower nascent peptide levels. Atf6 is a responsible for initiating the ERSR target gene transcription including xbp-1/hacA. (Korennykh and Walter, 2012)

1.3.1. *ire1* and *hacA*

ire1 was first identified in the lower eukaryote *S. cerevisiae* in 1993 and this was the initial discovery of the ERSR (Nikawa and Yamashita, 1992). *ire1* was named due to a *Δire1* strain proving lethal except when grown on media containing inositol. Inositol is a key component in many phospholipid biosynthetic pathways; given the importance of lipid synthesis to ER function it is unsurprising that deletion of *ire1* lead to lethality. This phenotype is not conserved

throughout the fungal kingdom or in higher eukaryotes however, and is still not entirely understood.

ire1 is the most conserved of the ERSR pathways as homologues can be found throughout eukaryotes such as plants, insects and mammals (Yoshida et al 2001, Lee et al 2011). *ire1* induces transcription of ERSR genes though the unconventional spliceosome-independent splicing of the mature yet inactive mRNA transcript *xbp-1/hac1/haca* (mammalian/*S. cerevisiae*/*A. nidulans*). The *hac1* transcript is exported from the nucleus despite containing an intron. In yeast the 252nt intron within *hac1* binds to its own 5' untranslated region (UTR) which inhibits translation, after splicing, the *hacA* transcript is translatable, resulting in production of a potent transcription factor. This intron removal is conserved but there are notable differences, *Aspergillus hacA* and mammalian *xbp-1* exhibit much smaller introns, 20nt and 26nt respectively. Translational inhibition of *hacA* and *xbp-1* is not due to binding of the 5'UTR and the intron. In *Aspergillus niger* the *hacA* transcript intron forms a stem-loop structure so is unable to bind to the 5'UTR. The *hacA* transcript is instead truncated in the 5'UTR as well as having its intron spliced; this removes an upstream Open Reading Frame (uORF) and subsequently translation of the transcript utilizes a downstream ORF which produces active HacA (Mulder and Nikolaev, 2009). *A. niger*, *A. nidulans* and *Trichoderma reesi* all exhibit this same truncation of *hacA* under ER stress (Valkonen, Penttilä and Saloheimo 2003; Dave *et al.*, 2006). Intron removal from *xbp*-1 causes a frame shift of the coding region which then encodes the active *xbp-1* (Yoshida *et al.*, 2001). After HacA synthesis the transcription factor relocates from the cytosol to the nucleus and binds to ER stress response elements (ERSE) upstream of target ERSR genes. The ERSE was identified through analysis of the *kar2*/*bipA* transcript promotor and is composed of 7 nucleotides (Mori et al., 1992. Mori et al., 1998). In an *A. niger* study results suggested that HacA was responsible for its own regulation (Mulder et al 2004).

IRE1 contains four distinct domains; the N-terminal sensory domain found within the lumen of the ER is responsible for the detection of protein accumulation, the transmembrane domain followed by the serine/threonine kinase domain and lastly the nuclease C-terminal domain which is responsible for splicing the *xbp-1*/*hacA* transcript (Lee *et al.*, 2008). When activated by protein aggregation in the lumen via its sensory domain, IRE1 oligomerizes. Subsequent to oligomerization, the kinase domains then auto-phosphorylate, activating the nuclease domain and splicing *hacA.* See Fig 1.5.

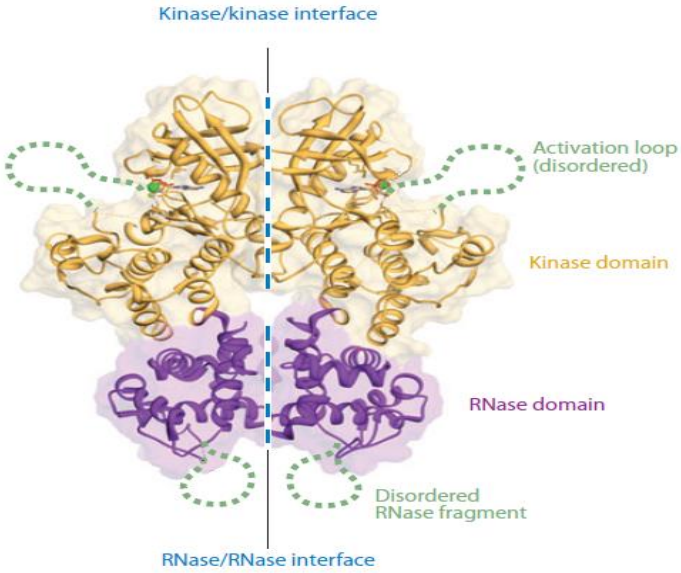

Figure 1. 5 IRE1 dimer. The image depicts the structure of homo sapiena ire1α highlighting the dimerization and activation of the cytosolic nuclease and kinase domains (Korennykh et al 2012).

IRE1's nuclease domain, in several metazoan organisms, recognises and cleaves transcripts other than *xbp-1*, specifically a subset of transcripts encoding proteins destined for the secretory pathway. This degradation of transcripts localized to the ER lowers the protein load entering the lumen. This secondary function has been termed regulated *ire1* dependent degradation (RIDD) and has been identified in insect, mammalian and plant cells (Hayashi *et al.*, 2016; Hollien *et al.*, 2006; Hollien *et al.*, 2009). To date the only *in vivo* study identifying RIDD in a fungal species examined *Schizosaccharomyces pombe* which has an unusual ERSR. Kimming

(2012) showed *S. pombe* has no homologue of *hac1* and so cannot exert transcriptional regulation to relieve ER stress. Selective degradation of transcripts encoding proteins that enter the lumen was observed, this loss of transcript did not occur in an *Δire1* strain, indicating the presence of RIDD. Further to this, it was shown that *bip1* (yeast homologue of *bip*/*bipA*) transcripts were cleaved by IRE1 but not degraded, instead cleavage by IRE1 increased stability of the transcript leading to *bip1* accumulation. This was observed although not entirely explained; through cleavage of the 3' UTR of *bip1* transcripts half-life increased from $T_{1/2}$ = 20min to $T_{1/2}$ = 70min. The improved transcript stability under ER stress, coinciding with degradation of other ER targeted transcripts, ensures *bip1* continues to be translated. Whilst this is an example of RIDD in a fungal spp it has yet to be replicated for another *in vivo* particularly where there is the canonical *ire1*/*hacA* pathway.

Candida glabrata, another fungal spp, was found to have an alternative method for mitigating ER stress than the otherwise conserved, ERSR. Unconventionally, *ire1* does not function to initiate the ERSR, contrary to the situation observed in almost all other species studied. Instead, microarray analysis shows transcriptional upregulation of the ERSR target genes is moderated by calcineurin signaling and marginally by the Slt2 MAPK pathway. Calcineurin is a serine/threonine protein kinase which binds Ca^{2+}. Whilst these results are unexpected, given the role the ER plays in Ca^{2+} regulation it is easily conceivable that *C. glabrata* has evolved to regulate ER stress through an alternative ER associated kinase. The study also revealed that an Δ*ire1* strain lacked the vulnerability observed in other UPR inhibited fungal mutants subjected to inducers of ER stress. The authors of this study postulate that the *C. glabrata* IRE1 has a nuclease activity similar to that observed in metazoans. This conclusion was drawn as there was no transcript degradation in response to ER stress in an Δ*ire1* strain (Miyazaki et al 2013).

1.3.2. *atf6*

atf6 was the last regulator of higher eukaryotic ERSR discovered and actually preceded the identification of *xbp-1* as the *hac1* homologue. ATF6 shows some homology with Hac1p as they both have a basic leucine zipper (bZIP) domain. Also like *hac1*, *aft6* is constitutively expressed. ATF6 consists of three domains, the ER stress sensing domain located in the ER lumen, a transmembrane domain anchoring the protein and a cytoplasmic domain which includes a transcription factor. ATF6 can detect ER stress directly through its lumenal domain initiating the cytoplasmic domains release into the cytoplasm. After its release, the cytoplasmic domain is targeted to the Golgi where it is cleaved by S1P and S2P releasing the ATF6 transcription factor, this translocates to the ER and initiates ERSR genes. S1P and S2P are Golgi localised proteases and also cleave an ER localised sterol response element binding protein (Haze *et al.*, 1999; Kaufman, 1999; Ye *et al.*, 2000; Shen *et al.*, 2002) As with *ire1* being involved in phospholipid biosynthesis, as evidenced by *S. cerevisiae's Δire1* inability to grow without inositol, it is unsurprising that there is overlap of sterol regulation and ER stress in higher eukaryotes. ATF6 is responsible for the upregulation of ERAD proteins, chaperones including *grp78*/*bipA* and *pdi* and also interestingly, *xbp-1*. While both XBP-1 and ATF6 act to upregulate ERSE they have been shown to differentially regulate genes when activated alone or in concert (Shoulders *et al.*, 2013)

.

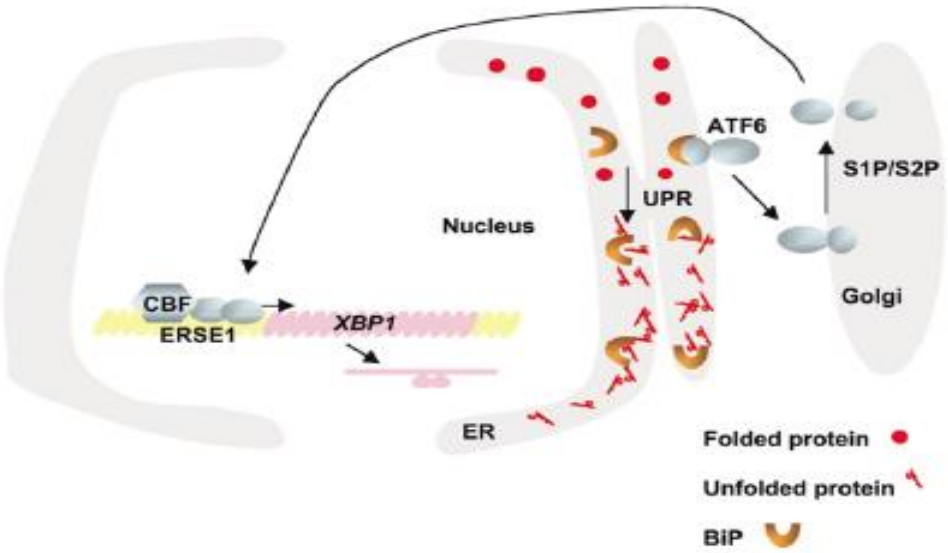

Figure 1. 6 ATF6 activation – transfer of protein to Golgi body, subsequent cleavage via S1P and S2P releases a transcription factor which within the nucleus binds to endoplasmic stress response elements (ERSE1) that are found upstream of target UPR genes including XBP1 and initiates transcription (Kaufman et al., 2002).

1.3.3. *perk*

The second of the transmembrane regulators of the ERSR to be discovered, PERK is responsible for global translational attenuation under ER stress. PERK belongs to a family of kinases which act upon the *eukaryotic initiation factor 2-α (eif2α)*. EIF2α is a component of the initiation complex, responsible for initiating translation of transcripts via addition of Met-$tRNA_i^{Met}$ thus beginning protein synthesis. This family of kinases each act upon the exact same serine residue (ser51) of *eif2α*, phosphorylation of which inhibits the 80s ribosomal assembly thus lowering rates of translation. Consisting of three domains, a lumenally located sensor of ER stress, a transmembrane domain and a cytoplasmic facing kinase domain. PERK also biases the EIF complex to translate alternate ORF's of a subset of transcripts including *atf4*. ATF4 is transcription factor regulating genes involved in cellular redox status, metabolism and regulates the induction of apoptosis. ATF4 also activates further transcription factors including CHOP

which is involved in cell apoptosis. (Harding *et al.*, 2000; Saito *et al.*, 2011; Kim *et al.*, 2014); PERKs activation is similar to IRE1 as they both undergo oligomerization under ER stress. In a murine model PERK was shown to be important for increasing activation of ATF6 and XBP-1, given ATF6s role in upregulating *xbp-1* this is unsurprising (Tsuru *et al.*, 2016). This finding highlights the degree of complexity and interactive nature of the three branches of the ERSR as they all impact on one another's effectiveness. While fungal spp have been shown to possess two of the four known *eif2a* kinases there is no homologue of PERK. There is no evidence of reduction in global translational rate during ER stress in fungal spp to date (Tom Payne *et al.*, 2008; Krishnan *et al.*, 2014).

1.3.4. Stress sensing

Sensing of ER stress by the ERSR was not understood for a long time even after the discovery of the three branches, however the consensus is that *bip* is key to negatively regulating each sensor. The most commonly held theory is that BIP/GRP78 associates with IRE1/PERK/ATF6 lumenal domains (see Fig 1. 4). When there is an increase in lumenal unfolded peptides BIP disassociates from IRE1/PERK/ATF6 to preferentially bind to unfolded peptides, freeing the sensory domains and thus activating the ERSR. As a target of the ERSR, BIP levels will rise until such a time as there is no unfolded protein to bind and will re-associate with IRE1/PERK/ATF6 again thus regulating the response (Bertolotti *et al.*, 2000; Shen *et al.*, 2002; X. Han *et al.*, 2013).

1.3.5. Filamentous fungal specific ER stress response

The *ire1*/*hacA* pathway is well established in fungi and is the only currently known pathway conserved throughout eukaryotes responsible for mitigating ER stress. Several studies have reported the repression of transcripts in filamentous fungi under ER stress, this has termed repression under secretion stress (RESS) (Pakula *et al.*, 2003; Al-sheikh *et al.*, 2004). This has

been proposed for *T. reesei*, *A. niger*, *A. oryzae* and *A. nidulans* (Sims *et al.*, 2005; Wang *et al.*, 2010). These studies determined the decrease in transcripts coding secreted proteins under ER stress was transcriptional downregulation rather than degradation (RIDD). This was proposed as altering the upstream regions of the transcripts examined, particularly the promotor, led to a loss of downregulation under ER stress (Pakula *et al.*, 2003; Al-sheikh *et al.*, 2004; Sims *et al.*, 2005; Wang *et al.*, 2010).

1.4. Recombinant protein production and ER stress

The biotech industry utilizes a broad range of species to produce commercially desirable proteins and enzymes (Faus *et al.*, 1998; Kunaparaju, Liao and Sunstrom, 2005; Sørensen and Mortensen, 2005; Jarvis, 2014; Chen and Lai, 2015). Protein production covers a wide range of applications including those involved in food and pharmaceutical industries as well as having applications in cosmetics, paper, and leather and textile industries (Lubertozzi and Keasling, 2009). *Aspergillus* spp. are used extensively to produce a variety of homologous (see Table 1) and heterologous extracellular enzymes.

Table 3. The table provides examples of the homologous proteins produced by asepergillus spp and the industrial use. (LUBERTOZZI AND KEASLING, 2009).

Homologous Extracellular enzyme	Industrial Application
Amylases	Ethanol fermentation
Proteases, lipases	Detergent additives
Cellobiohydrolase, cellulases	Textile processing
Cellulases, hemi-cellulases	Paper processing
proteases, lipases, cellulases	Leather processing
pectinases, cellulases, glycosidases	Wine and fruit juice production
glucose oxidase, amylase, metalloproteinase	Baking
lactase, proteases	Dairy product production

Aspergillus spp are particularly useful for the production of secreted proteins due to their filamentous structure and their evolution as saprophytic organisms which both lend to a large secretory surface. With much research having been carried out within *Aspergillus* spp. they are well characterised and can be genetically manipulated with relative ease to produce the desired protein, homologous or heterologous. However, it has been observed that the yield of heterologous protein is much lower than homologous (Sims *et al.*, 2005). Several studies identified the ER and the secretory pathway as a bottleneck for RPP in a variety of organisms (Ku *et al.*, 2010; Ward, 2012; Hoang, Maruyama and Kitamoto, 2015). This has been counteracted in some yeast species by overproducing the homologue of *bipA* to help with protein folding (Harmsen *et al.*, 1996; T. Payne *et al.*, 2008). However, this has

had limited success and has not been shown to help within *Aspergillus* species overexpressing *bipA* (Harmsen *et al.*, 1996) whereas increased levels of *pdiA* have been shown to have a positive impact on RPP yields (Ngiam *et al.*, 2000; Moralejo *et al.*, 2001). *A. niger* and *Aspergillus awamori* displayed increased yield of RPP when modified to overexpress *hacA*, highlighting its role on decreased yields in standard industrial strains (Valkonen *et al.*, 2003). Thaumatin, a low calorie sugar substitute isolated from *Thaumatococcus daniellii*, was also successfully overexpressed in *Pichia pastoris* through conjugation with the foldase *pdi* (Healey et al., 2017). An alternative approach to overexpression of chaperones/foldases which has successfully increased yields of RPP is alteration of the desired protein. Chymosin was upregulated by more than 100% in *A. niger* when a poorly utilized glycosylation site within prochymosin was altered to be more receptive to glycosylation (van den Brink et al., 2006). An earlier study found that by attaching a glycosylation site to a region of chymosin being produced heterologously by *A. awamori* led to a 10 fold increase in expression (Berka et al., 1991).

Comparative to other *Aspergillus* spp *A. nidulans* is less studied in regards to the ERSR. As this is the model organism for *Aspergillus* spp, characterizing the ERSR and its capabilities can be considered fundamental research and may provide further targets to increase recombinant protein yields.

1.5. Aims of this project

Given the ERSR has been implicated as limiting RPP for fungal spp I proposed three aims to the project;

- Investigate the known *ire1*/*hacA* pathway for RIDD
    - To investigate the *ire1*/*hacA* pathway I shall create a constitutively active *hacA* mutant for comparison with both the WT and *ΔhacA* strains.
    - To examine whether RIDD occurs in *A. nidulans* I shall utilize northern blotting and Q-PCR to determine levels of transcripts for both secreted and non-secreted proteins.
    - Measurement of transcripts during control and ER stress induced conditions will be examined as well as investigating the role that *hacA* plays in regulating ERSR targets.
- Identify potential targets for increasing RPP
    - Using results from investigating RIDD and ERSR target gene expression I will design further experiments to elucidate targets to increase RPP.
- Trial a new method for quantifying ER stress
    - A newly developed method for quantifying ER stress in mammalian cells has been identified, I will test applicability and feasibility of this new technique for measuring ER stress in *A. nidulans*.

2. Materials and Methods

2.1. General Solutions and Buffers

See appendix 1. A.

2.2. *Aspergillus* strains, oligonucleotides and strain growth

2.2.1. *Aspergillus* strains

Table 4 Genotypes of strains used in this study

Strain	Stock Number	Source
Wild Type (WT): veA+ ΔnkuA	1048	This Laboratory
ΔhacA: ΔnkuA	1057	This Laboratory
hacA Δintron ΔnkuA	1060	This work
Δgcn2 pyroA4 ΔnkuA	1159	FGSC
ΔhriA pryoA4 ΔnkuA	1161	FGSC
Δgcn2:ΔhriA riboB2 pabaB22 ΔnkuA	1357	This work
Δeif2α riboB2 pabaB22 ΔnkuA::argB+	1304	This work
P_{niiA}:ireA pyroA4 ΔnkuA	1308	This work

2.2.2. Oligonucleotides

Table 5 Oligonucleotides used in this study.

Oligonucleotide	5' - 3' sequence
hacA F1	GAAGGCAATAAAGGCGTGAC
hacA R2	GGTGAAGAGCATTGTTTGAGGCGCAACTAGACGGAAGCAGGT
hacA F3	CGCATCAGTGCCTCCTCTCAGACAAGCGGTACAGGGTCATACG
hacA R4	AGCGGCCTTCAACTCATTTA
hacA F2	CCAGGGTTAGGCCCCCTCCT
hacA R3	CGCGAGCGGCTTCCTTTTTC
prtA For 1	CGGTGAAACCTACGGTGTTT

prtA Rev 1	CAATCCAAGCGGAGAGGATA
pepJ For 1	AATGCCGGTCTACAGGTCAC
pepJ Rev 1	CATCGATGGTCAGTTCGTTG
hacA Splicing For	GAGAAGAAGCCAGCGAAGAA
hacA Splicing Rev	GACGCTGAAGAAGGAACTGG
PyrG_HacA_R	CTTGGGCTAGTTGAACTCCGCGGAGTTCAACTAGCCCAAG
PyrG_HacA_F	CAACTTCGCAACCTCATCAACGGAGTTTGTTACGAGAAGTGG
HacA_spliced_Rev	TCTGTCTTAGCGCGTTTTCTTGGAGGTAAGTTTG
HacA_spliced_for	GACAAACTTACCTCCAAGAAAACGCGCTAAGACA
PrtA_f1_intronless	GTACATTGACGCCCTGACCT
PrtA_r1_intronless	CATAGGCGTAAGTGCCCTCT
PrtA_f2_intronless	GCGCCAAATGCTCTTACTGT
PrtA_r2_intronless	CAATCCAAGCGGAGAGGATA
Ire1_F5	GGGTATGCTTGGCTCTGGTA
Ire1_R5	CCAAGGCACACCTACACCTT
18S_F1	CTTGGATTTGCTGAAGACTAAC
18S_R1	CTAACTTTCGTTCCCTGATTAATG
18S_F2	GGAAACTCACCAGGTCCAGA
18S_R2	GCTATTTAAGGGCCGAGGTC
Ubiquitin_RT_F1	GGTCGCACTCTTTCGGACTA
Ubiquitin_RT_R1	CTACACCACCCCCAAGAAGA
HrdC F1	GACTCTTGCCTATCGCCATC
HrdC R1	TCGATAGCCTTATCCGCAAC
derA F1	CGGCGTGTTAGTGTTCACAG
derA R1	CACCCCACAGATCTCATCCT
BipA F1	TCCATCTTGGAGGTGAGGAC
BipA R1	TGGCTTTTAGGTCCTTGGTG
18S_F4	GGGCTCCTTGGTGATTCATA

18S_R4	CTCCGGAATCGAACCCTAAT
BipA F2	ACGGTGTTTTCGAGGTTCTG
BipA R3	CAGACAGAACACCACCCTGA
pdiA F1	CTGGGTACATCGCGGTAAGT
pdiA R1	GGACATCCTTGTCGTTCTCG
Reverse Gcn2C PM	CTAGCTGCATCTATTAGTATATTGTCG*
Gcn2C_5_F	GGGTGTCATGAGGATGCTTT*
Gcn2C_3_R	CAGGGGTATGAACCTCCAGA*
Gcn2C_int_R	ATGGTGGCAATGTAACGACA*
Gcn2C_int_F	ATTTCGCTCAATCAGCCTTG*
Forward Gcn2C PM	CGACAATATACTAATAGATGCAGCTAG*
GCN2_5Fgib	CAACCAAAGCGAGAACAAAAATGTTGATCGTATCTTCATTGTCATTT*
GCN2_3_ R Gib	ATTTCCCCGACTCGAGAATTCAGGGGTATGAACCTCCAGA*
eIF2_5'_fwd	CCTGCCAACCAAAGCGAGAACAAAACTTGGTGCAGCACTGGTAG*
eIF2SA_5'_rev	TACGTCTCCGCGCAAGCTCAGAGAGCAGAATC*
eIF2SA_3'_fwd	GCTCTCTGAGCTTGCGCGGAGACGTATTCGT*
eIF2_3'_rev	CGCACATTTCCCCGACTCGAGAATTACGCTTAAACCATCGCAAAC*
eRF2_5'_delta_rev	AGAGCATTGTTTGAGGCCGACAATTTGTGAGCGAC*
pyrG_fwd_eIF2	TCACAAATTGTCGGCCTCAAACAATGCTCTTCAGCCTCAAACAATGCTCTTC*
pyrG_rev_eIF2	GAGAGGAGGCACTGATGTCTGAGAGGAGGCACTG*
eIF2_3'_delta_fwd	CCTCCTCTCAGACATCAGTGCCTCCTCTCAGACAGGAGGGTGTCCCCGAATAAATATG *
eIF2 5prime F	CTTGGTGCAGCACTGGTAGA*
eIF2 3prime R	ACGCTTAAACCATCGCAAAC*
PepJ F RT	GGAGGCTCAACCTTCACAAC
PepJ R RT	GTACTGGAGGACTCGGATGC
Ire1 F RT	AGCCAGGATGGCAGTCTCTA
Ire1 R RT	TACGGCGTCTCATCAACAAG

2.2.3. Oligonucleotide design and synthesis

I designed all primers except for those highlighted with an asterisk in Table 3, these were designed by Professor Mark X. Caddick. Genomic sequences for genes of interest were attained from www.aspgd.org. Once selected, Primer 3 software was utilized to adjust

parameters for desired oligonucleotides; including oligonucleotide length, melting temperature and size of desired product. All oligonucleotides were synthesised by Sigma.

2.2.4. General growth and harvesting

A. nidulans stock cultures were stored at – 80^{o}C in glycerol stocks prepared and stored using Protect beads (Technical Service consultants Ltd). Strains were grown on MM 3% agar plates that were appropriately supplemented and incubated at 37^{o}C for 3 days. Conidia were harvested from plates with a sterile spatula and 20 ml of 0.01% Tween water. Cells were grown in MM at a 1 in 4 volume proportionate to flask size ranging from 50 ml in a 200 ml flask to 250 ml in 1 L flasks. Cells were grown at 37^{o}C with shaking at 4g for a minimum of 16 hours. Harvesting of cells involved filtering through Miracloth (Calbiochem Corp.) and washing with the appropriate buffer before being pressed dry between paper towels and flash frozen in liquid nitrogen. Samples were then stored at – 80^{o}C.

2.2.5. Cassette synthesis for strain transformation

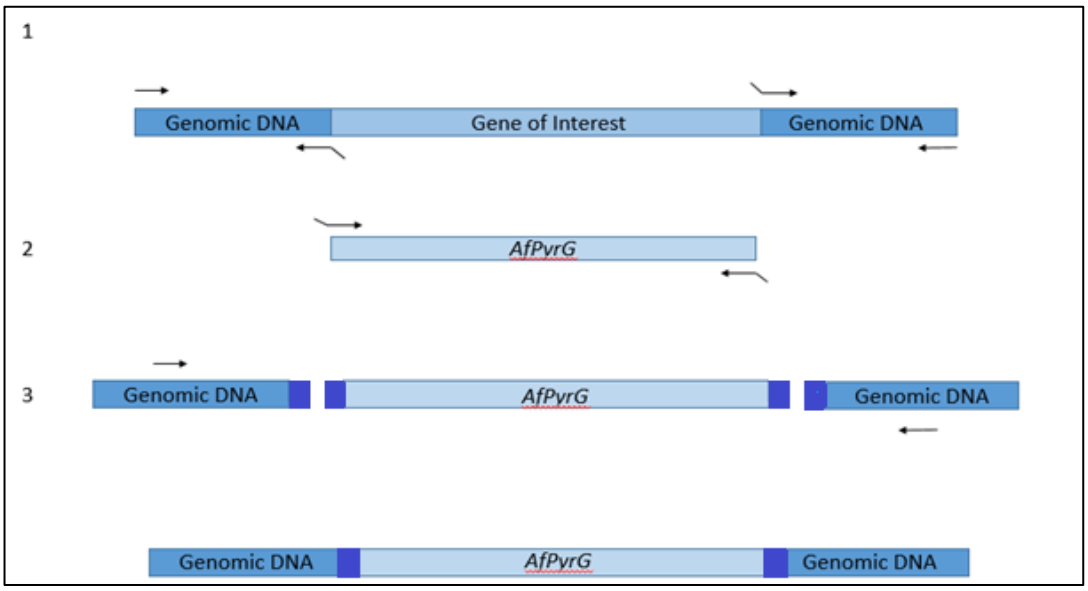

Figure 2. 1 Example of deletion cassette synthesis. 1 shows the initial PCR amplifying the up and downstream regions of the gene of interest. 2 shows the amplification of the selectable marker, *Aspergillus fumigatus PyrG*. The primers used in both steps one and two create overlapping sequences to ensure correct assembly which occurs in step 3. 3 shows PCR with nested primers to form the final product which is shown below.

Cassettes for transformations were produced utilizing the technique outlined in Fig 2.1 and described by (Szewczyk *et al.*, 2007). Flanking regions of genes of interest were 1500 bp to ensure correct localisation of DNA constructs. *Aspergillus fumigatus pyrg* was used as a selectable marker in cassette construction.

2.3. *A. nidulans* transformation and confirmation

The protocol to transform *A. nidulans* was as described by Szewczyk *et al*,.2007. All glassware used was washed with 10% (v/v) acetic acid prior to use to ensure removal of any potential contaminants. Putative transformants were grown on selective media, i.e only successful transformants could grow. *pyrG* encodes orotidine-5'-phosphate decarboxylase. An *A.*

nidulans pyrG mutation (*pyrG*89) leads to loss of function in orotidine-5'-phosphate decarboxylase and strains require uridine or uracil. I used as a selectable marker *AfpyrG*, this restores growth of *pyrG89* containing *A. nidulans* strains' on media deplete of uridine and uracil (Weidner et al., 1998). The *hacA Δintron* strain was created through transformation of *ΔhacA*, in this instance successful transformants *lost* the ability to grow without uridine and uracil as the intronless *hacA* cassette was reinserted into the *hacA's* original locus. To select for transformants in this case 5-fluoroorotic acid was used in the selective media. 5-fluoroorotic is decarboxylated to the toxic compound 5-fluorouracil by orotidine-5'-phosphate decarboxylase. Strains containing the *AfpyrG* are therefore selected against.

Confirminatory PCR was used to check the presence of the gene of interest. For confirmation of cassette insertion at the right locus, the forward primer will bind upstream of the homologous region the cassette is targeted to. A successful PCR therefore shows cassette insertion of the cassette at the correct locus. See Appendix 1. B.

See Figure 2. 3

2.4. RNA work

To minimise degradation of RNA by nucleases, all the solutions were autoclaved twice. During solution preparation and sample handling disposable gloves were worn. Diethyl pyrocarbonate (DEPC) water was prepared and used to as a solute for solutions involved in RNA work.

2.5. Polymerase Chain Reaction

Standard PCR was conducted using Bioline Redmix with a reaction volume of 20 µl;

- Bioline Redmix 10 µl
- DNA 200 ng
- Primers 0.5 µl each (20 µM)
- H_2O ▲20 µl

Typical PCR protocol consisted of the parameters described in Table 4.

Table 6. Standard PCR settings for Bioline Redmix and standard KOD hotstart reactions.

Step		Temperature (°C)	Time
1	Initial denaturation	95	1 mins
2	Denaturation	95	30 secs
3	Annealing	~56-64	20 secs
4	Elongation	72	1 min per KB
5	Cycle back to step 2 (x 30)		
5	Final elongation	72	10 mins

2.5.1. Fusion PCR

KOD hotstart proofreading DNA polymerase was used for the synthesis of deletion constructs. Reactions were carried out at a volume of 50 µl;

- KOD Buffer 5X 10 µl
- Primers 0.5 µl each
- DNA 1 µl
- $MgCl_2$ 3 µl
- dNTPs 5 µl
- KOD polymerase 1 µl
- H_2O_2 ▲50 µl

Table 7. Protocol for fusion pcr.

Step		Temperature °C	Time
1	Initial denaturation	98	30 secs
2	Denaturation	98	10 secs
3	Annealing	Primer specific	30 secs
4	Elongation	72	1min/KB
5	Cycle back to step 2 (x12)		
6	Denaturation	98	10 secs
7	Annealing	Primer specific	30 secs
8	Elongation	72	3 mins
9	Increase elongation by 5 secs each round Go back to 6 (x12)		
10	Denaturation	98	10 secs
11	Annealing	Primer specific	30 secs
12	Elongation	72	4 mins
13	Increase elongation by 5 secs each round Go back to 10 (x 12)		
14	Final Elongation	72	5mins

2.5.2. Reverse transcription and quantitative PCR

Reverse transcription of RNA was performed using Tetro reverse transcriptase from Bioline following the manufacturer's protocol.

Quantitative PCR (qPCR) was performed using SensiFast Sybr Hi Rox (Bioline) master mix at 10 µl per reaction.

- Primer (8mM) 0.5 µl
- cDNA 5 ng
- H_20_2 2 µl
- 2 x Mastermix 5 µl

Table 8. Protocol for Q-PCR with SensiFast Sybr Hi Rox master mix.

Step		Temperature (°C)	Time
1	Initial denaturation	95	10 mins
2	Denaturation	95	10 secs
3	Annealing	59	10 secs
4	Elongation	72	5 secs
5	Cycle back to step 2 (x 30)		
5	Melt Curve	60-95	

Q-PCRs were run on the Applied Biosystems Real Time PCR Step One Plus themocycler.

2.6. Nucleic acid quanfitication

DNA and RNA quantity and quality were measured with NanoDrop-1000 (Thermo Scientific) using 1-1.5 µl of the solution.

2.6.1. Electrophoresis gels

2.6.1.1. DNA

Gels were prepared with 1% (unless otherwise stated) agarose (Bioline), TAE buffer and 2 µl for every 100 ml of Midori Green. Electrophoresis was performed in horizontal gel tanks containing TAE buffer. Settings were 100 Volts and 400 Amps for 30-45 minutes or until sufficient separation of bands occurred.

2.6.1.2. RNA

Gels for northern blots were made with 2.5 g of agarose (Bioline) melted in 206 ml DEPC water. Once cooled to ~60^{O}C 25ml of 10X MOPS (20 mM MOPS, 5 mM sodium acetate, 1mM EDTA) and 14 ml formaldehyde were added. This was then poured into the appropriate gel tray.

2.7. RIDD analysis

2.7.1. Growth & harvesting

Strains were grown as described above in 2.2. After 16 hours of growth in 250 ml MM at 37 $^{\circ}$C in an orbital incubator at 4g. Mycelia were harvested by filtration and washed with pre-warmed nitrogen free MM. The mycelia were re-suspended in a further 250 ml of pre-warmed nitrogen free MM and incubated for a further 24 hours with shaking. Cells were then subjected to either 20 mM DTT, 20 mM DTT and 1.7 mM proflavin or 1.7 mM proflavin treatment alone. Harvesting of cells involved filtering through Miracloth (Calbiochem Corp.) and washing with

appropriate buffer before being pressed dry between paper towels, flash frozen in liquid nitrogen and stored at -80 ^{o}C.

2.7.2. RNA extraction

Mycelia (~250 mg) was ground in a mortar and pestle with liquid nitrogen. Ground mycelia was added to sterile 2ml Eppendorf tubes containing 800 µl of RNA extraction buffer (100 mM Tris-Cl pH8, 1.4 M sodium chloride, 10 mM EDTA and 5% SDS) and 800 µl phenol, vortexed briefly and agitated for 10 minutes. Samples were centrifuged at 25,200g for 30 min. 700 µl of the aqueous phase was transferred to a fresh Eppendorf tube containing 700 µl phenol: chloroform (1:1), vortexed and centrifuged for a further 10 min at 25,200g. 5 M lithium chloride was added in equal parts to the aqueous RNA solution removed after phenol/chloroform clean up and precipitated for at least 1 hour at 4^{O}C. After a further 20 min centrifugation the pellet was washed twice with 70% ethanol then re-dissolved in DEPC H_2O, ethanol precipitated and re-dissolved in DEPC H_2O.

2.7.3. Northern Blots

After extraction RNA samples were incubated at 65^{O}C for 10 min with 10 µl of 2X RNA loading buffer (see appendix 1. B) and then transferred to ice prior to gel loading. Gels were in a solution of 1X MOPS buffer and ran for 3 hours at 100V. The RNA from the gels were then transferred to Zeta-Probe GT blotting membrane (BioRad) in 10X SSC (1.5 M sodium chloride, 0.15 M sodium citrate, pH 7.0) overnight. After overnight transfer the membrane was rinsed in 2X SSC twice for 10 min and then left to air dry. Once dried the RNA was fixed by vacuum drying at 80^{o}C for 45 mins. Membranes were then exposed to radiolabelled (α32P – dCTP) DNA probes at 65 ^{o}C following the protocols for Zeta-Probe membrane. Imaging was conducted using a Molecular Dynamics STORM^{TM} scanner and quantification was done using ImageQuant TL Software.

2.8. Polysome profiling

2.8.1. Growth & Harvesting

Strains were initially grown and harvested from plates as described in 2.2. For polysome profiling experiments cells were grown in 125 ml of MM in a 500 ml flask with shaking (at 4g) at 37^{o}C. Prior to harvesting the cultures were treated with cycloheximide (1µg/ml). Cells were harvested by filtering through MiraCloth and washing with cold Polysome cell wash buffer (20 mM Tris-Cl pH 8.0, 140 mM potassium chloride, 1.5 mM magnesium chloride, 1% Triton X-100, 1 mg/ml heparin, 0.1 mg/ml cycloheximide) prior to snap freezing. All 3 replicates, for each condition, were grown and harvested concurrently.

2.8.2. Sucrose Gradient production

A 50% sucrose solution in sucrose buffer (20 mM Tris-Cl pH 8.0, 140 mM potassium chloride, 5 mM magnesium chloride, up to 0.5L with DEPC H_2O_2) was filter sterilized (0.22 µm filter). A portion of this was diluted with sucrose buffer to create a 10 % (w/v) solution. To each buffer 250 µl of 0.5 mM DTT and 0.1 mg/ml cycloheximide were added. The two buffers were then mixed using the BioRad Biologic LP to produce the desired gradients in 14 x 95mm polypropylene tubes (Beckman Coulter) centrifuge tubes. Gradients were allowed to settle overnight at 4 ˚C.

2.8.3. Fractionation and Profiling

800 µl of polysome lysis buffer was added to sterile tubes to which ~ 200mg of ground mycelia was added and agitated at 4^{o}C for 10 min. Samples were then centrifuged at 4,000g at 4^{o}C for 5 min. The supernatant was then transferred to a fresh tube and centrifuged again at 10,000g for another 5 min after which the supernatant was transferred to an Eppendorf tube.

Samples RNA concentrations were measured on the NanoDrop 2000. About 800 μg of RNA was loaded onto sucrose gradients and centrifuged at 459,984g at 4 ˚C for 2 hours and 50 min in the Beckman Optima XL-100K ultracentrifuge. All replicates for a particular strain and condition were fractionated on sucrose gradients derived from the same batch. 1.1 ml aliquots were collected using the BioRad Biologic LP machine with UV lamp which measured RNA absorption (260 nm). Samples were cleaned with 500µl Phenol + 10µl 10% SDS. The samples were then precipitated overnight at -80ºC in ethanol + 10% 3M sodium acetate.

2.8.4. qRT-PCR

Polysome fractions were spun at full speed for 20 mins at 4˚C. Pellets were washed with 70% ethanol and dried. Pellets were then resuspended in DEPC H_2O. Fractions were pooled into "high" and "low" expression as based on polysome profiles previously generated. Equal volumes of each fraction were added to the appropriate high and low pools. These samples were then converted to cDNA and used for Q-PCR as described in 2.6.

2.9. ER Stress Quantification

2.9.1. Growth and treatment

Strains were initially grown on plates as described in 2.2 and transferred to 50 ml of supplemented MM and grown overnight at 37 ºC . Aliquots of 400 µl were transferred to 24 well suspension culture plates from produced by Cellstar (Geiner Bio-one) and left to grow at 37 ºC for a further five hours. Specified treatments were then applied to individual wells; once treated, 2 ml of 4 % paraformaldehyde solution was added to each well and left for five mins. This was then removed and another 2 ml of the paraformaldehyde added for 5 min before being removed. Cells were stored at 4 ºC in the dark.

2.9.2. Visualisation

Stock Thioflavin T was added to each sample at a 5 µM final concentration and left to incubate for 20 min. Whole individual hyphae were imaged as replicates for each strain and condition. Imaging was primarily carried out on the EVOS FL Cell Imaging System from Thermofisher using the DAPI filter for ThT visualisation as per the manufacturer's specifications. The EVOS employs LED illumination, images taken using Objectives 10X and 40X. Initial imaging was performed on LSM 710 with Objective 10X. This microscope is located in the Centre for Cell Imaging at the University of Liverpool.

2.10. Computational Analysis

- Software
  - ImageJ was used in the analysis of microscopy fluorescence and polysome profile quantification.
  - ImageQuant was used to quantify northern blot images.
  - Jalview 2.8.2 was used for alignments of protein and nucleotide sequences.
  - Graphpad Prism 5.03 was used for figure design and statistical analysis. Statistical analysis included Two-Way ANOVA, Paired and Unpaired T-Tests.

- Databases
  - The *Aspergillus* genome database (www.aspgd.org).
  - Fungal Genetics Stock Centre (www.fgsc.com).
  - National Centre for Biotechnology Information (NCBI) (http://www.ncbi.nlm.nih.gov/).
- Online Tools
  - Primer 3 was used to design oligonucleotides.
  - Basic Local Alignment Search Tool (BLAST) (http://www.ncbi.nlm.nih.gov/)

    MUSCLE (Multiple Sequence Comparison by Log Expression) (https://www.ebi.ac.uk/Tools/msa/muscle/

3. Analysis of transcript stability during ER stress

3.1. Introduction

To investigate whether ER stress leads to a loss of secreted transcript, through either RESS or RIDD, I needed conditions in which there are measurable levels of mRNA transcripts encoding secreted proteins. Extracellular proteases in *Aspergillus spp* are regulated by a variety of factors including growth medium composition, initial pH and temperature (Ortiz et al., 2016). Extracellular substrate has long been known to effect protease secretion in *A. nidulans*, depletion of carbon, nitrogen or sulpher sources illicits extracellular neutral and alkaline protease production (Cohen, 1973). Whilst there are established conditions that induce protease expression there is still relatively little known about the regulatory circuits responsible. The only known example in *Aspergillus* is that of *prtT*, loss of this gene led to loss of extracellular proteases in *A. niger* mutants. Whilst this observation was found in 1992 the regulatory circuit wasn't identified until 2008 (Mattern et al., 1992, Punt et al., 2008). The production capacity of *Aspergillus* for extracellular proteases is actually a bottleneck for RPP as native proteases can target the heterologous protein product (Archer and Peberdy, 1997; van den Hombergh et al., 1997).

For examining mRNA transcript stability, I selected two well established extracellular proteases, *prtA* and *pepJ*. Firstly, *prtA*, which encodes a metallo-protease, was identified as being highly transcribed under nitrogen starved conditions. Secondly, *pepJ* was identified initially as upregulated during carbon starvation (Emri *et al.*, 2009, Katz, Rice and Cheetham, 1994; vanKuyk, Cheetham and Katz, 2000). Both proteases are linked with autolysis in *A. nidulans*, although they were not required for this response (Szilágyi et al., 2019). Preliminary analysis utilizing northern blotting confirmed that *prtA* was highly upregulated at 24 hrs of

nitrogen starvation (data not shown). I also probed for *pepJ* under the same nitrogen starved conditions and this was highly expressed. Therefore, these two proteases provide suitable targets for measuring the effect ER stress has upon secreted transcript stability under the one condition (Emri *et al.*, 2009).

To observe the effects of each aspect of the ERSR on transcript stability during ER stress, I wanted to create ERSR mutants. Prior to this study this lab created a *ΔhacA* strain, which based on literature, is unable to induce the transcriptional aspect of the ERSR (H. J. Mulder. M, 2004). From the *ΔhacA* strain I wanted to create a *hacA Δintron* strain through transformation with a DNA construct encoding an intronless version of the *hacA* gene. As mentioned chapter 1, *T. reesei*, *A. niger* and *A. nidulans* all express a truncated and spliced *hacA* mRNA when the ERSR is active (Valkonen, Penttilä and Saloheimo, 2003; Dave *et al.*, 2006). Whilst the *hacA Δintron* strain would not constitutively produce a truncated transcript, intron removal was found to be sufficient for constitutive ERSR induction in several studies examining *A. niger* (Mulder and Nikolaev, 2009; Carvalho *et al.*, 2012) The availability of both *ΔhacA* and *hacA Δintron* strains will allow for examination of both loss, and the constitutive activation of *ΔhacA*. I also wanted to create a *ΔireA* strain; as RIDD is performed by IRE1 in higher eukaryotes, a *ΔireA* strain would indicate whether IREA is responsible for degrading transcripts encoding secreted proteins during ER stress, if this occurs in *A. nidulans*. *ΔireA* was found to be lethal in a study examining the *A. nidulans* kinome (De Souza et al., 2013). A way to overcome this lethality would be to create a construct with *ireA* on a regulated promotor. This has been successful in an *A. niger* study which was able to repress *ireA* expression through the use of a thiamine riboswitch. The study found that in *A. niger* a fully functional ERSR is required for growth conditions that induce secreted hydrolytic enzymes (Tanaka, Shintani and Gomi, 2015). An inducible promotor for *ireA* may be the only option to study the endonuclease's role on transcript stability during ER stress.

To examine ER stress, dithiothreitol (DTT), a strong reducing agent, was administered to cultures at 20 mM. DTT is commonly used to examine the ERSR as it inhibits disulphide bond formation, thus impeding secondary structure attainment of nascent peptides (Harding *et al.*, 2000; Patil, Li and Walter, 2004; Oslowski and Urano, 2011). To confirm whether any loss of transcript that may be observed is due to active degradation rather than transcriptional repression we utilized the transcriptional inhibitor proflavin. Proflavin functions as a transcriptional inhibitor by intercalating with mRNA and DNA molecules, thereby restricting polymerases from transcribing DNA (Hurwitz and Rosano, 1965). This has allowed researchers to observe and measure transcript half-life (Et and Acta, 1965; Hershey, 1989; Morozov *et al.*, 2006; Krol *et al.*, 2013). To do this, an initial control sample of cells is taken followed by regularly timed samples after proflavin treatment. Measuring the initial level of an mRNA transcript from the the control and then throughout the time course will indicate the half-life of a transcript. This allows for comparison of any observed transcript loss during DTT treatment with that of proflavin treatment. If the rate of transcript loss via DTT treatment is greater than that of proflavin treatment, we can infer that transcripts are actively degraded as the loss is at a higher rate than the transcript's half-life. Combining both DTT and proflavin treatment should therefore lead to the greatest loss of transcript due to both inhibited synthesis of new transcripts and degradation of current transcripts. For this experient samples were taken every 10 min for 30 min.

3.2. Aims

- Create ERSR mutants to examine the role *hacA* and *ireA* may have on any regulation of transcripts that may be observed
- Determine if degradation of mRNA transcripts encoding secreted proteins occurs during ER stress
- Observe differences in *bipA* mRNA levels during ER stress between ERSR mutants

3.3. Results

3.3.1. Mutant strain creation

Transformation of the *ΔhacA* strain with a DNA construct encoding an intronless *hacA* was successful, see Fig 3.1. When attempting to generate a *ΔireA* strain, I found the same lethality as was found by De Souza *et al.*, in *A. nidulans*; to overcome this, a construct encoding *ireA* regulated by the *Niia* promotor was created. This construct will allow for the induction of *ireA* expression via NO_3^-. This led to the P_{Niia}:*ireA* strain which should express *ireA* when NO_3^- is present in the media and will strongly repress *ireA* expression when NH_4^+ is present (Caddick et al., 2006). Given the lethality that loss of *ireA* presents, it can be inferred that *ireA* is successfully expressed/repressed by examining growth on either NO_3^- or NH_4^+ containing media respectively. Fig 3.1 shows the P_{Niia}:*ireA* strain is unable to grow without induction of the P_{Niia}:*ireA* construct via NO_3^-, thus displaying the lethality observed in a *ΔireA* strain. *ΔireA* is lethal in *A. oryzae*, *A. niger* and *A. nidulans* yet is viable for *A. fumigatus* (Mulder and Nikolaev, 2009; Feng *et al.*, 2011; De Souza *et al.*, 2013). This is especially surprising as in *A. fumigatus*, *ireA* was found to be required for pathogenicity and the transcription of genes unrelated to ER homeostasis. A study in *Neurospora crassa* found a *ΔireA* strain is viable and that 223 genes are transcriptionally dependent on the kinase whereas only 186 are dependent

on *hac1* (Fan *et al.*, 2015). These studies taken together indicate *ireA*/*ire1* has a role separate from *hac1* activation in *N. crassa* and *A. fumigatus*. Interestingly, transformation of the *hacA ΔIintron* strain with the P_{Niia}:*ireA* construct did not recover the lethal phenotype when grown on media supplemented with NH_4+ (data not shown). If *ireA's* only role in *A. nidulans* was to splice out *hacA's* intron, then the *hacA ΔIintron* would not require *ireA*, however, this is not the case. This is a strong indication that in *A. nidulans*, *ireA* has another function separate to HacA activation.

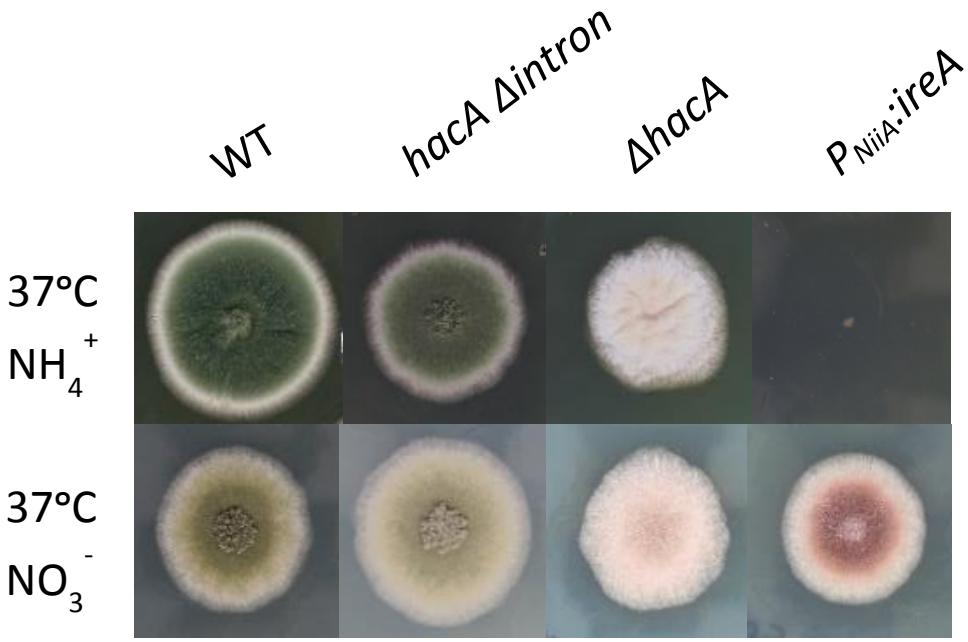

Figure 3.1 **Comparison of *ireA*/*hacA* mutants and WT grown for 72 hrs at 37°C on alternate nitrogen sources.** Successful growth of mutant strains. P_{NiiA}:*ireA* shows no growth on NH_4^+ but healthy growth on NO_3^- supplemented media.

Fig 3.1 shows successful growth of the *hacA ΔIintron* and *ΔhacA* strains. *ΔhacA* shows a severe phenotype with little conidiation. *hacA ΔIintron* grows well but has slightly diminished radial growth compared to WT on NH_4^+ supplemented media and improved growth on NO_3^- supplemented media. For further growth tests see Chapter 6.

3.3.2. Northern blot analysis

Initial experiments examined the half-life of *prtA*. Loss of transcript during ER stress, greater than that observed with proflavin treatment alone, indicates active degradation of transcripts rather than transcriptional repression. This would imply the presence of RIDD as opposed to RESS, although one does not preclude the other.

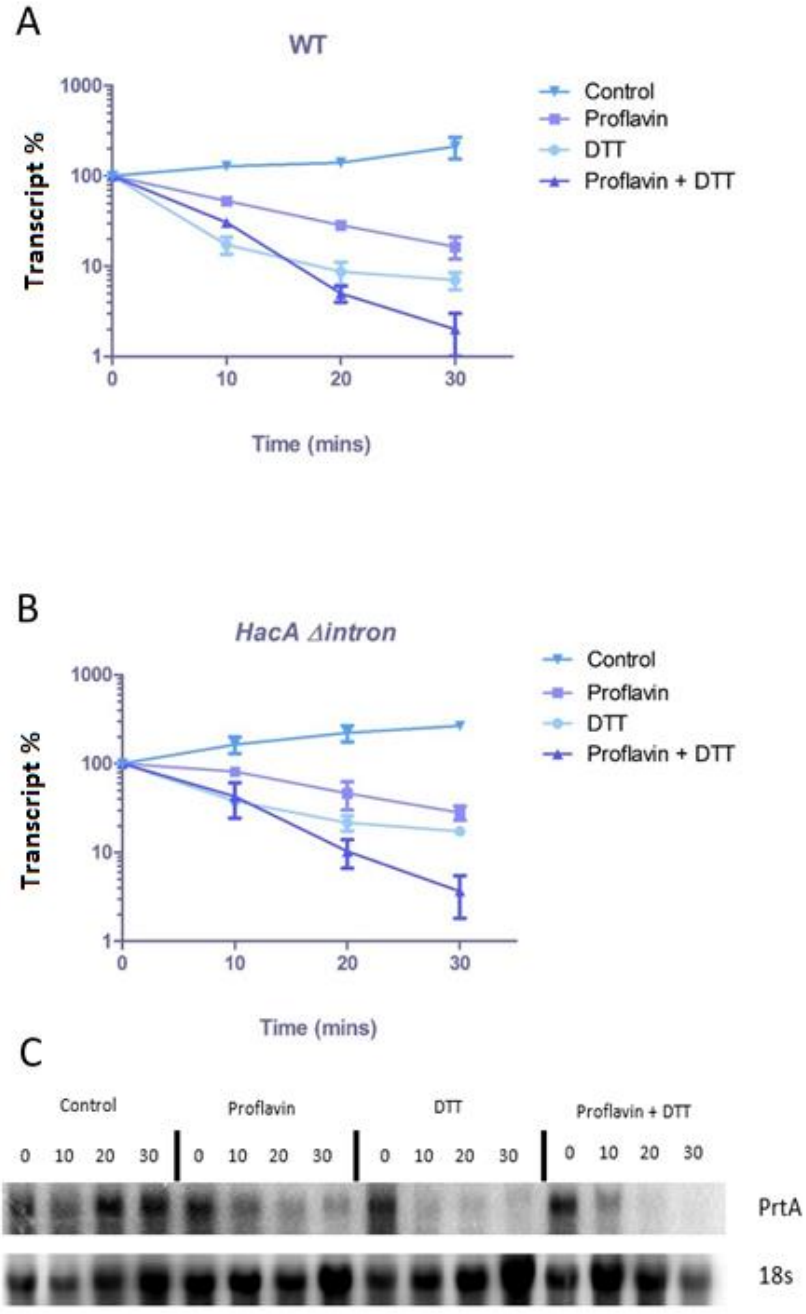

Figure 3 2 Northern blot analysis for *prtA* transcript levels under ER stress conditions in WT and *hacA Δintron*. Transcript level determined by northern blot using 18S rRNA to normalize data. 0 min is used as a starting reference for subsequent time points. A and B show *prtA* transcript level under control, 12 µm proflavin, 20 mM DTT and proflavin + DTT treatment for both WT and *hacA Δintron* strains. WT and *hacA Δintron* display loss of *prtA* under all conditions except the control which sees a steady increase. For both strains each time course and time point is significantly different from the control ($p = <0.0001$ and <0.0001 respectively) as determined by a 2-Way repeated measures Anova and Bonferroni post hoc tests. Combination of proflavin and DTT treatment led to the largest loss of *prtA* for both strains tested. C shows Northern blot of *prtA* and 18s from WT control, proflavin, DTT and proflavin + DTT conditions.

Fig 3.2 A shows WT *prtA* levels drop after treatment of proflavin, DTT and a combination of both, whereas during control conditions levels rise steadily. Each time point was significantly different from the same control time point (p=<0.0001). The 2-Way repeated measures Anova was selected to test for statistical significance as the data is parametric and I am examining a dependent variable (mRNA transcript level) between different conditions over a time course. The Bonferroni post hoc tests quantifies significant differences, where differences occurred, between the treatments i.e provides p-values for the same time point between conditions. From the results I can see DTT treatment alone causes a more rapid decrease in *prtA* transcript than proflavin treatment alone. DTT treatment led to the second largest loss in *prtA* levels as only 10% of the original level remained by 30 min of treatment. The combination of the DTT and proflavin led to the most significant decrease of *prtA* by 30 min with ~3% of the original transcript remaining. Therefore, I know the loss of *prtA* observed is due to transcript degradation not down-regulation. Fig 3.2 B shows *prtA* levels for *hacA Δintron* during control, DTT, DTT + proflavin and proflavin treatment alone. As with the WT, each time point was significantly different from the corresponding control (p=<0.0001). *hacA Δintron* displays the same trends observed in WT, proflavin treatment alone leads *prtA* loss but not as drastically as DTT or DTT + proflavin treatment. The data indicate that *hacA* is not responsible for degradation of transcripts.

Due to the scope of the analysis this project pursued, I decided to carry out subsequent experiments using Quantitative-PCR. This method provided a better means for quantifying and comparing samples as with northern blotting sample number is more limited.

3.3.3. Q-PCR

3.3.3.1. *prtA*

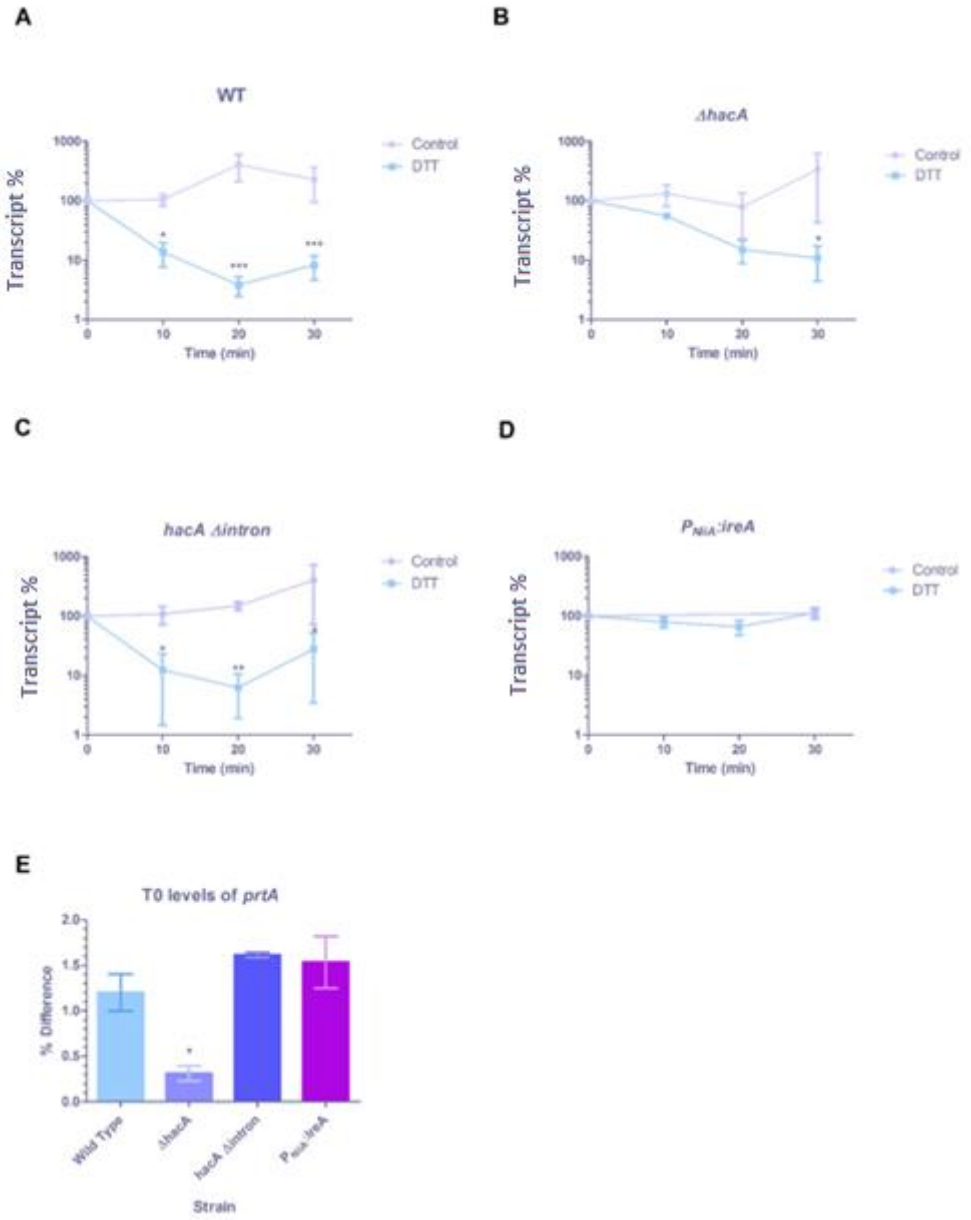

Figure 3 3 *prtA* transcript levels under ER stress conditions. A-D show the response of *prtA* transcript levels to DTT (20mM) treatment over a 30 min time course in WT, *ΔhacA*, *hacA Δintron* and P_{NiiA}:*IreA* strains, respectively. Transcript levels were determined by qRT PCR, using 18S rRNA to normalise data. 0 min is used as a starting reference for subsequent time points in A-D. WT has a significant decrease in prtA levels between control and DTT treatment (p=<0.0001). *ΔhacA* exhibits a significant difference also between conditions (p=<0.05). DTT treated *hacA Δintron* shows significant differences between conditions (p=<0.05). WT, *ΔhacA* and *hacA Δintron* all show a 90% decrease in prtA by 30 min of DTT treatment. P_{NiiA}:*IreA* shows no significant difference between conditions (p=0.9661). WT and *hacA Δintron* exhibit a mild increase in transcript at 30 min compared to 20 min DTT treatment. E compares relative abundance of initial transcript levels for each mutant compared to WT, *ΔhacA* has a significantly smaller transcript level (p=<0.05) Significance levels * {<0.05} ** {<0.01} *** {<0.0001}. N=3.

Using northern analysis I demonstrated in both the wild type and *hacA Δintron* strains that DTT treatment lead to rapid degradation of the *prtA* transcript. In order to monitor the transient regulatory response to DTT in a range of strains similar experiments were conducted in the absence of a transcriptional inhibitor. From Fig 3.3 A I can see in the WT that under control conditions *prtA* levels fluctuate but do not fall below the 10 min level in the WT. The DTT treated WT cells exhibit a ~90% decrease of *prtA* by 10 min ($p =<0.05$). This trend continued with the lowest level of *prtA* measured as a 97% decrease at 20 min ($p =<0.0001$). By 30 min *prtA* levels have begun to increase although still <90% lower than control levels. A paired T-test between the 20 min and 30 min values shows this increase is not considered significant at $p = 0.05$. The increase of *prtA* at 30 min compared to 20 min in the DTT treated cultures is not significant ($p = 0.05$). However, these data suggest a trend which may indicate that the degradation machinery responsible for this dramatic decrease has either slowed or ceased in degrading transcripts.

Degradation of *prtA* in response to DTT treatment was observed in *ΔhacA* as shown in Fig 3.3 B. However, the response was less dramatic than that observed in the wild type with the lowest measured level a 95% decrease at 30 min which was the only time point statistically significantly different from the control. Northern blot analysis of *ΔhacA* was previously attempted however there were no successful attempts to quantify *prtA* levels, this was assumed to be due to low levels of transcript given the extremely unhealthy phenotype. Fig 3.3.E shows that *prtA* levels in the *ΔhacA* strain were significantly lower under control conditions than the WT with 70% less transcript ($p =<0.05$). Fig 3.3 C shows *prtA* levels in the *hacA Δintron* mutant strain which also shows transcript degradation after DTT addition.

Analysis of the for *hacA Δintron* strain revealed *a* 97% decrease in *prtA* mRNA levels at 20 min DTT treatment. By 30 min, the level recovered slightly. This trend, of a slight increase in transcript at 30 min, is similar to the WT results. The data represented in Fig 3.3.A-C indicates

that *hacA* is not involved in this degradation response. The P_{NiiA}*:ireA* strain was grown with NH_4^+ as the sole nitrogen source and supplemented with 1mM 4-PBA to allow growth (see chapter 6) before transferring to nitrogen free media. Under these conditions *ireA* is repressed during growth. Fig 3.3 D shows that in the P_{NiiA}*:ireA* strain, *prtA* levels stay very similar from 0 to 30 min under control conditions. DTT treated P_{NiiA}*:ireA* shows relatively steady levels of *prtA* at 10 and 20 min, whilst by 30 min there is a very slight increase compared to the 0 min *prtA* level. From Fig 3.3 E it appears that in the P_{NiiA}*:ireA* strain the expression level of *prtA* at 0 min is higher than in the WT by ~50% although this was not statistically significant.. These results indicate the presence of RIDD for the first time *in vivo* within a fungus containing the canonical *ire1/XBP-1* (*ireA/hacA*) transcriptional pathway and the first instance for a filamentous fungi.

3.3.4. *pepJ*

To ensure this observation was not *prtA* specific I selected another transcript to examine for degradation. As RIDD degrades transcripts that are specifically processed within the ER, *pepJ* which is upregulated under these conditions should therefore also be subject to this observed degradation during ER stress.

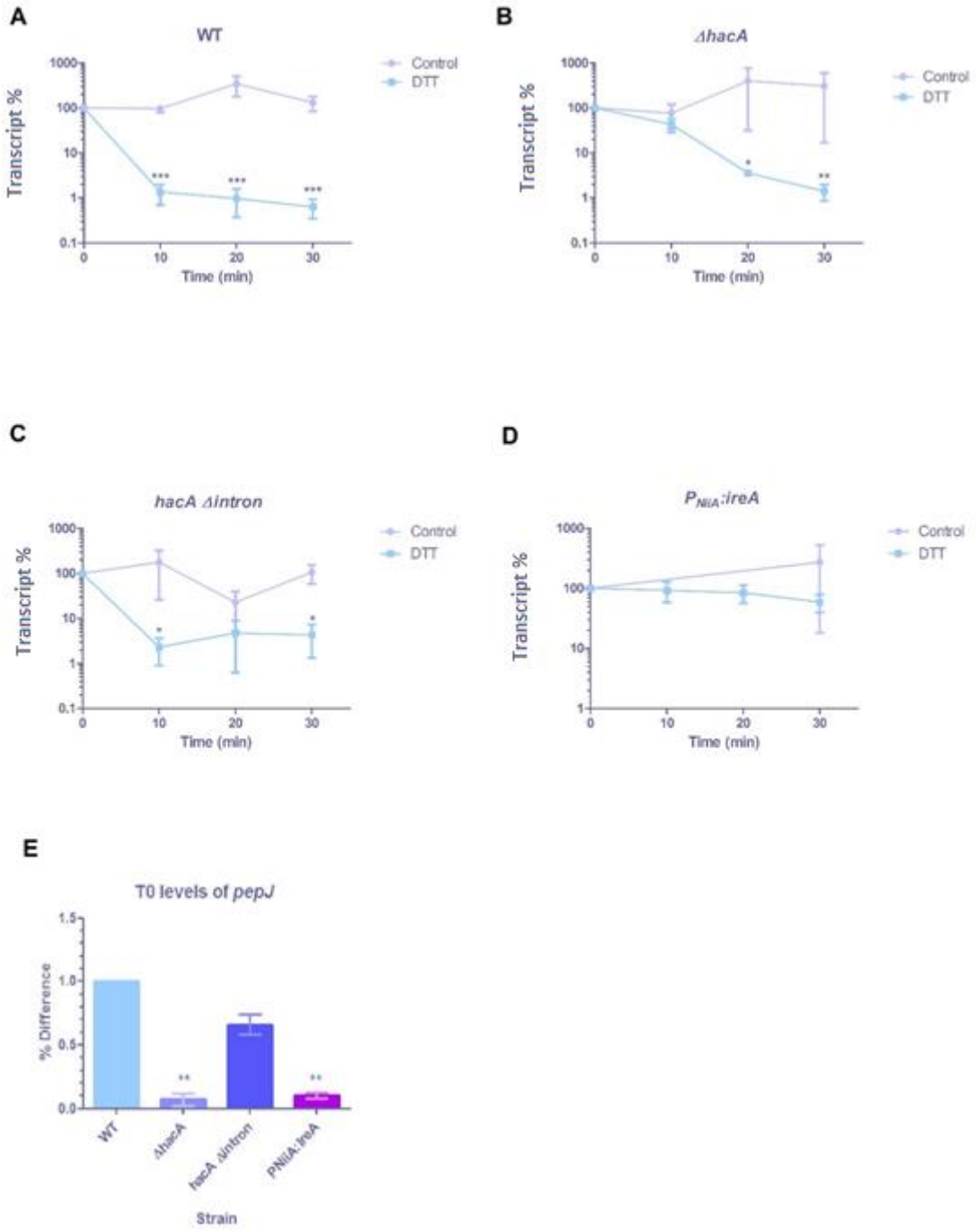

Figure 3.4 *pepJ* transcript levels under ER stress conditions. A-D show the response of *pepJ* transcript levels to DTT (20mM) treatment over a 30 min time course in WT, *ΔhacA*, *hacA Δintron* and P_{NiiA}:*ireA* strains, respectively. 0 min is used as a starting reference for subsequent time points in A-D. A-D show *pepJ* transcript levels under control and DTT (20mM) treated conditions from WT, *ΔhacA*, *hacA Δintron* and P_{NiiA}:*ireA* respectively. WT *pepJ* levels is significantly different between conditions (p=<0.0001). *ΔhacA* displays a significant difference between conditions (p=<0.01). *hacA Δintron* also shows significant differences between conditions (p=<0.05). A slight increase in pepJ transcript is seen at 30 min compared to 10 and 20 min. DTT treated WT, *ΔhacA* and *hacA Δintron* all exhibit >95% loss of *pepJ* levels during the time course. P_{NiiA}:*ireA* shows no significant difference and similar transcript levels between conditions (p=0.885). E compares initial *pepJ* levels comparative to WT. Both *ΔhacA* and P_{NiiA}:*ireA* show significantly lower initial *pepJ* levels (<10%) (p=<0.01). Significance levels * {<0.05} ** {<0.01} *** {<0.0001}. N=3.

Fig 3.4 A shows WT *pepJ* transcript remains above 0 min levels during the control time course. DTT treatment within the WT shows a marked loss of *pepJ* mRNA, which based on 2-Way Anova test is significant ($p =<0.0001$) by 10 min. The decrease in *pepJ* continues throughout the time course with no signs of a restoration of transcript levels, unlike *prtA*. By 30 min, in the WT under DTT treatment, there is <1% of the control level of *pepJ*. This is further indication of RIDD. DTT treatment of the *ΔhacA* strain, leads to a significant decrease in *pepJ* transcript levels by 20 min. At 30 min, *ΔhacA pepJ* levels were at ~2% of the 0 min level. Thus, with respect to both *prtA* and *pepJ*, RIDD is not dependent on *hacA*. Additionally, as with *prtA*, the *pepJ* transcript level under control conditions is significantly lower ($p =<0.01$) than WT, at only 6% of WT control levels.

For the *hacA Δintron* strain (Fig 3.4 C) *pepJ* transcript levels display quite a lot of variation under control conditions. Despite this, statistical analysis revealed a significant difference between control and DTT conditions ($p =<0.05$). The DTT treated cells show a marked decrease by 10 min in *pepJ* transcript levels, being reduced to ~1% of initial levels. This decreased transcript level is maintained through the time course with a very slight increase by 30 min which was determined not to be statistically significant by a paired T-test. Fig 3.4 E shows that *pepJ* transcript levels at 0 min in the *hacA Δintron* strain appear lower than the WT but this was not significant.

The P_{niiA}*:IreA* strain, showed no significant difference in *pepJ* transcript levels between control and DTT conditions (Fig 3.4 D). The P_{NiiA}*:IreA* mutant has 10% of WT *pepJ* levels at 0 min (Fig 3.4 E). I can observe from both Figs 3.3 B and 3.4 B that lower initial levels of transcript, such as within the *ΔhacA* strain, does not limit transcript degradation over the time course. For both *prtA* and *pepJ*, by 30 min of DTT treatment the *ΔhacA* strain has less than

10% of the starting level. Compared to the WT and *ΔhacA* strains, *hacA Δintron* has the highest relative level of *pepJ* by at 30 min DTT treatment.

3.3.5. *actA*

RIDD, which has been characterised in animal systems (Hollien *et al.*, 2009; Eletto *et al.*, 2016; Tavernier *et al.*, 2017), specifically targets transcripts encoding products which are processed through the ER. To confirm that the observed degradation is not a global effect on all transcripts but only those trafficked to the ER I decided to investigate a cystolically translated mRNA.

Actin (*actA* in *A.nidulans*) encodes one of the most abundant proteins within most eukaryotic cells, shows high conservation between species and is involved in more protein-protein interactions than any other known protein. *actA* is a soluble protein and does not contain a SS and it is often used as a reference gene for qPCR experiments. I selected *actA* mRNA for examination due to these properties (Lerner and Nicchitta, 2006).

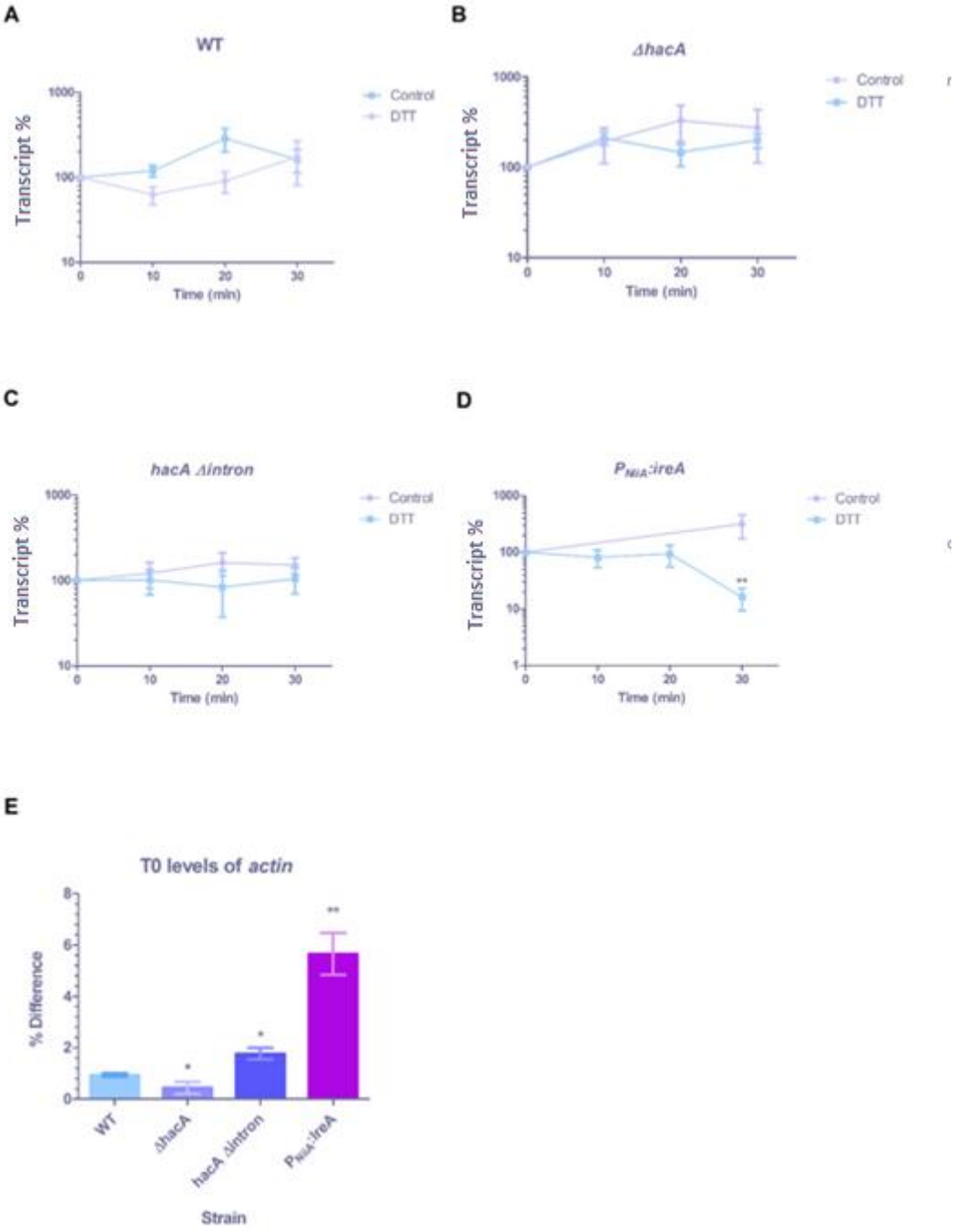

Figure 3.5 *actA* transcript levels under ER stress conditions. A-D show the response of actA transcript levels to DTT (20mM) treatment over a 30 min time course in WT, ΔhacA, hacA Δintron and P_{NiiA}:ireA strains, respectively. 0 min is used as a starting reference for subsequent time points in A-D. A-D show actA transcript levels under control and DTT (20mM) conditions from WT, ΔhacA, hacA Δintron and P_{NiiA}:ireA respectively. WT, ΔhacA and hacA Δintron show no significant difference in actA levels between treatments. P_{NiiA}:IreA displays an overall significant decrease between conditions (p=<0.05) with an almost 90% reduction reached by 30 min under DTT treatment. This large decrease occurs mainly between the 20 and 30 min time points. E compares initial actA transcript level comparative to WT. ΔhacA has significantly lower levels of the actA transcript whereas hacA Δintron and P_{NiiA}:ireA both have significantly higher levels. Significance levels * {<0.05} ** {<0.01. N=3.

Figure 3.5 A shows that there is no significant difference in *actA* transcript levels between control and DTT treated WT cells over the 30 min time course. Fig 3.5 B and C shows similar trends for *ΔhacA* and *hacA Δintron* in that control and DTT time courses are not significantly different. *ΔhacA* shows that there is an increase in *actA* during both control and DTT time courses. These data taken together implies that *actA* is not subject to the degradation observed for *prtA* and *pepJ*, this supports our hypothesis of RIDD. The 2-Way repeated measures Anova was selected to test for statistical significance as the data is parametric and I am examining a dependent variable (mRNA transcript level) between different conditions over a time course. The Bonferroni post hoc tests confirm differences where differences occurred between the treatments, i.e provides p-values for the same time point between conditions.

P_{NiiA}*:ireA* displays a decrease of *actA* at 10 min (~30% decrease) which is maintained until the 20 min time point before showing a significant drop in by 30 min (p=<0.01). At 30 min *actA* levels are ~10% of that of initial levels, see Fig 3.5 D. This is unusual and unlike the other strains tested. A potential explanation is the induction of apoptosis; given *ire1* appears to be responsible for degradation of secreted transcripts in the WT and *hacA* mutants; loss of this method to alleviate ER stress may lead to irreconcilable unfolded protein accrual when P_{NiiA}*:ireA* is presented with DTT. If this observation is ERSR induced apoptosis it raises the question of how this is initiated without *ireA/hacA*.

Levels of *actA* are significantly lower within *ΔhacA* compared to WT at ~50%, see Fig 3.5 E (p=<0.05). *hacA Δintron* displays significantly higher *actA* levels compared to WT measured at ~190% (p=<0.05). I can see from Fig 3.5 E that P_{NiiA}*:ireA* has a significantly higher level of *actA* at the at 0 min compared to WT at over 5x. This data does not imply that *ireA*/*hacA* are directly responsible for altering *actA* levels but it's clear that modifications to the ERSR components lead to an effect on *actA* transcription.

3.3.6. *bipA*

To ensure that the degradation observed for *prtA* and *pepJ* is associated with ER stress I decided to examine the classic ER stress target, *bipA*, induction of which is the hallmark of the ER stress response (Oslowski and Urano, 2011; Beriault and Werstuck, 2013b).

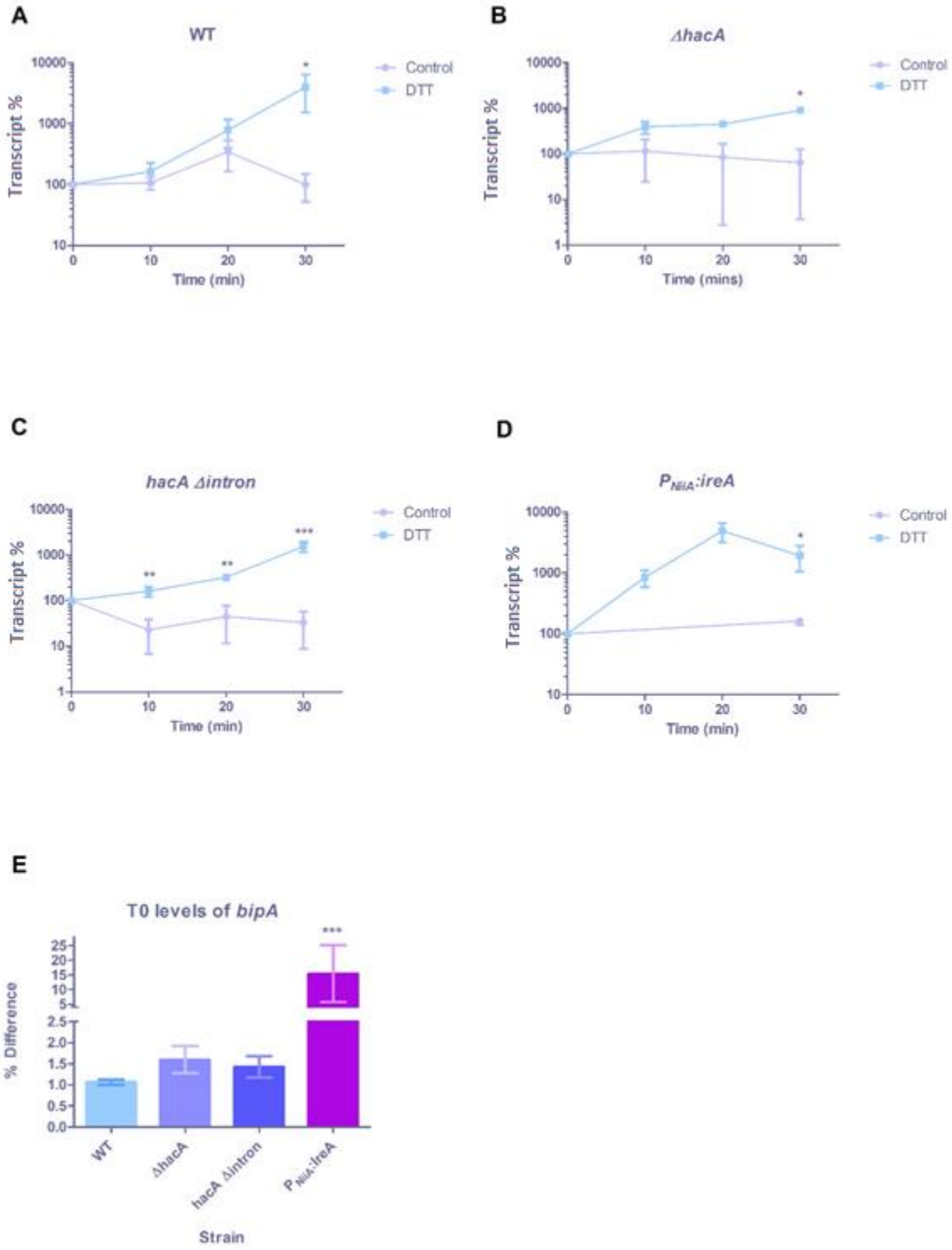

Figure 3 6 bipA transcript levels under ER stress conditions. A-D show the response of bipA transcript levels to DTT (20mM) treatment over a 30 min time course in WT, ΔhacA, hacA Δintron and P_{NiiA}:ireA strains, respectively. T_0 is used as a starting reference for subsequent time points in A-D. A-D show bipA transcript levels under control and DTT (20mM) conditions from WT, ΔhacA, hacA Δintron and P_{NiiA}:IreA respectively. WT does not display an overall significant difference between control and DTT treated samples but has a significantly higher level at 30 min (p=<0.05) ΔhacA displays an overall significant difference between conditions (p=<0.05). hacA Δintron shows significant differences of bipA levels between conditions (p=<0.0001). P_{NiiA}:ireA shows no overall significant difference in bipA (p=0.058) although 30 min levels are significantly higher (p=<0.05). E compares initial transcript level comparative to WT, both ΔhacA and P_{NiiA}:ireA have significantly higher initial bipA levels (p=<0.05). Significance levels * {<0.05} ** {<0.01} *** {<0.0001}. N=3.

Fig 3.6 A shows the WT has a steady increase in *bipA* transcript after DTT treatment, resulting in a significantly higher level at 30 min, where levels are >90% higher than in the untreated control. The WT control shows variation over the time course but with lower levels at 30 min compared to the initial level (p=<0.05). The observed induction of *bipA* is indicative of the ER stress response. Fig 3.6 B shows that the *ΔhacA* strain also induces *bipA* transcription under DTT treatment with a significant difference at 30 min (p=<0.05). The control shows a steady decrease in *bipA* levels although there was a lot of variation between replicates. Fig 3.6 E suggests higher levels of *bipA* in the *ΔhacA* strain under control conditions but this was not supported statistically. The *hacA Δintron* strain shows significant induction of *bipA* from 10 min DTT treatment onwards with the most significant increase at 30 min (>90%) (p=<0.0001 at 30 min). Initial levels of *bipA* in *hacA Δintron* again appear higher than the WT but are not significantly. These data indicate that while *bipA* is induced under ER stress conditions the transcriptional upregulation observed is not dependent on HACA. The P_{NiiA}*:ireA* mutant also showed induction of *bipA* after DTT treatment which is statistically significant at the 30 min time point (p=<0.05) (Fig 3.6 D). However, the P_{NiiA}*:ireA* strain differs from the WT and other mutants, as *bipA* transcript levels fell after 20 min. Despite this drop in *bipA* levels at 30 min during DTT treatment, this time point is significantly higher than the corresponding untreated control (p=<0.05). Fig 3.6 E shows that at 0 min P_{NiiA}*:ireA* has 16x higher levels of *bipA* compared to WT (p=<0.0001). These data confirm that the ER stress response has been induced under the conditions tested and also confirm that not all transcripts are subject to RIDD. The 2-Way repeated measures Anova was selected to test for statistical significance as the data is parametric and I am examining a dependent variable (mRNA transcript level) between different conditions over a time course. The Bonferroni post hoc tests confirm differences where differences occurred between the treatments, i.e provides p-values for the same time point between conditions.

3.3.7. *hrdC*

As *bipA* expression is not dependant on HACA, I decided to examine another transcript induced under ER stress, the ERAD gene *hrdC. hrdC* encodes a putative orthologue of *S. cerevisiae hrd3*. Hrd3p is a membrane protein which forms a complex with Hrd1p and ERAD components and helps coordinate lumen to cytosol coordination of ERAD events (Gardner *et al.*, 2000). *hrdC* was shown to be 3.3-fold over expressed in the *A. niger hacA ΔintronA* equivalent as well as being significantly upregulated under DTT treatment in an *A. nidulans* study (Sims *et al.*, 2005). *hrdC* and other ERAD components have been examined as targets in several studies aiming to increase heterologous protein production in filamentous fungi (Carvalho *et al.*, 2012) making this a suitable target for examination.

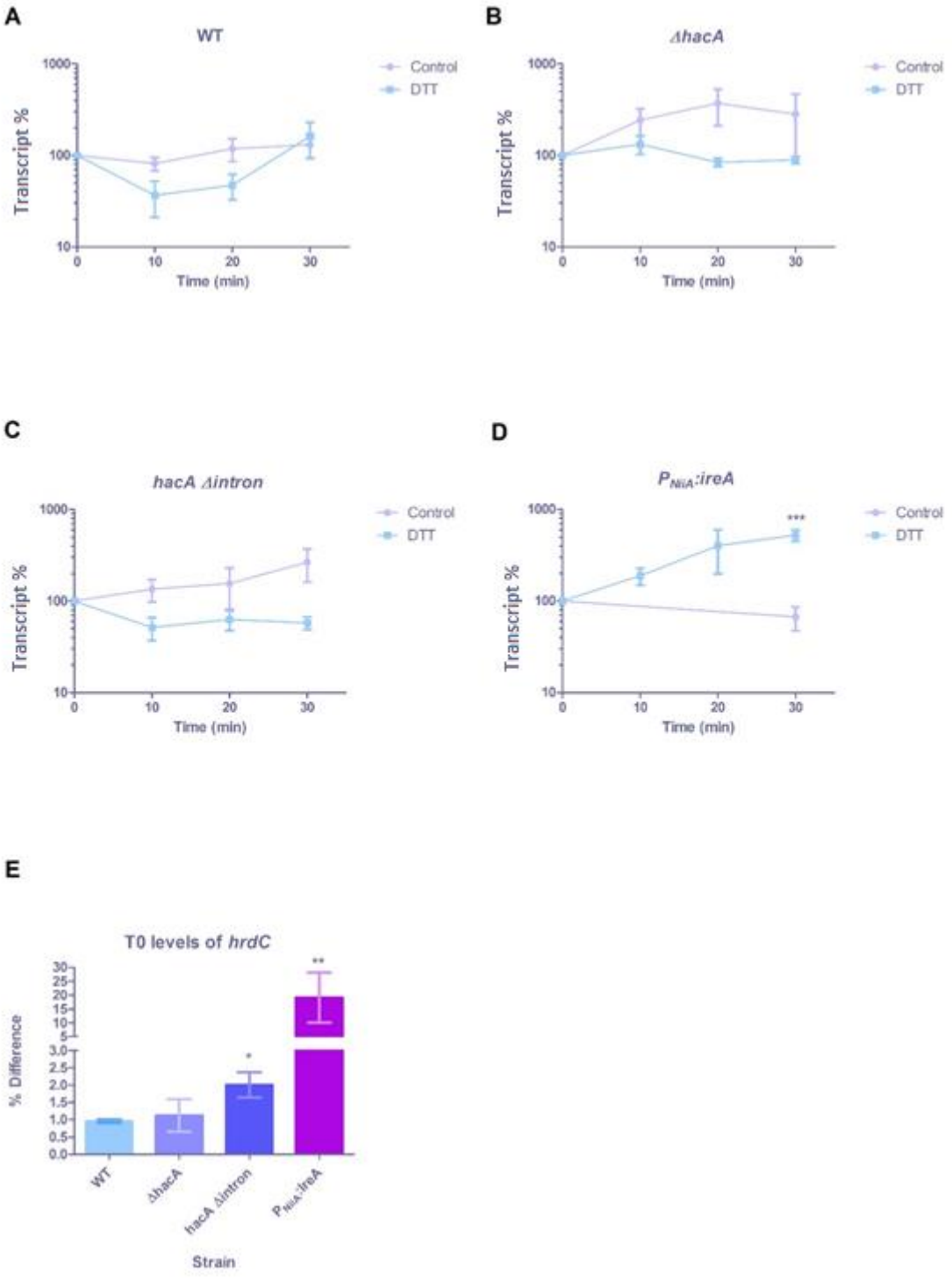

Figure 3 7 hrdC transcript levels under ER stress conditions. A-D show the response of hrdC transcript levels to DTT (20mM) treatment over a 30 min time course in WT, ΔhacA, hacA Δintron and P_{NiiA}:IreA strains, respectively. Transcript levels were determined by qRT PCR, using 18S rRNA to normalise data. T_0 is used as a starting reference for subsequent time points in A-D. T_0 is used as a starting reference for subsequent time points in A-D. A-D show the response of hrdC transcript levels to DTT (20mM) treatment over a 30 min time course in WT, ΔhacA, hacA Δintron and P_{NiiA}:IreA strains, respectively. WT, ΔhacA and hacA Δintron show no significant change in hrdC under DTT treatment. P_{NiiA}:ireA shows significant increase in hrdC transcript under DTT treatment at 30 min (p=<0.0001). E compares initial transcript level comparative to WT, hacA Δintron and P_{NiiA}:ireA both show significantly higher hrdC transcript levels. Significance levels *** {<0.0001}. N=3.

Fig 3.7 A shows WT levels of *hrdC* drop initially under DTT treatment at 10 min before rising gradually until 30 min where levels are slightly higher than the initial level. Control conditions remain stable throughout the time course. The results are not significantly different. *ΔhacA* shows no significant difference between conditions, see Fig 3.7 B. Fig 3.7 E shows that *ΔhacA* had slightly higher levels of *hrdC* although this varied between replicates and was not significantly different from WT 0 min levels. *hacA Δintron* shows a decrease in *hrdC* after DTT treatment and this level is maintained for the duration of the experiment. There is no significant difference between the control and DTT treated cells. Fig 3.7 E shows *hacA Δintron* has a 2x higher level of *hrdC* at 0 min compared to WT, this is statistically significant ($p=<0.05$) and shows similarity to the finding in of higher *hrdC* levels in an *A.niger hacA Δintron* mutant (Carvalho *et al.*, 2012). P_{NiiA}*:ireA* shows increased levels of *hrdC* after DTT treatment for all time points with a 4x increase observed by 30 min, see Fig 3.7 D. The increase observed is statistically significant ($p=<0.0001$). Fig 3.7 E shows that *hrdC* levels in the P_{NiiA}*:ireA* strain compared to WT are 20x higher than that of the WT at T0 although there was a large degree of variation between replicates ($p=<0.01$). The results indicate that HACA is not responsible for regulating *hrdC*. This is due to P_{NiiA}*:ireA* displaying significantly increased levels of *hrdC* at 0 mins which then rises dramatically after DTT addition. Without *ireA,* initiation of *hacA* splicing is not possible, therefore the strain should have similar or lower levels of *hrdC* to WT as observed in *ΔhacA*. This evidence as well as the *bipA* (Fig 3.6) results indicate a second regulator of transcription during ER stress.

3.3.8. *ireA*

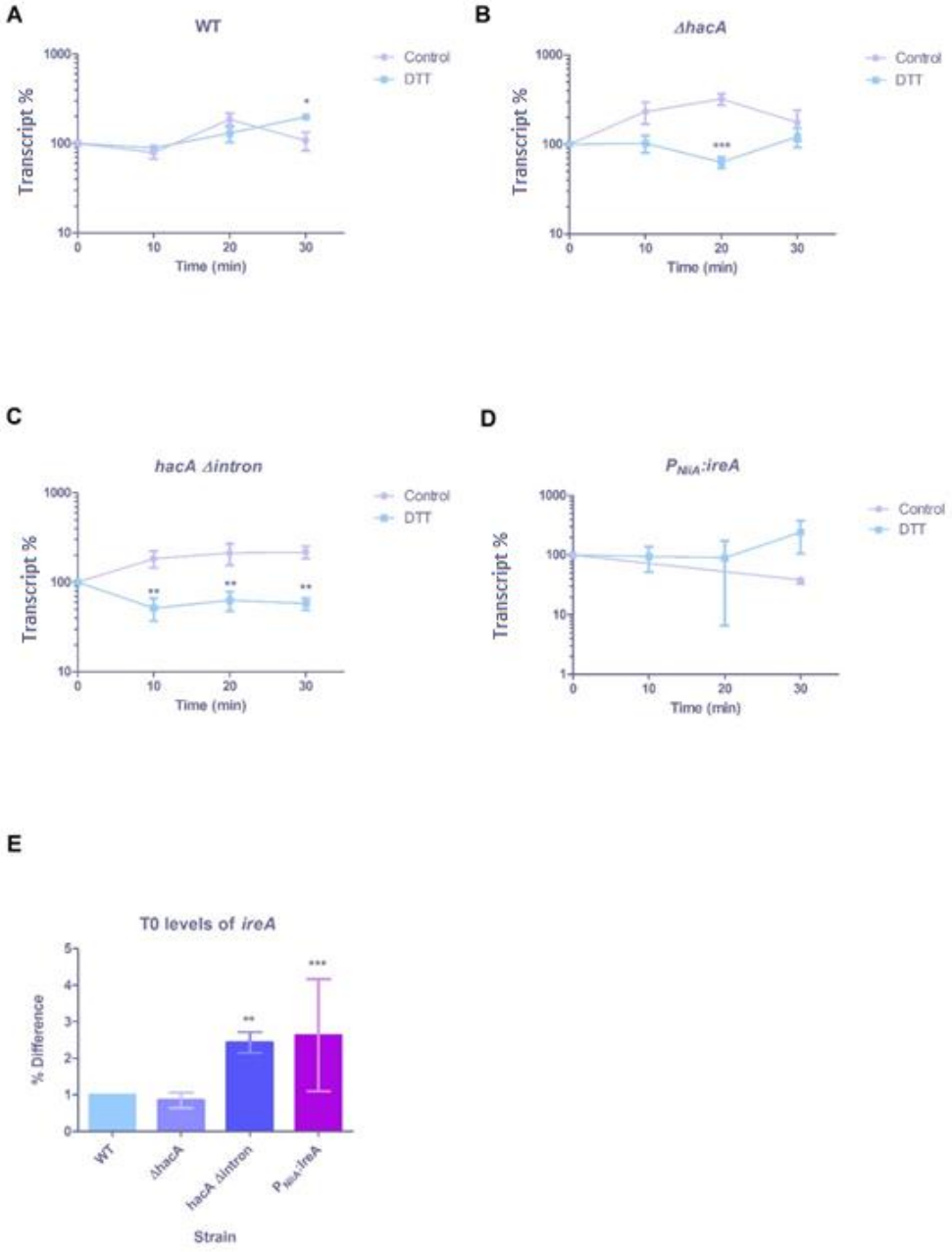

Figure 3 8 ireA transcript levels under ER stress conditions. A-D show the response of ireA transcript levels to DTT (20mM) treatment over a 30 min time course in WT, ΔhacA, hacA Δintron and P_{NiiA}:IreA strains, respectively. Transcript levels were determined by qRT PCR, using 18S rRNA to normalise data. T_0 is used as a starting reference for subsequent time points in A-D. A-D show ireA transcript levels under control and DTT (20mM) conditions from WT, ΔhacA, hacA Δintron and P_{NiiA}:ireA respectively. WT has a significant difference between conditions (p=<0.05) of ireA transcript level. The control condition shows fluctuation of ireA level whereas DTT treated cells showed a steady increase after a small initial decrease at 10 min. ΔhacA shows significance between conditions (p=<0.05). In ΔhacA control conditions there is a steady increase in ireA levels until 20 min wherein this drops by 30 min. hacA Δintron shows significant differences between conditions (p=<0.01). The control shows an initial increase which stays steady whereas the DTT treated cells display an initial 45% decrease which then remains steady. P_{NiiA}:ireA shows no significant difference between conditions. E compares initial transcript level comparative to WT, ΔhacA transcript levels are similar to WT and not significant. hacA Δintron and P_{NiiA}:ireA both display significantly higher levels of ireA. Significance levels * {<0.05} ** {<0.01} *** {<0.0001}. N=3.

Fig 3.8 shows *ireA* transcript levels under control and DTT treated conditions in WT. After DTT treatment *ireA* shows a negligible decrease at 10 min (>~5%). This is followed by a gradual increase leading to a final 200% higher level which is significantly different from control conditions at 30 mins (p=<0.05). From the WT I can see under control conditions that the transcript level varies over the 30 minute time period. Fig 3.8 B shows *ireA* levels within the *ΔhacA* strain initially decrease under DTT treatment leading to a significant difference from control conditions at 20 min (p=<0.0001). Transcript levels then return to control condition levels at 30 min. Fig 3.8 E shows that the *ΔhacA* strain has very similar levels of *ireA* to the WT. Fig 3.8 C shows that the *hacA Δintron* strain, like *ΔhacA*, has decreased levels of *ireA* after DTT treatment and the observed drop of ~40% is maintained throughout the time course. Control conditions for *hacA Δintron* show that at each time point there is a marginal increase of *ireA*, Fig 3.8 E shows that at 0 min the transcript level is 2.4x that of the WT (p=<0.01); this implies that HACA is responsible for upregulation of *ireA* under ER stress but not responsible for basal levels as evidenced by *ΔhacA's ireA* level. There is potential that *ireA* is subject to RIDD as processing of the nascent peptide occurs in the ER. If this is reflected in an increased level of IREA protein in *hacA Δintron* strain, it is presumably inactive without ER stress. However, upon DTT treatment IREA should be activated and this coincides with a drop of *ireA* transcript levels which remains steady. If *ireA* transcription is upregulated by HACA but also subject to RIDD, this could explain the initial drop in *ireA* levels which is then maintained during the time course rather than displaying the trends observed for *prtA* and *pepJ*. Fig 3.8 D shows *ireA* levels in the P_{NiiA}*:ireA* strain, under control conditions I can see the transcript has decreased over the 30 min time course. The DTT treated cells show a lot of variation between replicates but that there is a decrease in transcript at 20 min which appears to rise again by 30 min. However these results are not significantly different. Fig 3.8 E shows that P_{NiiA}*:ireA* has significantly different levels of the transcript compared to WT with an average 2.6x higher

level than the WT (p=<0.0001) though there is a very large degree of variation between the replicates. Initially this finding is very surprising given that the strain should have less *ireA* transcript. An explanation for the increased level of transcript would be due to the nitrogen starved conditions. The *NiiA* promotor is regulated by presence of exogenous NO_3^- and strongly suppressed by NH_4^+ (Caddick *et al.*, 2006). This time course was carried out under nitrogen starved conditions thereby removing suppression of *ireA* expression. Additionally, a key regulator of numerous nitrogen metabolism related genes, *areA*, is active under nitrogen limited conditions and *NiiA* is subject to *areA* regulation (Arst and Cove, 1973; Kudla *et al.*, 1990; Caddick, 2004) Therefore it is unsurprising that there is increased transcription of *ireA*, the creation of the mutant strain was performed without this time course in mind and was an unforeseen occurrence. This leads to a question of why there is reduced transcript degradation observed for this mutant as ER stress induced degradation was identified to be regulated by *ire1*/*ireA*. *ireA* being subject to RIDD would explain this findings; once repression was removed by transferring to nitrogen starved conditions, any IreA P_{NiiA}*:ireA* translated would presumably be activated as the strain prior to this point had no means of upregulating *hacA* or degrading transcripts. There is also the possibility the transcript measured is the antisense strand and thus not encoding *ireA*. As the P_{NiiA}*:ireA* strain's only mutation is in *ireA* promotor region and it displays little to no degradation of secreted transcripts, this study proposes *ireA* is performing RIDD during ER stress.

To try and identify if there any IREA was active in the P_{NiiA}*:ireA* strain I examined *hacA* splicing using RT PCR. Lack of the spliced form of *hacA*, when compared with WT, will indicate if there are similar levels of IREA in the P_{NiiA}*:ireA* strain.

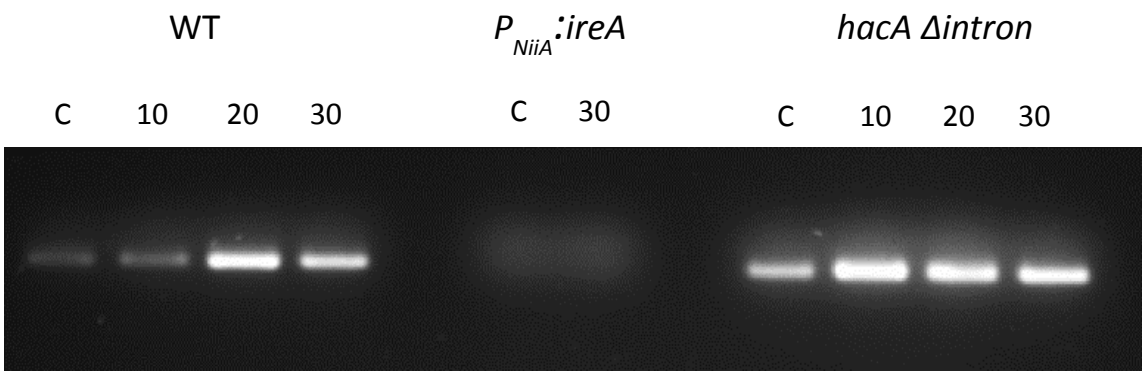

Figure 3 9 Gel image of *hacA* PCR products from primers amplifying the intron containing region from WT, P_{NiiA}:*ireA* and *hacA Δintron* cDNA. For WT and *hacA Δintron*, C – 30 indicate *hacA* from Control, DTT 10, 20 and 30 min treatment, spliced hacA is fully is present in each sample. P_{NiiA}:ireA displays *hacA* amplified from control and 30 min of 20mM DTT treated cells. There is no hacA amplified from the P_{NiiA}:ireA samples.

The results from Fig 3.9 show that during nitrogen starvation there is a low level of spliced *hacA* and this is increased in response to DTT treatment, indicating activation of the ERSR. It is worth noting that the nitrogen regime may itself affect splicing as *hac1* splicing in *S. cerevisiae* was repressed by nitrogen starvation whereas nitrogen addition to media was found to initiate *hac1* splicing (Schröder, Chang and Kaufman, 2000). *hacA Δintron* displays the expected results as the strain cannot produce the intron containing *hacA* transcript. P_{NiiA}*:ireA* appears to have lost the ability to splice the *hacA* transcript of both spliced and unspliced form; this strongly implies that *hacA* regulates its own transcription. Without *ireA* to activate the TF there is loss of the transcript altogether. *hacA* has been shown to upregulate its own expression in *A. niger* so this finding fits with the literature (H. J. Mulder. M, 2004).

Next I decided to confirm that the increased transcription of *ireA* within the P_{NiiA}*:ireA* strain is specific to this time course. To do this I performed a further experiment examining WT, *ΔhacA, hacA Δintron* and P_{NiiA}*:ireA* using MM supplemented with NH^{4+}. P_{NiiA}*:ireA* was grown overnight in MM supplemented with NO_3^- before being transferred to MM supplemented with NH_4^+ for 24 hrs.

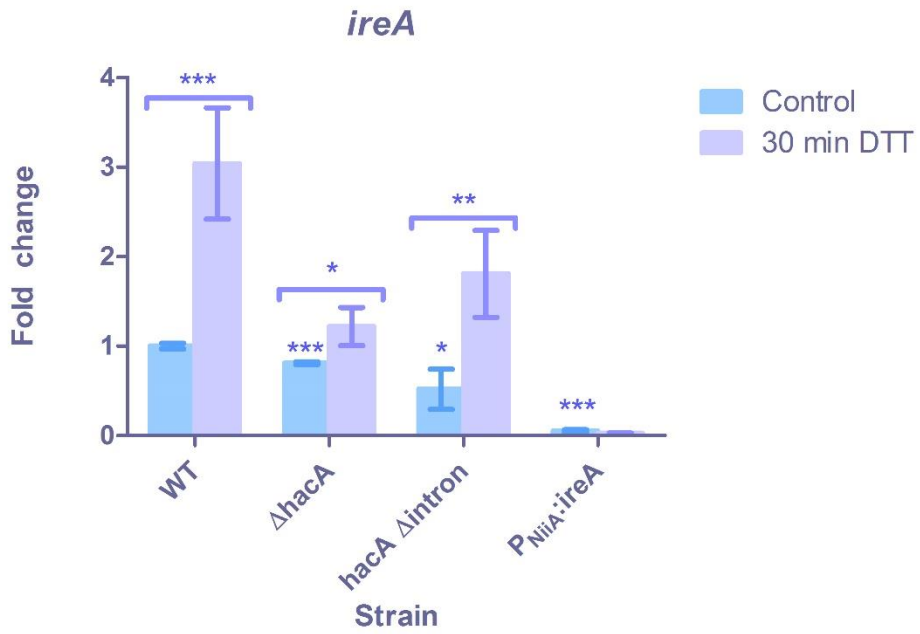

Figure 3.10 A comparison of *ireA* levels from WT, *ΔhacA*, *hacA Δintron* and P_{NiiA}:*ireA* under control and 30 min 20mM DTT treatment when grown on MM + NH^{4+}. WT, *ΔhacA* and *hacA Δintron* all exhibit significant increases in *ireA* after DTT treatment (p=<0.0001, 0.05 and 0.01 respectively) as determined by paired T-tests. *ΔhacA* and *hacA Δintron* have significantly lower levels of ireA under control conditions as determined by unpaired T-tests. P_{NiiA}:*ireA* has significantly lower ireA levels under control conditions at 5% of WT control levels, this does not show a significant change after DTT treatment. Significance determined by either Paired or Unpaired T-Tests. Significance levels * {<0.05} ** {<0.01} *** {<0.0001}. N=3.

Fig 3.10 shows WT displays a significant increase in *ireA* levels of 300% (p=<0.0001). *ΔhacA* shows a significant increase of 50% after DTT treatment although this is only slightly above WT control levels (p=<0.05). *hacA Δintron* shows an increase of *ireA* by 300% also. At both time points measured the *hacA Δintron* has 50% of WT levels of *ireA*. This is a different observation from Fig 3.8 where during the nitrogen starved control conditions *ireA* 2.6x higher than WT. P_{NiiA}:*ireA* has 5% of WT *ireA* levels which decreases after DTT addition although not significantly. *ΔhacA, hacA Δintron* and P_{NiiA}:*ireA* all display significantly lower levels of *ireA* under control conditions (p=< 0.0001, 0.05 and 0.0001 respectively). This is the expected observation for P_{NiiA}:*ireA* when in the presence of NH_4^+ and confirms that the large level of *ireA* observed during nitrogen starved conditions is due to loss of repression. Paired T-tests

were used for calculating the p-values between control and 30 mins of DTT treatment for each strain as these samples are related. Unpaired T-tests were used to calculate whether there was significant differences between the WT and mutant strain control values, this test was used as these are unrelated samples.

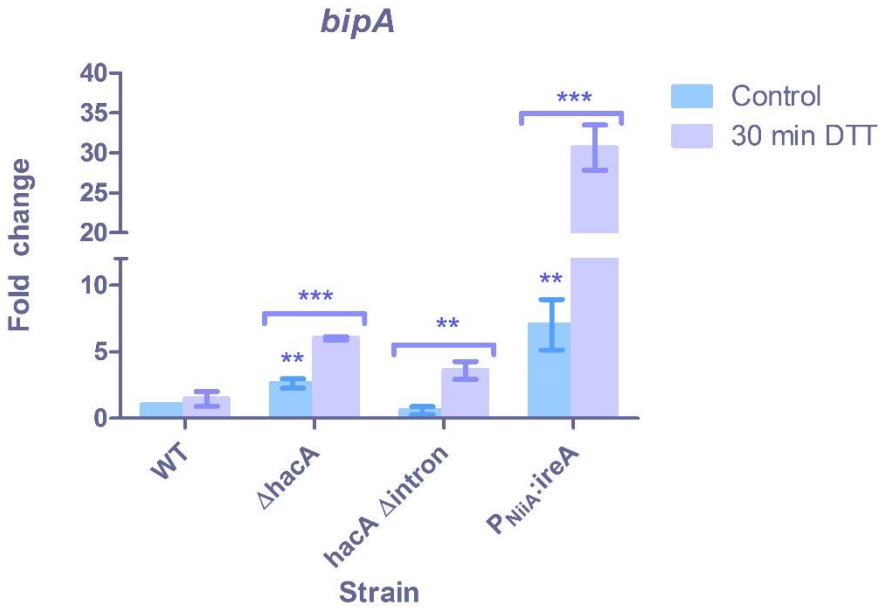

Figure 3.11 A comparison of *bipA* levels from WT, *ΔhacA*, *hacA Δintron* and P_{NiiA}*:ireA* under control and 30 min 20mM DTT treatment when grown on MM + NH^{4+}. WT shows a ~50% increase in bipA after DTT treatment which was not considered significant. ΔhacA and P_{NiiA}:ireA both have significantly higher levels of bipA under control conditions (~2.5 and 7 fold respectively) compared to WT (p=<0.01) and show significant increases after DTT treatment reaching 6 and 30 fold higher bipA levels (p=<0.0001). hacA Δintron displays slightly decreased levels of bipA under control conditions which significantly increases to 3.6 fold higher than WT control levels after DTT addition (p=<0.01). Significance determined by either Paired or Unpaired T-Tests. Significance levels ** {<0.01} *** {<0.0001}. N=3.

Fig 3.11 shows WT displays a 40% increase in *bipA* after DTT treatment, this contrasts the increase of 10x increase observed under nitrogen starvation for the same time period. *ΔhacA* initial levels were significantly higher than WT at 2.6x the level (p=<0.01) and showed a significant further increase of 2x after DTT treatment (p=<0.0001). *hacA Δintron* control levels were similar though slightly smaller than WT control levels and displayed a significant 7x increase after DTT treatment. P_{NiiA}*:ireA bipA* levels initially were 7x the WT (p=<0.01) and displayed a further significant increase to 15x WT DTT treated levels after DTT treatment (p=<0.0001). *ΔhacA, hacA Δintron* and P_{NiiA}*:ireA* all display higher levels of *bipA* in nitrogen

replete media than starved, indicative of an increased level of ER stress when supplemented with a sufficient nitrogen source. Nitrogen starvation induces autophagy, this compensates for the lack of extracellular nitrogen through turnover of cellular components to scavenge available nitrogen sources (Onodera and Ohsumi, 2005; Kohda *et al.*, 2007; Guiboileau *et al.*, 2012). The depletion of amino acids could explain the lower level of stress during nitrogen starvation, based on *bipA* induction, as there is less substrate available for protein synthesis. Paired T-tests were used for calculating the p-values between control and 30 mins of DTT treatment for each strain as these samples are related. Unpaired T-tests were used to calculate whether there was significant differences between the WT and mutant strain control values, this test was used as these are unrelated samples.

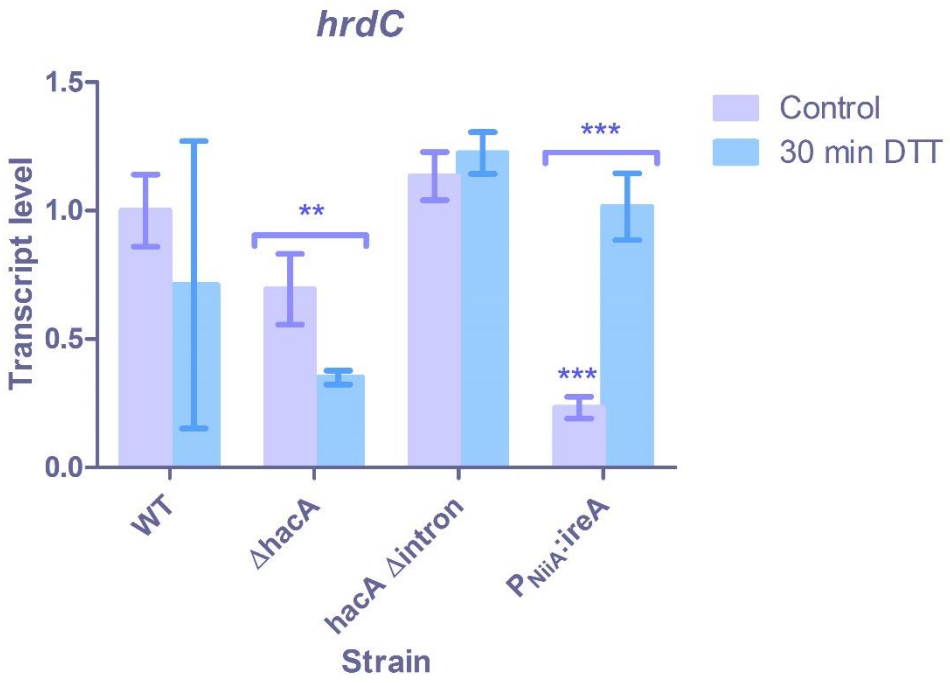

Figure 3.12 A comparison of *hrdC* levels from WT, *ΔhacA*, *hacA Δintron* and P_{NiiA}:*ireA* under control and 30 min 20mM DTT treatment when grown on MM + NH^{4+}. WT and *ΔhacA* display a drop in hrdC after DTT treatment although this was not significantly different for the WT. *hacA Δintron* displays similar levels to WT which shows a slight increase after DTT treatment. P_{NiiA}:*ireA* shows a significantly smaller level of *hrdC* under control conditions which increase significantly after DTT treatment. Significance determined by either Paired or Unpaired T-Tests. Significance levels * {<0.05} ** {<0.01} *** {<0.0001}. N=3.

Fig 3.12 WT shows a drop in *hrdC* levels after DTT treatment which was not considered significantly different by a paired T-test. *ΔhacA* also displays a decrease in *hrdC* after 30 min DTT treatment which was significant by an unpaired T-test (p =<0.01). *hacA Δintron* displays elevated levels of hrdC by 20% compared to WT. This was not considered significant. P_{NiiA}*:ireA* and *ΔhacA* have 75% and 25% of WT *hrdC* control levels respectively. This decreased *hrdC* level was significantly different for P_{NiiA}*:ireA*, this contrasts the findings from Fig 3.11 where it can be observed *bipA* transcript levels are very high. *hacA Δintron* displayed a non-significant increase in *hrdC* of ~9% after DTT treatment. Paired T-tests were used for calculating the p-values between control and 30 mins of DTT treatment for each strain as these samples are related. Unpaired T-tests were used to calculate whether there was significant differences between the WT and mutant strain control values, this test was used as these are unrelated samples.

3.4. Discussion

3.4.1. RIDD

From the data presented (Figs 3.3 and 3.4) I can see that WT, *ΔhacA* and *hacA Δintron* strains all show a significant loss of the transcripts encoding secreted proteases *pepJ* and *prtA* during ER stress. Importantly, I have confirmed that in the case of *prtA* the reduction in mRNA levels is primarily due to degradation as opposed to transcriptonal repression as it persists when transcription is blocked chemically (Fig 3.2). ERSR induction was confirmed utilising *bipA* as a marker (Fig 3.6). Additionally, *actA* transcript remained relatively unaltered by DTT treatment, consistent with the observed transcript degradation during ER stress being specific to those processed in the ER and not the cytosol (Fig 3.5). Further to this, P_{NiiA}*:ireA*, displayed

no significant loss of transcript. The lethality of a *ΔireA* strain in several *Aspergillus spp* indicate a secondary function to activation of HACA, particularly given the inability of a P_{NiiA}*:ireA hacA ΔintronA* strain to grow (Carvalho *et al.*, 2010; De Souza *et al.*, 2013; Tanaka, Shintani and Gomi, 2015). This essential function could potentially be its role in RIDD in *A. nidulans*. Based on the findings of this study I propose that RIDD occurs in *A. nidulans* and is likely to be present in other filamentous fungi. Whilst RESS has been shown in *A. niger* none of the studies combined transcriptional inhibition and ER stress induction to confirm loss of transcript was active degradation as opposed to down-regulation alone. The study by Al-Sheikh *et al* (2004) confirmed that loss of transcript was due to repression of transcription through nuclear run on assays. Nuclear run on assays examine transcripts through the isolation of the nuclei of cells and application of radioactive nucleotides. The nucleotides become incorporated into actively transcribed genes which can then be probed for on a blot (Gariglio, Bellard and Chambon, 1981). The presence of RIDD in *A. nidulans* leads to the question of whether or not this occurs in other *Aspergillus spp* as well. RESS does not rule out the presence of RIDD and vice versa, I would venture that filamentous fungi are capable of both. The dual process of RESS and RIDD, inhibiting new transcripts encoding secreted proteins as well as degrading those already present, would help to alleviate ER stress more rapidly than either alone.

3.4.2. The role of *hacA*

The *ΔhacA* strain has significantly lower levels of *prtA* and *pepJ* (Fig 3.1 and 3.2) despite the nitrogen deplete media inducing expression of these proteases in the wild type (Katz, Ricea and Cheetham, 1994). This poorly growing strain is likely to be subject to severe ER stress due to loss of the transcription factor which is known to regulate key component of the ER stress response. In the absence of HacA, RIDD still occurs, and this could be contributing to the lower levels of secreted transcripts. Given the loss of both *prtA* and *pepJ* transcripts after ER stress induction in the *ΔhacA* strain (Figs 3.3 and 3.4), I propose that this is due to transient RIDD,

or activation of a portion of the IreA present, impeding transcript levels rising to an unmanageable level. The controls lowered level of secreted transcripts implies that *hacA* does play a role in mediating ER stress which would fit with the literature.

From Figs 3.6 E, 3.7 E and 3.8 E I observe that during nitrogen starvation the *hacA ΔIintron* strain has significantly higher levels of *ireA* and *hrdC* but not *bipA*. Nitrogen replete media show *ireA* and *hrdC* are at similar levels to WT; this indicates nitrogen starvation elicits a different transcriptional response in the *hacA ΔIintron* strain. I can see from Fig 3.9 that WT exhibits only the fully spliced form of *hacA* during nitrogen starvation. The higher levels of *hrdC* and *ireA* in nitrogen starved *hacA ΔIintron*, are therefore an indirect response to growth with overexpression of *hacA* during nitrogen starvation and not a direct result of constitutive *hacA* expression. *bipA* regulation is not solely coordinated by *hacA*. This is clear due to the ER stress induced *bipA* transcription observed for *ΔhacA, hacA ΔIintron* and P_{NiiA}*:ireA*. From Fig 3.9 I can see complete loss of *hacA* transcript for P_{NiiA}*:ireA*, which is the same for *ΔhacA*, therefore any induction of *bipA* is elicited via a different means of transcriptional upregulation. This is confirmed by *hacA ΔIintron* exhibiting an increase in *bipA* after ER stress induction; presumably *bipA* levels would be constitutively higher regardless of ER stress due to the presence of only the translatable *hacA* transcript. HacA does not appear to be responsible for regulating *hrdC* either due to the increased expression in the P_{NiiA}*:ireA* strain. The only significant upregulation of the *hrdC* occurs in the P_{NiiA}*:ireA* strain (see Fig 3.12), this indicates that loss of both *ireA* and *hacA* leads to increased ER stress, as opposed to loss of *hacA* alone.

HacA independent *bipA* regulation has previously been proposed by a study in *A. niger* (Dave et al., 2006). The researchers showed increased *bipA* transcript levels in strains overproducing select membrane proteins, despite no splicing or truncation of *hacA* transcript. The authors suggested this may be evidence of another regulator of the fungal ERSR but highlighted the possibility that increased *bipA* levels could be due to increased transcript stability rather than

upregulation. Increased transcript stability was found to occur in *S. cerevisiae* for several ERSR target genes including *sec61* and *bipA*/*kar2* during ER stress (Hyde et al., 2002). This may account for the increased *bipA* in the Dave *et al.*, study. Another study in *S. cerevisiae* identified a hac1p-independent transcriptional response by regulating *hac1* expression with an inducible promoter. In this study they were able to induce ER stress via DTT/tunicamycin whilst inhibiting *hac1* expression. Comparison of ER stressed cells both producing and repressing *hac1* identified genes which were upregulated during ER stress independent of hac1p (Pincus et al., 2014). I examined the supplementary data which showed that *bipA*/*kar2* is found at higher levels during ER stress independent of hac1p. Whilst *bipA*/*kar2* have been confirmed at higher transcript number in a hac1p/HacA independent manner, no study has identified if this is due to active transcription or improved transcript stability. The data in Fig 3.6 is the first identification of HacA independent *bipA* induction/increased stability in *A. nidulans*. This is important considerating there may be differences between the *Aspergillus spp* and their ERSR given the first identification of RIDD in *A. nidulans*.

3.4.3. Future work

Further analysis for degradation of secreted transcripts upregulated during different conditions would be beneficial to confirm that the apparent RIDD is not specific to nitrogen starved conditions. Examining amylolytic genes during growth exacerbating their induction could provide further confirmation of RIDD. Nuclear run on studies should also be carried out in *A. nidulans* under the conditions tested in Figs 3.3-3.9 to observe whether RESS is occurring in tandem. Confirming whether rates of *bipA* transcription, or its stability, is increased during ER stress could be achieved through Q-PCR analysis of the *ΔhacA* when exposed to DTT, DTT + proflavin and proflavin alone. Proflavin treatment alone would provide the *bipA* half-life while

DTT treatment alone would provide results as seen in Fig 3.6. Combining DTT and proflavin would indicate whether *bipA* is upregulated or simply stabilized – if upregulation is responsible then there would be no increase in transcription due to proflavin. *bipA* levels in this instance should stay steady or show normal transcript turnover. An increase in transcript stability would show *bipA* remaining steady or decreasing at a slower rate than proflavin treatment alone.

Growth of the P_{niiA}*:ireA* strain, prior to the nitrogen starvation time course, relied on growth with 4-PBA to achieve the sufficient biomass. It is clear from Figs 3.6, 3.7, 3.11 and 3.12 that the P_{niiA}*:ireA* strain underwent ER stress in response to induction via DTT treatment. These data imply any stress alleviation conveyed by 4-PBA is lost at the time of sampling. However, it would be prudent to conduct parallel experiments with the wild type to confirm that this pre-treatment does not affect the ERSR/RIDD directly.

Initial experiments suggest that in the P_{niiA}*:ireA* strain, the IreA is activity is disrupted under the conditions tested. However, preliminary data suggested that under the N-starvation conditions *ireA* transcription was restored but additionally *hacA* transcription is lost. The basis of these observations need to be tested. With respect to *ireA*, it may be that this was a not functional transcript, such as an antisense. It will be important to test this directly. Regarding *hacA* mRNA levels in P_{niiA}*:ireA*, it is possible that loss of *hacA* splicing due to the initial growth in the presence of NH_4^+ and the associated repression of *ireA* may have led to loss of the *hacA* transcription due to the absence of HacA and a subsequent inability to restore transcript levels and HacA. This should be tested further. Ideally a different regulatory system should be tested with respect to *ireA* expression, such as the Tet-on system, which has been used successfully in *Aspergillus spp* (Wanka *et al.*, 2016).

3.4.4. Conclusions

At this point in the study I propose previously unseen levels of complexity to the filamentous fungal ERSR. This is due to the presence of RIDD, but also the evidence of a potential second transcriptional pathway as indicated by *bipA* upregulation being independent of HacA. This is the second instance of this response being observed in an *Aspergillus* spp (Dave *et al.*, 2006). Despite there being no experimentally confirmed fungal homologue of *atf6* the findings indicate the potential of a second transcriptional branch to the fungal ERSR.

4. ERSR in *A. nidulans*

4.1. Introduction

Based on the ERSR targets *bipA* and *hrdC* levels from the control samples of P_{NiiA}*:ireA* being significantly elevated, the induction of *bipA* in both the *ΔhacA* and *hacA Δintron* strains (see Figs 3.6 and 3.11) during ER stress and the similar findings in *A. niger* (Dave *et al.,* 2006), I propose there is a second transcriptional pathway in *A. nidulans*. a*tf6* is the regulator of the second transcriptional branch to the ERSR in higher eukaryotes and during the majority of this study there was no known fungal homologue.

Based on the findings from Chapter 3 I had decided to try and identify a homologue of *atf6* in *A. nidulans*.

4.2. Results

To search for potential homologues of Atf6 in *A. nidulans* I first selected organisms known to possess functional orthologues. I selected *Homo sapiens*, *Mus musculus*, *Rattus norvegicus*, *Drosophila melanogaster* and *Caenorhabditis elegans* to identify the most conserved aspects of Atf6 across a range of organisms. I used the online tool MUSCLE (Multiple Sequence Comparison by Log Expression), which aligns sequences and Jalview, which allows for manipulation and better visualization of alignments.

The result of this alignment was identification of 46 conserved residues, with 15 and 17 residues clustered in two areas, indicated with red and purple arrows respectively (see Fig 4.1). The 15AA sequence corresponds to the bZIP domain of Atf6. I used this sequence in a p-blast, based on the assumption that if there were to be a homologue in *A. nidulans*, it would display similarity within the DNA binding domain. Blast is an online tool that allows for the

comparison of a sequence of nucleotides or AAs to determine similarity between DNA or protein sequences. A p-blast compares a submitted protein sequence with all others available. Results are returned with an "e-value" which refers to the number of hits one can expect to see by chance, the lower the e-value the more significant the result. I limited the p-blast analysis to *Aspergillus* spp (taxid: 5052). The results provided 33 hits but all below the e-value threshold 0.01.

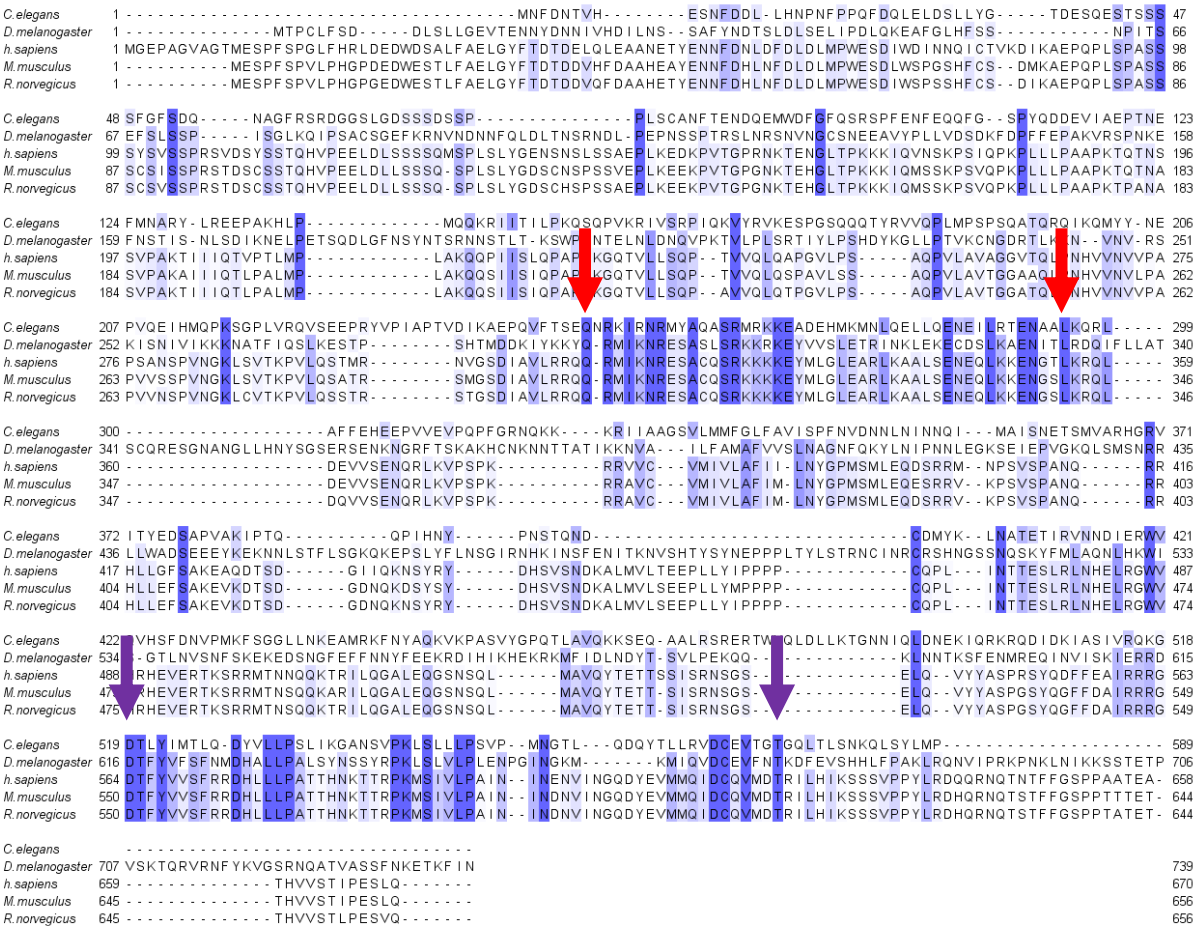

Figure 4 1 Alignment of ATF6 protein sequences. ATF6 sequences from *C. elegans*, *D. melanogastor*, *H. sapiens*, *M. musculus* and *R. norvegicus* were aligned using MUSCLE and presented in Jalview. The red arrows highlight a region of 12 conserved residues. The purple arrows highlight a region of 17 conserved residues.

Next, I ran the 17AA sequence identified in Fig 4.1 which yielded one result; *A. nidulans* gene AN5327. This is an uncharacterised protein, through gene ontology listed on the aspgd.org website it is purported to have GTPase activity and seemed an unlikely candidate. I expanded

the search parameters to include all fungal genomes (taxid: 4751) available. The results of this search led to identification of over 20 transcription factors which could potentially function in a similar role to Atf6. At this point in the project I was deciding what avenues of investigation I should take to try and identify targets to potentially increase RPP. I decided to look for other genes that may have a role in ER stress sensing and alleviation. As I had evidence of RIDD and a potential second transcriptional pathway in *A. nidulans*, I decided to look for genes that could potentially downregulate rates of translation (RT) in response to ER stress as is observed in higher eukaryotes. Due to the pressures on fungi as saprophytic organisms to secrete large volumes of protein and the filamentous fungal large surface area facilitating this, I hypothesised there could be a means of regulating RT during ER stress.

4.3. *perk* and the *eif2α* kinase family

As Perk is responsible for translational attenuation during ER stress and achieves this through the conserved mechanism of eIF2α phosphorylation, I examined the *A. nidulans* genome to identify candidates which may potentially undertake this role within the fungal ERSR. Four distinct eIF2α kinases have been identified in eukaryotic organisms: PERK, protein kinase double stranded RNA-dependent (PKR), heme-regulated inhibitor (HRI) and general non-repressible control 2 (Gcn2p). Attenuation of RT is mediated through phosphorylation of a highly conserved serine residue in eIF2α. Not only do all four kinases act upon the same residue but the amino acid sequence surrounding Ser51 is extremely conserved through the eukaryotic phyla (see Fig 4.2).

Figure 4.2 Amino acid sequence alignment of EIF2A kinase Serine 51 region from *A .thaliana*, *A. nidulans*, *D. melanogaster*, *H. sapiens*, *M. musculus*.

The four kinases each initiate translational attenuation under different conditions, with Perk acting in response to ER stress. PKR regulates translation when its N-terminal domain binds double stranded RNA which is an indicative of viral infection (Nanduri *et al.*, 1998; Weber *et al.*, 2006). Hri lowers translation in response to heme depletion while GCN2 is activated during AA starvation (Dong *et al.*, 2000; Uma, Yun and Matts, 2001). There is a large degree of homology between these four kinases; the coding sequence of HRI in rabbits for example shares such high levels of similarity with both yeast Gcn2p and human PKR that the authors of the study suggested Gcn2 acted as an eIF2α kinase before experimental confirmation (Chen *et al.*, 1991). Of the four kinases, fungal spp have homologues of HriA and Gcn2, which I will discuss.

4.3.1. *hri*

Heme-regulated inhibitor is key to cell survival through its regulation of heme levels. Heme is important for aspects of cellular health, such as respiration and O_2 transport. Cytochrome P450 is a key component of the electron transport system within mitochondria and contains heme, as does haemoglobin, which is an O_2 transporter (Klingenberg, 1958; Garfinkel, 2003). Regulation of heme is therefore critical to cellular energy homeostasis. The majority of literature on HRI is derived from mammalian work which identified the kinase is predominantly functional in developing erythroid cells, this is unsurprising given its role in O_2 transport (Crosby *et al.*, 1994; Han *et al.*, 2001). Recently HRI has been proposed as a target for cancer therapeutics due to its ability to induce apoptosis, achieved via the translational bias

implemented upon phosphorylation of eIF2α (see 1.3.3) (Burwick *et al.*, 2017; Yefidoff-Freedman *et al.*, 2017).

Interestingly, there is little work done within the fungal kingdom on *hri* with work primarily carried out within *S. pombe*. There is no homologue of *hri* in *S. cerevisiae* as eIF2α phosphorylation is entirely under Gcn2p control (Zaborske *et al.*, 2010). *S. pombe* has *hri* paralogues; *hri1* and *hri2*. Deletion of either *hri* loci was not lethal but reduced growth rate following heat shock, which was further reduced in the double null mutant. Interestingly, *Δhri1* led to slightly improved growth under control conditions. Arsenic stress inducing compounds produced similar results to heat shock with *Δhri1* mutant displaying the least inhibited growth whilst the *Δhri1Δhri2* double mutant was the most inhibited. Both kinases were found to be inhibited by hemin (the oxidized form of heme), which is the same finding for HRI in rabbit reticulocytes. (Zhan *et al.*, 2002). Subsequent studies in *S. pombe* identified Hri2p as being the primary kinase responsible for translational attenuation during heat shock (Berlanga *et al.*, 2010). In *A. nidulans*, an *hri* orthologue, *hriA*, has been identified. However, there are no publications for *Aspergillus* spp describing *hriA* except a study examining the *A. nidulans* kinome which found that *ΔhriA* is viable (De Souza *et al.*, 2013). The lack of research into *hriA* is surprising as there are several studies describing the effect of heme levels' on industrial peroxidase production (Conesa *et al.*, 2002; Conesa, Punt and Van Den Hondel, 2002; Franken *et al.*, 2011), where said peroxidases contained heme co-factors.

4.3.2. *gcn2*

gcn2 is extremely well studied throughout a range of eukaryotes including plants, yeast, mammalians and insects (Dever *et al.*, 1992; Olsen *et al.*, 1998; Berlanga, Santoyo and De Haro, 1999; Lageix *et al.*, 2008). Initially discovered in *S. cerevisiae*, *gcn2* regulates protein

synthesis and mediates selective translation of the *gcn4* transcript (homologous to *atf4/cpcA* in *H. sapiens*/*A. nidulans*, see 1.3.3) during AA starved conditions; this response was termed "general amino acid control" GAAC (Delforge, Messenguy and Wiame, 1975; Wolfner *et al.*, 1975; Hoffmann *et al.*, 2001; Li and Miller, 2015). Gcn4p initiates transcriptional upregulation of genes involved in AA biosynthesis, AA transport, autophagy, vitamin biosynthetic enzymes and peroxisomal compartments; fitting with the role of nutrient sensing as these responses free nitrogen metabolites and increase available AAs (Natarajan *et al.*, 2001). However, these gene targets only accounted for 25% of the upregulated genes in *S. cerevisiae,* indicating Gcn2p/Gcn4p are regulators of gene expression in response to stimuli other than nutrient sensing. A later study showed *gcn2/gcn4* were required for the upregulation of the majority of ERSR target genes (Patil, Li and Walter, 2004). The work of Travers *et al,*. (2000) identified 381 genes upregulated during ER stress, however these genes did not have the 7 nt ERSE sequence identified by Mori *et al.,* (1992, 1998). Patil *et al.,* identified a further two ERSE they termed ERSE-2 and ERSE-3 (with the first ERSE found being termed ERSE-1). All three ERSEs require both *gcn2*/*gcn4* for their upregulation during ER stress, in fact, loss of *gcn4* prevents hac1p induction of ERSR genes. These data are highly reminiscent of *perk/atf4* in higher eukaryotes and makes *gcn2* a likely protagonist in translational repression during ER stress, if identified in a fungal species.

As research into *gcn2* continued so did the kinase's role expand; *A. thaliana* for instance was shown to require *gcn2* in response to wounding (Lageix *et al.*, 2008). *gcn2* is crucial for survival during hypertonic stress and affects lifespan during dietary restriction in *C. elegans* (Choung-Hee Lee and Strange, 2012; Rousakis *et al.*, 2013). Roles for the kinase during development have been shown for both *D. melanogaster* and *M. musculus.* Loss of *gcn2* in *D. melanogaster* lead to inhibited growth during larval development whilst *M. musculus* displays heightened *gcn2* levels within oocytes (Alves *et al.*, 2009; Malzer *et al.*, 2013). A very

interesting finding, due to its overlap with PKR function, is that *gcn2* plays a role in regulating translation during viral infection. Disruption of *gcn2* led to increased levels of viral proteins in early days of infection by several viruses (Berlanga *et al.*, 2006). HIV-1 encodes a protein which cleaves Gcn2, dramatically lowering its kinase activity; the evolution of a viral protein which specifically cleaves a translational regulator indicates strongly a key role for GCN2 in fighting viral infection (del Pino *et al.*, 2012; Cosnefroy *et al.*, 2013). GCN2*'s* role has expanded so much that there are several reviews to cover the findings (Towle, 2007; Grallert and Boye, 2013; Castilho *et al.*, 2014). Further to these stimuli, yeast Gcn2p regulates the cell cycle after DNA damage and UV irradiation as well as being initiated during oxidative stress (Shenton *et al.*, 2006; Menacho-Marquez *et al.*, 2007; Tvegard *et al.*, 2007). What is very interesting about the majority of these stimuli is that they impact on the ER stress response (Komori *et al.*, 2012; Zhang and Wang, 2012; C. Han *et al.*, 2013; Crambert *et al.*, 2014; Wang, Yang and Zhang, 2016), taken together this strongly implies that the *gcn2* orthologue, AN2246, will have a complex regulatory role in the *A. nidulans*, that this may extend to ERSR and may prove to be a target for increasing RPP.

4.4. Discussion

Whilst writing up this research I carried out more bioinformatics work - I had decided that, given the continually increasing availability of genomic data, there may be suitable matches. I re-blasted the entire 64AA bZIP domain of *H. sapien* Atf6 I had retrieved from the Uniprot website. This yielded the maximum results, one that was particularly interesting and showed 46% similarity was termed Cyclic AMP-dependent transcription factor *Atf*-6 from *Smittium culicis*. Current computational methods allow for genomes to be annotated automatically based on sequence similarity with characterised genes from other organisms. It is likely *Atf*-6 of *S. culicis* was attributed during such a process and not investigated as this would be the first known homologue in a fungal system. Unfortunately there is no publication or information

available regarding confirmation of *atf6* functionality in *S. culicis*. Subsequent attempts to access the GenBank assembly (GCA_001970855.1) has been met with an error message advising it is unavailable. Nevertheless, I used the full protein sequence of *S. culicis* ATF-6 to blast the genomes of all *Aspergillus* spp. The best hits were all annotated as *hacA* within various *Aspergillus* spp. I next ran the blast again limiting the analysis to *A. nidulans*. Five results returned with *hacA* accounting for four of these due to re-annotations of the *A. nidulans* genome creating multiple entries. The additional hit was another TF listed as activating transcription factor A (AtfA). AtfA was one of the over 20 I had initially identified when deciding on the direction of this project. AtfA has been implicated as having a role in temperature and oxidative stress resistance in *A. nidulans* (Balázs *et al.*, 2010) as well as conidial germination and stress tolerance in *Aspergillus oryzae*. Another study examined *A. nidulans* when treated with farnosel, an isoprenoid that induces mitochondrial-associated apoptosis. *atfA* was found to inhibit the accumulation of *apoptosis-inducing factor* (*Aif*)-like mitochondrial oxidoreductase which is involved in mitochondrial associated apoptosis (Savoldi *et al.*, 2008; Sakamoto *et al.*, 2009). Studies have shown there is a relationship between the mitochondria and the ERSR during ERSR induced apoptosis (Nutt *et al.*, 2002). Research in human cell lines has shown that farnesol induces apoptosis via ERSR activation (Joo *et al.*, 2007; Hyuck *et al.*, 2015). Another very recent study in *A. nidulans* found *atfA* regulates transduction of stress signals. The study examined a variety of oxidative stress inducing compounds and not the ERSR specifically but it was found that a *ΔatfA* mutant had decreased vesicular transport in response to the stressors tested (Orosz *et al.*, 2017). Oxidative stress and the ERSR cross talk is well established and has been reviewed several times (Wang, Yang and Zhang, 2016; Chong, Shastri and Eri, 2017). Therefore, in addition to showing homology to *atf6*, it is probable that *atfA* plays a similar functional role in *A. nidulans.* Unfortunately the annotation of *S. culicis* Atf6,

followed by the interesting findings from Orosz *et al.,* occurred during the final year of my research and I had already taken a different course of investigation.

My decision to investigate the possibility that RT were attenuated during ER stress was partly due to the compelling data on *gcn2*/*gcn4* by Patil *et al.,* (2004), but also *gcn2's* reported activation under numerous ERSR associated stimuli in other organisms (Komori *et al.,* 2012; Zhang and Wang, 2012; C. Han *et al.*, 2013; Crambert *et al.*, 2014; Wang, Yang and Zhang, 2016). Also, Professor Caddick's lab was well versed to carry out polysome profiling which can be used to observe translational rates (Molon et al., 2016) and I wished to expand my skill set with new techniques. I decided to investigate *hriA* alongside *gcn2*, as its role is unexplored in filamentous fungi and these represent the only likely *eif2α* kinases in *A. nidulans*.

5. Translational attenuation during ER stress

5.1. Introduction

Several studies have shown yeast amd filamentous fungi undergo alterations to the translatome during ER stress. Firstly, a study found after treating *S. cerevisiae* to DTT (2mM for 1 hour) there is a marked difference in the translatome. Whilst DTT is well established at illiciting the ERSR via *ire1*/*hac1* in regards to transcriptome regulation this study examined the translatome. The authors showed that 363 genes were translationally upregulated whereas 140 were downregulated. Translationally upregulated genes included *hac1* and *der1* as well as other ERSR gene targets. Downregulated genes included those involved in ribosome synthesis and assembly (Payne et al., 2008). Inhibiting ribosome biogenesis whilst biasing translation to ERSR targets help cells to alleviate ER stress through effective use of the translational machinery. The ability to bias ribosomes to translate specific transcripts in response to ER stress is reminiscent of *perk*/*atf4's* regulation over the translatome in higher eukaryotes. Both *A. fumigatus* and *A. niger* undergo significant alterations to their translatomes (Guillemette *et al.*, 2007; 2008; Krishnan *et al.*, 2014). In *A. niger*, a similar response to that of *S. cerevisiae* was observed; ribosomal machinery was translationally downregulated in response to ER stress whereas ERSR targets were upregulated. This study represents the first instance of translational regulation in response to ER stress in a filamentous fungi (Guillemette *et al.*, 2007). Contrary to the findings in *S. cerevisiae* and *A. niger*, in *A. fumigatus* ER stress displayed limited alterations to the secretory pathway translatome – distinct from the secretory pathway transcriptome which is upregulated during ER stress. Instead, *A. fumigatus* was found to increase translation of transcripts encoding translational machinery and maintain translation rates of ERSR targets; this is the reverse of observations in *S. cerevisiae* and *A. niger* and highlights the differences within *Aspergillus* spp and their ERSRs (Krishnan *et al.*, 2014). The

author did note that there was no observed shift in RT under the conditions examined (1 mM DTT for 1 hour and 10 μg/ml tunicamycin for 1 hour). Attenuation of RT is a key feature of the higher eukaryotic translational pathway. Given the newly indicated RIDD in *A. nidulans*, I wished to see if there were other aspects of the higher eukaryotic ERSR present. Translatome alteration during ER stress is established in fungi yet altering the RT to help mitigate ER stress is not. Identification of any regulation over RT during ER stress could prove a potent target to increase RPP.

To examine ER stress and its potential effect on RT, I utilised sucrose density centrifugation to examine the effect of DTT treatment on the polysome profile. Polysome profiling separates mRNA by the level of bound ribosomes, through the use of a sucrose gradient. Transcripts associated with numerous ribosomes, termed "polysomes" sediment at higher sucrose concentrations whilst transcripts with single or ribosomal subunit association remain in the lower sucrose concentration (Chassé *et al.*, 2016). UV measurement of the gradient generates a "polysome profile", alterations of the profile indicate changes in rates of translation. This technique is widely used and allows for further mRNA interrogation by fractioning the gradient into distinct pools (Coudert, Adjibade and Mazroui, 2014; Gandin *et al.*, 2014; King and Gerber, 2016). As in Chapter 3, I used DTT at 20mM as it was shown to induce degradation of transcripts encoding secreted proteins, which is consistent with RIDD observed in other organisms (Kimmig *et al.*, 2012; Bright *et al.*, 2015; Guydosh *et al.*, 2017). I hypothesised that if ER stress leads to an alteration to the RT it would occur quickly, given the rapid transcriptional degradation response observed under these treatment conditions. The previously published studies in yeast and filamentous fungi did not identify regulation over the RT during ER stress (Guillemette *et al.*, 2007; Tom Payne *et al.*, 2008; Krishnan *et al.*, 2014). However, these studies examined the response after an extended time-period (>1h) and potentially this would not identify a rapid, transient response in global translation. The work by Travers

showed that the ERSR is essentially fully induced by 15 min after DTT exposure (Travers *et al*., 2000) in S. cerevisiae. I therefore decided to initially investigate the polysome profiles of strains within a 15-min time frame.

5.2. Results

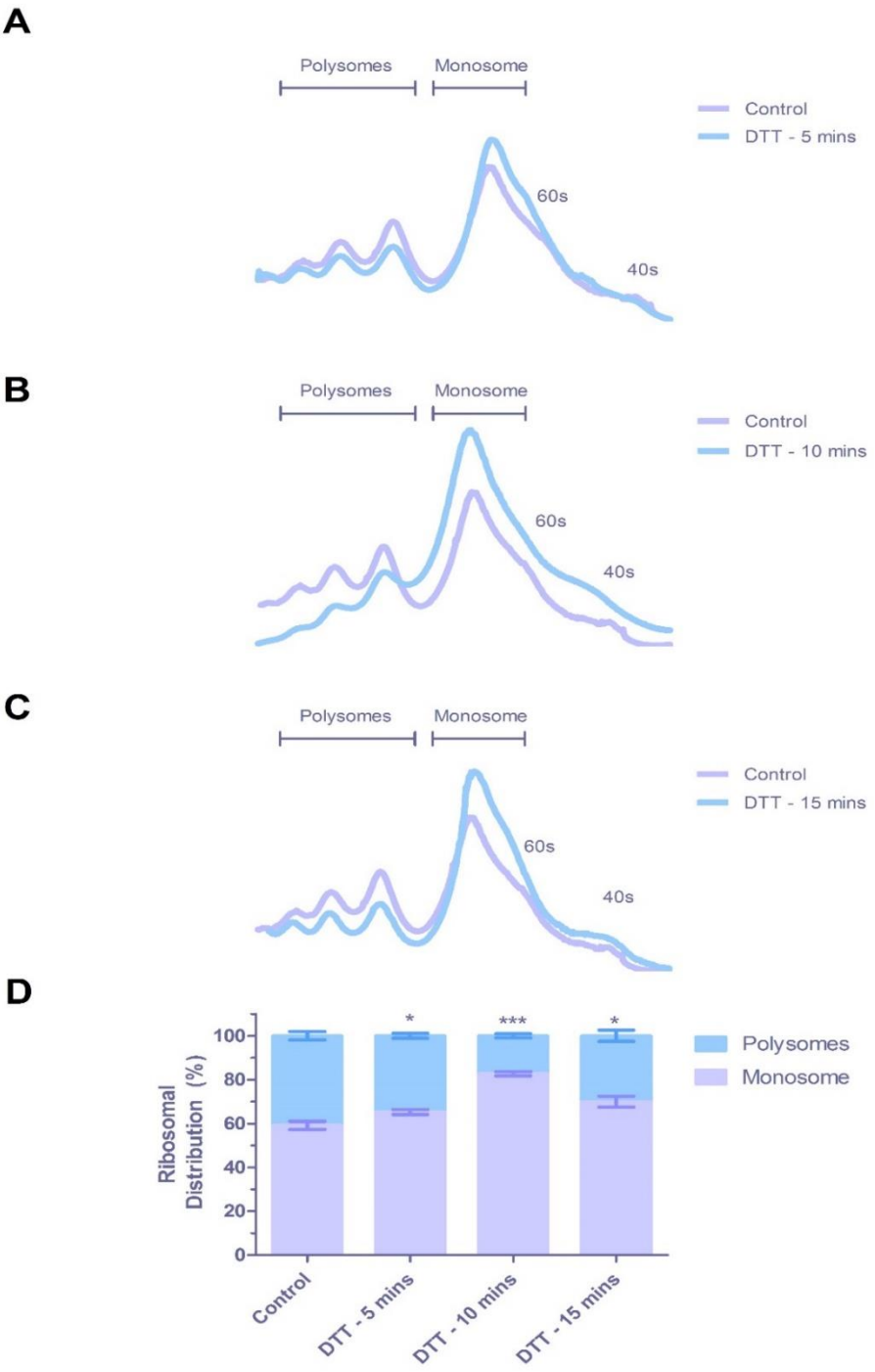

Figure 5 1 Polysome profiles of WT in response to 20mM DTT treatment. A-C show polysome profiles, obtained by sucrose density centrifugation, for the WT under control conditions compared to DTT treatment (20 mM) for 5, 10 and 15 min, respectively. D shows the percentage of polysome/monosome+subunit fractions for control and each of the DTT conditions. 5 min of DTT treatment leads to a 6% decrease in the polysome fractions compared to the control, 10 min of treatment shows a 22% decrease and at 15 minutes the polysome fraction was closer to the control level although still with 10% less polysomes. Each DTT treatment led to a significant reduction in the polysome fraction, with the most significant difference (p=<0.0001) observed 10 minutes after treatment. Significance was determined by unpaired T-Tests. Significance levels * {<0.05} ** {<0.01} *** {<0.0001}. N=3.

From Fig 5.1 A I can see that under control conditions the polysome profile can be clearly separated into distinct components, including the individual ribosome subunits (40 and 60S), the monosomes (80S) through to the polysome fraction, which extends from the disomes and trisomes. Based on triplicate experiments the proportion of the profile in the polysome fraction or the monosome and subunit fraction were quantified and are displayed in Fig 5.1 D. From these data for the untreated samples the polysomes account for ~40% of the total. At five min of DTT treatment I can see the polysome fraction has decreased slightly and that there is a corresponding increase in the monosome. This shift is significant ($p < 0.05$) and is consistent with findings in other eukaryotes of an ER stress associated shift in the translational profile (REFs). At 10 min this shift is much more obvious with a 22% reduction ($p > 0.0001$) in the polysome fraction with a corresponding increase in the monosome and ribosomal subunit fractions (Fig 5.1 B and D). This was the most dramatic shift was observed. At 15 min (Fig 5.1 C) there is a reduced but significant shift from the polysomes to the monosome fractions ($p >= 0.05$) compared to the control profile. Unpaired T-Tests were used as each sample was grown in its own flask so must be treated as separate during statistical analysis.

Analysis of the effect of DTT treatment on the polysome profile over the 15 min time-course shows that this translational shift is very transient, already being reversed between 10 and 15 min. This would account for why this has not been observed previously as studies utilizing a fungal system have not tested for this response in such a short time frame. In mammalians, the shift in the polysome profile from the polysomes to the monosome induced by DTT treatment begins to attenuate between 3-4 hours. However, it can still be observed 6 hours after ER stress induction (Kochetov and Montaner, 2012; Baird *et al.*, 2014). Interestingly, while the control shows little variation between replicates as shown by the standard error of the mean (SEM), this variation becomes even smaller after DTT treatment until 15 min where I see a return to

control conditions (control ± 1.87, $_{T5}$ ± 1.12, $_{T10}$ ± 0.97, and $_{T15}$ ± 2.49). This is evidence of an incredibly robust response to ER stress in filamentous fungi.

5.2.1. *hacA's* role in translational attenuation

I looked next at the effect of the transcription factor, HacA, on the DTT induced polysome shift by examining the mutants, *ΔhacA* and *hacA Δintron*. The mechanism of *perk* mediated *eif2α* phosphorylation is well established and reviewed; to date there is no known regulation of translation via the mammalian *hacA* homologue *xbp-1* (Pavitt and Ron, 2012; Liu *et al.*, 2015). However, as the *ireA*/*hacA* related pathway is currently the only known aspect of the ERSR in fungi, determining the effect, if any, the TF has on the observed translational regulation seemed prudent before examining the *eif2α* kinases.

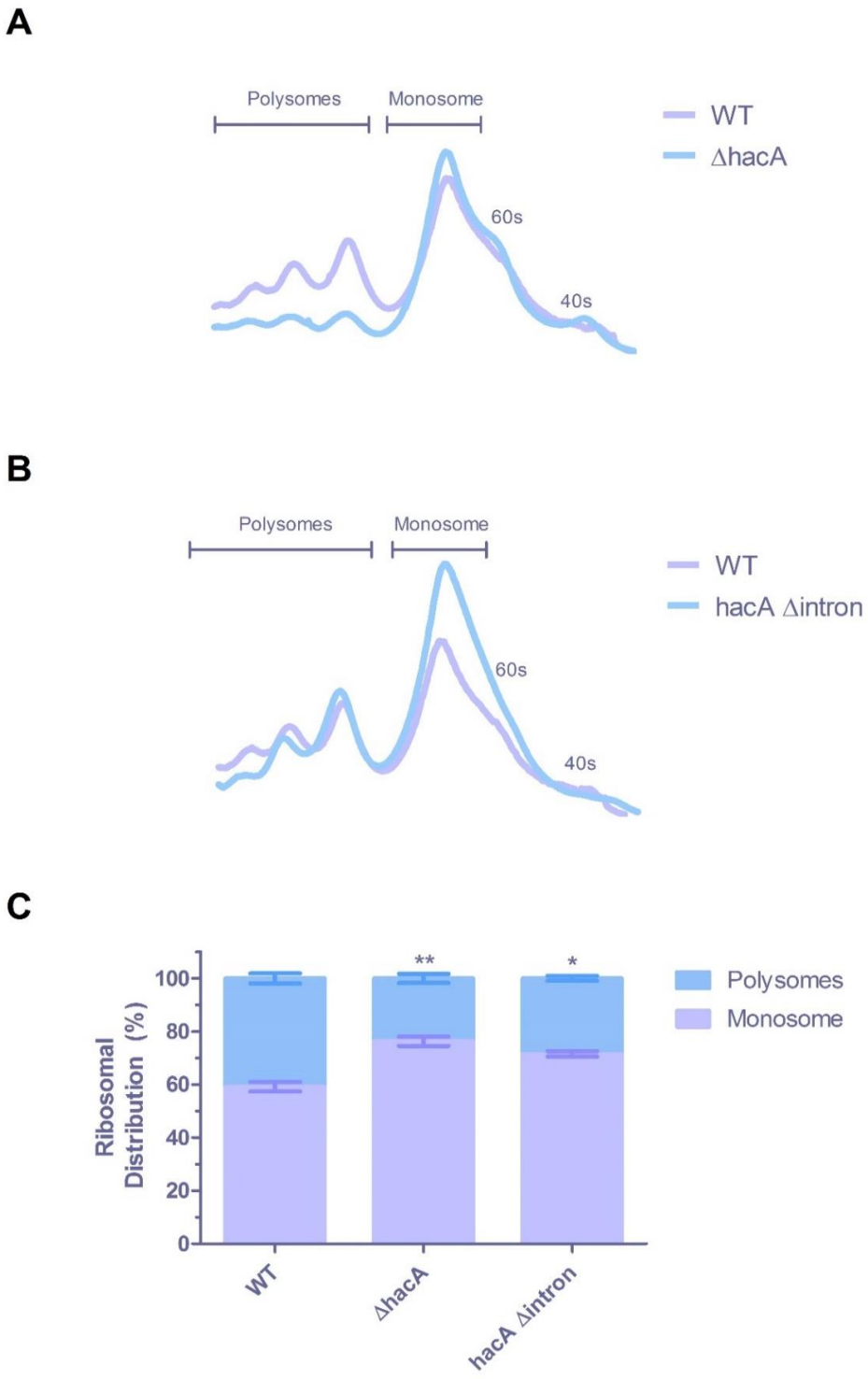

Figure 5 2 Comparison of WT and transcriptional mutants' polysome profiles under control conditions. A shows the WT and ΔhacA's polysome profile under control conditions. ΔhacA has lower and less well defined polysome peaks compared to WT and defined 60s and 40s peaks. B shows the WT control and the hacA Δintron control polysome profiles. hacA Δintron has clear peaks within the polysome region however these are lower and the monosome peak higher compared to the WT. Figure C shows a comparison of ribosomal distribution as a percentage for the two mutants and WT under control conditions. Both ΔhacA and hacA Δintron have significantly lower mRNA within the polysome fractions (p-values = <0.01 and <0.05 respectively as determined by unpaired T-Tests). Significance levels * {<0.05} ** {<0.01}. N=3.

Fig 5.2 A shows that under control conditions the *ΔhacA* strain has decreased polysome peaks which are poorly defined compared to the WT which account for ~24% and ~40% of the total respectively. The 60s and 40s peaks represent ribosomal subunits that are translationally inactive and are more apparent in *ΔhacA*. This implies that rates of translation are much lower within *ΔhacA* under normal conditions and possibly a factor for its abnormal phenotype (see Fig 6.1) and poor growth. The *ΔhacA* strain is likely to suffer from ER stress, due to its probable inability to upregulate ER stress target genes. As I have shown ER stress reduces RT in the WT, *ΔhacA's* unusual polysome profile under control conditions is likely due to initiation of this newly identified response. Fig 5.2 C shows *ΔhacA* polysome fractions are significantly smaller than the WT by ~17% ($p = <0.01$). Fig 5.2 B shows that the profiles of WT and *hacA Δintron* are similar in that there are clear polysomes and relatively less distinguished subunit peaks (compared to the profile of the *ΔhacA* strain for example, Fig 5.2 A). *hacA Δintron* has a larger monosome than the WT (monosome/subunits are 12% higher, $p = <0.05$, see Fig 5.2 B) but the profile implies there is a higher rate of translation compared to *ΔhacA* as there is little or no peak in the regions that corresponds to the inactive subunits. These data imply that loss of HACA leads a large degree of translational repression whereas its overexpression leads to a more moderate decrease in repression. HACA's role in translational repression in *hacA Δintron* is therefore indirect as complete loss of the TF shows the largest degree of repression. I next examined the ability of *ΔhacA* and *hacA Δintron* to initiate translational repression during DTT treatment. As DTT treatment for 10 min gave the most significant response in the WT, this time point was selected for these experiments.

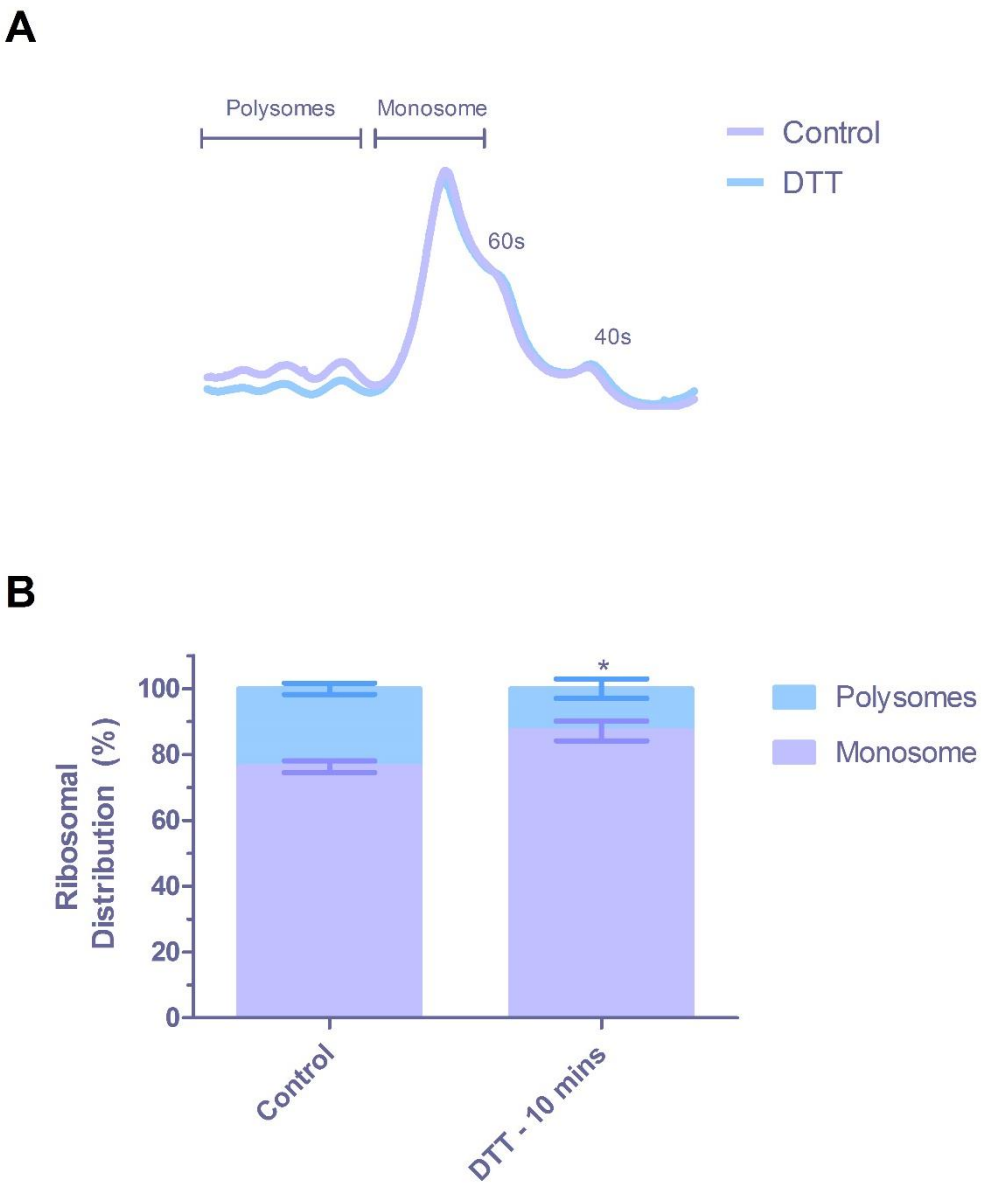

Figure 5 3 Polysome profile analysis of the ΔhacA strain's response to DTT treatement. A compares the polysome profiles of control and 10 min 20 mM DTT treated cells for ΔhacA. There is a relatively low level of polysomes in the control condition, a large monosome with very pronounced 60s and 40s subunits. DTT treatment led to a modest decrease in the polysome fractions. Both conditions show largely the same profile. B shows the ribosomal distribution when calculated as a percentage between the polysomes and ribosomes/subunits. The polysome fractions account for ~24% of the total in the control. DTT treated cells have a reduced polysome fraction, where they account for ~13% of the total. The difference is significant (p=<0.05) as determined by an unpaired T-Test. Significance levels * {<0.05} N=3.

Fig 5.3 show *ΔhacA* control and 10 min DTT treated polysome profiles. I can see there is a significant shift from the polysomes to the monosome/subunit fractions (p=<0.05). Polysomes

account for 24% under control conditions and 13% after DTT treatment. These data further imply that HacA is not required for the observed DTT induced translational shift.

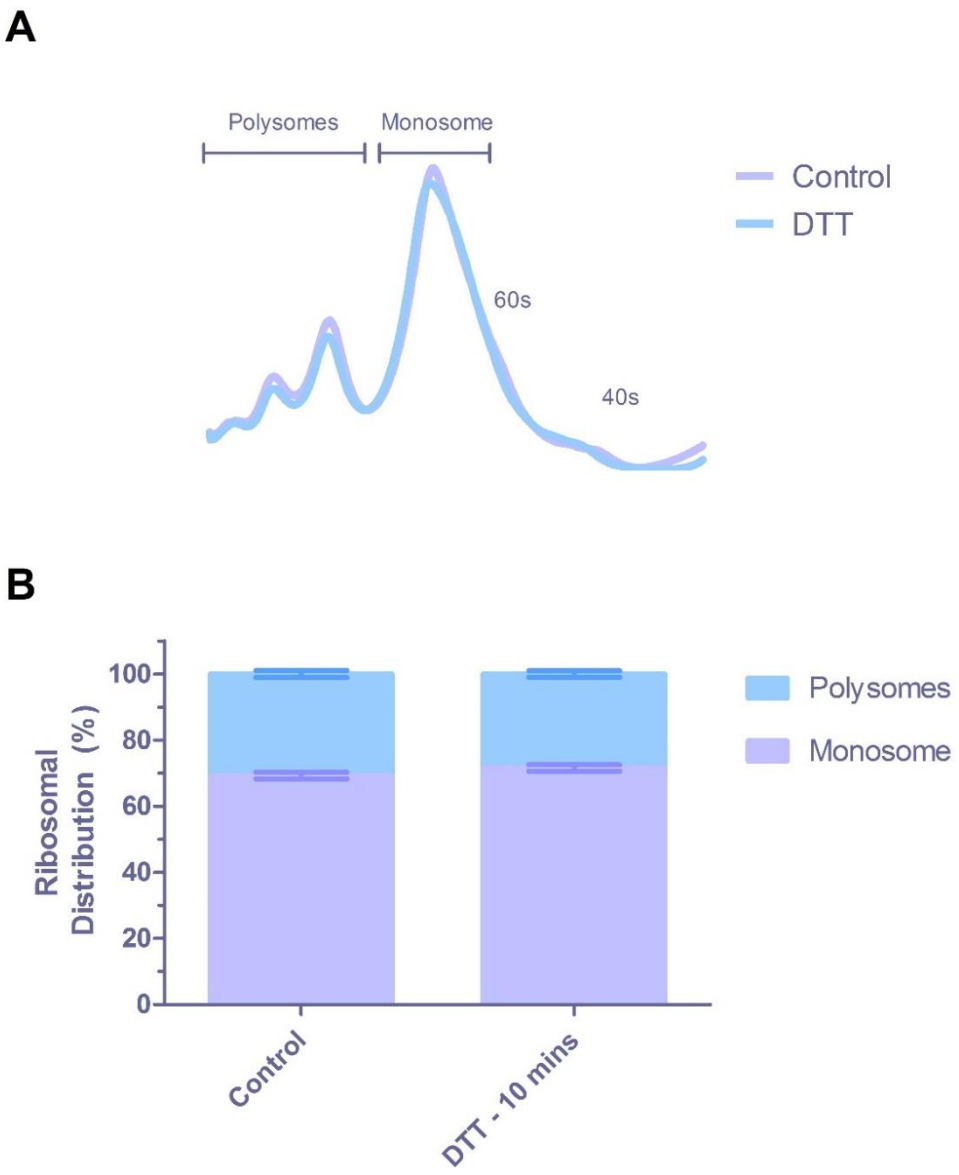

Figure 5.4 Polysome profile analysis of hacA Δintron strain's response to DTT treatment. A compares polysome profiles for control conditions and DTT treated cells from hacA Δintron. There is almost no observable difference between profiles as evidenced by A. B shows the ribosomal distribution when calculated as a percentage between the polysomes and ribosomes/subunits. B shows that there is a decrease in polysome size after DTT treatment of ~2.5%. This is not significantly different as determined by an unpaired T-Test. N=3.

From Fig 5.4 A I can see that there are clear polysomes present in the *hacA Δintron* strain and only small proportion associates with the 60s and 40s subunit fractions. After 10 minutes of

DTT treatment the profile as a whole remains largely unchanged. This is confirmed by Fig 5.4 B which highlights only a modest shift in ribosomal distribution of ~2.5% from polysomes to monosome and subunits. Based on other filamentous fungal systems the *hacA ⊿intron* strain is likely to constitutively express active HACA (Valkonen and Penttila, 2003; Valkonen *et al.*, 2003; Carvalho *et al.*, 2012). This is likely to result in increased levels of ER chaperones and upregulation of other HACA targets, all of which potentially provide a better intracellular environment to deal with ER stress. The shift in translational profile may therefore be absent from this strain due to the buffer provided by the presence of relatively high levels of ER response proteins. Alternatively I know that in the WT this transient response has significantly diminished by 15 minutes, therefore it is possible that in the *hacA ⊿intron* strain at 10 minutes the response is completed and polysome profile returned to that of control conditions.

Whilst the *hacA ⊿intron* strain's polysome fraction is 12% lower than the WT, this does not account for the lack of a shift under DTT treatment as *⊿hacA* has even smaller polysome fractions but still exhibits a significant shift when stressed. The *hacA ⊿intron* strain appears to deal with ER stress more efficiently. This fits with the observations of transcript degradation, as *hacA ⊿intron* had marginally higher levels of both *prtA* and *pepJ* compared to WT and showed increasing transcripts at 30 mins (Fig 3.3 and 3.4)

I can also observe that HACA constitutive expression leads to less variation between the control and DTT treated replicates with SEM values of ± 1.02 and ± 0.99 respectively. This control SEM value is lower than that of the WT control SEM and almost equal to 10 min DTT treated samples SEM value. This implies that in the WT ERSR, induction is transient in nature, as there is more variability in control conditions where cells deal with their individual ER homeostasis compared to the unilateral stress induced via DTT treatment.

Whilst DTT is used in numerous studies examining the ERSR, I decided to confirm this decrease in RT occurred during ER specific stress which led to the use of tunicamycin. Tunicamycin is an antibiotic produced by *Streptomyces spp,* and acts as an of inhibitor of *N*-linked glycosylation via the inhibition of Guanosine-5'-triphosphate (GTP), the first and key regulator of N-glycan biosynthesis (see Fig 1.3) (Koizumi *et al.*, 1999). Due to this function it effectively inhibits glycosylated proteins attaining their correct conformation but does not alter existing proteins; this makes it a very specific ER stress inducer. Therefore, it is a widely used treatment for eukaryotic species to examine the ERSR (Welihinda, Tirasophon and Green, 1998; Shang, 2005; Wakasa *et al.*, 2011). Additionally, studies have shown that in *A. niger*, DTT treatment led to over 800 genes being upregulated compared to 38 for tunicamycin treatment, this highlights the more specific nature of tunicamycin induced stress (Guillemette *et al.*, 2007). For these reasons I selected tunicamycin to examine if it induced a shift in RT similar to that of DTT - this would be expected if the DTT induced response was a function of the ERSR.

5.2.2. Tunicamcyin

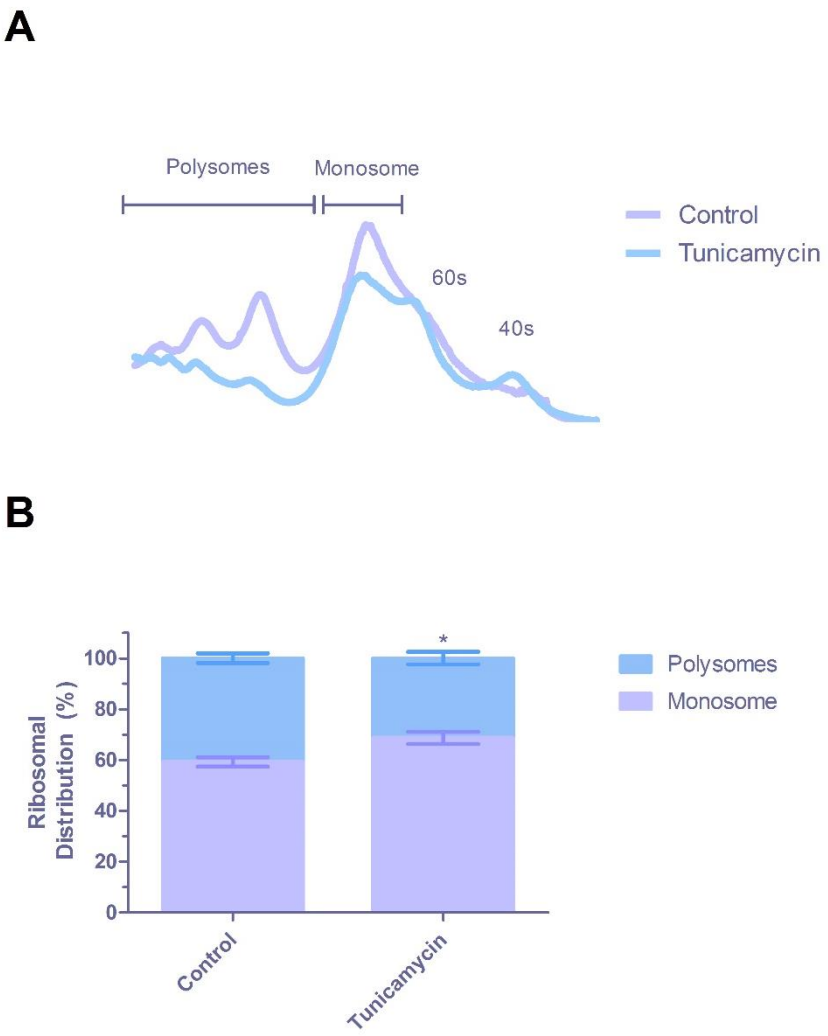

Figure 5 5 Polysome profile analysis of WT response to 1µg/µl tunicamycin treatment for 10 min. A compares polysome profiles for control conditions and after 10 min of 1µg/µl tunicamycin treatment in WT cells. There is a drop in the disome/trisomes particularly and a large increase in the subunit peaks after tunicamycin treatment compared to WT. B shows the ribosomal distribution when calculated as a percentage between the polysomes and ribosomes/subunits. B shows that there is a decrease in polysome size after tunicamycin treatment of from ~40% to ~31%. This is significantly different as determined by an unpaired T-Test. Significance levels * {<0.05}. N=3

Fig 5.5 A shows that tunicamycin treatment leads to very clear remodelling of the WT polysome profile compared to control conditions. A significant decrease (p=<0.05) of the polysome fractions is observed through a ~9% reduction. Interestingly, tunicamycin treatment led to very clear ribosomal subunit disassociation as evidenced by very large subunit peak appearance, this has not observed for the DTT treated cells. This is surprising as 10 min of DTT treatment reduced polysome fractions to 18% of the profile as opposed to tunicamycin's

31% (see Fig 5.1). Another interesting aspect of tunicamycin treatment is that whilst polysomes decreased overall this appears specific to the disome/trisome peaks. The initial polysomes peaks (representing the highest levels of translation) are still relatively high. This is confirmation of altered translational profiles during ER stress.

I wanted to investigate other stressors that *gcn2* has been attributed to translationally regulating. I next examined AA starvation, the first role attributed to *gcn2*. To test for decreased translation during AA starvation I used *3*-Amino-1,2,4-triazole (3-AT). 3-AT acts to induce synthetic AA starvation through disruption of the histidine biosynthetic pathway (Klopotowski and Wiater, 1965; Natarajan *et al.*, 2001). I added 3-AT to a concentration of 5mM and examined polysome profiles at 10 min.

5.2.3. Alternative stressors

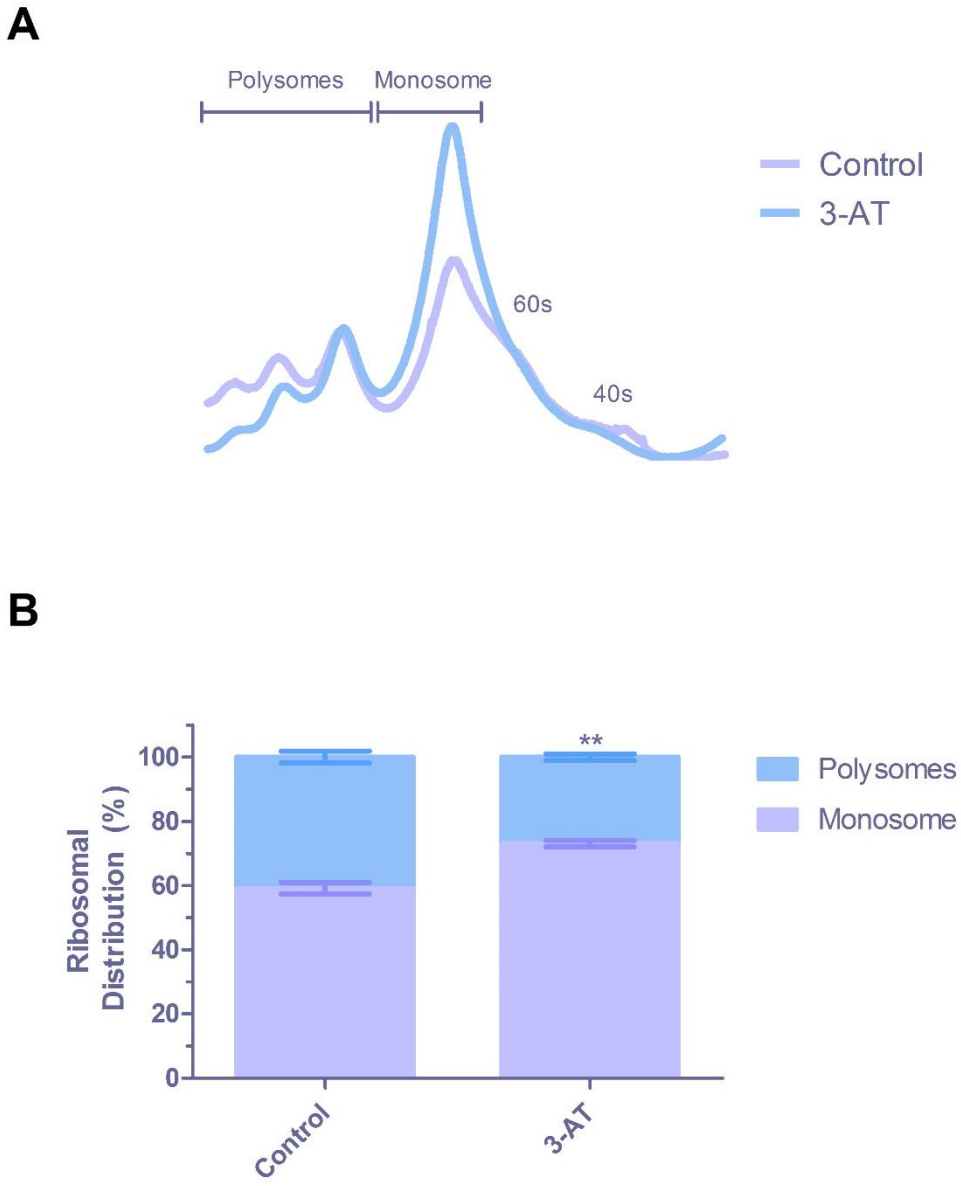

Figure 5.6 Comparison of 5mM 3-AT treatment and control conditions on polysome profiling for WT. A shows the polysome profile generated under control conditions against that of 10 min of 3-AT treatment in WT cells. The control shows the expected profile of defined polysomes, a large monosome followed by the appearance of 60s and 40s ribosomal subunits. The 3-AT treated cells show diminished polysomes excluding the disome. The monosome peak is very well defined and the peaks for the subunits have diminished. B shows ribosomal distribution as a % of total mRNA with separation of polysomes and monosomes/subunits. There is a decrease of polysomes from ~41% to ~27% after 3-AT treatment. The change is significant ($p<0.01$) as determined by an unpaired T-Test. Significance levels ** = {<0.01}. N=3

Fig 5.6 A compares the control and 5mM 3-AT treated WT polysome profiles. I can see that amino acid starvation induces a shift from the polysome fractions to the monosome/subunit fractions. There is a clear and sharp increase in the monosome peak at these conditions. The

subunit peaks lose definition at this time point implying increased use total ribosomes. I can see from Fig 5.6 B that this is a significant change ($p<0.01$) in ribosomal distribution compared to the control. The change in polysome size between control and 3-AT treatment is ~40% (SEM = ± 1.87) and ~27% (SEM = ± 1) respectively. The variation between replicates is also decreased after 3-AT treatment as shown for other treatments.

I examined oxidative stress next as *gcn2* has also been linked to translational attenuation under these conditions in other fungal *spp* (Morano, Grant and Moye-Rowley, 2012; Martin, Berlanga and de Haro, 2013). I tested the WT first to determine to what extent oxidative stress affects polysome profiles. Hydrogen peroxide (H_2O_2) at a final concentration of 5 mM for ten minutes was used to induce an oxidative stress response.

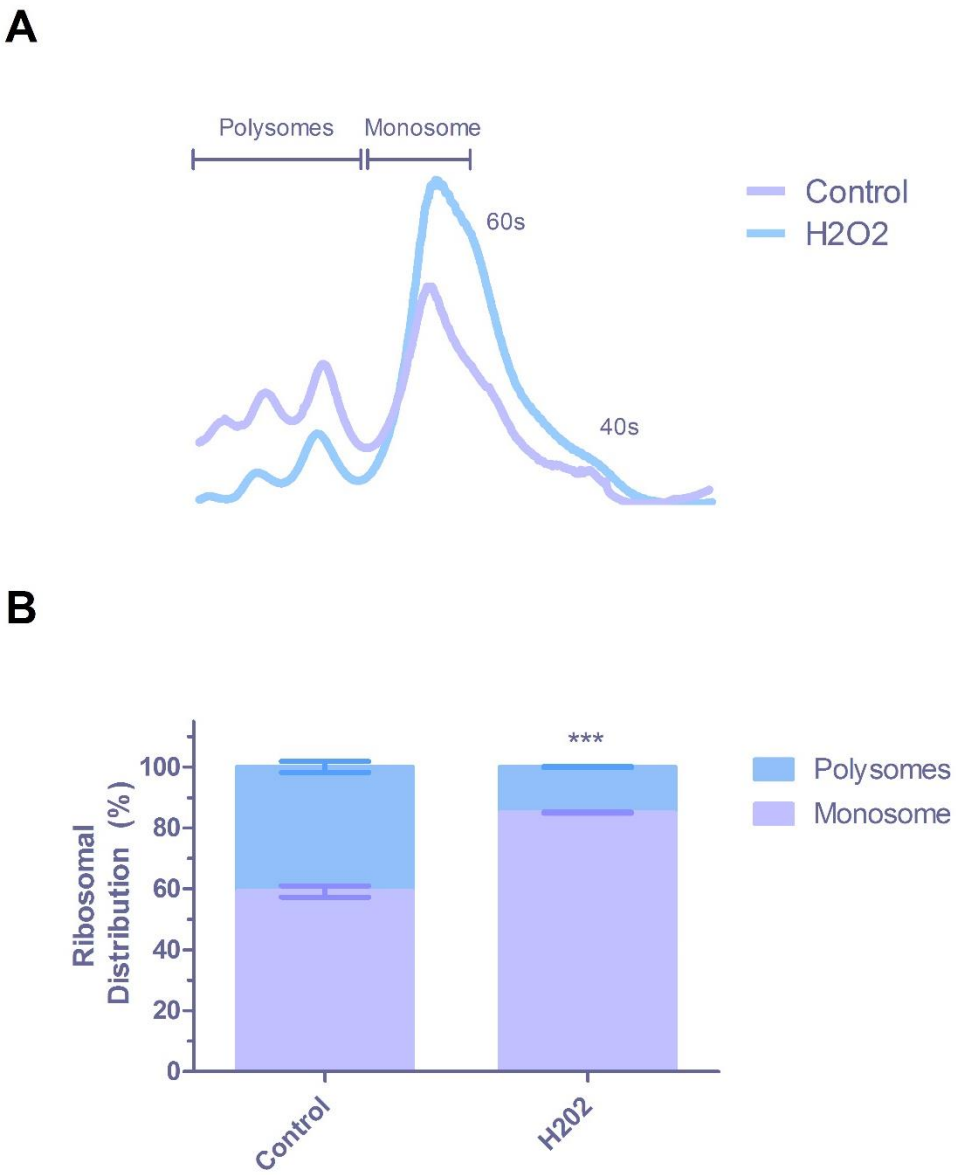

Figure 5.7 Comparison of 5mM H_2O_2 treatment and control conditions on polysome profiling for WT. A shows the polysome profiles for the control and 10 minutes of 5 mM H_2O_2 treated conditions for WT. The control shows well defined polysomes and a larger monosome followed by slight peaks for the ribosomal subunits 60s and 40s. The H_2O_2 treated cells have lowered polysomes and a larger monosome and an increased size of both the 60s and 40s subunits. B shows ribosomal distribution as a percentage of polysomes to monosome/subunits. Polysomes decrease from ~41% to ~15% in H_2O_2 treated cells. There is a significant difference between the conditions ($P<0.0001$) as determined by an unpaired T-Test. Significance levels *** {<0.0001}. N=3

Fig 5.7 A shows polysome profiles for both the control and H_20_2 treatment for WT cells. There is a clear shift from the polysome fractions to the monosome, which increased dramatically. There are also a much larger 60s and 40s peaks. These data show that there is an overall down regulation of translation as the monosome peak is significantly higher, there is also an increase in the level of disassociated ribosomes, both of which are indicative of translational repression.

From Fig 5.7 B I can observe the translational shift for oxidative stress is more extreme than the DTT treatment at 10 min (15% and 18% polysomes respectively, see Fig 5.1). After oxidative stress induction I can see again that the variation between replicates becomes smaller, ±1.87 and ± 0.14 respectively.

As *hriA* has been shown to regulate translation in response to heat shock in *S. pombe* I decided to examine the effects of heat shock to the *A. nidulans* polysome profile (Martin, Berlanga and de Haro, 2013). Interestingly, the heat shock response, which is the upregulation of specific chaperones in response to alterations in environmental temperature, has been shown in several studies to interact with the ERSR (Marcu *et al.*, 2002; Kennedy, Mnich and Samali, 2014). This relationship is obvious when considering the role of temperature on protein conformation and interactions. The finding that the heat shock response, oxidative stress response and the ERSR are related is less obvious but has been demonstrated in yeast (Hou *et al.*, 2014). If translational repression during heat shock occurs and *hriA* is responsible, it does lead to a question of whether the kinase has a role in dealing with ER stress, perhaps cooperatively or in concert with *gcn2* due to its role in the oxidative stress response (Hou *et al.*, 2014). WT was exposed to 5 min at 42^{O}C after growth at 37^{O}C to determine if this led to a change in translation. I already confirmed that growth at 30^{O}C led to significantly decreased polysome fractions ($p=<0.05$), see appendix 1. D.

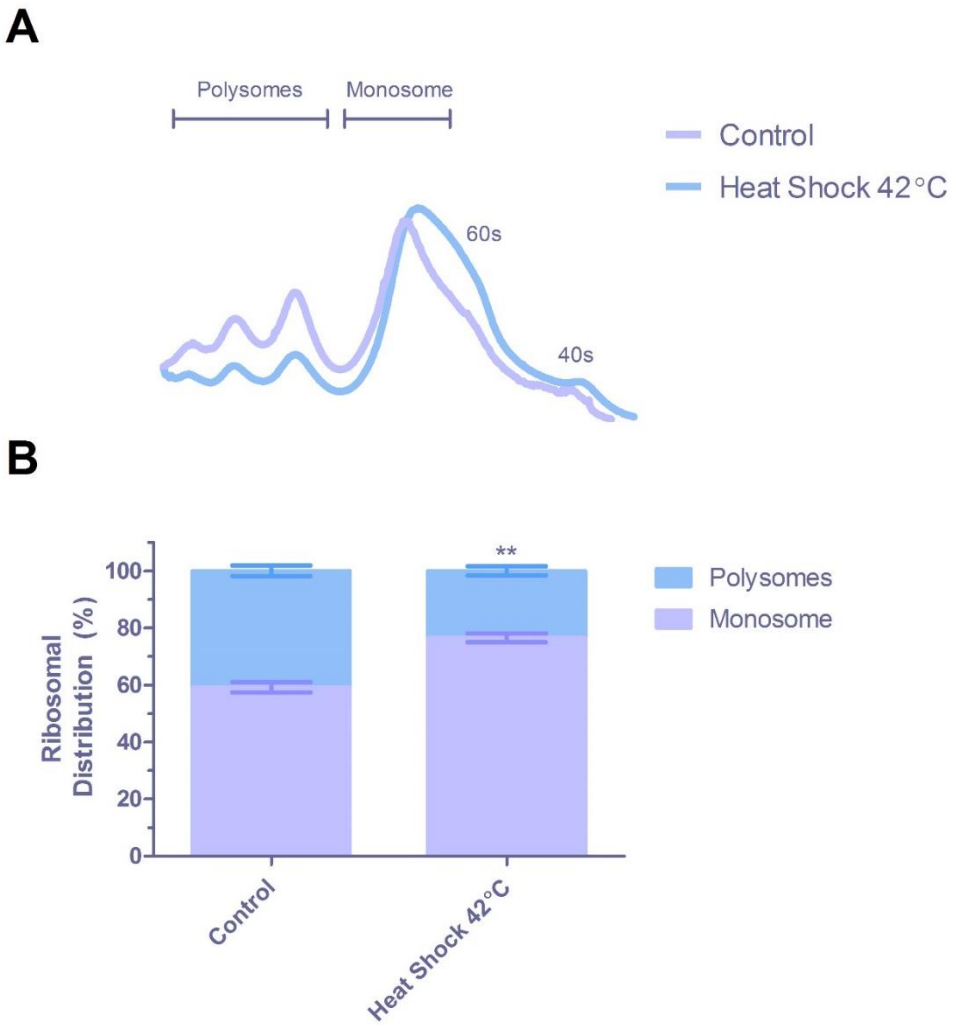

Figure 5.8 Comparison of polysome profiles of WT control conditions and 5 minutes of 42^{O}C heat shock. A shows the polysome profiles for the control (37^{O}C) and 5 min 42^{O}C heat shock for WT. The control shows well defined polysomes and a larger monosome followed by slight peaks for the ribosomal subunits 60s and 40s. The heat shocked cells have lowered polysomes, a large monosome and an increased size of both the 60s and 40s subunits. B shows ribosomal distribution as a percentage of polysomes to monosome/subunits. Polysomes decrease from ~41% to ~23% in heat shocked cells. There is a significant difference between the conditions (p=<0.01). Significance levels ** {<0.01}. Significance determined by Unpaired T-test N=3

Fig 5.8 A shows the polysome profiles for the WT under control conditions which includes incubation at 37^{O}C and heat shocked cells treated to 5 min at 42^{O}C. I can see that after 5 min of heat shock there appears to be disassociation of ribosomes as evidenced by an increased 60s peak which appears merged with the monosome peak. A study in *A.fumigatus* has shown altered polysome profiles after heat shock induced by transfer from 25^{O}C to 37^{O}C and measured at 30 min (Krishnan *et al.*, 2014), so likely I are observing the initiation of this change. Fig 5.8

B shows the distribution of ribosomes shifts to the monosome/subunit fractions from the polysomes, a decrease from ~41% to ~23%, indicative of translational repression. This shift is significantly different from control conditions ($p=<0.01$).

As the WT displayed significant changes in polysome profiles under all the conditions tested I next examined *Δgcn2* for its ability to initiate repression of translation. I began with comparing polysome profiles generated under control conditions and 10 min of 20mM DTT treatment.

5.2.4. *eif2α* kinase mutants

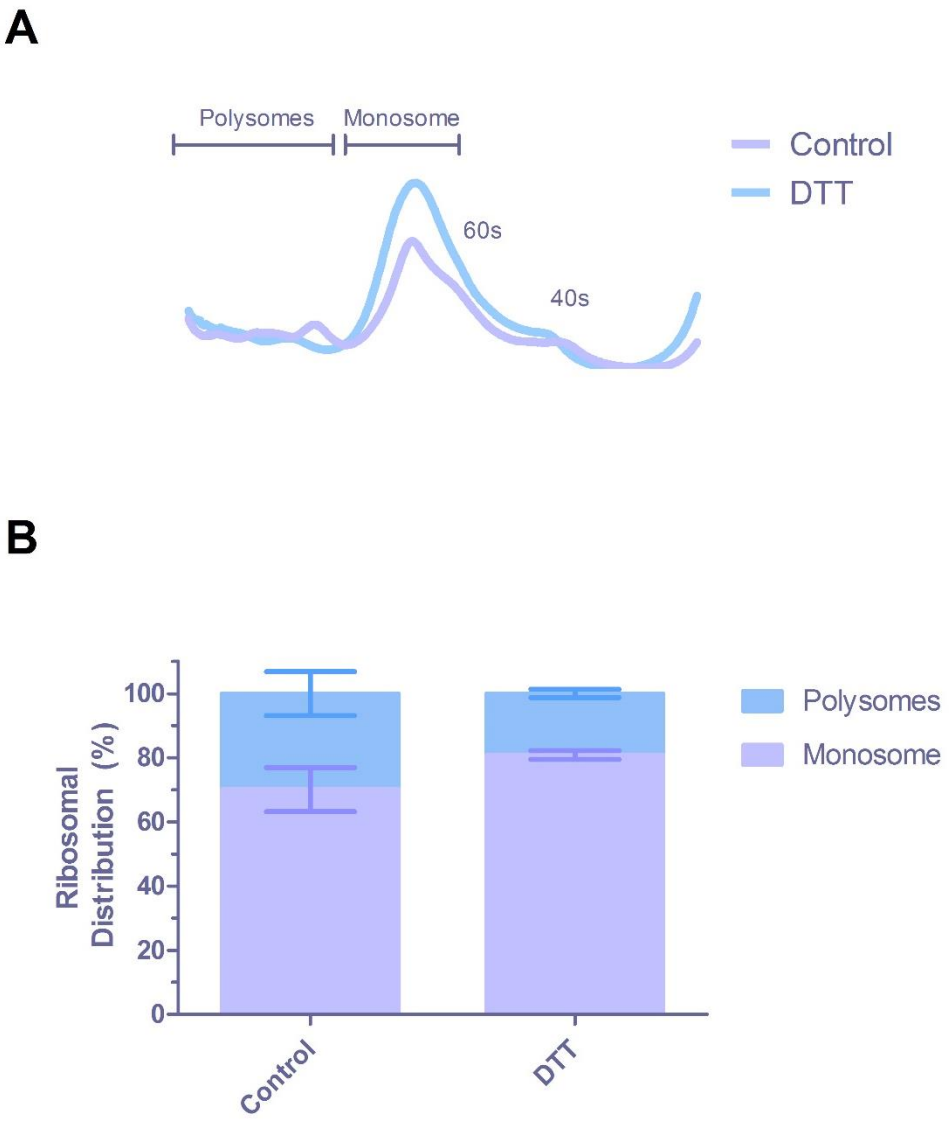

Figure 5.9 Polysome profiles of control and 10 min 20mM DTT treated Δgcn2strain. A shows the polysome profile for both control and DTT treated cells for Δgcn2. The control shows small poorly defined polysome peaks, a large monosome, a mild 60s and a clearly defined 40s peak. After DTT treatment the polysomes are decreased and less clearly defined and the monosome shows an increase in size. B shows the ribosomal distribution when calculated as a percentage between the polysomes and monosome/subunits. The polysomes account for ~30% of the total mRNA and this decreases to 20% after DTT treatment. This was not considered significant as determined by an unpaired T-Test. N=3.

The *Δgcn2* strain's polysome profile has the least defined polysome peaks of any strain tested (Fig 5.9 A). Based on our analysis (Fig 5.9 B) this represents ~30% of the ribosome distribution. This implies that this strain has low rates of translation. As *gcn2* is likely to be required for amino acid biosynthesis (Dever *et al.*, 1992; Zhang *et al.*, 2002), it is not surprising if growth and translation rates are low, particularly in MM. DTT addition causes an apparent

shift of mRNA from the polysomes to monosome/subunit fractions by 10% which implies that deletion of *gcn2* does not lead to loss of translational attenuation under ER stress. However, this was not statistically significant (p= 0.1985). From the data it is apparent that the variation in the control conditions is a significant issue. The *Δgcn2* strain has a sick phenotype and grew very poorly on minimal media. In liquid culture I observed wide variation in growth between flasks despite inoculations of equal volumes from the same mycelial culture, this led to occasionally having some replicates or conditions providing less mRNA to load during polysome profiling. Despite this, I do observe a decrease in variation between DTT treated replicates compared to the controls (SEM = ± 6.86 and ±1.302 respectively). I next examined tunicamycin's effect on the *Δgcn2* polysome profile.

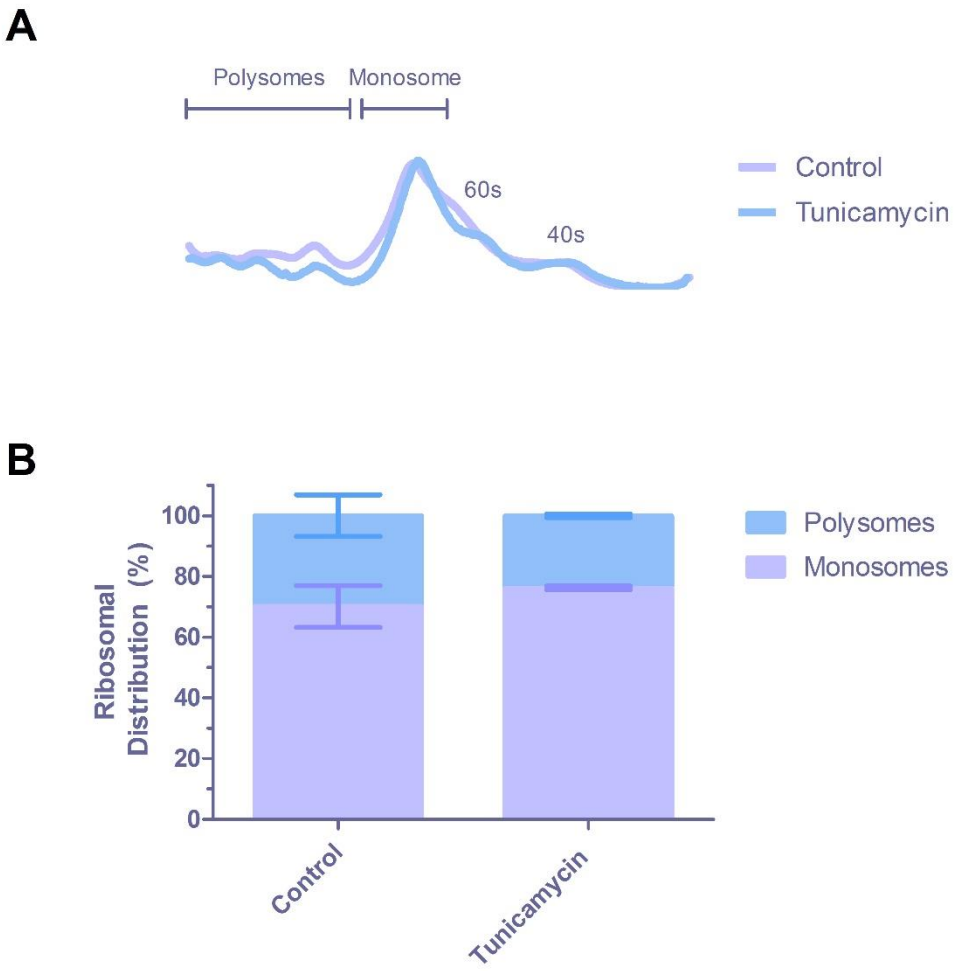

Figure 5.10 Comparison of control and 10 min 1µl/ml tunicamycin treated polysome profiles for Δgcn2. A shows that the control Δgcn2 has poorly defined polysomes peaks a large monosome and 60s peak and a clearly defined 40s peak. Tunicamycin treatment lowered the polysomes which are more defined and noticeably decreased the 60s peak which along with the 40s peak became clearer. B shows that there is an increase in the monosome/subunit fractions compared to the control. This was not considered significant as determined by unpaired T-Tests. N=3.

From Fig 5.10 A I can see that treatment with 1µl/ml tunicamycin induces a minor shift in the polysome profile for the *Δgcn2* mutant strain; there is a reduction in the proportion of the profile in the polysome fraction. This is possibly indicative of a translational response. However this was not significant (p=0.4283). Another piece of evidence for increased translational regulation is that as with DTT treatment I see that the SEM of tunicamycin treated cells is has lowered to ± 0.57 as opposed to ± 6.86 in the control.

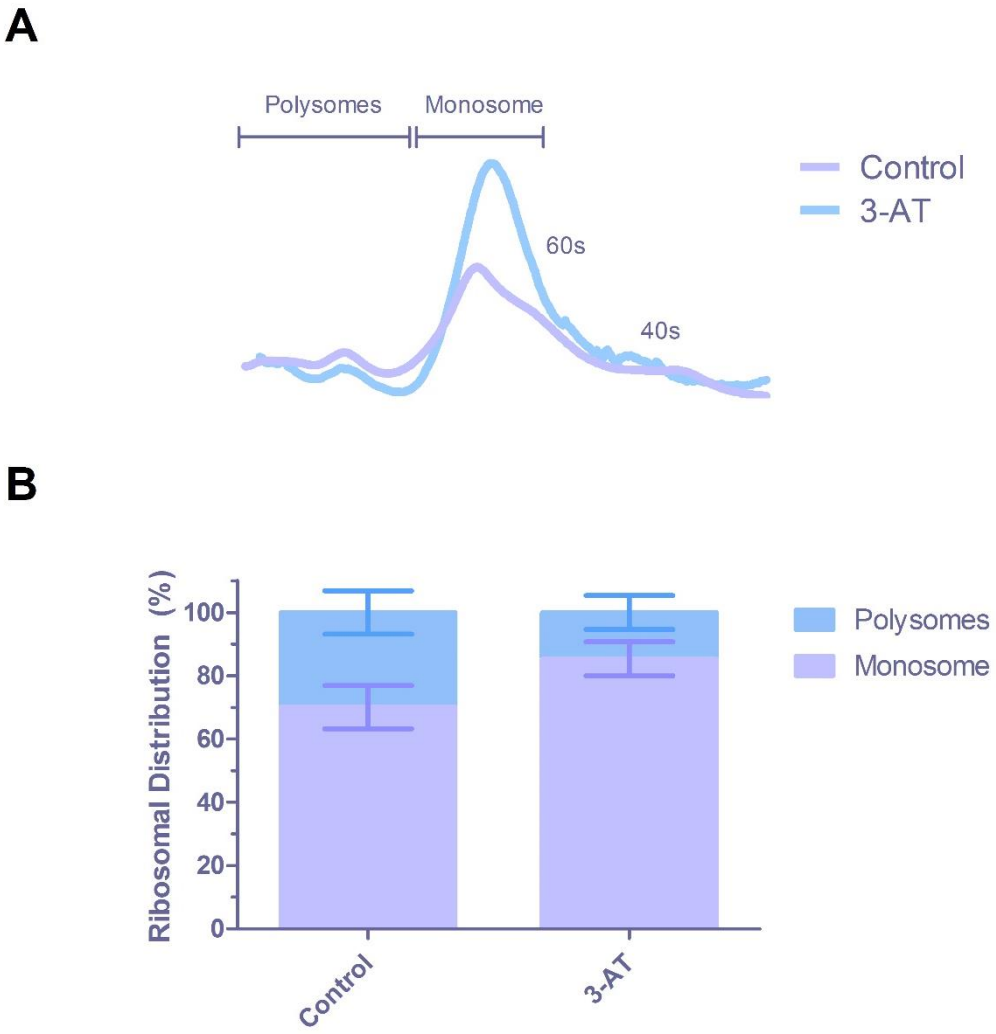

Figure 5.11 **Comparison of 5mM 3-AT treatment and control conditions on polysome profiling for *Δgcn2*.** **A** shows a comparison of polysome profiles generated under control and 10 min 3-AT treated *Δgcn2* cells. The control shows poorly defined polysomes, a large monosome, 60s and 40s subunit peaks. 3-AT treated cells show a reduction in the polysome fraction primarily the disome, a large and more clearly defined monosome and decreased 60s and 40s peaks. **B** shows ribosomal distribution as a % of total mRNA with separation of polysomes and monosomes/subunits of the control and 3-AT treated cells. Polysomes account for 30% and 15% of total mRNA in the control and 3-AT conditions respectively. This result was not significant as determined by an unpaired T-Test. **N=3.**

Fig 5.11 A compares the control and 5mM 3-AT treated *Δgcn2* cells' polysome profiles. From this I can see there is a decrease in the polysome fractions and an increase in the monosome peak and a decrease in the subunit peaks although not a disappearance. Fig 5.11 B shows the ribosomal distribution between the two conditions which did not show a significant difference. This is the most varied response seen for the *Δgcn2* so far with a SEM of ± 5.36. These data indicate that loss of *gcn2* could be contributing to the diminished and varied response which

would fit with the literature that shows this kinase is responsible for attenuated translation under amino acid starved conditions.

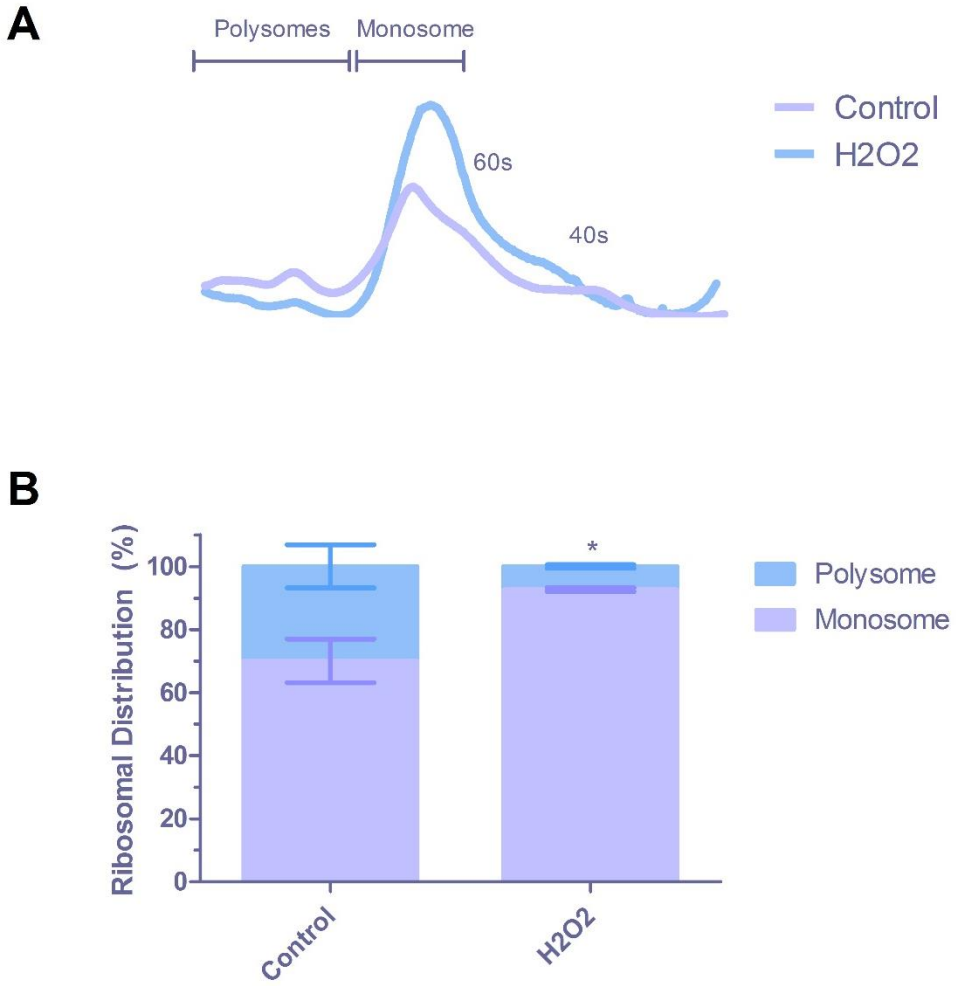

Figure 5.12 Comparison of 5mM H2O2 treatment and control conditions on polysome profiling for *Δgcn2*. A shows the profiles for control and 10 min H_2O_2 treatment for the Δgcn2 strain. The control has poorly defined polysomes followed by a clear monosome and subsequent subunit peaks with the 40s being most prominent. The H_2O_2 profile shows decreased polysomes and an enlarged monosome, the 40s subunit peak is still present but diminished whereas the 60s is much less apparent. B shows ribosomal distribution as a % of total mRNA with separation of polysomes and monosome/subunits. Polysomes decrease from ~30% to ~8%. This is significant at $p<0.05$ as determined by an unpaired T-Test. Significance levels *{<0.05}. N=3

Fig 5.12 A shows the polysome profiles for the control and 5mM H202 treated cells from *Δgcn2*. I can see that there is a large decrease in the polysome fractions and an increase into the monosome peak in the H202 treated cells comparative to the control. The 60s and 40s peaks have lost their definition also. Fig 5.12 B shows a significant difference between the control and H_2O_2 ($p<0.05$) and I can see that there is a decrease in the polysome fractions of ~30% to ~8%. I can observe that the same trend for the WT under oxidative stress is found within *Δgcn2*;

this treatment leads to a large loss of polysome fractions to the monosome/subunits. After H_2O_2 treatment the polysomes account for ~8% rather than the DTT treated ~20% (see Fig 5.1). Therefore *gcn2* does not appear to regulate attenuation of RT during oxidative stress.

At this stage it was apparent the variation between replicates under control conditions, likely due to the varied but consistently poor growth between replicates, needed to be addressed. The *ΔhriA* strain also displayed very similar growth despite increased inoculum size, flasks would take between 5-7 days to have sufficient biomass to carry out polysome profiling. I found that addition of AA via the casein hydrolysate (case) addition to media largely recovered growth on solid and liquid media (Fig 6.3). I therefore compared the profiles generated by gcn2 under control and control + case conditions.

5.2.5. Casein hydrolysate

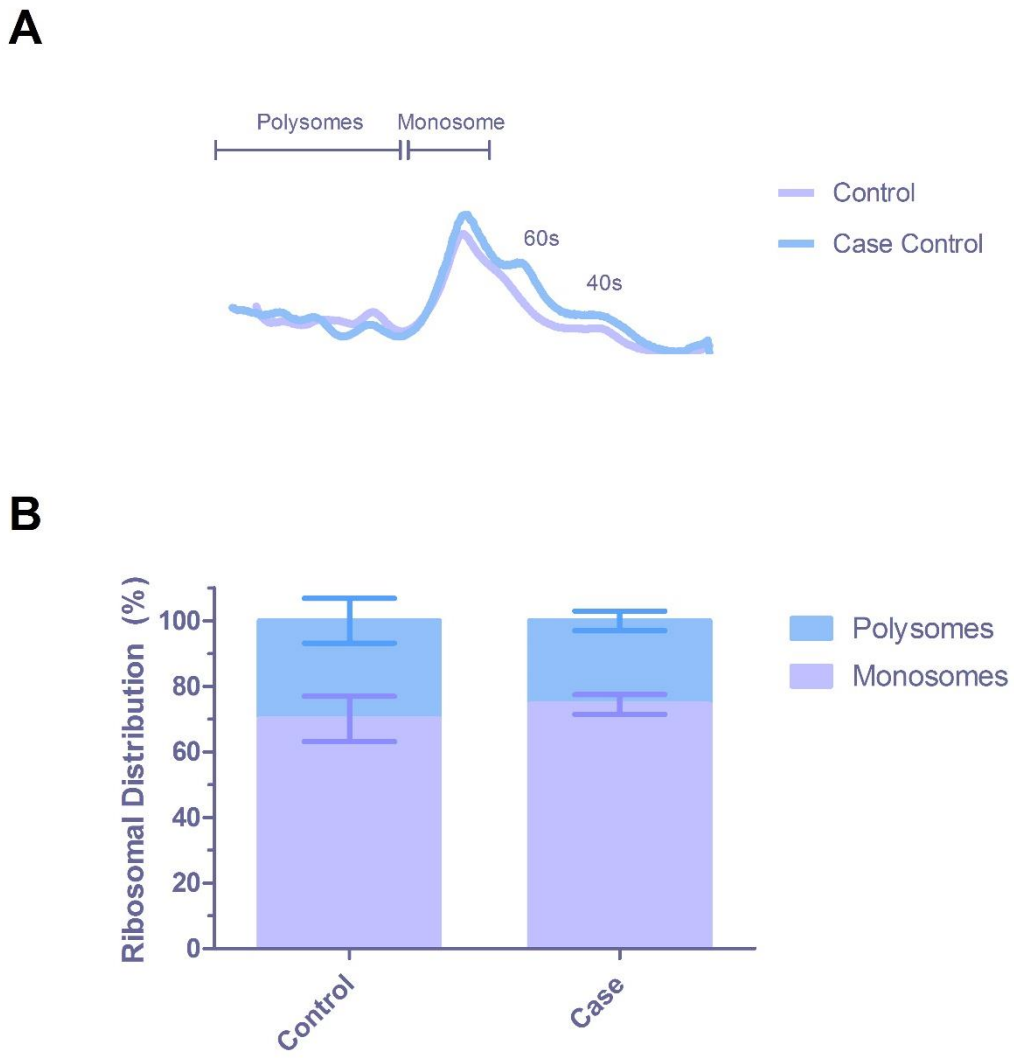

Figure 5.13 Comparison of polysome profiles generated under control conditions and control + case from Δgcn2. A shows the polysome profiles for control and control + case show. With addition of case there is a small fourth polysome observed and the peaks are more clearly defined that the control without case. The subunits for both the 60s in particular and the 40s to a lesser extent are larger and more pronounced. B shows ribosomal distribution as a % of total mRNA with separation of polysomes and monosome/subunits. With addition of case there is a decrease in the level of polysomes from ~30% to ~26%. This result was not significant as determined by an unpaired T-Test. N=3.

Fig 5.13 A shows that with the addition of case, under control conditions, there is the appearance of a small fourth polysome peak which until now was not observed for *Δgcn2*. There is also a very distinct 60s and 40s peak which implies that there is an increase in the level of ribosomes not actively engaged in translation. Fig 5.13 B shows that there is a slight decrease

in the polysome fraction, despite the extra polysome present. From Fig 6.3 I know that the addition of case improves *Δgcn2's* growth, this has also led to a decrease in the level of variation between replicates, as the SEM is ± 3.02 with case and ± 6.86 without. Whilst this is an improvement, this is still the most varied control samples taken for any strain in this study. I next wanted to examine WT control + case and the effect 20mM DTT has on the polysome profiles generated.

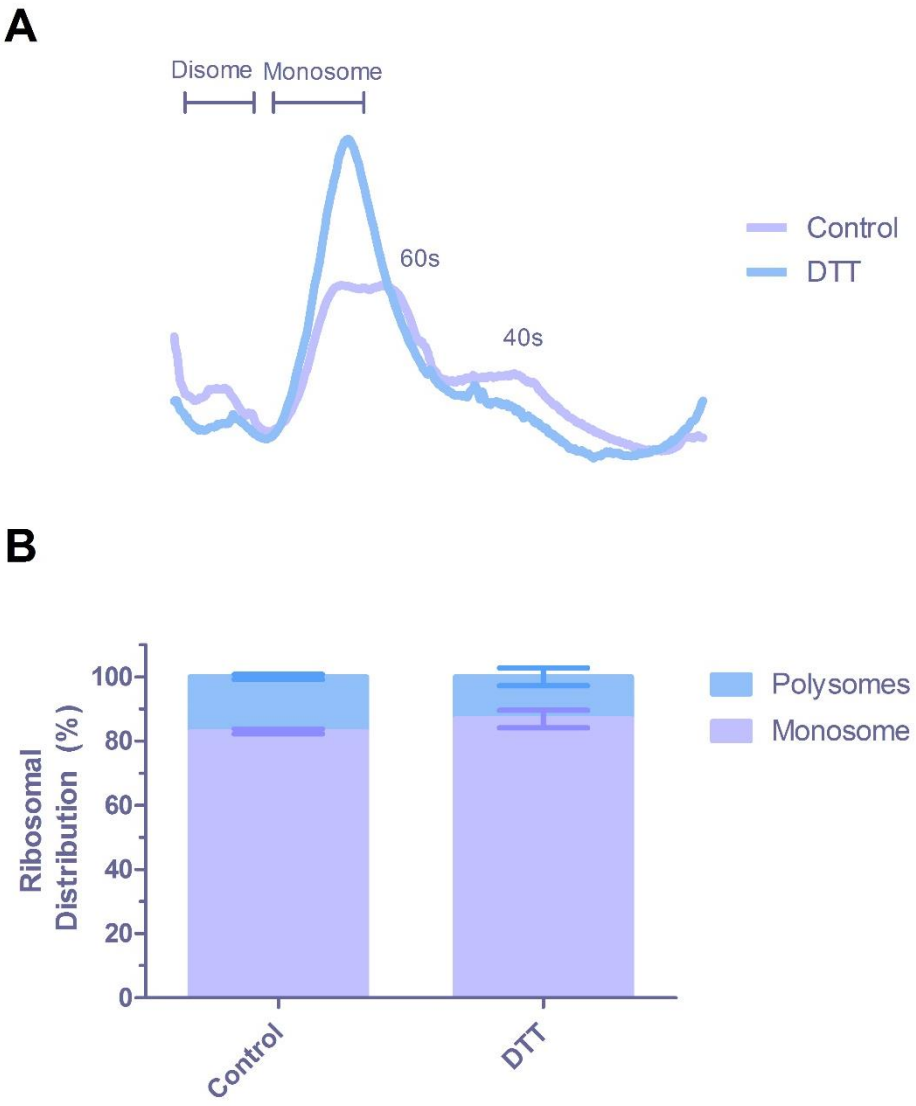

Figure 5.14 Comparison of control conditions and 20mM DTT treatment on polysome profiling for WT with casein hydrolysate. A shows profiles for control conditions + case and 10 minute 20mM DTT treated cells. The top of the tubes were crushed during ultracentrifugation and subsequently a large portion of the polysome fraction was lost. I can see that under control + case treatment that the monosome is at the same level as the 60S and a large and clear 40S peak. DTT treatment led to formation of a large monosome, disappearance of the 60S peak and lowering of the 40S peak. B shows ribosomal distribution as a % of total mRNA with separation of polysomes and monosome/subunits, in this instance only the disome was visible from the polysome fractions. This result was not significant as determined by an unpaired T-Test. N=3

Fig 5.14 A shows a comparison of control and 20mM DTT treated cells after 10 min from the WT. Unfortunately during ultracentrifugation each of the 3 tubes for both conditions collapsed. This altered the polysome profile drastically as I lost the polysome fractions excluding the disome. This means that whilst I can examine the monosome and subunit peaks I can't ascertain the difference to the control without case or any other conditions. However, I can clearly see that there is a large 60s peak under control conditions, almost equal to the monosome. A clear

40s which is even larger than the disome is also present. This is an observation I haven't seen previously for the WT. After DTT treatment there is a clear and enlarged monosome comparatively and a decrease in both the 60s and 40s peaks. These findings would imply that with a supply of amino acids present in the media there is a decrease in the level of ribosomes actively translating. That is not necessarily surprising as with a plentiful supply of peptide monomers there is less importance on all the associated biosynthetic pathways. Fig 5.14 B shows the ribosomal distribution, again this can't accurately reflect the true state of polysome to ribosome/subunit distribution. There was no significant difference between conditions.

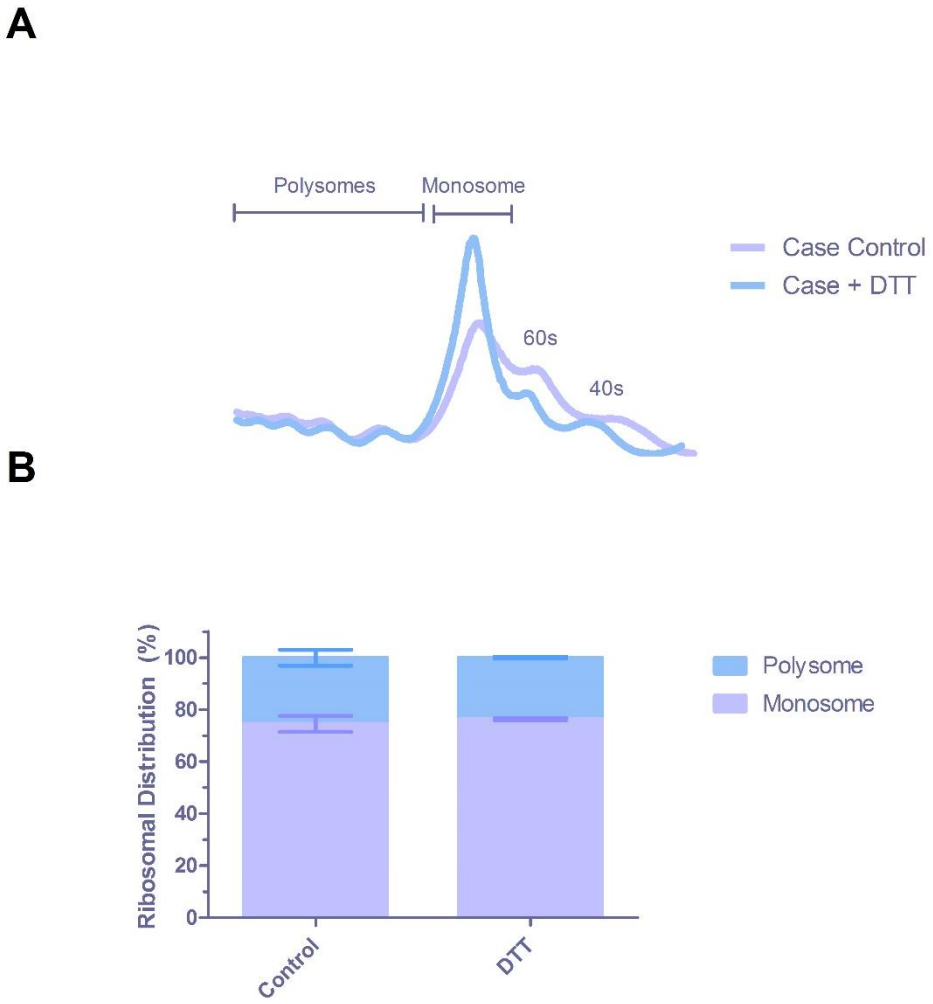

Figure 5.15 Comparison of polysome profiles generated under control and 10 min 20mM DTT treatment with casein hydrolysate supplementation from the Δgcn2 strain. A shows the control vs 20mM DTT after 10 min with case included in the growth media. The control displays polysomes, monosome and defined subunit peaks. There is a decrease of the 60s and 40s peaks after DTT treatment and an obvious increase in the monosome which has become more clearly defined from the 60s peak. B shows ribosomal distribution as a % of total mRNA with separation of polysomes and monosome/subunits. There is a slight change in polysome size from ~26% to ~24% after DTT treatment. This was not a significant change as determined by an unpaired T-Test. N=3.

Fig 5.15 A shows a comparison of control and 20mM DTT treated cells after 10 min from the *Δgcn2*. Under control conditions I see small but clear polysome peaks as well as the presence of clear and relatively large subunit peaks. After DTT treatment I see a decrease in the subunit peaks and a concomitant increase in the monosome, this is indicative of an increase in translation due to the loss of disassociated ribosomes. This appears to follow the trend indicated from the WT. Fig 5.15 B shows the distribution of ribosomes into polysomes and monosomes/subunits. There is no significant change.

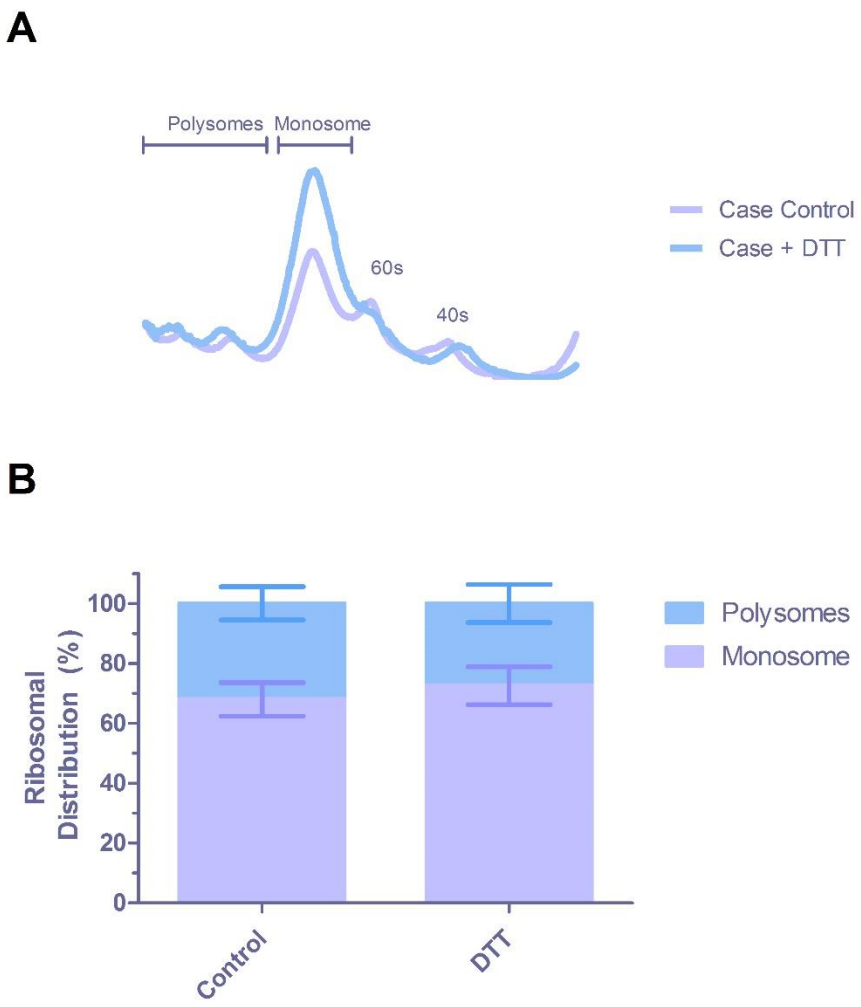

Figure 5.16 Comparison of polysome profiles generated under control and 10 min 20mM DTT treatment from the ΔhriA strain. A shows the control vs 20mM DTT after ten min with case included in the growth media for ΔhriA. The control displays a few polysome peaks followed by clear and separate monosome and subunit peaks. There is a decrease in the definition of the 60s and 40s peaks after DTT treatment and an obvious increase in the monosome. B shows ribosomal distribution as a % of total mRNA with separation of polysomes and monosome/subunits. There is a slight change in polysome size from ~32% to ~27% after DTT treatment. This was not a significant change as determined by an unpaired T-Test. N=3.

Fig 5.16 A shows a comparison of control and 20 mM DTT treated cells after 10 min from the *ΔhriA* strain. I can see the presence of two polysome peaks (disome and trisome) followed by monosome and subunit peaks which are very well defined indicating a lower level of translation compared to the *Δgcn2* strain. After DTT treatment the profile changes, indicating that

previously inactive ribosomal subunits become active as evidence by the increase in the monosome peak. The appearance of the polysomes remain consistent between control and DTT treated conditions. Fig 5.16 B shows ribosomal distribution as a % separated into polysomes and monosomes/subunits. From this I can see there is a slight increase, however there is a relatively large degree of variation between replicates and this change is not considered significantly different as determined by an unpaired T-test.

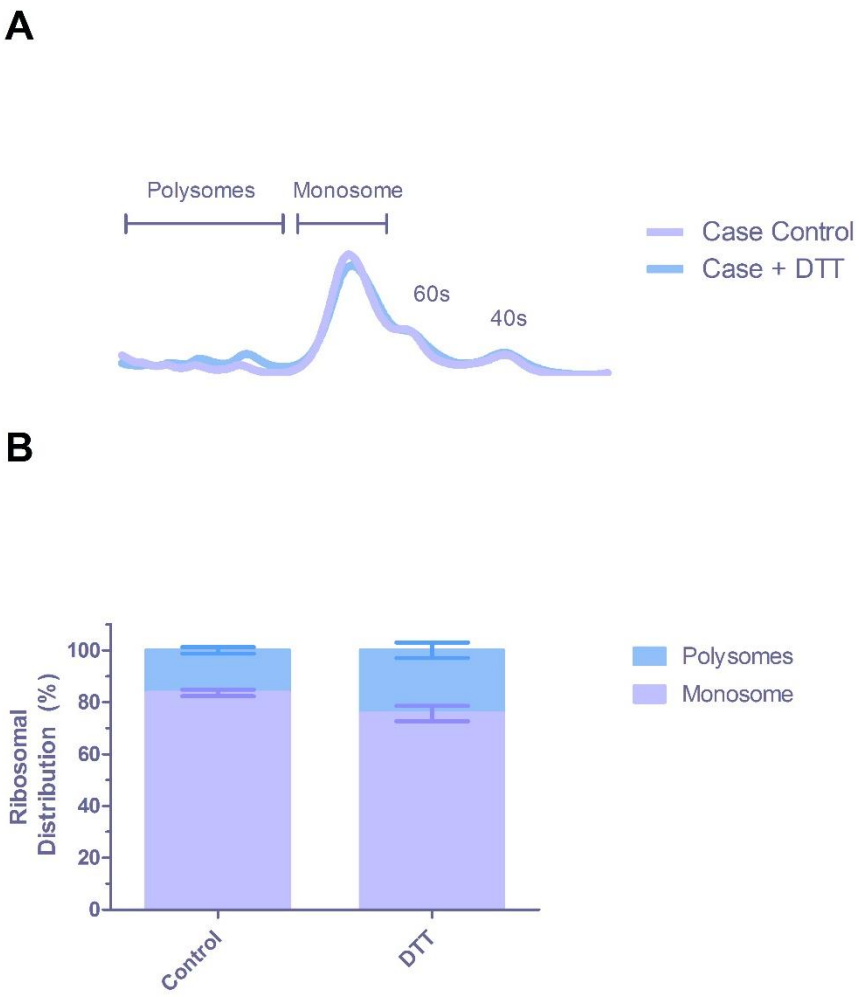

Figure 5.17 Comparison of polysome profiles generated under control and 10 min 20mM DTT treatment with casein hydrolysate from Δgcn2ΔhriA. A shows the control vs 20mM DTT after 10 min with case included in the growth media. The control displays several small polysome peaks, a large monosome and subunit peaks. There is a slight decrease of the monosome peak after DTT treatment and an increase in the polysome peaks. B shows ribosomal distribution as a % of total mRNA with separation of polysomes and monosome/subunits. There is an increase of polysomes from ~16% to ~24% after DTT treatment. This was not a significant change as determined by an unpaired T-Test. N=3.

Fig 5.17 A shows a comparison of control and 10 min 20mM DTT treated cells with case from the *Δgcn2ΔhriA* strain. I see a similar profile as to that of *Δgcn2* and *ΔhriA* under control conditions although the subunit peaks appear less defined for *Δgcn2ΔhriA* (see Figs 5.15 and 5.16). DTT treatment shows very little change compared to the control, there is a slight increase in the polysomes which is the first instance of this occurring during this study. Fig 5.17 B shows ribosomal distribution as a % with polysomes separated from monosomes/subunits. There is an increase in polysomes after DTT treatment from ~16% to ~24%. This change was not considered significantly different as determined by an unpaired T-test.

For both *Δgcn2* and *ΔhirA*, there appeared to be a response to DTT but this was not significant, in either case. However, in the double mutant the response to DTT was negligible and potentially reversed. It is therefore likely that both GCN2 and HRIA act to regulate the translational response to DTT and it is possible that they are acting independently. I need further data to be certain.

Polysome profiling is usually used in combination with transcriptomics. Unfortunately at this point in the research, funds were limited, so I utilized Q-PCR and focused on *bipA* transcript levels for the WT under various conditions. I also examined the *ΔhacA* and *hacA Δintron* strains to observe what effect, if any, loss and overexpression of HacA caused.

5.2.6. *bipA* transcript levels and ribosomal association

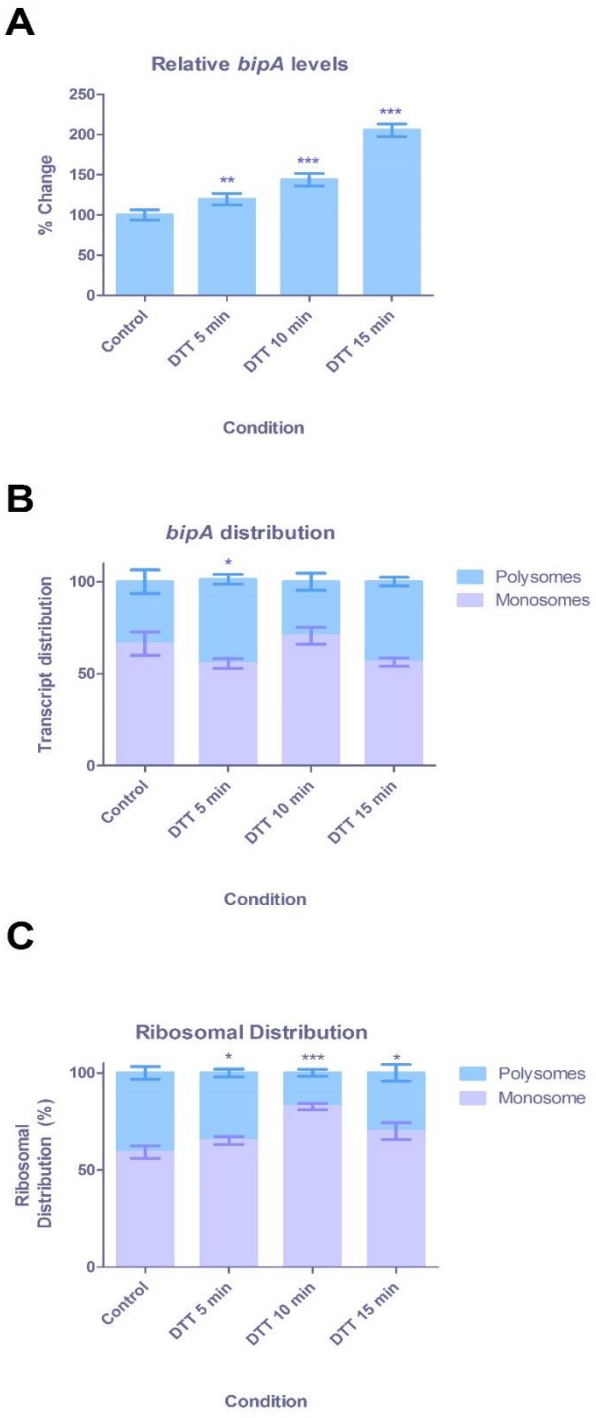

Figure 5.18 Comparison of bipA level and distribution in control and 20mM DTT treated cells for WT. A shows bipA transcript levels from control, 5, 10 and 15 min DTT treated cells. There is significant increases of bipA after DTT treatment for each time point measured. B shows bipA distribution between polysomes and monosomes/subunits. 5 min of DTT treatment led to a significant change in transcript distribution towards the polysomes as determined by an unpaired T-test. C shows ribosomal distribution as a % of total mRNA with separation of polysomes and monosome/subunits, which shows significantly decreased polysome fractions after DTT treatment. Significance levels * {<0.05} ** {<0.01} *** {<0.0001} Significance determined by unpaired T-tests. N=3.

Fig 5.18 A shows *bipA* levels after 20mM DTT treatment compared to control conditions. I see a steady and significant increase at each time point after DTT addition. By 15 min of DTT treatment *bipA* levels have nearly doubled. Fig 5.18 B shows *bipA* distribution between polysomes and monosome/subunit fractions. 5 min of DTT treatment led to a significant change in *bipA* association with polysomes which increased by ~11%. 10 and 15 min treatment were not significantly different from the control. Fig 5.18 C shows ribosomal distribution as a % with polysomes and monosomes/subunits separated. Next I compared DTT and tunicamycin treatment for *bipA* induction and ribosomal association.

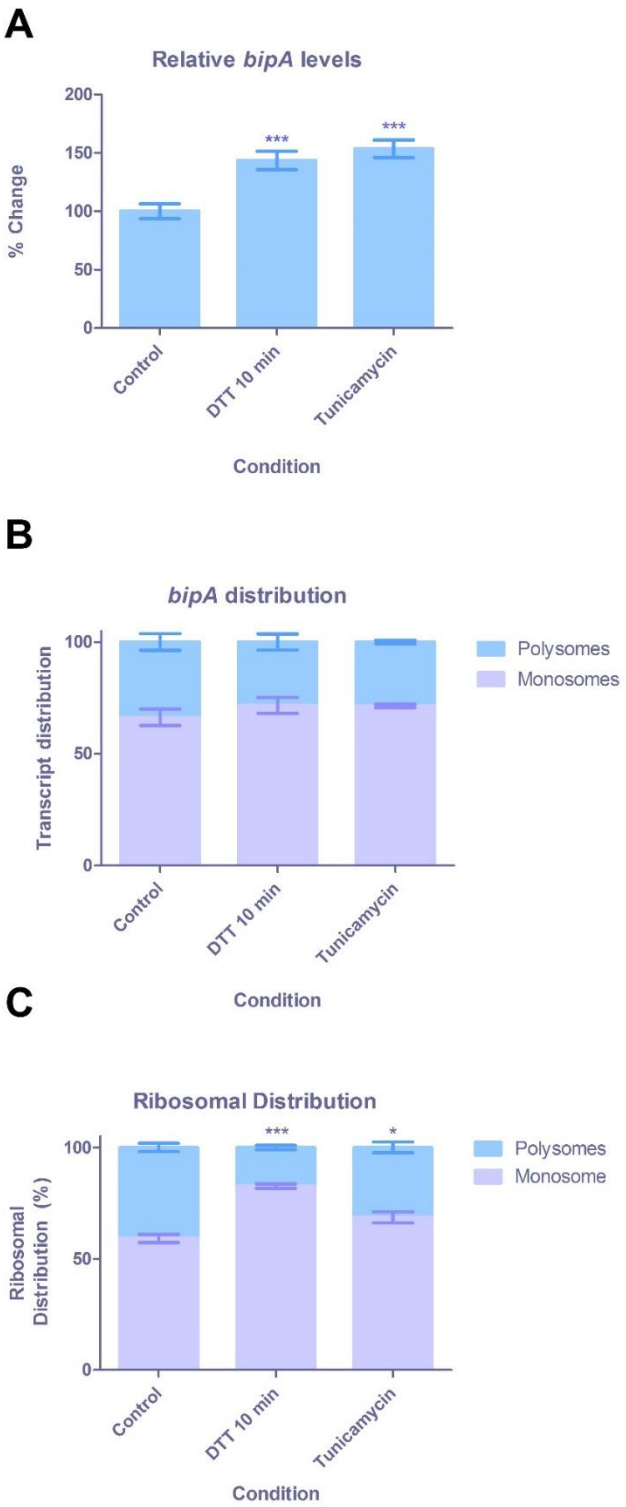

Figure 5.19 Comparison of bipA transcript level and distribution in control, 10 min 20mM DTT and 1µg/µl tunicamycin treated cells for WT. A shows bipA transcript levels from control, 10 min DTT and 1µg/µl tunicamycin treated cells. There is significant increases of bipA after DTT and tunicamycin treatment. B shows bipA distribution between polysomes and monosomes/subunits which was not significantly altered (determined by unpaired T-tests).. C shows ribosomal distribution as a % of total mRNA with separation of polysomes and monosome/subunits. Significance levels * {<0.05} *** {<0.0001}. N=3.

Fig 5.19 A shows *bipA* levels after 10 min treatment with 20mM DTT and 10 min treatment with 1µg/µl tunicamycin compared to control conditions. Whilst both treatments significantly induced *bipA* transcription, tunicamycin treatment induced a higher level of *bipA* compared to the DTT. Fig 5.19 B shows *bipA* ribosomal association and I can see that there is no difference between control and the treated samples at 10 mins ($p=0.2480$ for tunicamycin and $p=0.3636$ for DTT). Fig 5.19 C shows ribosomal distribution as a % with polysomes and monosomes/subunits. By comparing the Fig 5.19 A-C I estimate that tunicamycin treatment led to the highest levels of *bipA* translation; not only was *bipA* transcript more abundant after tunicamycin treatment but I can see the proportion associated with the polysomes represented ~31% of the total mRNA as opposed to ~18% for DTT. This implies that there are more active polysomes translating a higher number of *bipA* transcripts. These data imply that tunicamycin treatment, whilst not displaying as drastic a shift in polysome profile as DTT, induces a higher degree of ER stress based on *bipA* induction.

I next examined *hacA's* role in *bipA* induction and association.

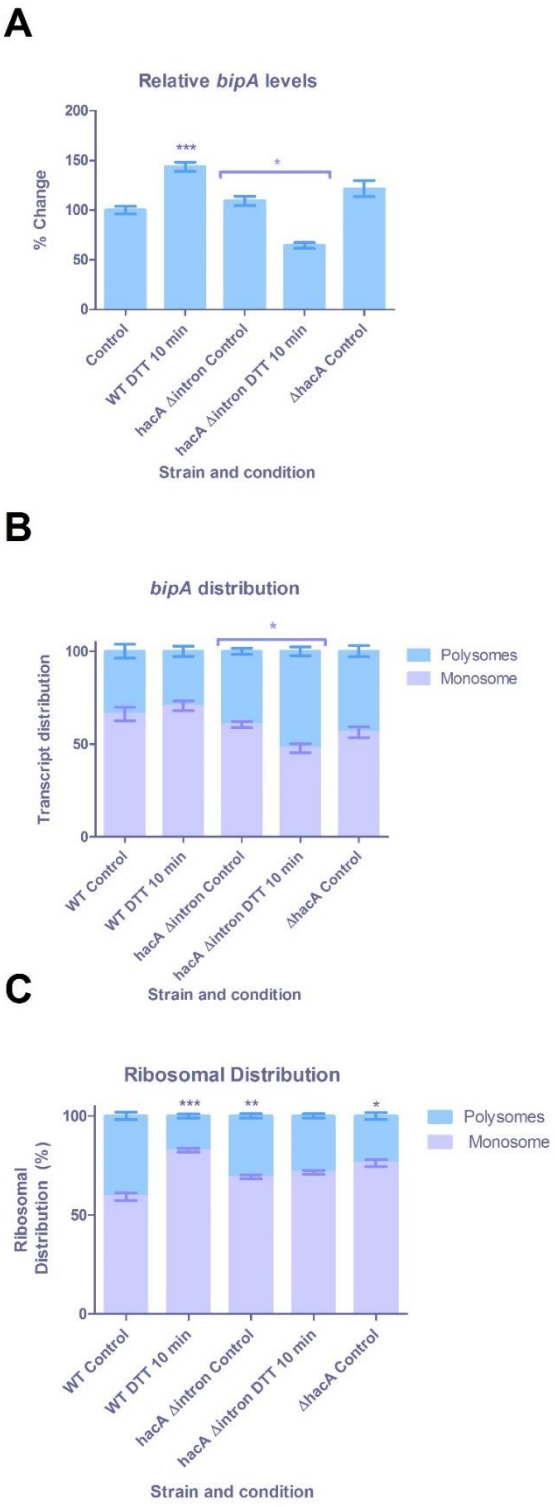

Figure 5.20 Comparison of bipA transcript level and distribution from WT and hacA mutants under control and 10 min 20mM DTT treatment. A shows bipA transcript levels from control conditions for WT, ΔhacA and hacA Δintron as well as 10 min DTT treated samples of WT and hacA Δintron. A shows both hacA mutants had slightly increased levels of bipA but not significantly different. hacA Δintron shows a significant decrease in bipA after DTT treatment whereas WT displays a significant increase (determined by unpaired T-tests). B shows bipA distribution between polysomes and monosomes/subunits which was not significantly different for the hacA mutants under control conditions. hacA Δintron displays a significant difference in bipA distribution after DTT treatment with a significant shift to the polysome fractions. C shows ribosomal distribution as a % of total mRNA with separation of polysomes and monosome/subunits, both hacA mutants have significantly smaller polysomes than the WT. Significance levels * {<0.05} ** {<0.01} *** {<0.0001}. N=3.

Fig 5.20 A shows *bipA* levels under control conditions for WT, *ΔhacA* and *hacA Δintron* strains as well as 10 min DTT treatment for WT and *hacA Δintron* mutant. *ΔhacA* DTT treated samples were lost and so I were unable to examine any *bipA* level or ribosomal association changes. Both *ΔhacA* and *hacA Δintron* mutants exhibit elevated levels of *bipA* under control conditions although this is not considered significantly different (p=0.1025 and p=0.1958 respectively). Whilst WT showed a significant increase in *bipA* at 10 min, the *hacA Δintron* strain shows a significant decrease from ~109% of WT control levels to ~65% (p= 0.0118). Fig 5.20 B shows *bipA* ribosomal association, both *ΔhacA* and *hacA Δintron* mutants display higher levels of transcript associated with polysomes (~44% and ~40% respectively) than the WT under control conditions (~36% *bipA* association with polysomes). *hacA Δintron* strain exhibits a significant increase of *bipA* polysome association from ~40% to ~52% after DTT treatment. Fig 5.20 C shows ribosomal association as a % with polysomes and monosomes/subunits separated. By comparing Fig 5.20 A-C I can see that although *hacA Δintron* strain shows a decrease in *bipA*, there is a concomitant shift to the polysome fractions and I can see from C that the ribosomal distribution stays almost unchanged. These data taken together imply that for the *hacA Δintron* strain *bipA* transcript decreases in abundance but the remainder are being more actively translated. I next compared the *eif2α* mutants' *bipA* levels.

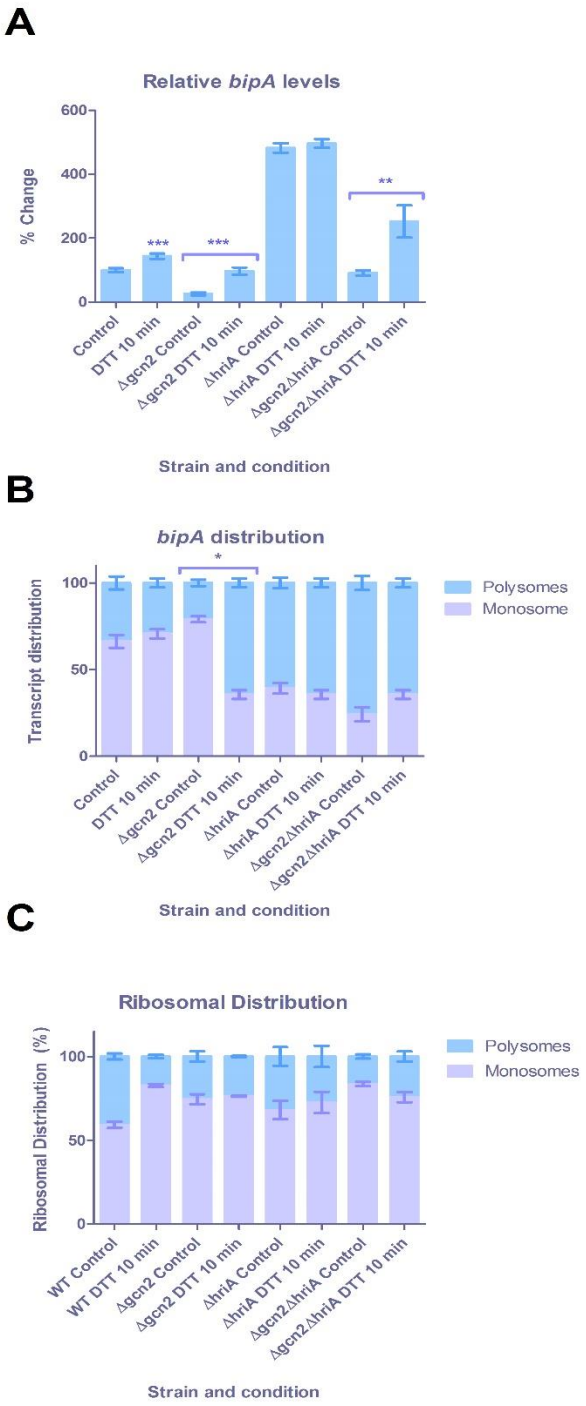

Figure 5 21 Comparison of WT control and 10 min 20mM DTT treated conditions and eif2α kinase mutants control and 10 min DTT treatment bipA levels (supplemented with casein hydrolysate. A shows relative bipA levels for WT under control and DTT treated conditions control conditions + casein hydrolysate and 10 min 20mM DTT treated cells for Δgcn2, ΔhriA and Δgcn2ΔhriA. WT, Δgcn2 and Δgcn2ΔhriA show significant increases in bipA levels after DTT treatment. ΔhriA has over 4-fold bipA under control + case conditions and shows no significant increase after DTT treatment. B shows bipA distribution between polysomes and monosomes/subunits. Δgcn2 displays a significant redistribution of bipA towards the polysomes after DTT treatment. ΔhriA and Δgcn2ΔhriA show that ~60% and ~75% of bipA transcript is associated with polysomes. C shows ribosomal distribution as a % of total mRNA with separation of polysomes and monosome/subunits. This result was not significant as determined by an unpaired T-Test. Significance levels * {<0.05} ** {<0.01} *** {<0.0001}. N=3.

5.3. Discussion

5.3.1. Translational remodelling

I have observed decreases in RT in response to a variety of different stimuli (Figs 5.1, 5.5, 5.6, 5.7 and 5.8). *S. cerevisiae* and *S pombe* have both been shown to alter rates of translation in response to glucose starvation, AA deprivation, oxidative stress and heat shock (Tzamarias, Roussou and Thireos, 1989; Ashe, De Long and Sachs, 2000; Shenton *et al.*, 2006). Whilst polysome profile alterations have been shown in *A. niger* during heat shock (Krishnan *et al.*, 2014), this study is the first example of decreased RT being observed during ER stress in filamentous fungi. Likely this observed decrease in polysome size has been missed to date due to the rapid nature of the response. This in itself implies a very robust system present in *A. nidulans* due to what appears to be a rapid return to the control profile (see Fig 5.1 C). In mammalian systems ER stress translational repression is observable after 3 hrs of stress exposure (Novoa *et al.*, 2001; Ventoso *et al.*, 2012). Given the inherent differences between mammalian and fungal systems - mammals being supplied with the requirements for metabolism whereas fungi are dependent on the breakdown of extracellular materials; it is unsurprising that fungi would display a more vigorous system for attenuating, and then reinstating rates of translation in response to ER stress.

5.3.2. Tunicamycin and DTT as ER stressors

Fig 5.5 shows that whilst 10 min DTT treatment led to a larger shift to the polysome profile, tunicamycin treatment for the same time period led to the higher level of *bipA* expression. This implies that tunicamycin was providing a larger induction of the ERSR. DTT treatment is not specific to the ER; the disulphide bond formation inhibition is not relegated to the ER but effects cytosolically translated proteins also. Examining *bipA* ribosomal association also implies that tunicamyin illicits a higher ERSR level; not only was *bipA* more abundant, there

was also a larger portion of polysomes retained after tunicamycin treatment. Taken together, this indicates *bipA* is more actively translated during tunicamycin treatment as well as being in higher abundance. For future work, tunicamycin would provide a more specific means of examining the ERSR.

5.3.3. The role of *hacA* in ER stress induced translation remodelling

Figs 5.3 and 5.4 show that over expression or loss of *hacA* do not play a role in translational attenuation during ER stress. This can be ascertained due to *ΔhacA* showing a significant decrease in polysomes after DTT addition. Also the loss of *hacA* led to a profile similar to that of WT 10 min DTT treated, indicating that the presence of the inducible HacA is important to regulating normal translation. The *hacA Δintron* displayed little to no remodelling after 10 min DTT treatment (see Fig 5.4). I hypothesise that this is due to the increased abundance of HacA targets being constitutively present and that remodelling may occur at different time points. However, further investigation is needed to ascertain this. There is potential that *hacA Δintron* is capable of mitigating DTT induced ER stress without translational remodelling which would make this a potential target to increase RPP, but more experiments are needed to confirm this. The constitutive expression of the active form of *hacA* led to a significantly smaller level of polysomes compared to WT; this indicates that the increased abundance of ERSR targets may induce a degree of ER stress which provides the altered translational profile seen in *hacA Δintron*. Interestingly, after DTT treatment I can see from Fig 5.20 there is a decrease in *bipA*, this occurs at the same time that *bipA* becomes more highly associated with polysomes implying increased translation. The shift from monosome to polysome association of *bipA* in *hacA Δintron* was not witnessed for the WT except at 5 min DTT treatment, this was the only instance of a change to *bipA* association for the WT.

5.3.4. *eif2α* kinase mutants and translational remodelling

Fig 5.15 and 5.16 show that both the *Δgcn2* and *ΔhriA* mutants have altered polysome profiles at 10 min of DTT treatment (with casein hydrolysate supplemented in the media). This remodelling consists of an increase in the level of actively translating ribosomes as evidenced by a decrease in the subunit peaks and a concomitant increase in the monosome. This is unexpected, although a similar trend is observed for the WT under the same conditions from the available data (Fig 5.14). A loss of polysome fractions cannot be confirmed for the WT due to the collapse of the tubes during ultracentrifugation. These samples for the WT will need to be repeated to ascertain if there is a decrease in polysomes during DTT treatment as seen without casein hydrolysate supplementation. The *Δgcn2ΔhriA* mutant shows remarkably similar profiles with and without DTT addition (Fig 5.17). The only slight difference, which wasn't considered significant, was a small increase of the polysomes. This seems unusual; however when you consider that the ERSR upregulates a host of genes to mitigate stress, and there are no kinases present which can attenuate translation in this strain, an increase in the polysome peaks is almost expected as there is an increased level of genes being transcribed. These data, taken together, imply that both kinases are needed for altered RT during ER stress. Studies in mammalian cells have shown that the *gcn2* and *hri* both function as part of the ERSR. *gcn2* is capable of phosphorylating *eif2α* during ER stress in a $PERK^{-/-}$ cell line, while *hri* was found to help regulate basal ER stress levels (Hamanaka *et al.*, 2005; Acharya, Chen and Correia, 2010). Therefore, it is likely given the results of Fig 5.21 that *gcn2* and *hriA* both have a role in regulating translation during ER stress in *A. nidulans*.

Loss of *gcn2* led to decreased levels of *bipA* under control conditions, this was extremely surprising. After DTT addition there was significant upregulation of *bipA* as expected. Loss of *hriA* alone led to 4 x the level of WT *bipA* under control conditions; this was also

extremely surprising, particularly as *Δgcn2ΔhriA* displays similar to WT levels of *bipA* under control conditions. An explanation for this could be that *gcn2* is responsible for biasing translation of transcripts towards ERSR targets such as *perk* does in mammalian systems. Therefore, loss of *gcn2* without an external ER stressor, may lead to lower levels of *bipA* until the ERSR is induced leading to upregulation of *bipA*. *hri* has been shown to be involved in maintaining ER stress in mammals, loss of the kinase led to higher levels of PERK mediated *eif2α* phosphorylation. Loss of *hriA*, therefore could lead to ER stress, leading to ERSR induction; with GCN2 present, translational machinery bias toward ERSR targets is achievable, leading to the high levels of *bipA*. This theory would also explain why there isn't the same high levels of *bipA* in the *Δgcn2ΔhriA* double mutant; loss of *hriA* leads to ER stress but loss of *gcn2* removes the translational bias toward *bipA*, leading to levels not seen in either kinase KO. Both *ΔhriA* and *Δgcn2ΔhriA* display a very large level of *bipA* associated with polysomes than any other strain tested. This indicates *hriA* may play a role in regulating ribosomal association of transcripts, interestingly the Δ*gcn2* strain displayed a significant change in *bipA* polysome association after DTT addition, resembling the *ΔhriA* and *Δgcn2ΔhriA* strains. Taken together, I conclude that both Gcn2 and HriA have roles in regulating RT in response to ER stress as well as fidelity of transcript/ribosome interactions during ER stress.

5.3.5. Future work and considerations

Polysome profiling is usually used in concert with extensive transcriptomic analysis (Kuersten et al., 2013. McGlincy and Ingolia, 2017). Whilst this approach generates a large amount of data, the purpose of this section of research was specifically looking for attenuation of RT during ER stress, as is seen in higher eukaryotes. Polysome profiling in and of itself indicates the translational state of a sample and can be used to measure translational iniation or even as

an indicator of cell health (Coudert, Adjibade and Mazroui, 2014. Molon et al., 2016). Polysome profiling therefore offered a suitable and reliable means for examining alterations to rates of translation.

The *Δgcn2*, *ΔhriA* and *Δgcn2ΔhriA* strains all displayed poor growth in MM, although this was improved with casein hydrosylate addition. Their incubation times were at least three days to garner sufficient biomass to run polysome profiling as opposed to overnight growth for WT, *ΔhacA* and *hacA Δintron*. This poses an issue for comparison with other strains due to there potentially being other factors at play, including altered ribosome numbers. Ribosome quantification is generally carried out using rRNA and can be analyzed on agarose or polyacrylamide gels. This is perfomed by comparing relative intensities of the bands produced (Zundel, Basturea and Deutscher 2009; Basturea, Zundel and Deutscher 2011). An approach termed capillary gel electrophoresis with laser-induced fluorescemce detection (CGE-LIF) is able to not only analyze rRNA *in vivo* but follow its degradation *in vitro* (Hardiman et al. 2008, Failmezger et al. 2016). These techniques however are difficult, time consuming and potentially dangerous as some utilize harmful chemicals (Boedtker 1971; Reijnders, Sloof and Borst 1973). There are more recent techniques being developed that could be useful for checking ribosome numbers in each strain; tagging of ribosomal proteins with fluorescent proteins. This method has successfully been used to examine intracellular ribosomal distribution during cell division, growth and drug treatment (Chai *et al*., 2014. Bakshi *et al*., 2014). Whilst the ribosomal number may differ between strains, thus making comparisons between them difficult, we can make observations on the changes between control and DTT treated samples for each strain as these were grown and harvested in concert.

Further experiments should be carried out utilizing tunicamcyin to investigate the responses of the *Δgcn2*, *ΔhriA* and *Δgcn2ΔhriA* strains as this appears to be a more ER specific stressor.

Also further analysis to determine if each kinase has a specific stressor to which it initiates translational attenuation, such as the observed response to heat shock and whether *hriA* is responsible as seen in *S. pombe* (Zhan *et al.*, 2002).

5.3.6. Conclusion

Based on these findings I conclude that there is a response to mitigate ER stress in filamentous fungi through attenuation of RT and this appears to be regulated by *eif2α* kinases as their loss results in no shift from polysome to monosome fractions. If this response occurs in industrially used *Aspergillus spp* it could represent a potent target for increasing RPP.

6. Growth Tests

6.1. Introduction

In this chapter, I examined the effects of alternative media on each mutant strains growth and morphology. Initially, I established growth for all strains at 37° C and 30°C on solid minimal media with glucose as the carbon source and either ammonium or nitrate as nitrogen source. NO_3 was included as this is the requirement for the P_{niiA}*::ireA* strain. I then examined several media that induce or exacerbate ER stress and several that potentially alleviate ER stress.

6.1.1. ER Stressors

To ascertain the impact the mutations that were made have upon ER stress handling capability I grew strains under control conditions with known ER stressors, DTT and Tunicamycin. The concentration of DTT used was 5 mM as opposed to the 20 mM concentration used for examining RIDD and polysome profiles as the higher concentration led to very little or no growth (data not shown). I also tested a different carbon source, dextran, as this has been shown to be the largest up-regulator of the amylolytic genes in *A. nidulans* (Kato *et al.*, 2002; Nakamura *et al.*, 2014).

In *A.niger* ER stress induction was shown to downregulate secreted proteins encoded by the amylolytic genes. Non-secreted proteins such as glyceraldehyde 3'-phosphate dehydrogenase were not downregulated (Al-Sheikh 2004). This fits with the current model of the fungal ER stress response see 1.1.15. The highest level of induction of amylolytic genes in *A.nidulans* is initiated by extracellular isomaltose (Kato *et al.*, 2002; Nakamura *et al.*, 2014). Dextran is a branched polysaccharide which when broken down releases isomaltose, this makes it a suitable carbon source for intensifying amylolytic gene output, leading to higher levels of secreted proteins. I hypothesised that the range of genes being upregulated for breakdown of dextran

would be more difficult to achieve and sustain for ER stress response deficient strains. Secretion capacity of each mutant is likely to be altered and this can be viewed by examining clear zones around a fungal colony (Hankin and Anagnostakis, 1975). Due to dextrin's turbidity in media its use allowed us to examine levels of clearing around each colonies.

6.1.2. Stress alleviators

As the majority of the mutant strains in this study displayed poor growth compared to the WT, I examined several substances for their ability to supress the aberrant growth phenotype. Firstly I looked at the addition of 1% proline to control media. Proline has been proven to be a protectorate of cell health during various stress conditions including, osmotic, freezing, oxidative, heavy metal and UV damage induced stress, amongst others (Choudhary, Sairam and Tyagi, 2005; Yang, Lan and Gong, 2009; Sasano *et al.*, 2012; Takagi, Taguchi and Kaino, 2016). Presence of proline has even been shown to be a requirement for regulating the ER stress response due to its role in redox regulation (Liang, Dickman and Becker, 2014). Casein hydrolysate is a mixture of amino acids derived through the hydrolysis of casein. Addition of casein hydrolysate to media removes the cells need to synthesize AAs as these can be taken from the extracellular environment. I decided to incorporate this into media as *gcn2* is responsible for nutrient sensing and appropriate translational responses to high/low AA levels (Wek, Zhu and Wek, 1995; Harding *et al.*, 2000). I hypothesised that this would have an impact on growth of both *Δgcn2*, *Δgcn2ΔhriA* and *Δeif2α.* In *S. cerevisiae* GCN2 acts to induce higher expression of GCN4 under AA starved conditions -GCN4 being responsible for upregulating 30 different genes involved in various AA biosynthetic pathways (Ramirez, Wek and Hinnebusch, 1991). *Δgcn2* therefore does not have a means of increasing AA synthesizing pathways so is potentially less efficient at utilizing exogenous NH_4 and act as though starved. The *A.nidulans* homologue of GCN4, termed CPCA, has been shown to be upregulated under

AA starved conditions and be translationally repressed when AAs are present (Hoffmann *et al.*, 2000; Bernd Hoffmann *et al.*, 2001). CPCA is a relatively unstudied TF in *A.nidulans*.

4-phenyl butyric acid (4-PBA) is an FDA approved drug for the treatment of urea cycle disorders and cystic fibrosis. A study in 2007 found 4-PBA acts as a chemical chaperone capable of decreasing ER stress, for this reason I wished to examine its impact on strains' growth (Yam *et al.*, 2007).

6.2. Results

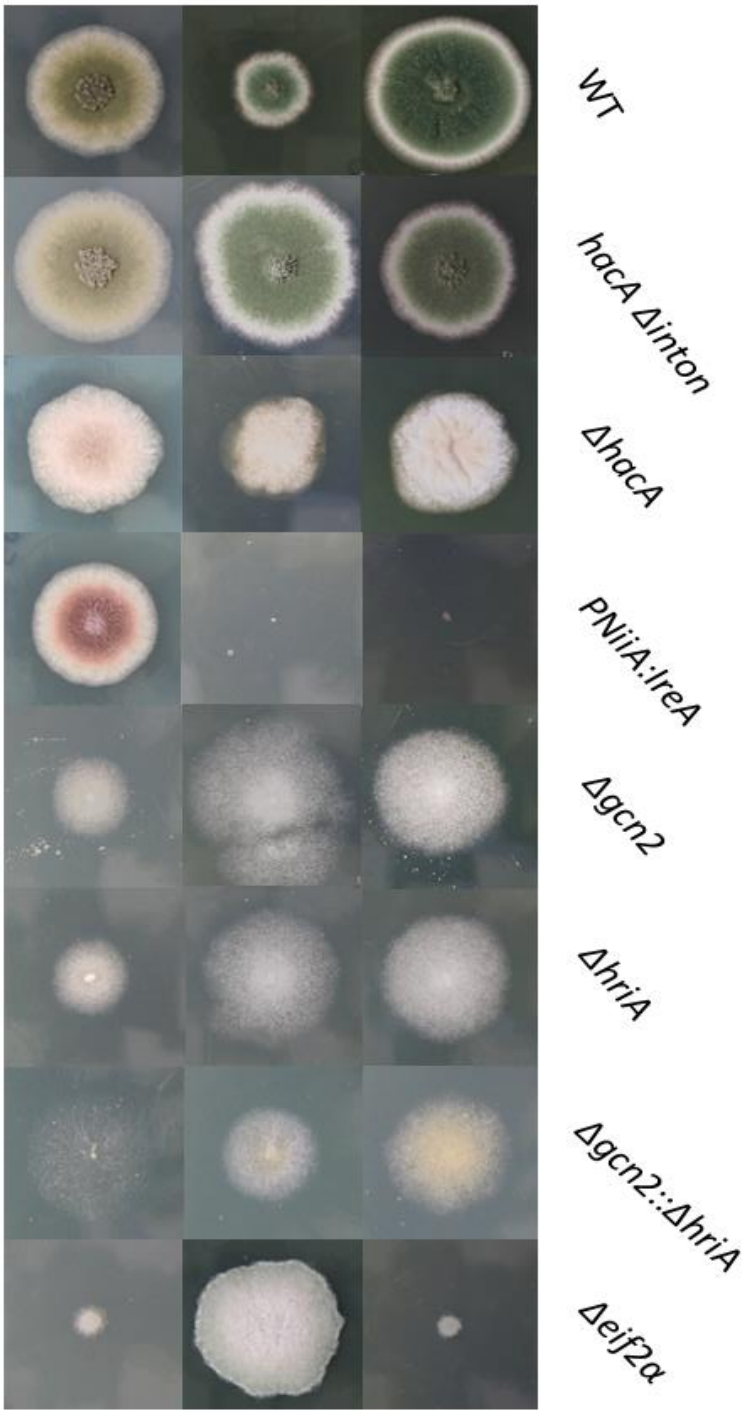

Figure 6. 1 Growth phenotypes of *hacA* and *ireA* mutants. Comparison of WT and mutant strains after 72 hours growth on MM with ammonium as nitrogen source at 37°C and 30°C and growth on NaNO3 as the nitrogen source at 37oC. I can see that the PniiA::IreA strain does not grow without NO3. Δgcn2ΔhriA shows similar growth under control conditions as Δgcn2 and ΔhriA and only slightly diminished growth at 30°C. Δeif2α shows very good growth at 30°C.

Fig 6.1 shows that under control conditions (37°C + NH_4^+) that the WT grows the most efficiently, with *ΔhacA*, *hacA Δintron*, *Δgcn2* and *ΔhriA* strains all displaying approximately equal diameters of colony growth. Other than a marginal reduction in colony size *hacA Δintron* strain appears similar to WT, with good conidiation while the *ΔhacA* mutant displays no conidiation. The *Δgcn2*, *ΔhriA* and *Δgcn2ΔhriA* strains display sparse colonies with media clearly visible. The *Δeif2α* mutant displays very poor growth while the *PniiA::ireA* strain shows no growth.

At 30°C on NH_4^+ WT grows well but not as efficiently as at 37°C, while the *hacA Δintron* mutant produces a slightly larger colony at the lower temperature. The poor growth morphologies of the *ΔhacA, Δgcn2* and *ΔhriA* strains and the failure of the *PniiA::ireA* mutant to grow were not rescued at the lower temperature. *Δgcn2ΔhriA* displays reduced growth at 30 °C compared to 37 °C. The *Δeif2α* strain displays a large increase in growth compared to 37°C.

Altering the nitrogen source to $NaNO_3$ leads to the *hacA Δintron* strain showing a marginally larger colony than WT and for both strains the conidiation is reduced and its pigmentatoin altered. The *ΔhacA* and *Δeif2α* mutants show similar growth to that observed on NH_4^+, while both *Δgcn2* and *ΔhriA* show marginally decreased growth. The reduced growth for the single *eif2α* kinase mutants is not as drastic as the reduced growth of the double mutant *Δgcn2ΔhriA* The most striking difference is for the *PniiA::ireA* strain, which shows healthy growth with $NaNO_3$. This is consistent with *ireA* being expressed in the presence of NO_3 due to the *niiA* promotor, *ireA* being essential.

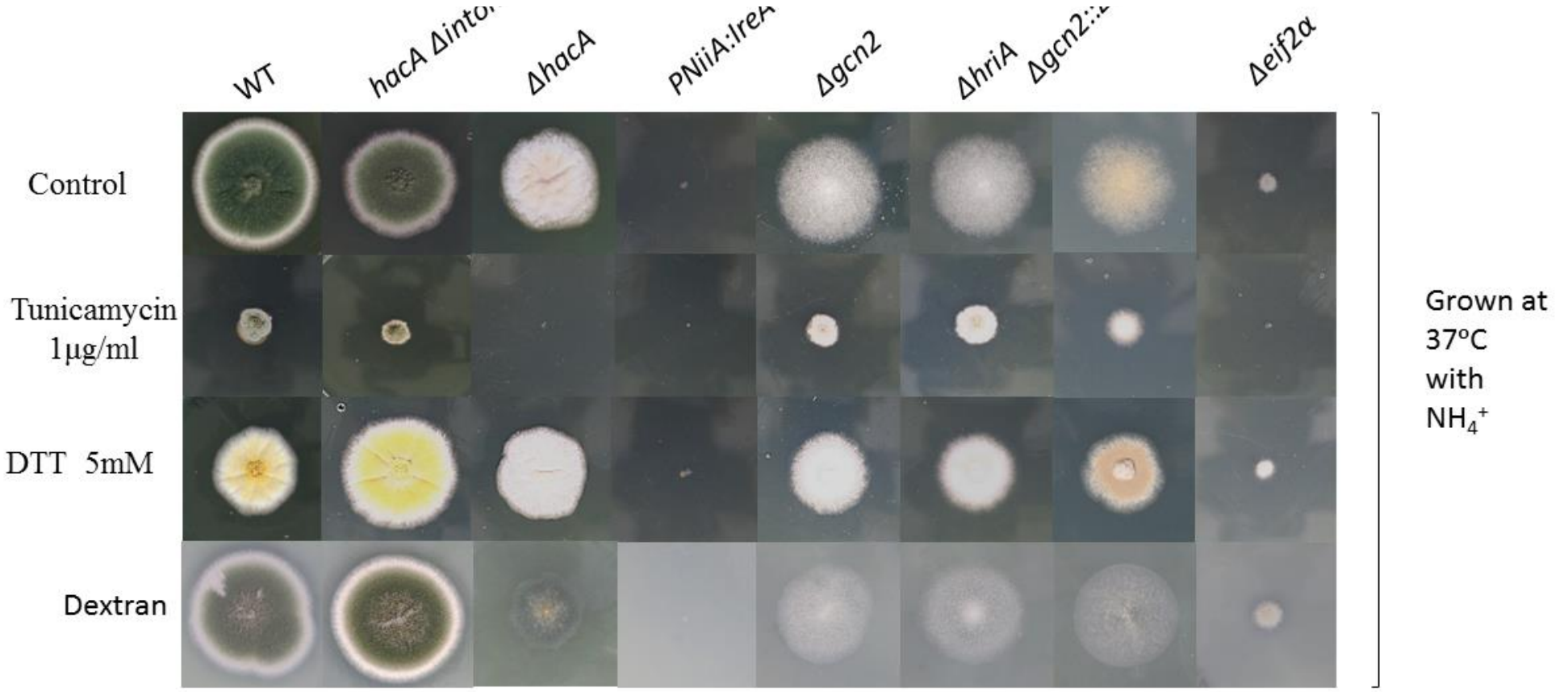

Figure 6.2 **Comparison of growth for wild type and mutant strains under ER stress inducing conditions.** WT and mutant strains (as indicated) were grown on minimal media at 37°C for 72 hours. The effect of tunicamycin, DTT or replacing glucose with dextrin was assessed. The *PNiiA:ireA* strain displayed no growth. Tunicamycin inhibits colony size for all strains or halts growth entirely. The *hacA Δintron* mutant displayed better growth than WT in the presence of DTT. The *Δeif2α* mutant showed similar growth on all media except tunicamycin containing media, where there is no visible growth. Dextrin (1%) inhibits *ΔhacA* growth. Both the WT and *hacA Δintron* strains showed distinct zones of clearance on the dextrin media.

Fig 6.2 compares control conditions and media containing ER stressors DTT and tunicamycin as well as an inducer of amylolytic genes, dextrin. Tunicamycin, which disrupts protein glycosylation and induces ER stress significantly reduces colony growth of WT, *Δgcn2, ΔhriA*, *Δgcn2ΔhriA* and *hacA Δintron* strains, *w*hilst both the *ΔhacA* and *Δeif2α* mutants showed no signs of growth. DTT showed inhibitory effects on growth for WT, *Δgcn2* and *ΔhriA* strains while the poor growth of *ΔhacA* and *Δeif2α* mutants was not exacerbated by DTT. The *hacA Δintron* strain, showed similar colony size in the presence and absence of DTT, sugesting that it is capable of mitigating DTT induced stress more efficiently than WT. Interestingly WT and *hacA Δintron* both show yellow pigmentation. An increase in yellow pigment production has been shown in other fungal spp. when under various stresses such as high temperature and high glucose conditions. This was found to be due to secondary metabolite production during altered metabolic pathways to cope with external stress (Babitha, Soccol and Pandey, 2007; Huang *et al.*, 2017). Dextran as sole carbon source shows inhibitory effects for the *ΔhacA* strain, as evidenced by poor and undefined growth. The *Δgcn2* and *ΔhriA* strains, whilst able to grow, show patchy weak colonies indicating difficulty utilizing dextrin as a substrate. WT and *hacA Δintron* strains show strong growth, with clear zones around the colony indicating succesfull breakdown of dextrin, this clearing is not evident for the *Δgcn2, ΔhriA* and *Δgcn2ΔhriA* strains. This may indicate less efficient secretion capacity for the *eif2α* kinase mutants. The *Δeif2α* mutant displays marginally better growth than under control conditions and there is mild clearing around the colony. This indicates succesful secretion of the required enzymes for growth on dextran.

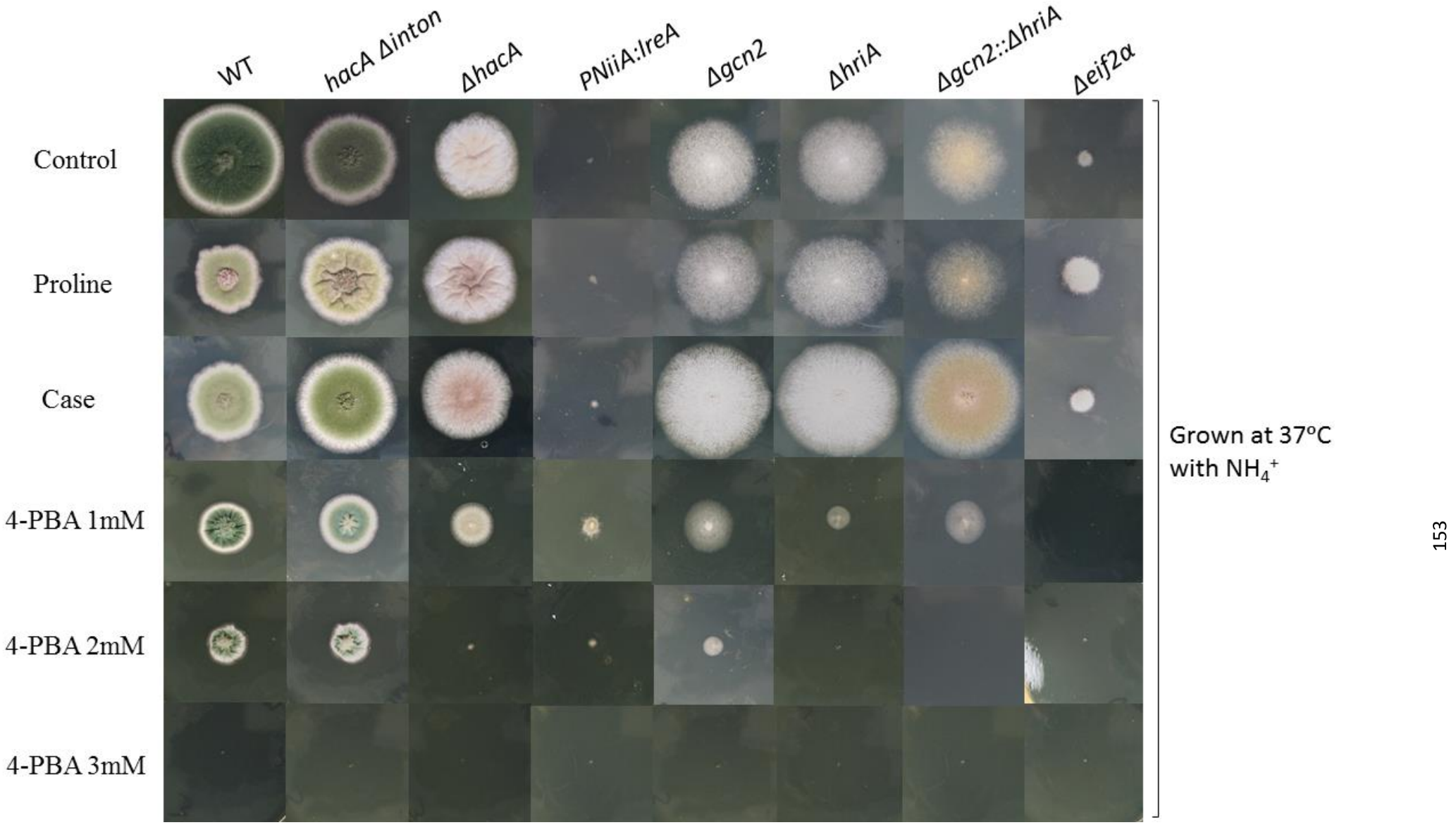

Figure 6 3 Comparison of growth for wild type and mutant strains under potential ER stress reducing conditions. WT and mutant strains (as indicated) were grown on minimal media at 37°C for 72 hours. The effect of proline, casein hydrolysate (case) and 4-phenylbutyrate (4-PBA) was assessed. The *P_{NiiA}::IreA* strain displays growth with 4-PBA at 1 mM and small growth at 2 mM. *P_{NiiA}::IreA* does not grow otherwise. Proline inhibits WT growth and increases *Δeif2α* growth, no obvious changes for other strains with proline. Case appears to slightly limit WT growth while improving growth for *Δeif2α* kinases mutants. No visible change in growth for other mutants with case.

Fig 6.3 displays growth for WT and each mutant strain when grown with potential ER stress alleviators. With the exception of the WT and *Δeif2α* strains 1% proline addition does not have a striking differential effect on growth, when compared to control conditions. WT has diminished growth whereas *Δeif2α* displays larger colony size with proline addition. Casein hydrolysate (case) led to *Δgcn2*, *ΔhriA* and *Δgcn2ΔhriA* strains to grow more efficiently as evidenced by larger colony sizes and more conidiation. This is consistent with both mutants leading to reduced ability to synthesise amino acids. The *ΔhacA* mutant grows to a similar degree but displays improved conidiation with case. The *Δeif2α* strain on case containing media has a slightly increased diameter compared to control media. WT grew less efficiently with case addition compared to control media. While the *hacA Δintron mutant* displayed similar growth in the presence and absence of case.

4-PBA diminishes growth of all strains tested except the *PniiA::ireA* strain and no strain was able to grow at 3 Mm 4-PBA. The rescue of *PniiA::ireA* by exogenous 4-PBA is most apparent at the 1 mM concentrations but also apparent at 2 mM. This is occuring in spite of the presence of NH_4^+ and absence of NO_3^- in the media which imply ireA is not being expressed. Interestingly 4-PBA is the only condition that appears to differentiate the growth phenotypes of *Δgcn2* and *ΔhriA* mutants, *Δgcn2* showing better growth with 4-PBA than *ΔhriA* at both 1 and 2 mM concentrations. The *Δgcn2ΔhriA* shows growth similar but slightly improved to that of *ΔhriA* with exogenous 4-PBA. The *Δeif2a* mutant was unable to grow.

6.3. Discussion

From these results it would appear that the biggest impact on the cells health is disruption of *ireA*. This is expected due to the lethality of *ireA* deletion. Whilst the *Δgcn2, ΔhriA* and *Δgcn2ΔhriA* grow well with case addition to media, loss of either kinase is more detrimental than deletion of *hacA*. The *ΔhacA* strain displays a sick phenotype but this remains relatively unaltered regardless of the media with the exceptions of tunicamycin and casein addition, tunicamycin inhibiting growth and casein inducing conidiation. These data would imply that all four strains showing improved conidiation with casein hydrosylate, are unable to iniate AA biosynthesis pathways. Increased conidiation by *ΔhacA* with casein supplementation implies that when grown on MM the strain is behaving as though there is limited nutrients in the environment. This fits with the work of Walter and Patil who identified *gcn2* is linked with the ERSR. *Δgcn2, ΔhriA* and *Δgcn2ΔhriA* all have colonies where growth is not evenly spread as the medium is visible. Every other strain shows thick growth over the media from the point of inoculation. The poorer growth of *eif2α* kinase mutants compared to *ΔhacA* combined with the newly confirmed RIDD, it is clear that upon ER stress, limiting nascent peptides entering the lumen is more beneficial to stress attenuation than upregulation of ERSR gene targets. Of note is that both *Δgcn2, ΔhriA* and *Δgcn2ΔhriA* displayed poor growth in liquid cultures without the addition of casein hydrolysate. Before discovering the benefit of adding casein hydrolysate, attaining enough biomass for experimentation of the *eif2α* kinase KO mutants required 5-7 days growth. Also, biomass varied between replicates despite the same volume of inoculation. The most interesting result from this section of the research is the growth of *PNiiA::ireA* while retaining repression of *ireA* through NH_4. The presence of 4-PBA, known to lower ER stress, recovers this strains ability to grow. 1 mM 4-PBA addition to liquid MM was sufficient to grow *PNiiA::ireA* overnight (data not shown). This finding is by far the largest indicator that *ireA* is involved in a role related to ER stress that is distinct from *hacA* activation; loss of *hacA* does

not lead to inviability whereas *ireA* loss (without 4-PBA) does. If *ireA's* only role were HACA activation then the *ΔhacA* should be inviable also. I consider this further confirmation of RIDD. 4-PBA also seems to have a detrimental effect at 1mM concentration as evidence by decreased growth for the majority of strains. Interestingly, *gcn2* and *ΔhriA* show very similar phenotypes on each media except for those containing 4-PBA where *Δgcn2* clearly grew better; this indicates a role for *gcn2* in alleviating ER stress which would fit with the role of *gcn2* in *S. cerevisiae* in biasing translation towards ERSR target genes. For this experiment 4-PBA was dissolved in ethanol which was then added to the media; this could explain the apparent toxic effect and why larger concentrations led to diminished growth. Further work would be utilizing 4-PBA to observe its effects on growth.

7. ER stress quantification

7.1. Introduction

7.1.1. Current quantification methods

The majority of research into the ER stress response relies on the stress response being quantified after samples have been treated, harvested and then subject to techniques to measure mRNA/protein levels of specific targets. These techniques are both old and new, including northern/western blotting, RNA-seq derived data and the use of reporter constructs providing a quantifiable response. Other means include measuring dilation of the ER to specific pathway quantification such as quantifying IRE1 or PERK phosphorylation (Oslowski and Urano, 2011). Whilst measuring ER dilation is a viable approach to view induction of ER stress it does not provide insight into how quickly protein aggregation is mitigated nor does it allow for a means of standardizing quantification due to the varied structure of the ER. ER dilation occurs in response to protein aggregation, however as can be seen through the persistence of ERSE altered translatomes more than three hours after stressing of mammalian cells, dilation may persist after protein aggregation has been resolved (Kochetov and Montaner, 2012). So dilation/constriction of the ER is only one aspect of the response and may not be indicative in itself of unfolded protein attenuation. A method of measuring real time protein aggregation is far more beneficial. This would be of great benefit for both academic and industrial research purposes. An industrial example being a company with a host of recombinant proteins as potential products; some will be more difficult for strains to produce due to the limitations of the cells folding machinery, protein toxicity etc. The ability to screen which proteins induce less ER stress, thereby avoiding protein accumulation, potential apoptosis etc. would be beneficial in selecting which protein candidates are carried through to large scale fermentation. From an academic research

viewpoint, being able to determine the effect of a genes impact on ER stress mitigation would save on costly quantification methods. This would allow for honing of research time by focusing on the genes which have the most significant roles in the ER stress response.

In this chapter I examine a new method of quantifying ER stress, via protein aggregation, through the use of confocal microscopy and the fluorescent dye Thioflavin T (ThT). I wished to determine the viability of this technique for use in fungal systems.

7.1.2. Thioflavin T based ER stress quantification

Originally used as a histochemical dye, ThT is a benzothiazole salt which has increased fluorescence when bound to protein aggregates (Vassar and Culling, 1959; Hospital, 1967). Due to this property, it has been used in various studies ranging from Alzheimer's and prion disease research to extracellular protein characterization (Khurana *et al.*, 2005; Polyneuropathy *et al.*, 2006; Hawe, Sutter and Jiskoot, 2008). ThT was identified as being highly specific to amyloid plaques, earning itself the title of the "gold standard" for examining amyloid fibrils (Biancalana and Koide, 2010). Despite this, the mechanism of how ThT binds amyloid fibrils has not been confirmed; it is thought ThT binds to channels that exist along the long axis of amyloid fibrils (Krebs, Bromley and Donald, 2005. Xue et al., 2017).

A study utilizing mammalian cells found it is possible to quantify ER stress *in vivo* with the use of a ThT and confocal micrscopy. ThT was found to be a suitable dye to use for measuring ER stress response as they found a direct correlation between fluorescence and ER stress, which they determined by subsequent measuring of *bipA* induction. The study carried out analysis of both live and fixed cells making this a useful tool for studying ER stress (Beriault and Werstuck, 2013).

Whilst this technique has shown promise in mammalian cells, it is as yet undetermined if it is applicable to fungal strains. I therefore carried out a time course experiment to determine if ThT is able to diffuse across the fungal cell wall and if there is measurable changes in fluorescence levels upon stress induction.

7.2. Results

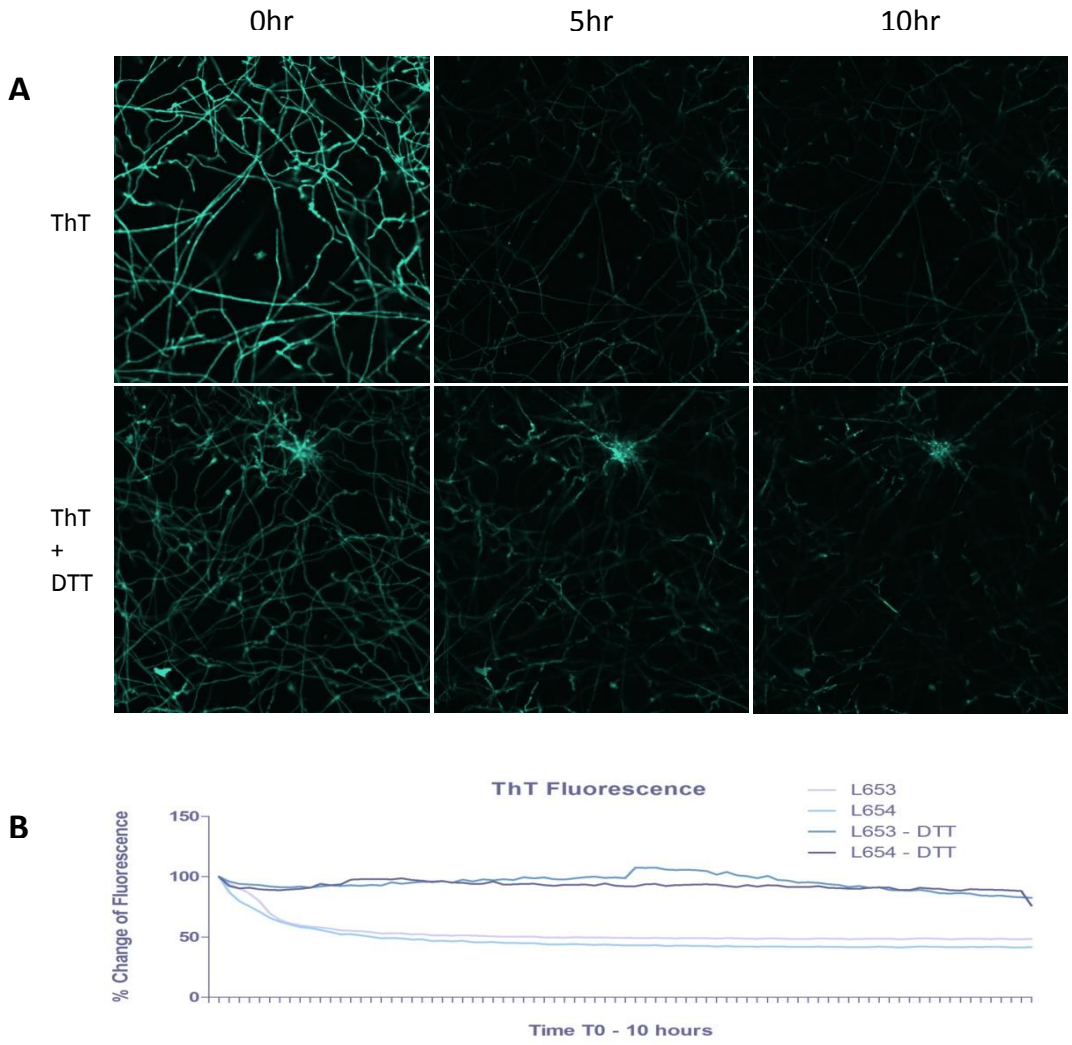

Figure 7.1 Images of *A. nidulans* subjected to ER stress in the presence of ThT. A shows Images taken on the LS 710 confocal microscope. WT cells were either treated with 5 µM ThT and 20 mM DTT or 5 µM ThT alone. B shows levels of fluorescence levels of the entire visible region over a 10 hour time period. Quantification of fluorescence carried out with ImageJ software.

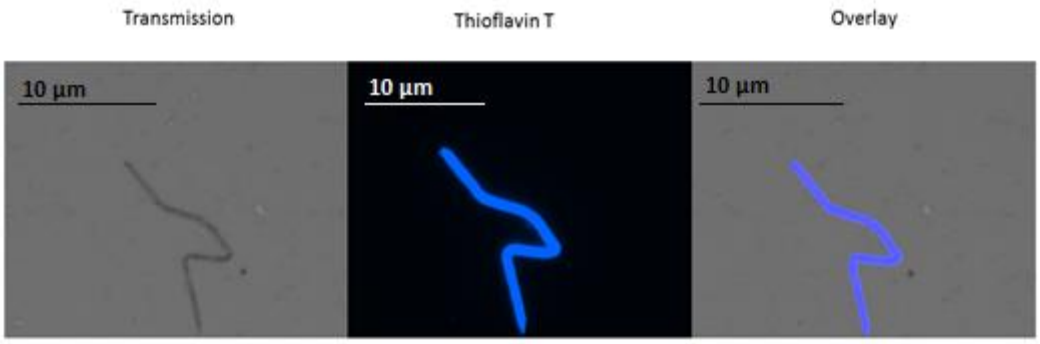

Figure 7.2 An example of images taken on the EVOS microscope of WT under control conditions. Transmission and DAPI images are shown plus an overlay of the two.

From Fig 7.1 and 7.2 I can observe that ThT is able to penetrate the fungal cell well allowing for further exploration of the dye's suitability from quantifying ER stress in fungi. I carried out a time course experiment treating cells to 20mM DTT and then fixing them with paraformaldehyde at 10, 20 and 30 min. Control samples were left untreated and fixed. Results are presented with transcriptional mutants and translational mutants collated separately.

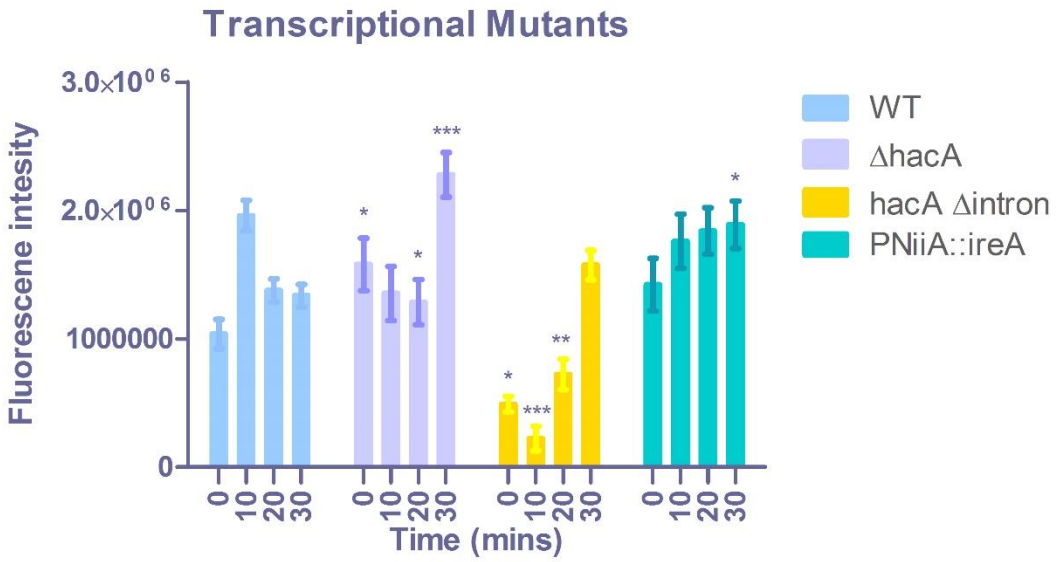

Figure 7 3 A comparison of ER stress between WT and ER stress response transcriptional mutants over a 30 min time course. WT shows an initial increase in fluorescence after 20 mM DTT treatment at 10 min which then lowers over the time period but does not return to control levels. ΔhacA shows a decrease after DTT treatment until 30 min which see an increase. hacA Δintron has the lowest level at control conditions, an initial drop after DTT addition which then rises over at 20 min and 30 min. P_{NiiA}::ireA shows an initial high level under control conditions which gradually increases throughout until 30 min. Statistical analysis conducted with 2-Way ANOVA comparing mutant time points with WT equivalent. Significance levels * {<0.05} ** {<0.01} *** {<0.0001}. N=15

Fig 7.3 shows that the WT experiences a sharp increase in fluorescence at 10 min of DTT treatment which then drops by 20 min and further by t_{30} but does not return to control levels within the times measured. *ΔhacA* has a significantly higher level of fluorescence under control conditions than the WT ($p < 0.05$). At 10 and 20 min of DTT treatment there is a small decrease in intensity until 30 min which sees a sharp rise to levels above the highest level observed in the WT at 10 min. *hacA Δintron* has the lowest levels of fluorescence under control conditions for any strain. After DTT treatment there is a drop in intensity followed by large increases throughout the rest of the time course. This was considered significantly different ($p<0.0001$). *P_{niiA}::ireA* was grown overnight in NO_3^- before washing and incubating with MM + NH_4^+ for 24 hours repressing *ireA* transcription. *P_{niiA}::ireA* shows higher levels of fluorescence under control conditions compared to WT and has modest increases in intensity over the times measured. The WT is the only strain observed to show an increase in fluorescence that is then lowered over the remaining time points. *ΔhacA* and *hacA Δintron*

time course results are significantly different based on 2-way ANOVA analysis ($p < 0.0001$) whereas the *PNiiA:ireA* was not. Specific time points were analysed with the Bonferroni post-test with each strain being compared to the WT.

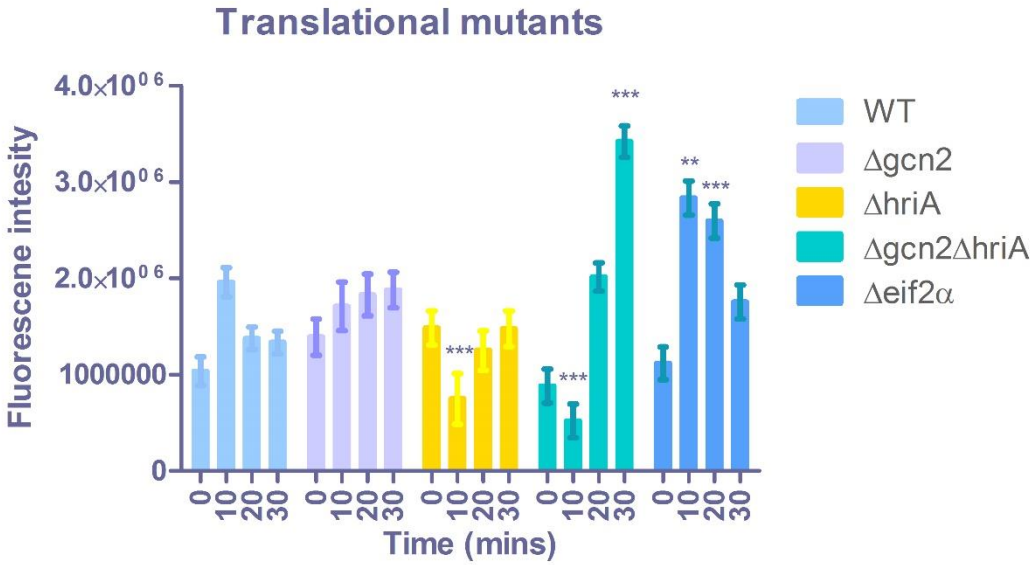

Figure 7.4 A comparison of ER stress between WT Δeif2a, Δgcn2, Δgcn2ΔhriA and ΔhriA mutants over a 30 min. Strains were grown in MM + NH_4^+ and treated with 20 mM DTT before fixing and staining. WT shows an initial increase in fluorescence after DTT addition which then decreases but does not return to control conditions by 30 min. Δgcn2 shows a gradual increase in fluorescence over the time course. ΔhriA has an initial decrease at 10 min followed by an increase at 20 and 30 min. Δgcn2ΔhriA shows an initial decrease followed by large increases in fluorescence leading to the highest level measured for all strains at 30 min. Δeif2a shows a large increase after DTT treatment followed by a slow decline which doesn't reach control levels by 30 min. Statistical analysis conducted with 2-Way ANOVA comparing mutant time points with WT equivalent. Significance levels * {<0.05} ** {<0.01} *** {<0.0001}. N=15

Fig 7.4 shows the WT results as shown in Fig 7.3. The *Δgcn2* strain shows a steady increase over the time course after DTT treatment. There was no significant difference between the WT and *Δgcn2* results. *ΔhriA*, *Δgcn2ΔhriA* and *Δeif2α* results are significantly different based on 2-way ANOVA analysis ($p < 0.001$, < 0.0001 and < 0.05 respectively). The *ΔhriA* strain has similar levels of fluorescence as can be seen in *Δgcn2* under control conditions but has an initial drop in fluorescence intensity at 10 min, this is then followed by gradual increase until 30 min which sees a return to control levels. The *Δgcn2ΔhriA* double mutant, under control conditions, has slightly lower levels of fluorescence comparative to the WT. DTT treatment

at 10 min shows a modest decrease as observed for *ΔhriA*. Samples at 10 min and 30 min see dramatic increases with 30 min providing the highest level of fluorescence observed for all strains tested. Overall the *Δgcn2ΔhriA* displays the same trend as *ΔhriA* but more exaggerated. *Δeif2α* has similar control levels of fluorescence as the WT but has a larger increase in intensity at 10 min than the WT. Similarly to WT, *Δeif2α* showed decreasing levels of fluorescence at 10 min and 30 min but do not return to control levels. *Δeif2α* shows the most similar trend to that of the WT.

7.3. Discussion

7.3.1. Thioflavin T as a means of ER stress quantification

I can see from Fig 7.1 and 7.2 that the ThT is capable of fungal cell entry suggesting that this new method of ER stress quantification is viable for fungal systems. However, the uniformity of the ThT binding is a concern as it is not localised to the ER. The study validating ThT flouresence as a proxy for ER stress displayed clear localisation (Beriault and Werstuck, 2013). I carried out a literature search for the presence of amyloid fibrils in fungi to clarify why the fluorescence wasn't localising to the ER; amyloid fibrils and amyloid like proteins are a key component in fungal cell walls (Kalebina et al., 2008. Lipke et al., 2012. Nayyar et al., 2017). This is therefore a major issue for using this dye as a means of quantifying ER stress. We can see from Fig 7.1 that DTT induced ER stress prolongs fluorescence of ThT compared to ThT alone; at best the results of this chapter could be used as a preliminary indicator of which component of the ERSR has the largest effect on stress alleviation. Optimization and a fungal specific protocol need to be developed before this could be considered a realible means of quantifying ER stress in fungal systems. This may be an insurmountable issue.

7.3.2. Transcriptional mutants and ER stress

Fig 7.3 shows that there is variation between the *hacA* mutants comparative to the WT with respect to dealing with protein aggregates. From the results, loss of HacA leads to high levels of protein aggregation after DTT treatment. This is unsurprising given a key component of the transcriptional response to ER stress has been removed, presumably leading to a reduced capacity to deal with it. From Fig 3.11 I can see both *ΔhacA* and *hacA Δintron* have elevated levels of *bipA* and in the case of *hacA Δintron* increased levels of *hrdC* also (Fig 3.12). These ERSR targets already present may account for the initial observed decrease in fluorescence for both mutants. Two theories could explain this; the increased levels of *bipA, hrdC* and potentially functionally related transcripts may be able to initially attenuate DTT induced stress. Secondly, without substrates to act upon the accumulated ERSR targets may form aggregates themselves and thus account for a portion of the fluorescence measured under control conditions, upon DTT treatment they disassociate and deal with the misfolded proteins. Whereas the WT has to initiate the response after aggregation of protein has reached the threshold for ERSR induction, leading to an initial increase of aggregates that is then dealt with by a fully functional ERSR lowering protein aggregation over the time course. The subsequent increase of fluorescence in *hacA Δintron* could be that the unregulated overexpression of ER stress response genes in the continued presence of DTT leads to further protein aggregation. Under control conditions both *ΔhacA* and *hacA Δintron* have significantly different fluorescence levels. Unsurprisingly, *ΔhacA* having an aspect of the ERSR pathway transcriptionally inert, has higher basal levels of protein aggregation whereas *hacA Δintron,* with the same pathway constitutively active has lower levels of protein aggregation The P_{niiA}*::ireA* strain shows increases of protein aggregation over the time despite exhibiting high levels of *bipA* (see Fig 3.11).This implies increased ERSR targets by themselves are not enough to deal with protein aggregation without *ireA* limiting influx of

new proteins via degradation of transcripts. This provides further evidence that *ireA* plays a role out with *hacA* regulation in regards to ER stress otherwise they would display similar results. However, without HacA to activate its portion of the stress response this would eventually led to an increase in fluorescence as shown at 30 min.

7.3.3. Translational mutants and ER stress

Fig 7.3 shows that loss of *eif2α* or both the putative *eif2α* kinases, leads to the highest fluorescence intensity observed for any strains tested: the most extreme being the double mutant *Δgcn2ΔhriA.* This strongly implies that the newly found translational attenuation observed under ER stress is a key component of the *A. nidulans'* ER stress response. Loss of *gcn2* led to small increases in fluorescence over the time course but these were not considered statistically significant. The *ΔhriA* strain showed a similar trend to the *hacA Δintron* mutant in that there was an initial drop in fluorescence after DTT addition, although it was again not significantly different from the WT control. This result was also unexpected and merits further investigation especially as the same initial decrease after DTT treatment is observed for the double mutant *Δgcn2ΔhriA.* The *Δgcn2 ΔhriA* double mutant exhibits the highest level of fluorescence but with a similar profile to the *ΔhriA* single mutant. This would be consistent with HRIA having the major role in signalling the translational response but GCN2 being able to partially replace its activity. Interestingly *Δeif2α*, whilst showing the highest levels of fluorescence at 10 min begins to recover and show decreases over the time course, implying attenuation of ER stress. This could be explained by loss of *eif2α* causing decreased rates of translation.

8. Discussion

8.1. *hacA* and the ERSR

By examining all the data generated within this project, I can see that although *hacA*'s role isn't entirely as purported by current literature, its loss leads to significant decreases to the cells' growth, translational ability and capacity to secrete products and overall level of ER stress during control conditions. That *hacA* plays a role in the ERSR isn't in doubt, however the importance of the TF to regulating the ERSR as a whole is questionable with the evidence of a second transcriptional pathway. Overexpression of the TF does lead to some benefits; I see reduced or removed translational down regulation in *hacA ΔIintron*, enhanced growth comparative to WT on ER stress inducing media and also based on the limited growth test data, retention of a secretion capacity similar to WT (See Fig 5.4 and 6.2). Further experimentation would need to be carried out with the *hacA ΔIintron* strain to determine whether translational remodelling does occur but at a different time point. I can see from Fig 7.2 that *hacA ΔIintron* displays an initial decrease in fluorescence at 10 min DTT treatment, under the same conditions during polysome profiling I see little to no change in polysome distribution; however at 30 mins during the microscopy experiment I see increasing levels of ER stress. Whilst the microscopy is data is tentative at best, the implication from this data is that loss of translational remodelling observed for the *hacA ΔIintron* may have been temporarily repressed by the abundance of HacA targets present, rather than the remodelling being absent altogether. Another strain that could be produced to identify *hacA* targets more readily would be to create a strain with *hacA ΔIintron* on an inducible promotor. Growth would be impaired but viable based on the Δ*hacA* strain and through sampling before and after induction of *hacA ΔIintron* RNA-seq analysis would allow for a direct comparison of the

HacA targets. This would be more beneficial than constitutive overexpression as there may be unforeseen downstream effects to an overabundance of ERSR targets.

8.2. *ireA* and importance to the ERSR

Now that RIDD has been confirmed in a filamentous fungi, it presents a new avenue to explore as a target to increase RPP. Further extensive experimental work should be carried out to confirm that the observed degradation of *pepJ* and *prtA* isn't specific to these proteases, or specific to nitrogen starved conditions. Ideally several different conditions could be examined, including observations of transcript stability during induction of an industrially relevant enzyme/product. Also, as seen in Fig 3.5 and 3.6, there is a decrease in *actin* and *bipA* transcript levels in the P_{niiA}*:ireA* strain – I believe that this could represent the iniation of ERSR induced apoptosis. This should be tested, The previous publications displaying RESS have already made headway on this; one study found that altering the 5'UTR of the transcripts being monitored negatively affected the subsequent loss after ERSR induction (Al-Sheikh et al., 2004). By altering transcripts' 5'UTR's this may hinder *ireA*'s endoribonuclease domains ability to recognise and cleave them, leading to an increase in the encoded proteins. Future work could involve modifications to *ireA's* RNAse domain in order to determine if the efficacy of RIDD can be diminished. Although, given the lethal nature of an *ΔireA* mutant, dimishing the capacity of the RNAse domain will very likely lead to poor growth. As mentioned in Chapter 3's discussion, an alternative regulatred promotor for *ireA* would be beneficial for analysing transcript degradation given that my time course experiment relied on nitrogen starvation and the *niiA* promotor is involved in nitrogen metabolism. Determining characteristics of RIDD targets in order to modify desirable products would be very beneficial to industry. This could be achieved through RNA-seq work carried out during conditions that exacerbate enzyme secretion, dextran for example.

That *ireA* has a role outside of HacA activation is clear, and that this is linked to the ERSR is also clear due to P_{niiA}*:ireA's* ability to grow with 4-PBA addition while repressing *ireA* expression. Whilst I have confirmed RIDD, there is also the possibility that *ireA* is responsible for signalling *gcn2*/*hriA* and initiating the translational remodelling observed. *ireA* is currently the only known ER bound protein with a role in the ERSR and this potential crosstalk to *gcn2*/*hriA* should be explored. Is there physical interaction between the three kinases, or is any regulation a downstream effect of *ireA* activation? The literature is clear that throughout eukaryotes there is e cross talk between the various aspects of the ERSR (Ron and Walter, 2007, Tsuru *et al.*, 2016). An interesting avenue of investigation would be to cross the *Δgcn2*, *ΔhriA* and *Δgcn2hriA* strains with the P_{niiA}:*ireA* strain. Four conditions for each strain would be needed to assess the potential cross talk between *ireA* and the *eif2α* kinases; all conditions would need overnight growth in MM + casein hydrosylate + NO^{3-}. The controls therefore are the *eif2αK*:P_{niiA}:*ireA* grown in *ireA* inducing media and either left untreated or exposed to DTT. These cells would need to be washed and returned to MM + casein hydrosylate + NO^{3-} whilst the biomass for the experimental work would be transferred to MM + casein hydrosylate + NH^{4+} to inhibit *ireA* expression. These flasks would then need to be left untreated and DTT treated. This would be a large piece of work but the data would be very interesting and yield a large amount of data if followed up with transcriptomic analysis beyond just *bipA* measurement.

8.3. Translational attenuation and the importance to regulating ER stress

From Fig 7.3 I can see loss of both *gcn2* and *hriA* leads to the largest level of ER stress measured for any strain over the time course. This would propose that translational attenuation during ER stress is a more significant aspect of the ERSR than the roles of *ireA* or *hacA*. While the microscopy data is only tentative it does fit with some other observations such as the rapid decrease then increase in RT observed within just 15 min of DTT exposure

(Fig 5.1) .This would be logical; altering the transcriptome will help mitigate ER stress through induction of genes that can act to lower the accumulation of misfolded protein. However, without a means of regulating rates of protein translation, and in particular biasing translational machinery to desirable targets, altering the transcriptome will only help alleviate ER stress so much when there is still a constant influx of nascent peptide. Further testing is necessary to confirm if the *eif2α* kinases do illicit biasing of translational machinery to specific transcripts as is seen with gcn2p/gcn4p in S. cerevisiae. Limiting this influx gives the ER time to return to homeostasis. This is a significant find for researchers examining the ERSR in filamentous fungi. Whilst this response has been identified a lot more work needs to be carried out to clarify the roles *gcn2* and *hriA* perform, including which kinase is responsible for specific stressors. Particularly interesting would be determining the role *hriA* appears to have on ribosomal association of transcripts. The loss of *hriA* in both the single and double mutant led to very high levels of *bipA* association with polysomes. Determining the mechanism/machinery responsible for a transcripts RT would be very beneficial for RPP.

8.4. Relevance to RPP

The newly found attenutation of RT in the fungal ERSR could prove a very potent target for increasing RPP yield. This could be achieved through determining what properties transcripts that are biased for translation during ER stress have that can be conveyed to transcripts encoding desired products. Utilization of this in concert with inducible constitutive expression of *hacA Δintron* for example could lead to increased yields. Ascertaining if *atfA* is indeed responsible for the second transcriptional pathway I have identified evidence for would further this ability to modify the ERSR to increase RPP yields. Further to this, including the findings of Pakula's work, whereby they altered the 5'UTR of transcripts and this appeared to show less down-regulation/degradation, there is potential to modify transcripts to avoid RIDD whilst being actively translated during ER stress in a strain which

is already resistant to translational remodelling (Pakula *et al.*, 2003). This endeavour would take a large amount of work to create all the necessary combinations of mutants and a suitable assay for protein secretion would need to be employed to determine any alterations in yields. However, the new targets of the ERSR provide innovative avenues to increase protein production which includes homologous as well as heterologous proteins. Whilst the ThT assay does is not specific in fungi due to the amyloid fibril adhesion motifs displayed on cell walls, another dye following the same principle could allow for screening of new strains derived from ERSR mutants with relative ease. The potential an optimized functioning assay to quantify ER stress could have for screening mutant's warrants further investigation. Future work should also include examining each of this projects strains for protein aggregation levels during production of a recombinant protein as well as secretion levels of the product. This would give insight into which strain copes better with recombinant protein production at a translational stage while also analysing secretion output. This would indicate which aspect of the ERSR is providing the largest bottleneck to RPP.

8.5. Conclusions

In regards to this projects purpose to examine the ERSR and identify potential new targets for increasing RPP yield, I consider this very successful. There is still a lot of work to be done in order to clarify each regulator of the ERSR and their exact function. I propose that the fungal ERSR is functionally no different, and certainly no less complex, than that of higher eukaryotes (see Fig 8.1). Indeed, in regards to translational attenuation during ER stress, *A. nidulans* has an incredibly robust system compared to mammalian cells.

The RPP industry impacts on numerous fields, the hope of this researcher is that the findings in this project may someday increase RPP, particularly for pharmaceuticals and those industries impacting people's everyday quality of life.

9. References

Acharya, P., Chen, J. and Correia, M. (2010). Hepatic heme-regulated inhibitor (HRI) eukaryotic initiation factor 2 kinase: A protagonist of heme-mediated translational control of CYP2B enzymes and a modulator of basal endoplasmic reticulum stress tone. *Molecular Pharmacology*, 77(4), pp.575-592.

Aebi, M. (2001). Congenital disorders of glycosylation: genetic model systems lead the way. *Trends in Cell Biology*, 11(3), pp.136-141.

Alder, N., Shen, Y., Brodsky, J., Hendershot, L. and Johnson, A. (2005). The molecular mechanisms underlying BiP-mediated gating of the Sec61 translocon of the endoplasmic reticulum. *The Journal of Cell Biology*, 168(3), pp.389-399.

Al-Sheikh, H., Watson, A., Lacey, G., Punt, P., MacKenzie, D., Jeenes, D., Pakula, T., Penttilä, M., Alcocer, M. and Archer, D. (2004). Endoplasmic reticulum stress leads to the selective transcriptional downregulation of the glucoamylase gene in *aspergillus niger*. *Molecular Microbiology*, 53(6), pp.1731-1742.

Alves, V., Motta, F., Roffé, M., Delamano, A., Pesquero, J. and Castilho, B. (2009). GCN2 activation and eIF2α phosphorylation in the maturation of mouse oocytes. *Biochemical and Biophysical Research Communications*, 378(1), pp.41-44.

Anderson, D. and Hetzer, M. (2008). Shaping the endoplasmic reticulum into the nuclear envelope. *Journal of Cell Science*, 121(2), pp.137-142.

Appenzeller-Herzog, C., Riemer, J., Zito, E., Chin, K., Ron, D., Spiess, M. and Ellgaard, L. (2010). Disulphide production by Ero1α–PDI relay is rapid and effectively regulated. *The EMBO Journal*, 29(19), pp.3318-3329.

Arst, H. and Cove, D. (1973). Nitrogen metabolite repression in *Aspergillus nidulans*. *MGG Molecular & General Genetics*, 126(2), pp.111-141.

Archer, D. and Peberdy, J. (1997). The Molecular Biology of Secreted Enzyme Production by Fungi. *Critical Reviews in Biotechnology*, 17(4), pp.273-306.

Ashe, M., De Long, S. and Sachs, A. (2000). Glucose depletion rapidly inhibits translation initiation in Yeast. *Molecular Biology of the Cell*, 11(3), pp.833-848.

Babitha, S., Soccol, C. and Pandey, A. (2007). Effect of stress on growth, pigment production and morphology of *Monascus sp*. in solid cultures. *Journal of Basic Microbiology*, 47(2), pp.118-126.

Baird, T., Palam, L., Fusakio, M., Willy, J., Davis, C., McClintick, J., Anthony, T. and Wek, R. (2014). Selective mRNA translation during eIF2 phosphorylation induces expression of IBTKα. *Molecular Biology of the Cell*, 25(10), pp.1686-1697.

Balázs, A., Pócsi, I., Hamari, Z., Leiter, É., Emri, T., Miskei, M., Oláh, J., Tóth, V., Hegedűs, N., Prade, R., Molnár, M. and Pócsi, I. (2010). *AtfA* bZIP-type transcription factor regulates

oxidative and osmotic stress responses in *Aspergillus nidulans*. *Molecular Genetics and Genomics*, 283(3), pp.289-303.

Backhaus, R., Zehe, C., Wegehingel, S., Kehlenbach, A., Schwappach, B. and Nickel, W. (2004). Unconventional protein secretion: membrane translocation of FGF-2 does not require protein unfolding. *Journal of Cell Science*, 117(9), pp.1727-1736.

Basturea, G., Zundel, M. and Deutscher, M. (2010). Degradation of ribosomal RNA during starvation: Comparison to quality control during steady-state growth and a role for RNase PH. *RNA*, 17(2), pp.338-345.

Biancalana, M. and Koide, S. (2010). Molecular mechanism of Thioflavin-T binding to amyloid fibrils. *Biochimica et Biophysica Acta (BBA) - Proteins and Proteomics*, 1804(7), pp.1405-1412.

Bernales, S., McDonald, K. and Walter, P. (2006). Autophagy counterbalances endoplasmic reticulum expansion during the unfolded protein response. *PLoS Biology*, 4(12), p.e423.

Bernales, S., Papa, F. and Walter, P. (2006). Intracellular Signaling by the Unfolded Protein Response. *Annual Review of Cell and Developmental Biology*, 22(1), pp.487-508.

Berka, R., Kodama, K., Rey, M., Wilson, L. and Ward, M. (1991). The development ofAspergillus nigervar.awamorias a host for the expression and secretion of heterologous gene products. *Biochemical Society Transactions*, 19(3), pp.681-685.

Boedtker, H. (1971). Conformation independent molecular weight determinations of RNA by gel electrophoresis. *Biochimica et Biophysica Acta (BBA) - Nucleic Acids and Protein Synthesis*, 240(3), pp.448-453.

Bogdanov, M., Sun, J., Kaback, H. and Dowhan, W. (1996). A phospholipid acts as a chaperone in assembly of a membrane transport protein. *Journal of Biological Chemistry*, 271(20), pp.11615-11618.

Bright, M., Itzhak, D., Wardell, C., Morgan, G. and Davies, F. (2015). Cleavage of BLOC1S1 mRNA by IRE1 is sequence specific, temporally separate from XBP1 splicing, and dispensable for cell viability under acute endoplasmic reticulum stress. *Molecular and Cellular Biology*, 35(12), pp.2186-2202.

Burke, B. and Ellenberg, J. (2002). Remodelling the walls of the nucleus. *Nature Reviews Molecular Cell Biology*, 3(7), pp.487-497.

Burwick, N., Zhang, M., de la Puente, P., Azab, A., Hyun, T., Ruiz-Gutierrez, M., Sanchez-Bonilla, M., Nakamura, T., Delrow, J., MacKay, V. and Shimamura, A. (2017). The eIF2-alpha kinase HRI is a novel therapeutic target in multiple myeloma. *Leukemia Research*, 55, pp.23-32.

Caddick, M., Jones, M., van Tonder, J., Le Cordier, H., Narendja, F., Strauss, J. and Morozov, I. (2006). Opposing signals differentially regulate transcript stability in *Aspergillus nidulans*. *Molecular Microbiology*, 62(2), pp.509-519.

Caddick, M., Peters, D. and Platt, A. (1994). Nitrogen regulation in fungi. *Antonie van Leeuwenhoek*, 65(3), pp.169-177.

Caldwell, S., Hill, K. and Cooper, A. (2001). Degradation of endoplasmic reticulum (ER) quality control substrates requires transport between the ER and Golgi. *Journal of Biological Chemistry*, 276(26), pp.23296-23303.

Carrasco, S. and Meyer, T. (2011). STIM proteins and the endoplasmic reticulum-plasma membrane junctions. *Annual Review of Biochemistry*, 80(1), pp.973-1000.

Carvalho, N., Arentshorst, M., Jin Kwon, M., Meyer, V. and Ram, A. (2010). Expanding the ku70 toolbox for filamentous fungi: establishment of complementation vectors and recipient strains for advanced gene analyses. *Applied Microbiology and Biotechnology*, 87(4), pp.1463-1473.

Carvalho, N., Jørgensen, T., Arentshorst, M., Nitsche, B., van den Hondel, C., Archer, D. and Ram, A. (2012). Genome-wide expression analysis upon constitutive activation of the HacA bZIP transcription factor in *Aspergillus niger* reveals a coordinated cellular response to counteract ER stress. *BMC Genomics*, 13(1), p.350.

Carvalho, P., Goder, V. and Rapoport, T. (2006). Distinct Ubiquitin-Ligase Complexes Define Convergent Pathways for the Degradation of ER Proteins. *Cell*, 126(2), pp.361-373.

Castilho, B., Shanmugam, R., Silva, R., Ramesh, R., Himme, B. and Sattlegger, E. (2014). Keeping the eIF2 alpha kinase Gcn2 in check. *Biochimica et Biophysica Acta (BBA) - Molecular Cell Research*, 1843(9), pp.1948-1968.

Chanat, E., Le Parc, A., Lahouassa, H. and Badaoui, B. (2016). Isolation of endoplasmic reticulum fractions from mammary epithelial tissue. *Journal of Mammary Gland Biology and Neoplasia*, 21(1-2), pp.1-8.

Chassé, H., Boulben, S., Costache, V., Cormier, P. and Morales, J. (2016). Analysis of translation using polysome profiling. *Nucleic Acids Research*, p.gkw907.

Chen, J., Throop, M., Gehrke, L., Kuo, I., Pal, J., Brodsky, M. and London, I. (1991). Cloning of the cDNA of the heme-regulated eukaryotic initiation factor 2 alpha (eIF-2 alpha) kinase of rabbit reticulocytes: homology to yeast GCN2 protein kinase and human double-stranded-RNA-dependent eIF-2 alpha kinase. *Proceedings of the National Academy of Sciences*, 88(17), pp.7729-7733.

Chen, Q. and Lai, H. (2015). Gene delivery into plant cells for recombinant protein production. *BioMed Research International*, 2015, pp.1-10.

Chen, X., Karnovsky, A., Sans, M., Andrews, P. and Williams, J. (2010). Molecular characterization of the endoplasmic reticulum: Insights from proteomic studies. *Proteomics*, 10(22), pp.4040-4052.

Chong, W., Shastri, M. and Eri, R. (2017). Endoplasmic Reticulum Stress and Oxidative Stress: A Vicious Nexus Implicated in Bowel Disease Pathophysiology. *International Journal of Molecular Sciences*, 18(4), p.771.

Choudhary, N., Sairam, R. and Tyagi, A. (2005). Expression of delta1-pyrroline-5-carboxylate synthetase gene during drought in rice (*Oryza sativa* L.). *Journal of biological chemistry*, 42(6), pp.366-70.

Cohen, B. (1973). The Neutral and Alkaline Proteases of Aspergillus nidulans. *Journal of General Microbiology*, 77(2), pp.521-528.

Conesa, A., Jeenes, D., Archer, D., van den Hondel, C. and Punt, P. (2002). Calnexin overexpression increases manganese peroxidase production in *Aspergillus niger*. *Applied and Environmental Microbiology*, 68(2), pp.846-851.

Conesa, A., Punt, P. and van den Hondel, C. (2002). Fungal peroxidases: molecular aspects and applications. *Journal of Biotechnology*, 93(2), pp.143-158.

Corbett, E., Oikawa, K., Francois, P., Tessier, D., Kay, C., Bergeron, J., Thomas, D., Krause, K. and Michalak, M. (1999). Ca^{2+} regulation of interactions between endoplasmic reticulum chaperones. *Journal of Biological Chemistry*, 274(10), pp.6203-6211.

Cosnefroy, O., Jaspart, A., Calmels, C., Parissi, V., Fleury, H., Ventura, M., Reigadas, S. and Andréola, M. (2013). Activation of GCN2 upon HIV-1 infection and inhibition of translation. *Cellular and Molecular Life Sciences*, 70(13), pp.2411-2421.

Coudert, L., Adjibade, P. and Mazroui, R. (2014). Analysis of translation initiation during stress conditions by polysome profiling. *Journal of Visualized Experiments*, (87).

Crambert, G., Ernandez, T., Lamouroux, C., Roth, I., Dizin, E., Martin, P., Féraille, E. and Hasler, U. (2014). Epithelial sodium channel abundance is decreased by an unfolded protein response induced by hyperosmolality. *Physiological Reports*, 2(11), p.e12169.

Crosby, J., Lee, K., London, I. and Chen, J. (1994). Erythroid expression of the heme-regulated eIF-2 alpha kinase. *Molecular and Cellular Biology*, 14(6), pp.3906-3914.

Cullinan, S., Zhang, D., Hannink, M., Arvisais, E., Kaufman, R. and Diehl, J. (2003). *Nrf2* Is a direct PERK substrate and effector of PERK-dependent cell survival. *Molecular and Cellular Biology*, 23(20), pp.7198-7209.

Dave, A., Jeenes, D., Mackenzie, D. and Archer, D. (2006). HacA-independent induction of chaperone-encoding gene *bipA* in *Aspergillus niger* strains overproducing Membrane proteins. *Applied and Environmental Microbiology*, 72(1), pp.953-955.

De Souza, C., Hashmi, S., Osmani, A., Andrews, P., Ringelberg, C., Dunlap, J. and Osmani, S. (2013). Functional analysis of the *Aspergillus nidulans* kinome. *PLoS ONE*, 8(3), p.e58008.

del Pino, J., Jiménez, J., Ventoso, I., Castelló, A., Muñoz-Fernández, M., de Haro, C. and Berlanga, J. (2012). GCN2 has inhibitory effect on human immunodeficiency virus-1 protein synthesis and is cleaved upon viral infection. *PLoS ONE*, 7(10), p.e47272.

DELFORGE, J., MESSENGUY, F. and WIAME, J. (1975). The regulation of arginine biosynthesis in *Saccharomyces cerevisiae*. The specificity of *argR*- mutations and the general control of amino-acid biosynthesis. *European Journal of Biochemistry*, 57(1), pp.231-239.

Demaurex, N. and Frieden, M. (2003). Measurements of the free lumenal ER Ca 2+ concentration with targeted "cameleon" fluorescent proteins. *Cell Calcium*, 34(2), pp.109-119.

Dever, T., Feng, L., Wek, R., Cigan, A., Donahue, T. and Hinnebusch, A. (1992). Phosphorylation of initiation factor 2α by protein kinase GCN2 mediates gene-specific translational control of GCN4 in yeast. *Cell*, 68(3), pp.585-596.

DeVries-Seimon, T., Li, Y., Yao, P., Stone, E., Wang, Y., Davis, R., Flavell, R. and Tabas, I. (2005). Cholesterol-induced macrophage apoptosis requires ER stress pathways and engagement of the type A scavenger receptor. *The Journal of Cell Biology*, 171(1), pp.61-73.

Donahue, T., Cigan, A., Pabich, E. and Castilho Valavicius, B. (1988). Mutations at a Zn(II) finger motif in the yeast elF-2β gene alter ribosomal start-site selection during the scanning process. *Cell*, 54(5), pp.621-632.

Dong, J., Qiu, H., Garcia-Barrio, M., Anderson, J. and Hinnebusch, A. (2000). Uncharged tRNA activates GCN2 by displacing the protein kinase moiety from a bipartite tRNA-binding domain. *Molecular Cell*, 6(2), pp.269-279.

Du, Y. (2004). Dynamics and inheritance of the endoplasmic reticulum. *Journal of Cell Science*, 117(14), pp.2871-2878.

Duran, J., Anjard, C., Stefan, C., Loomis, W. and Malhotra, V. (2010). Unconventional secretion of Acb1 is mediated by autophagosomes. *The Journal of Cell Biology*, 188(4), pp.527-536.

Dynamicscience.com.au. (2019). *biology-the cell-endoplasmic reticulum*. [online] Available at: http://www.dynamicscience.com.au/tester/solutions1/biology/cell/endoplsmretsmth.html [Accessed 6 Sep. 2017].

Eletto, D., Eletto, D., Boyle, S. and Argon, Y. (2016). PDIA6 regulates insulin secretion by selectively inhibiting the RIDD activity of IRE1. *The FASEB Journal*, 30(2), pp.653-665.

Emri, T., Szilágyi, M., László, K., M-Hamvas, M. and Pócsi, I. (2009). *PepJ* is a new extracellular proteinase of *Aspergillus nidulans*. *Folia Microbiologica*, 54(2), pp.105-109.

Engling, A. (2002). Biosynthetic FGF-2 is targeted to non-lipid raft microdomains following translocation to the extracellular surface of CHO cells. *Journal of Cell Science*, 115(18), pp.3619-3631.

Failmezger, J., Nitschel, R., Sánchez-Kopper, A., Kraml, M. and Siemann-Herzberg, M. (2016). Site-Specific Cleavage of Ribosomal RNA in Escherichia coli-Based Cell-Free Protein Synthesis Systems. *PLOS ONE*, 11(12), p.e0168764.

Fan, F., Ma, G., Li, J., Liu, Q., Benz, J., Tian, C. and Ma, Y. (2015). Genome-wide analysis of the endoplasmic reticulum stress response during lignocellulase production in *Neurospora crassa*. *Biotechnology for Biofuels*, 8(1).

Fankhauser, c., Homans, S., Thomas-Oates, J., McConville, M., Desponds, C., Conzelmann, A. and Ferguson, M. (1993). Structures of glycosylphosphatidylinositol membrane anchors from *Saccharomyces cerevisiae*. *Journal of Biological Chemistry*, 268(35), pp.26365-74.

Faus, I., del Moral, C., Adroer, N., del Río, J., Patiño, C., Sisniega, H., Casas, C., Bladé, J. and Rubio, V. (1998). Secretion of the sweet-tasting protein thaumatin by recombinant strains of *Aspergillus niger* var. *awamori*. *Applied Microbiology and Biotechnology*, 49(4), pp.393-398.

Feng, X., Krishnan, K., Richie, D., Aimanianda, V., Hartl, L., Grahl, N., Powers-Fletcher, M., Zhang, M., Fuller, K., Nierman, W., Lu, L., Latgé, J., Woollett, L., Newman, S., Cramer, R., Rhodes, J. and Askew, D. (2011). HacA-Independent functions of the ER stress sensor *ireA* synergize with the canonical UPR to influence virulence traits in *Aspergillus fumigatus*. *PLoS Pathogens*, 7(10), p.e1002330.

Fidel, S., Doonan, J. and Morris, N. (1988). Aspergillus nidulans contains a single actin gene which has unique intron locations and encodes a γ-actin. *Gene*, 70(2), pp.283-293.

Flis, V. and Daum, G. (2013). Lipid Transport between the Endoplasmic Reticulum and Mitochondria. *Cold Spring Harbor Perspectives in Biology*, 5(6), pp.1-22.

Franken, A., Lokman, B., Ram, A., Punt, P., van den Hondel, C. and de Weert, S. (2011). Heme biosynthesis and its regulation: towards understanding and improvement of heme biosynthesis in filamentous fungi. *Applied Microbiology and Biotechnology*, 91(3), pp.447-460.

Freedman, R., Dunn, A. and Ruddock, L. (1998). Protein folding: A missing redox link in the endoplasmic reticulum. *Current Biology*, 8(13), pp.R468-R470.

Fueller, J., Becker, M., Sienerth, A., Fischer, A., Hotz, C. and Galmiche, A. (2008). C-RAF activation promotes BAD poly-ubiquitylation and turn-over by the proteasome. *Biochemical and Biophysical Research Communications*, 370(4), pp.552-556.

Gallwitz, D. and Seidel, R. (1980). Molecular cloning of the actin gene from yeast *Saccharomyces cerevisiae*. *Nucleic Acids Research*, 8(5), pp.1043-1059.

Gandin, V., Sikström, K., Alain, T., Morita, M., McLaughlan, S., Larsson, O. and Topisirovic, I. (2014). Polysome fractionation and analysis of mammalian translatomes on a genome-wide scale. *Journal of Visualized Experiments*, (87).

Gardner, R., Swarbrick, G., Bays, N., Cronin, S., Wilhovsky, S., Seelig, L., Kim, C. and Hampton, R. (2000). Endoplasmic reticulum degradation requires lumen to cytosol signalling. *The Journal of Cell Biology*, 151(1), pp.69-82.

Garfinkel, D. (2003). Studies on pig liver microsomes I. Enzymic and pigment composition of different microsomal fractions. *Archives of Biochemistry and Biophysics*, 409(1), pp.7-15.

Gariglio, P., Bellard, M. and Chambon, P. (1981). Clustering of RNA polymerase B molecules in the 5′ moiety of the adult β-globin gene of hen erythrocytes. *Nucleic Acids Research*, 9(11), pp.2589-2598.

Gilbert, H. (1994). Protein chaperones and protein folding. *Current Opinion in Biotechnology*, 5(5), pp.534-539.

Goll, D., thompson, V., li, H., wei, W. and Cong, J. (2003). The Calpain System. *Physiological Reviews*, 83(3), pp.731-801.

Görlach, A., Klappa, P. and Kietzmann, D. (2006). The Endoplasmic Reticulum: folding, calcium homeostasis, signaling, and redox control. *Antioxidants & Redox Signaling*, 8(9-10), pp.1391-1418.

Grallert, B. and Boye, E. (2013). GCN2, an old dog with new tricks. *Biochemical Society Transactions*, 41(6), pp.1687-1691.

Griffing, L. (2010). Networking in the endoplasmic reticulum. *Biochemical Society Transactions*, 38(3), pp.747-753.

Gronostajski, R., Goldberg, A. and Pardee, A. (1984). The role of increased proteolysis in the atrophy and arrest of proliferation in serum-deprived fibroblasts. *Journal of Cellular Physiology*, 121(1), pp.189-198.

Gruss, O., Feick, P., Frank, R. and Dobberstein, B. (1999). Phosphorylation of components of the ER translocation site. *European Journal of Biochemistry*, 260(3), pp.785-793.

Guiboileau, A., Yoshimoto, K., Soulay, F., Bataillé, M., Avice, J. and Masclaux-Daubresse, C. (2012). Autophagy machinery controls nitrogen remobilization at the whole-plant level under both limiting and ample nitrate conditions in Arabidopsis. *New Phytologist*, 194(3), pp.732-740.

Guillemette, T., Ram, A., Carvalho, N., Joubert, A., Simoneau, P. and Archer, D. (2011). Methods for investigating the UPR in filamentous fungi. *Methods in enzymology*, 490, pp.1-29.

Guillemette, T., van Peij, N., Goosen, T., Lanthaler, K., Robson, G., van den Hondel, C., Stam, H. and Archer, D. (2007). Genomic analysis of the secretion stress response in the enzyme-producing cell factory *Aspergillus niger*. *BMC Genomics*, 8(1), p.158.

Guydosh, N., Kimmig, P., Walter, P. and Green, R. (2017). Regulated Ire1-dependent mRNA decay requires no-go mRNA degradation to maintain endoplasmic reticulum homeostasis in *S. pombe*. *eLife*, 6.

Hamanaka, R., Bennett, B., Cullinan, S. and Diehl, J. (2005). PERK and GCN2 Contribute to eIF2α Phosphorylation and Cell Cycle Arrest after Activation of the Unfolded Protein Response Pathway. *Molecular Biology of the Cell*, 16(12), pp.5493-5501.

Hampton, R., Gardner, R. and Rine, J. (1996). Role of 26S proteasome and HRD genes in the degradation of 3-hydroxy-3-methylglutaryl-CoA reductase, an integral endoplasmic reticulum membrane protein. *Molecular Biology of the Cell*, 7(12), pp.2029-2044.

Han, A. (2001). Heme-regulated eIF2alpha kinase (HRI) is required for translational regulation and survival of erythroid precursors in iron deficiency. *The EMBO Journal*, 20(23), pp.6909-6918.

Han, C., Jin, L., Mei, Y. and Wu, M. (2013). Endoplasmic reticulum stress inhibits cell cycle progression via induction of p27 in melanoma cells. *Cellular Signalling*, 25(1), pp.144-149.

Han, X., Zhou, J., Zhang, P., Song, F., Jiang, R., Li, M., Xia, F. and Guo, F. (2013). IRE1α dissociates with BiP and inhibits ER stress-mediated apoptosis in cartilage development. *Cellular Signalling*, 25(11), pp.2136-2146.

Hankin, L. and Anagnostakis, S. (1975). The use of solid media for detection of enzyme production by fungi. *Mycologia*, 67(3), p.597.

Hardiman, T., Ewald, J., Lemuth, K., Reuss, M. and Siemann-Herzberg, M. (2008). Quantification of rRNA in Escherichia coli using capillary gel electrophoresis with laser-induced fluorescence detection. *Analytical Biochemistry*, 374(1), pp.79-86.Harding, H., Novoa, I., Zhang, Y., Zeng, H., Wek, R., Schapira, M. and Ron, D. (2000). Regulated translation initiation controls stress-induced gene expression in mammalian cells. *Molecular Cell*, 6(5), pp.1099-1108.

Harmsen, M., Bruyne, M., Raué, H. and Maat, J. (1996). Overexpression of binding protein and disruption of the PMR1 gene synergistically stimulate secretion of bovine prochymosin but not plant Thaumatin in yeast. *Applied Microbiology and Biotechnology*, 46(4), pp.365-370.

Hawe, A., Sutter, M. and Jiskoot, W. (2008). Extrinsic fluorescent dyes as tools for protein characterization. *Pharmaceutical Research*, 25(7), pp.1487-1499.

Haze, K., Yoshida, H., Yanagi, H., Yura, T. and Mori, K. (1999). Mammalian transcription factor ATF6 is synthesized as a transmembrane protein and activated by proteolysis in response to endoplasmic reticulum stress. *Molecular Biology of the Cell*, 10(11), pp.3787-3799.

Hershey, J. (1989). Protein phosphorylation controls translation rates. *Journal of Biological Chemistry*, 264(35), pp.20823–20826.

Healey, R., Lebhar, H., Hornung, S., Thordarson, P. and Marquis, C. (2017). An improved process for the production of highly purified recombinant thaumatin tagged-variants. *Food Chemistry*, 237, pp.825-832.

Hessa, T., Meindl-Beinker, N., Bernsel, A., Kim, H., Sato, Y., Lerch-Bader, M., Nilsson, I., White, S. and von Heijne, G. (2007). Molecular code for transmembrane-helix recognition by the Sec61 translocon. *Nature*, 450(7172), pp.1026-1030.

Hetzer, M., Walther, T. and Mattaj, I. (2005). PUSHING THE ENVELOPE: Structure, Function, and Dynamics of the Nuclear Periphery. *Annual Review of Cell and Developmental Biology*, 21(1), pp.347-380.

Hoang, H., Maruyama, J. and Kitamoto, K. (2014). Modulating Endoplasmic Reticulum-Golgi cargo receptors for improving secretion of carrier-fused heterologous proteins in the filamentous fungus *Aspergillus oryzae*. *Applied and Environmental Microbiology*, 81(2), pp.533-543.

Hoffmann, B., Valerius, O., Andermann, M. and Braus, G. (2001). Transcriptional autoregulation and inhibition of mrna translation of amino acid regulator gene *cpca* of filamentous fungus *Aspergillus nidulans*. *Molecular Biology of the Cell*, 12(9), pp.2846-2857.

Hoffmann, B., Wanke, C., LaPaglia, S. and Braus, G. (2000). c-Jun and RACK1 homologues regulate a control point for sexual development in *Aspergillus nidulans*. *Molecular Microbiology*, 37(1), pp.28-41.

Hollien, J., Lin, J., Li, H., Stevens, N., Walter, P. and Weissman, J. (2009). Regulated Ire1-dependent decay of messenger RNAs in mammalian cells. *The Journal of Cell Biology*, 186(3), pp.323-331.

Hospital (1967). Hospital Digest. *Hospital Topics*, 45(3), pp.25-32.

Hou, J., Tang, H., Liu, Z., Österlund, T., Nielsen, J. and Petranovic, D. (2013). Management of the endoplasmic reticulum stress by activation of the heat shock response in yeast. *FEMS Yeast Research*, 14(3), pp.481-494.

Huang, T., Wang, M., Shi, K., Chen, G., Tian, X. and Wu, Z. (2017). Metabolism and secretion of yellow pigment under high glucose stress with *Monascus ruber*. *AMB Express*, 7(1), p.79.

Hurwitz, C. and Rosano, C. (1965). Measurement of rates of transcription and translation by means of proflavine or borate. *Biochimica et Biophysica Acta (BBA) - Nucleic Acids and Protein Synthesis*, 108(4), pp.697-700.

Hwang, S., Kim, M. and Kim, J. (2000). Cloning of hHRI, Human Heme-regulated Eukaryotic Initiation Factor 2α Kinase: Down-regulated in Epithelial Ovarian Cancers. *Molecules and Cells*, 10(5), pp.584-591.

Hyde, M., Block-Alper, L., Felix, J., Webster, P. and Meyer, D. (2002). Induction of secretory pathway components in yeast is associated with increased stability of their mRNA. *The Journal of Cell Biology*, 156(6), pp.993-1001.

Iula, L., Keitelman, I., Sabbione, F., Fuentes, F., Guzman, M., Galletti, J., Gerber, P., Ostrowski, M., Geffner, J., Jancic, C. and Trevani, A. (2018). Autophagy Mediates Interleukin-1β Secretion in Human Neutrophils. *Frontiers in Immunology*, 9.

Iwata, Y., Sakiyama, M., Lee, M. and Koizumi, N. (2010). Transcriptomic response of *Arabidopsis thaliana* to tunicamycin-induced endoplasmic reticulum stress. *Plant Biotechnology*, 27(2), pp.161-171.

Jarai, G., Kirchherr, D. and Buxton, F. (1994). Cloning and characterization of the pepD gene of Aspergillus niger which codes for a subtilisin-like protease. *Gene*, 139(1), pp.51-57.

Jarvis, D. (2014). Recombinant protein expression in baculovirus-infected insect cells. *Methods in enzymology*, 536, pp.149-63.

Jørgensen, T., Goosen, T., van den Hondel, C., Ram, A. and Iversen, J. (2009). Transcriptomic comparison of *Aspergillus niger* growing on two different sugars reveals coordinated regulation of the secretory pathway. *BMC Genomics*, 10(1), p.44.

Jonikas, M., Collins, S., Denic, V., Oh, E., Quan, E., Schmid, V., Weibezahn, J., Schwappach, B., Walter, P., Weissman, J. and Schuldiner, M. (2009). Comprehensive characterization of genes required for protein folding in the endoplasmic reticulum. *Science*, 323(5922), pp.1693-1697.

Joo, J., Liao, G., Collins, J., Grissom, S. and Jetten, A. (2007). Farnesol-induced apoptosis in human lung carcinoma cells is coupled to the endoplasmic reticulum stress response. *Cancer Research*, 67(16), pp.7929-7936.

Joo, J., Ueda, E., Bortner, C., Yang, X., Liao, G. and Jetten, A. (2015). Farnesol activates the intrinsic pathway of apoptosis and the ATF4-ATF3-CHOP cascade of ER stress in human T lymphoblastic leukemia Molt4 cells. *Biochemical Pharmacology*, 97(3), pp.256-268.

Jüschke, C., Ferring, D., Jansen, R. and Seedorf, M. (2004). A Novel Transport Pathway for a Yeast Plasma Membrane Protein Encoded by a Localized mRNA. *Current Biology*, 14(5), pp.406-411.

Kapp, K., Schrempf, S., Lemberg, M. and Dobberstein, B. (n.d.). *Post-Targeting Functions of Signal Peptides*. Austin: Landes Bioscience, pp.2000-2013.

Kasuya, T., Nakajima, H. and Kitamoto, K. (1999). Cloning and characterization of the bipA gene encoding ER chaperone BiP from Aspergillus oryzae. *Journal of Bioscience and Bioengineering*, 88(5), pp.472-478.

Kato, N., Murakoshi, Y., Kato, M., Kobayashi, T. and Tsukagoshi, N. (2002). Isomaltose formed by α-glucosidases triggers amylase induction in *Aspergillus nidulans*. *Current Genetics*, 42(1), pp.43-50.

Katz, M., Ricea, R. and Cheetham, B. (1994). Isolation and characterization of an *Aspergillus nidulans* gene encoding an alkaline protease. *Gene*, 150(2), pp.287-292.

Kaufman, R. (1999). Stress signalling from the lumen of the endoplasmic reticulum: coordination of gene transcriptional and translational controls. *Genes & Development*, 13(10), pp.1211-1233.

Kaufman, R., Scheuner, D., Schröder, M., Shen, X., Lee, K., Liu, C. and Arnold, S. (2002). The unfolded protein response in nutrient sensing and differentiation. *Nature Reviews Molecular Cell Biology*, 3(6), pp.411-421.

Kennedy, D., Mnich, K. and Samali, A. (2014). Heat shock preconditioning protects against ER stress-induced apoptosis through the regulation of the BH3-only protein BIM. *FEBS Open Bio*, 4(1), pp.813-821.

Khurana, R., Coleman, C., Ionescu-Zanetti, C., Carter, S., Krishna, V., Grover, R., Roy, R. and Singh, S. (2005). Mechanism of thioflavin T binding to amyloid fibrils. *Journal of Structural Biology*, 151(3), pp.229-238.

Kim, E., Lee, Y., Kang, S. and Lim, Y. (2014). Ionizing radiation activates PERK/eIF2α/ATF4 signaling via ER stress-independent pathway in human vascular endothelial cells. *International Journal of Radiation Biology*, 90(4), pp.306-312.

Kimmig, P., Diaz, M., Zheng, J., Williams, C., Lang, A., Aragón, T., Li, H. and Walter, P. (2012). The unfolded protein response in fission yeast modulates stability of select mRNAs to maintain protein homeostasis. *eLife*, 1.

King, H. and Gerber, A. (2014). Translatome profiling: methods for genome-scale analysis of mRNA translation. *Briefings in Functional Genomics*.

Kinseth, M., Anjard, C., Fuller, D., Guizzunti, G., Loomis, W. and Malhotra, V. (2007). The Golgi-Associated Protein GRASP Is Required for Unconventional Protein Secretion during Development. *Cell*, 130(3), pp.524-534.

Klingenberg, M. (1958). Pigments of rat liver microsomes. *Archives of Biochemistry and Biophysics*, 75(2), pp.376-386.

Klopotowski, T. and Wiater, A. (1965). Synergism of aminotriazole and phosphate on the inhibition of yeast imidazole glycerol phosphate dehydratase. *Archives of Biochemistry and Biophysics*, 112(3), pp.562-566.

Kohda, T., Tanaka, K., Konomi, M., Sato, M., Osumi, M. and Yamamoto, M. (2007). Fission yeast autophagy induced by nitrogen starvation generates a nitrogen source that drives adaptation processes. *Genes to Cells*, 12(2), pp.155-170.

Koizumi, N., Ujino, T., Sano, H. and Chrispeels, M. (1999). Overexpression of a gene that encodes the first enzyme in the biosynthesis of asparagine-linked glycans makes plants resistant to tunicamycin and obviates the tunicamycin-induced unfolded protein response. *Plant Physiology*, 121(2), pp.353-362.

Komori, R., Taniguchi, M., Ichikawa, Y., Uemura, A., Oku, M., Wakabayashi, S., Higuchi, K. and Yoshida, H. (2012). Ultraviolet A induces endoplasmic reticulum stress response in human dermal fibroblasts. *Cell Structure and Function*, 37(1), pp.49-53.

Koreishi, M., Gniadek, T., Yu, S., Masuda, J., Honjo, Y. and Satoh, A. (2013). The Golgin tether giantin regulates the secretory pathway by controlling stack organization within Golgi apparatus. *PLoS ONE*, 8(3), p.e59821.

Korennykh, A. and Walter, P. (2012). Structural basis of the unfolded protein response. *Annual Review of Cell and Developmental Biology*, 28(1), pp.251-277.

Krebs, M., Bromley, E. and Donald, A. (2005). The binding of thioflavin-T to amyloid fibrils: localisation and implications. *Journal of Structural Biology*, 149(1), pp.30-37.

Krishnan, K., Ren, Z., Losada, L., Nierman, W., Lu, L. and Askew, D. (2014). Polysome profiling reveals broad translatome remodeling during endoplasmic reticulum (ER) stress in the pathogenic fungus *Aspergillus fumigatus*. *BMC Genomics*, 15(1), p.159.

Krol, K., Morozov, I., Jones, M., Wyszomirski, T., Weglenski, P., Dzikowska, A. and Caddick, M. (2013). *RrmA* regulates the stability of specific transcripts in response to both nitrogen source and oxidative stress. *Molecular Microbiology*, 89(5), pp.975-988.

Ku, S., Toh, P., Lee, Y., Chusainow, J., Yap, M. and Chao, S. (2009). Regulation of XBP-1 signalling during transient and stable recombinant protein production in CHO cells. *Biotechnology Progress*, 26(2), pp.517-526.

Kudla, B., Caddick, M., Langdon, T., Martinez-Rossi, N., Bennett, C., Sibley, S., Davies, R. and Arst, H. (1990). The regulatory gene *areA* mediating nitrogen metabolite repression in *Aspergillus nidulans*. Mutations affecting specificity of gene activation alter a loop residue of a putative zinc finger. *The EMBO Journal*, 9(5), pp.1355-1364.

Kuersten, S., Radek, A., Vogel, C. and Penalva, L. (2013). Translation regulation gets its 'omics' moment. *Wiley Interdisciplinary Reviews: RNA*, 4(6), pp.617-630.

Kunaparaju, R., Liao, M. and Sunstrom, N. (2005). Epi -CHO, an episomal expression system for recombinant protein production in CHO cells. *Biotechnology and Bioengineering*, 91(6), pp.670-677.

Kwon, H., Kawaguchi, K., Kikuma, T., Takegawa, K., Kitamoto, K. and Higuchi, Y. (2017). Analysis of an acyl-CoA binding protein in Aspergillus oryzae that undergoes unconventional secretion. *Biochemical and Biophysical Research Communications*, 493(1), pp.481-486.

Lageix, S., Lanet, E., Pouch-Pélissier, M., Espagnol, M., Robaglia, C., Deragon, J. and Pélissier, T. (2008). *Arabidopsis* eIF2α kinase GCN2 is essential for growth in stress conditions and is activated by wounding. *BMC Plant Biology*, 8(1), p.134.

Lavoie, C., Lanoix, J., Kan, F. and Paiement, J. (1996). Cell-free assembly of rough and smooth endoplasmic reticulum. *Journal of cell science*, 109(6), pp.1415-25.

Lee, K., Dey, M., Neculai, D., Cao, C., Dever, T. and Sicheri, F. (2008). Structure of the dual enzyme Ire1 reveals the basis for catalysis and regulation in nonconventional RNA splicing. *Cell*, 132(1), pp.89-100.

Lerner, R. (2006). mRNA translation is compartmentalized to the endoplasmic reticulum following physiological inhibition of cap-dependent translation. *RNA*, 12(5), pp.775-789.

Li, W. and Miller, R. (2014). Elevated ATF4 Function in Fibroblasts and Liver of Slow-Aging Mutant Mice. *The Journals of Gerontology Series A: Biological Sciences and Medical Sciences*, 70(3), pp.263-272.

Liang, X., Dickman, M. and Becker, D. (2014). Proline Biosynthesis Is Required for Endoplasmic Reticulum Stress Tolerance in *Saccharomyces cerevisiae*. *Journal of Biological Chemistry*, 289(40), pp.27794-27806.

Lipke, P., Garcia, M., Alsteens, D., Ramsook, C., Klotz, S. and Dufrêne, Y. (2012). Strengthening relationships: amyloids create adhesion nanodomains in yeasts. *Trends in Microbiology*, 20(2), pp.59-65.

Liu, Z., Lv, Y., Zhao, N., Guan, G. and Wang, J. (2015). Protein kinase R-like ER kinase and its role in endoplasmic reticulum stress-decided cell fate. *Cell Death & Disease*, 6(7), pp.e1822-e1822.

Lizarbe, M., Barrasa, J., Olmo, N., Gavilanes, F. and Turnay, J. (2013). Annexin-Phospholipid Interactions. Functional Implications. *International Journal of Molecular Sciences*, 14(2), pp.2652-2683.

Lubertozzi, D. and Keasling, J. (2009). Developing *Aspergillus* as a host for heterologous expression. *Biotechnology Advances*, 27(1), pp.53-75.

Lucchini, G., Hinnebusch, A., Chen, C. and Fink, G. (1984). Positive regulatory interactions of the HIS4 gene of Saccharomyces cerevisiae. *Molecular and Cellular Biology*, 4(7), pp.1326-1333.

Malzer, E., Szajewska-Skuta, M., Dalton, L., Thomas, S., Hu, N., Skaer, H., Lomas, D., Crowther, D. and Marciniak, S. (2013). Coordinate regulation of eIF2 phosphorylation by PPP1R15 and GCN2 is required during *Drosophila* development. *Journal of Cell Science*, 126(6), pp.1406-1415.

Marcu, M., Doyle, M., Bertolotti, A., Ron, D., Hendershot, L. and Neckers, L. (2002). Heat shock protein 90 modulates the unfolded protein response by stabilizing IRE1. *Molecular and Cellular Biology*, 22(24), pp.8506-8513.

Martin, R., Berlanga, J. and de Haro, C. (2013). New roles of the fission yeast eIF2 kinases Hri1 and Gcn2 in response to nutritional stress. *Journal of Cell Science*, 126(14), pp.3010-3020.

Mattanovich, D., Gasser, B., Hohenblum, H. and Sauer, M. (2004). Stress in recombinant protein producing yeasts. *Journal of Biotechnology*, 113(1-3), pp.121-135.

Mattern, I., van Noort, J., van den Berg, P., Archer, D., Roberts, I. and van den Hondel, C. (1992). Isolation and characterization of mutants of *Aspergillus niger* deficient in extracellular proteases. *Molecular and General Genetics MGG*, 234(2), pp.332-336.

Marui, J., Yoshimi, A., Hagiwara, D., Fujii-Watanabe, Y., Oda, K., Koike, H., Tamano, K., Ishii, T., Sano, M., Machida, M. and Abe, K. (2010). Use of the *Aspergillus oryzae* actin gene

promoter in a novel reporter system for exploring antifungal compounds and their target genes. *Applied Microbiology and Biotechnology*, 87(5), pp.1829-1840.

McGlincy, N. and Ingolia, N. (2017). Transcriptome-wide measurement of translation by ribosome profiling. *Methods*, 126, pp.112-129.

Menacho-Márquez, M., Perez-Valle, J., Arino, J., Gadea, J. and Murguía, J. (2007). Gcn2p regulates a G1/S cell cycle checkpoint in response to DNA damage. *Cell Cycle*, 6(18), pp.2302-2305.

Menon, A. and Stevens, V. (1992). Phosphatidylethanolamine is the donor of the ethanolamine residue linking a glycosylphosphatidylinositol anchor to protein. *The Journal of biological chemistry*, 267(22), pp.15277-80.

Meyer, V., Arentshorst, M., van den Hondel, C. and Ram, A. (2008). The polarisome component SpaA localises to hyphal tips of *Aspergillus niger* and is important for polar growth. *Fungal Genetics and Biology*, 45(2), pp.152-164.

Milner, R., Famulski, K. and Michalak, M. (1992). Calcium binding proteins in the sarcoplasmic/endoplasmic reticulum of muscle and nonmuscle cells. *Molecular and Cellular Biochemistry*, 112(1).

Mishiba, K., Nagashima, Y., Suzuki, E., Hayashi, N., Ogata, Y., Shimada, Y. and Koizumi, N. (2013). Defects in IRE1 enhance cell death and fail to degrade mRNAs encoding secretory pathway proteins in the *Arabidopsis* unfolded protein response. *Proceedings of the National Academy of Sciences*, 110(14), pp.5713-5718.

Miura, N. and Ueda, M. (2018). Evaluation of Unconventional Protein Secretion by Saccharomyces cerevisiae and other Fungi. *Cells*, 7(9), p.128.

Miwa, T. and Kamada, S. (1990). The nucleotide sequence of a human smooth muscle (enteric type) γ-actin cDNA. *Nucleic Acids Research*, 18(14), pp.4263-4263.

Molon, M., Szajwaj, M., Tchorzewski, M., Skoczowski, A., Niewiadomska, E. and Zadrag-Tecza, R. (2016). The rate of metabolism as a factor determining longevity of the Saccharomyces cerevisiae yeast. *AGE*, 38(1).

Mooradian, A. and Haas, M. (2011). Glucose-induced endoplasmic reticulum stress is independent of oxidative stress: A mechanistic explanation for the failure of antioxidant therapy in diabetes. *Free Radical Biology and Medicine*, 50(9), pp.1140-1143.

Moralejo, F., Watson, A., Jeenes, D., Archer, D. and Martín, J. (2001). A defined level of protein disulfide isomerase expression is required for optimal secretion of thaumatin by Aspergillus awamori. *Molecular Genetics and Genomics*, 266(2), pp.246–253.

Morano, K., Grant, C. and Moye-Rowley, W. (2011). The response to heat shock and oxidative stress in *Saccharomyces cerevisiae*. *Genetics*, 190(4), pp.1157-1195.

Mori, K., Sant, A., Kohno, K., Normington, K., Gething, M. and Sambrook, J. (1992). A 22 bp cis-acting element is necessary and sufficient for the induction of the yeast KAR2 (BiP) gene by unfolded proteins. *The EMBO Journal*, 11(7), pp.2583-2593.

Mori, K., Kawahara, T., Yoshida, H., Yanagi, H. and Yura, T. (1996). Signalling from endoplasmic reticulum to nucleus: transcription factor with a basic-leucine zipper motif is required for the unfolded protein-response pathway. *Genes to Cells*, 1(9), pp.803-817.

Mori, K., Ogawa, N., Kawahara, T., Yanagi, H. and Yura, T. (1998). Palindrome with Spacer of One Nucleotide Is Characteristic of the cis-Acting Unfolded Protein Response Element in *Saccharomyces cerevisiae*. *Journal of Biological Chemistry*, 273(16), pp.9912-9920.

Morozov, I., Negrete-Urtasun, S., Tilburn, J., Jansen, C., Caddick, M. and Arst, H. (2006). Nonsense-mediated mRNA decay mutation in *Aspergillus nidulans*. *Eukaryotic Cell*, 5(11), pp.1838-1846.

Mulder, H. and Nikolaev, I. (2009). HacA-dependent transcriptional switch releases *hacA* mRNA from a translational block upon endoplasmic reticulum stress. *Eukaryotic Cell*, 8(4), pp.665-675.

Mulder, H., Saloheimo, M., Penttil, M. and Madrid, S. (2004). The transcription factor HACA mediates the unfolded protein response in Aspergillus niger, and up-regulates its own transcription. *Molecular Genetics and Genomics*, 271(2), pp.130-140.

Nakagawa, T., Zhu, H., Morishima, N., Li, E., Xu, J., Yankner, B. and Yuan, J. (2000). Caspase-12 mediates endoplasmic-reticulum-specific apoptosis and cytotoxicity by amyloid-β. *Nature*, 403(6765), pp.98-103.

Nakamura, T., Maeda, Y., Tanoue, N., Makita, T., Kato, M. and Kobayashi, T. (2006). Expression profile of amylolytic genes in *Aspergillus nidulans*. *Bioscience, Biotechnology, and Biochemistry*, 70(10), pp.2363-2370.

Nanduri, S., Carpick, B., Yang, Y., Williams, B. and Qin, J. (1998). Structure of the double-stranded RNA-binding domain of the protein kinase PKR reveals the molecular basis of its dsRNA-mediated activation. *The EMBO Journal*, 17(18), pp.5458-5465.

Natarajan, K., Meyer, M., Jackson, B., Slade, D., Roberts, C., Hinnebusch, A. and Marton, M. (2001). Transcriptional profiling shows that Gcn4p is a master regulator of gene expression during amino acid starvation in yeast. *Molecular and Cellular Biology*, 21(13), pp.4347-4368.

Nayyar, A., Walker, G., Wardrop, F. and Adya, A. (2017). Flocculation in industrial strains of Saccharomyces cerevisiae: role of cell wall polysaccharides and lectin-like receptors. *Journal of the Institute of Brewing*, 123(2), pp.211-218.

Ngiam, C., Jeenes, D., Punt, P., Van Den Hondel, C. and Archer, D. (2000). Characterization of a foldase, protein disulfide isomerase A, in the protein secretory pathway of *Aspergillus niger*. *Applied and Environmental Microbiology*, 66(2), pp.775-782.

Nickel, W. and Rabouille, C. (2009). Erratum: Mechanisms of regulated unconventional protein secretion. *Nature Reviews Molecular Cell Biology*, 10(3), pp.234-234.

Nikawa, J. and Yamashita, S. (1992). IRE1 encodes a putative protein kinase containing a membrane-spanning domain and is required for inositol phototrophy in *Saccharomyces cerevisiae*. *Molecular Microbiology*, 6(11), pp.1441-1446.

Novoa, I., Zeng, H., Harding, H. and Ron, D. (2001). Feedback inhibition of the unfolded protein response by GADD34-mediated dephosphorylation of eIF2α. *The Journal of Cell Biology*, 153(5), pp.1011-1022.

Nutt, L., Pataer, A., Pahler, J., Fang, B., Roth, J., McConkey, D. and Swisher, S. (2001). *Bax* and *Bak* promote apoptosis by modulating endoplasmic reticular and mitochondrial Ca^{2+} stores. *Journal of Biological Chemistry*, 277(11), pp.9219-9225.

Oliveira, D., Nakayasu, E., Joffe, L., Guimarães, A., Sobreira, T., Nosanchuk, J., Cordero, R., Frases, S., Casadevall, A., Almeida, I., Nimrichter, L. and Rodrigues, M. (2010). Characterization of Yeast Extracellular Vesicles: Evidence for the Participation of Different Pathways of Cellular Traffic in Vesicle Biogenesis. *PLoS ONE*, 5(6), p.e11113.

Olsen, D., Jordan, B., Chen, D., Wek, R. and Cavener, D. (1998). Isolation of the gene encoding the Drosophila melanogaster homolog of the *Saccharomyces cerevisiae* GCN2 eIF-2α kinase. *Genetics*, 149(3), pp.1495–1509.

Onodera, J. and Ohsumi, Y. (2005). Autophagy Is Required for Maintenance of Amino Acid Levels and Protein Synthesis under Nitrogen Starvation. *Journal of Biological Chemistry*, 280(36), pp.31582-31586.

Orosz, E., Antal, K., Gazdag, Z., Szabó, Z., Han, K., Yu, J., Pócsi, I. and Emri, T. (2017). Transcriptome-Based Modeling Reveals that Oxidative Stress Induces Modulation of the *AtfA*-Dependent Signaling Networks in *Aspergillus nidulans*. *International Journal of Genomics*, 2017, pp.1-14.

Ortiz, G., Noseda, D., Ponce Mora, M., Recupero, M., Blasco, M. and Albertó, E. (2016). A Comparative Study of New Aspergillus Strains for Proteolytic Enzymes Production by Solid State Fermentation. *Enzyme Research*, 2016, pp.1-11.

Oslowski, C. and Urano, F. (2011). Measuring ER stress and the unfolded protein response using mammalian tissue culture system. *The Unfolded Protein Response and Cellular Stress, Part B*, pp.71-92.

Pakula, T., Laxell, M., Huuskonen, A., Uusitalo, J., Saloheimo, M. and Penttilä, M. (2003). The effects of drugs inhibiting protein secretion in the filamentous fungus *Trichoderma reesei*. *Journal of Biological Chemistry*, 278(45), pp.45011-45020.

Palade, G. (1956). The endoplasmic reticulum. *The Journal of Cell Biology*, 2(4), pp.85-98.

Patil, C. and Walter, P. (2001). Intracellular signalling from the endoplasmic reticulum to the nucleus: the unfolded protein response in yeast and mammals. *Current Opinion in Cell Biology*, 13(3), pp.349-355.

Patil, C., Li, H. and Walter, P. (2004). Gcn4p and Novel Upstream Activating Sequences Regulate Targets of the Unfolded Protein Response. *PLoS Biology*, 2(8), p.e246.

Pavio, N., Romano, P., Graczyk, T., Feinstone, S. and Taylor, D. (2003). Protein synthesis and endoplasmic reticulum stress can be modulated by the hepatitis C virus envelope protein E2 through the eukaryotic initiation factor 2 kinase PERK. *Journal of Virology*, 77(6), pp.3578-3585.

Pavitt, G. and Ron, D. (2012). New insights into translational regulation in the endoplasmic reticulum unfolded protein response. *Cold Spring Harbor Perspectives in Biology*, 4(6), pp.a012278-a012278.

Payne, T., Finnis, C., Evans, L., Mead, D., Avery, S., Archer, D. and Sleep, D. (2008). Modulation of chaperone gene expression in mutagenized *Saccharomyces cerevisiae* strains developed for recombinant human albumin production results in increased production of multiple heterologous proteins. *Applied and Environmental Microbiology*, 74(24), pp.7759-7766.

Payne, T., Hanfrey, C., Bishop, A., Michael, A., Avery, S. and Archer, D. (2008). Transcript-specific translational regulation in the unfolded protein response of *Saccharomyces cerevisiae*. *FEBS Letters*, 582(4), pp.503-509.

Pehar, M., Lehnus, M., Karst, A. and Puglielli, L. (2012). Proteomic Assessment Shows That Many Endoplasmic Reticulum (ER)-resident Proteins Are Targeted by Nϵ-Lysine Acetylation in the Lumen of the Organelle and Predicts Broad Biological Impact. *Journal of Biological Chemistry*, 287(27), pp.22436-22440.

Pfeffer, S. (1996). TRANSPORT VESICLE DOCKING: SNAREs and Associates. *Annual Review of Cell and Developmental Biology*, 12(1), pp.441-461.

Pichler, H., Gaigg, B., Hrastnik, C., Achleitner, G., Kohlwein, S., Zellnig, G., Perktold, A. and Daum, G. (2001). A subfraction of the yeast endoplasmic reticulum associates with the plasma membrane and has a high capacity to synthesize lipids. *European Journal of Biochemistry*, 268(8), pp.2351-2361.

Piccioli, P. and Rubartelli, A. (2013). The secretion of IL-1β and options for release. *Seminars in Immunology*, 25(6), pp.425-429.

Pincus, D., Aranda-Diaz, A., Zuleta, I., Walter, P. and El-Samad, H. (2014). Delayed Ras/PKA signaling augments the unfolded protein response. *Proceedings of the National Academy of Sciences*, 111(41), pp.14800-14805.

Porter, K. (1945). A study of tissue culture cells by electron microscopy: methods and preliminary observations. *Journal of Experimental Medicine*, 81(3), pp.233-246.

Prinz, W., Grzyb, L., Veenhuis, M., Kahana, J., Silver, P. and Rapoport, T. (2000). Mutants affecting the structure of the cortical endoplasmic reticulum in *Saccharomyces cerevisiae*. *The Journal of Cell Biology*, 150(3), pp.461-474.

Punt, P., Schuren, F., Lehmbeck, J., Christensen, T., Hjort, C. and van den Hondel, C. (2008). Characterization of the *Aspergillus niger prtT*, a unique regulator of extracellular protease encoding genes. *Fungal Genetics and Biology*, 45(12), pp.1591-1599.

Ramirez, M., Wek, R. and Hinnebusch, A. (1991). Ribosome association of GCN2 protein kinase, a translational activator of the GCN4 gene of *Saccharomyces cerevisiae*. *Molecular and Cellular Biology*, 11(6), pp.3027-3036.

Reijnders, L., Sloof, P. and Borst, P. (1973). The Molecular Weights of the Mitochondrial-Ribosomal RNAs of Saccharomyces carlsbergensis. *European Journal of Biochemistry*, 35(2), pp.266-269.

Rexach, M. (1994). Characteristics of endoplasmic reticulum-derived transport vesicles. *The Journal of Cell Biology*, 126(5), pp.1133-1148.

Rock, K., Gramm, C., Rothstein, L., Clark, K., Stein, R., Dick, L., Hwang, D. and Goldberg, A. (1994). Inhibitors of the proteasome block the degradation of most cell proteins and the generation of peptides presented on MHC class I molecules. *Cell*, 78(5), pp.761-771.

Rousakis, A., Vlassis, A., Vlanti, A., Patera, S., Thireos, G. and Syntichaki, P. (2013). The general control nonderepressible-2 kinase mediates stress response and longevity induced by target of rapamycin inactivation in *Caenorhabditis elegans*. *Aging Cell*, 12(5), pp.742-751.

Rose, M., Misra, L. and Vogel, J. (1989). KAR2, a karyogamy gene, is the yeast homolog of the mammalian BiP/GRP78 gene. *Cell*, 57(7), pp.1211-1221.

Ruddock, L. and Molinari, M. (2006). N-glycan processing in ER quality control. *Journal of Cell Science*, 119(21), pp.4373-4380.

Saito, A., Ochiai, K., Kondo, S., Tsumagari, K., Murakami, T., Cavener, D. and Imaizumi, K. (2010). Endoplasmic Reticulum Stress Response Mediated by the PERK-eIF2α-ATF4 Pathway Is Involved in Osteoblast Differentiation Induced by BMP2. *Journal of Biological Chemistry*, 286(6), pp.4809-4818.

Sakamoto, K., Iwashita, K., Yamada, O., Kobayashi, K., Mizuno, A., Akita, O., Mikami, S., Shimoi, H. and Gomi, K. (2009). *Aspergillus oryzae atfA* controls conidial germination and stress tolerance. *Fungal Genetics and Biology*, 46(12), pp.887-897.

Saloheimo, M., Valkonen, M. and Penttilä, M. (2003). Activation mechanisms of the HACI-mediated unfolded protein response in filamentous fungi. *Molecular Microbiology*, 47(4), pp.1149-1161.

Sasano, Y., Haitani, Y., Ohtsu, I., Shima, J. and Takagi, H. (2012). Proline accumulation in baker's yeast enhances high-sucrose stress tolerance and fermentation ability in sweet dough. *International Journal of Food Microbiology*, 152(1-2), pp.40-43.

Savitz, A. and Meyer, D. (1990). Identification of a ribosome receptor in the rough endoplasmic reticulum. *Nature*, 346(6284), pp.540-544.

Savoldi, M., Malavazi, I., Soriani, F., Capellaro, J., Kitamoto, K., da Silva Ferreira, M., Goldman, M. and Goldman, G. (2008). Farnesol induces the transcriptional accumulation of the *Aspergillus nidulans* Apoptosis-Inducing Factor (AIF)-like mitochondrial oxidoreductase. *Molecular Microbiology*, 70(1), pp.44-59.

Schroder, M. (2000). The unfolded protein response represses nitrogen-starvation induced developmental differentiation in yeast. *Genes & Development*, 14(23), pp.2962-2975.

Schwarz, D. and Blower, M. (2015). The endoplasmic reticulum: structure, function and response to cellular signaling. *Cellular and Molecular Life Sciences*, 73(1), pp.79-94.

Shang, J. (2005). Quantitative measurement of events in the mammalian unfolded protein response. *Methods*, 35(4), pp.390-394.

Shen, J., Chen, X., Hendershot, L. and Prywes, R. (2002). ER stress regulation of ATF6 localization by dissociation of BiP/GRP78 binding and unmasking of Golgi localization signals. *Developmental Cell*, 3(1), pp.99-111.

Shenton, D., Smirnova, J., Selley, J., Carroll, K., Hubbard, S., Pavitt, G., Ashe, M. and Grant, C. (2006). Global translational responses to oxidative stress impact upon multiple levels of protein Synthesis. *Journal of Biological Chemistry*, 281(39), pp.29011-29021.

Shibata, Y., Voeltz, G. and Rapoport, T. (2006). Rough sheets and smooth tubules. *Cell*, 126(3), pp.435-439.

Shoulders, M., Ryno, L., Genereux, J., Moresco, J., Tu, P., Wu, C., Yates, J., Su, A., Kelly, J. and Wiseman, R. (2013). Stress-independent activation of XBP1s and/or ATF6 reveals three functionally diverse ER proteostasis environments. *Cell Reports*, 3(4), pp.1279-1292.

Sims, A., Gent, M., Lanthaler, K., Dunn-Coleman, N., Oliver, S. and Robson, G. (2005). Transcriptome analysis of recombinant protein secretion by *Aspergillus nidulans* and the unfolded-protein response In Vivo. *Applied and Environmental Microbiology*, 71(5), pp.2737-2747.

Sørensen, H. and Mortensen, K. (2005). Advanced genetic strategies for recombinant protein expression in *Escherichia coli*. *Journal of Biotechnology*, 115(2), pp.113-128.

Sosa, B., Rothballer, A., Kutay, U. and Schwartz, T. (2012). LINC Complexes Form by Binding of Three KASH Peptides to Domain Interfaces of Trimeric SUN Proteins. *Cell*, 149(5), pp.1035-1047.

Staehelin, L. (1997). The plant ER: a dynamic organelle composed of a large number of discrete functional domains. *The Plant Journal*, 11(6), pp.1151-1165.

Subramanian, K. and Meyer, T. (1997). Calcium-Induced Restructuring of Nuclear Envelope and Endoplasmic Reticulum Calcium Stores. *Cell*, 89(6), pp.963-971.

Suntharalingam, M. and Wente, S. (2003). Peering through the Pore. *Developmental Cell*, 4(6), pp.775-789.

Szewczyk, E., Nayak, T., Oakley, C., Edgerton, H., Xiong, Y., Taheri-Talesh, N., Osmani, S. and Oakley, B. (2006). Fusion PCR and gene targeting in *Aspergillus nidulans*. *Nature Protocols*, 1(6), pp.3111-3120.

Szilágyi, M., Kwon, N., Bakti, F., M-Hamvas, M., Jámbrik, K., Park, H., Pócsi, I., Yu, J. and Emri, T. (2011). Extracellular proteinase formation in carbon starving Aspergillus nidulans cultures - physiological function and regulation. *Journal of Basic Microbiology*, 51(6), pp.625-634.

Szpigel, A., Hainault, I., Carlier, A., Venteclef, N., Batto, A., Hajduch, E., Bernard, C., Ktorza, A., Gautier, J., Ferré, P., Bourron, O. and Foufelle, F. (2017). Lipid environment induces ER stress, TXNIP expression and inflammation in immune cells of individuals with type 2 diabetes. *Diabetologia*, 61(2), pp.399-412.

Takagi, H., Taguchi, J. and Kaino, T. (2016). Proline accumulation protects *Saccharomyces cerevisiae* cells in stationary phase from ethanol stress by reducing reactive oxygen species levels. *Yeast*, 33(8), pp.355-363.

Tamano, K., Sano, M., Yamane, N., Terabayashi, Y., Toda, T., Sunagawa, M., Koike, H., Hatamoto, O., Umitsuki, G., Takahashi, T., Koyama, Y., Asai, R., Abe, K. and Machida, M. (2008). Transcriptional regulation of genes on the non-syntenic blocks of Aspergillus oryzae and its functional relationship to solid-state cultivation. *Fungal Genetics and Biology*, 45(2), pp.139-151.

Tanaka, M., Shintani, T. and Gomi, K. (2015). Unfolded protein response is required for *Aspergillus oryzae* growth under conditions inducing secretory hydrolytic enzyme production. *Fungal Genetics and Biology*, 85, pp.1-6.

Tapley, E. and Starr, D. (2013). Connecting the nucleus to the cytoskeleton by SUN–KASH bridges across the nuclear envelope. *Current Opinion in Cell Biology*, 25(1), pp.57-62.

Tavernier, S., Osorio, F., Vandersarren, L., Vetters, J., Vanlangenakker, N., Van Isterdael, G., Vergote, K., De Rycke, R., Parthoens, E., van de Laar, L., Iwawaki, T., Del Valle, J., Hu, C., Lambrecht, B. and Janssens, S. (2017). Regulated IRE1-dependent mRNA decay sets the threshold for dendritic cell survival. *Nature Cell Biology*, 19(6), pp.698-710.

Taxis, C., Hitt, R., Park, S., Deak, P., Kostova, Z. and Wolf, D. (2003). Use of Modular Substrates Demonstrates Mechanistic Diversity and Reveals Differences in Chaperone Requirement of ERAD. *Journal of Biological Chemistry*, 278(38), pp.35903-35913.

Teixeira, P., Cerca, F., Santos, S. and Saraiva, M. (2006). Endoplasmic reticulum stress associated with extracellular aggregates. *Journal of Biological Chemistry*, 281(31), pp.21998-22003.

Terasaki, M., Shemesh, T., Kasthuri, N., Klemm, R., Schalek, R., Hayworth, K., Hand, A., Yankova, M., Huber, G., Lichtman, J., Rapoport, T. and Kozlov, M. (2013). Stacked endoplasmic reticulum sheets are connected by helicoidal membrane motifs. *Cell*, 154(2), pp.285-296.

TING, J. and LEE, A. (1988). Human Gene Encoding the 78,000-Dalton Glucose-Regulated Protein and Its Pseudogene: Structure, Conservation, and Regulation. *DNA*, 7(4), pp.275-286.

Towle, H. (2007). The metabolic sensor GCN2 branches out. *Cell Metabolism*, 5(2), pp.85-87.

Travers, K., Patil, C., Wodicka, L., Lockhart, D., Weissman, J. and Walter, P. (2000). Functional and genomic analyses reveal an essential coordination between the unfolded protein response and ER-associated degradation. *Cell*, 101(3), pp.249-258.

Trucco, A., Polishchuk, R., Martella, O., Pentima, A., Fusella, A., Giandomenico, D., Pietro, E., Beznoussenko, G., Polishchuk, E., Baldassarre, M., Buccione, R., Geerts, W., Koster, A., Burger, K., Mironov, A. and Luini, A. (2004). Secretory traffic triggers the formation of tubular continuities across Golgi sub-compartments. *Nature Cell Biology*, 6(11), pp.1071-1081.

Tsuru, A., Imai, Y., Saito, M. and Kohno, K. (2016). Novel mechanism of enhancing IRE1α-XBP1 signalling via the PERK-ATF4 pathway. *Scientific Reports*, 6(1).

Tvegard, T., Soltani, H., Skjolberg, H., Krohn, M., Nilssen, E., Kearsey, S., Grallert, B. and Boye, E. (2007). A novel checkpoint mechanism regulating the G1/S transition. *Genes & Development*, 21(6), pp.649-654.

Tzamarias, D., Roussou, I. and Thireos, G. (1989). Coupling of GCN4 mRNA translational activation with decreased rates of polypeptide chain initiation. *Cell*, 57(6), pp.947-954.

Tzur, Y., Wilson, K. and Gruenbaum, Y. (2006). SUN-domain proteins: 'Velcro' that links the nucleoskeleton to the cytoskeleton. *Nature Reviews Molecular Cell Biology*, 7(10), pp.782-788.

Uma, S., Yun, B. and Matts, R. (2001). The heme-regulated eukaryotic initiation factor 2α kinase. *Journal of Biological Chemistry*, 276(18), pp.14875-14883.

Valkonen, M., Penttila, M. and Saloheimo, M. (2003). Effects of inactivation and constitutive expression of the unfolded- protein response pathway on protein production in the yeast *Saccharomyces cerevisiae*. *Applied and Environmental Microbiology*, 69(4), pp.2065-2072.

Valkonen, M., Ward, M., Wang, H., Penttila, M. and Saloheimo, M. (2003). Improvement of foreign-protein Production in *Aspergillus niger* var. *awamori* by constitutive induction of the unfolded-protein response. *Applied and Environmental Microbiology*, 69(12), pp.6979-6986.

van den Hombergh, J., van de Vondervoort, P., Fraissinet-Tachet, L. and Visser, J. (1997). Aspergillus as a host for heterologous protein production: the problem of proteases. *Trends in Biotechnology*, 15(7), pp.256-263.

van Kuyk, P., Cheetham, B. and Katz, M. (2000). Analysis of two *Aspergillus nidulans* genes encoding extracellular proteases. *Fungal Genetics and Biology*, 29(3), pp.201-210.

van den Brink, H., Petersen, S., Rahbek-Nielsen, H., Hellmuth, K. and Harboe, M. (2006). Increased production of chymosin by glycosylation. *Journal of Biotechnology*, 125(2), pp.304-310.

Velickovska, V. and van Breukelen, F. (2007). Ubiquitylation of proteins in livers of hibernating golden-mantled ground squirrels, Spermophilus lateralis. *Cryobiology*, 55(3), pp.230-235.

Ventoso, I., Kochetov, A., Montaner, D., Dopazo, J. and Santoyo, J. (2012). Extensive translatome remodeling during ER stress response in mammalian cells. *PLoS ONE*, 7(5), p.e35915.

Voeltz, G., Rolls, M. and Rapoport, T. (2002). Structural organization of the endoplasmic reticulum. *EMBO reports*, 3(10), pp.944-950.

Volmer, R. and Ron, D. (2015). Lipid-dependent regulation of the unfolded protein response. *Current Opinion in Cell Biology*, 33, pp.67-73.

Wakasa, Y., Yasuda, H., Oono, Y., Kawakatsu, T., Hirose, S., Takahashi, H., Hayashi, S., Yang, L. and Takaiwa, F. (2011). Expression of ER quality control-related genes in response to changes in BiP1 levels in developing rice endosperm. *The Plant Journal*, 65(5), pp.675-689.

Wang, B., Guo, G., Wang, C., Lin, Y., Wang, X., Zhao, M., Guo, Y., He, M., Zhang, Y. and Pan, L. (2010). Survey of the transcriptome of *Aspergillus oryzae* via massively parallel mRNA sequencing. *Nucleic Acids Research*, 38(15), pp.5075-5087.

Wang, C., Chen, J., Yin, S. and Chuang, W. (2006). Predicting the redox state and secondary structure of cysteine residues in proteins using NMR chemical shifts. *Proteins: Structure, Function, and Bioinformatics*, 63(1), pp.219-226.

Wang, J., Yang, X. and Zhang, J. (2016). Bridges between mitochondrial oxidative stress, ER stress and mTOR signaling in pancreatic β cells. *Cellular Signalling*, 28(8), pp.1099-1104.

Wang, Q., Groenendyk, J. and Michalak, M. (2015). Glycoprotein Quality Control and Endoplasmic Reticulum Stress. *Molecules*, 20(8), pp.13689-13704.

Wang, Y., Shen, J., Arenzana, N., Tirasophon, W., Kaufman, J. and Prywes, R. (2000). Activation of ATF6 and an ATF6 DNA binding site by the endoplasmic reticulum stress response. *The Journal of biological chemistry*, 275(35), pp.27013–20.

Wanka, F., Cairns, T., Boecker, S., Berens, C., Happel, A., Zheng, X., Sun, J., Krappmann, S. and Meyer, V. (2016). Tet-on, or Tet-off, that is the question: Advanced conditional gene expression in Aspergillus. *Fungal Genetics and Biology*, 89, pp.72-83.

Ward, O. (2012). Production of recombinant proteins by filamentous fungi. *Biotechnology Advances*, 30(5), pp.1119-1139.

Weber, F., Wagner, V., Rasmussen, S., Hartmann, R. and Paludan, S. (2006). Double-stranded RNA is produced by positive-strand RNA viruses and DNA viruses but not in

detectable amounts by negative-strand RNA viruses. *Journal of Virology*, 80(10), pp.5059-5064.

Weids, A., Ibstedt, S., Tamás, M. and Grant, C. (2016). Distinct stress conditions result in aggregation of proteins with similar properties. *Scientific Reports*, 6(1).

Weidner, G., d'Enfert, C., Koch, A., Mol, P. and Brakhage, A. (1998). Development of a homologous transformation system for the human pathogenic fungus *Aspergillus fumigatus* based on the *pyrG* gene encoding orotidine 5′-monophosphate decarboxylase. *Current Genetics*, 33(5), pp.378-385.

Wek, S., Zhu, S. and Wek, R. (1995). The histidyl-tRNA synthetase-related sequence in the eIF-2 alpha protein kinase GCN2 interacts with tRNA and is required for activation in response to starvation for different amino acids. *Molecular and Cellular Biology*, 15(8), pp.4497-4506.

Welihinda, A., Tirasophon, W., Green, S. and Kaufman, R. (1998). Protein serine/threonine phosphatase ptc2p negatively regulates the unfolded-protein response by dephosphorylating Ire1p kinase. *Molecular and Cellular Biology*, 18(4), pp.1967-1977.

West, M., Zurek, N., Hoenger, A. and Voeltz, G. (2011). A 3D analysis of yeast ER structure reveals how ER domains are organized by membrane curvature. *The Journal of Cell Biology*, 193(2), pp.333-346.

Wetmore, D. and Hardman, K. (1996). Roles of the propeptide and metal ions in the folding and stability of the catalytic domain of stromelysin (Matrix Metalloproteinase 3)†. *Biochemistry*, 35(21), pp.6549-6558.

Wiertz, E., Tortorella, D., Bogyo, M., Yu, J., Mothes, W., Jones, T., Rapoport, T. and Ploegh, H. (1996). Sec6l-mediated transfer of a membrane protein from the endoplasmic reticulum to the proteasome for destruction. *Nature*, 384(6608), pp.432-438.

Wolfner, M., Yep, D., Messenguy, F. and Fink, G. (1975). Integration of amino acid biosynthesis into the cell cycle of *Saccharomyces cerevisiae*. *Journal of Molecular Biology*, 96(2), pp.273-290.

Wooding, F. (1967). Endoplasmic reticulum aggregates of ordered structure. *Planta*, 76(2), pp.205-208.

Wynn, R., Davie, J., Cox, R. and Chuang, D. (1994). Molecular chaperones: heat-shock proteins, foldases, and matchmakers. *The Journal of laboratory and clinical medicine*, [online] 124(1), pp.31–6. Available at: http://www.ncbi.nlm.nih.gov/pubmed/8035099 [Accessed 8 Apr. 2017].

Xue, C., Lin, T., Chang, D. and Guo, Z. (2017). Thioflavin T as an amyloid dye: fibril quantification, optimal concentration and effect on aggregation. *Royal Society Open Science*, 4(1), p.160696.

Yam, G., Gaplovska-Kysela, K., Zuber, C. and Roth, J. (2007). Sodium 4-phenylbutyrate acts as a chemical chaperone on misfolded myocilin to rescue cells from endoplasmic reticulum stress and apoptosis. *Investigative Opthalmology & Visual Science*, 48(4), p.1683.

Yamaguchi, S., Ishihara, H., Tamura, A., Yamada, T., Takahashi, R., Takei, D., Katagiri, H. and Oka, Y. (2004). Endoplasmic reticulum stress and N-glycosylation modulate expression of WFS1 protein. *Biochemical and Biophysical Research Communications*, 325(1), pp.250-256.

Yang, S., Lan, S. and Gong, M. (2009). Hydrogen peroxide-induced proline and metabolic pathway of its accumulation in maize seedlings. *Journal of Plant Physiology*, 166(15), pp.1694-1699.

Ye, J., Rawson, R., Komuro, R., Chen, X., Davé, U., Prywes, R., Brown, M. and Goldstein, J. (2000). ER Stress Induces Cleavage of Membrane-Bound ATF6 by the Same Proteases that Process SREBPs. *Molecular Cell*, 6(6), pp.1355-1364.

Ye, L. and Pan, L. (2008). A Comparison of the Unfolded Protein Response in Solid-State with Submerged Cultures ofAspergillus oryzae. *Bioscience, Biotechnology, and Biochemistry*, 72(11), pp.2998-3001.

Yefidoff-Freedman, R., Fan, J., Yan, L., Zhang, Q., dos Santos, G., Rana, S., Contreras, J., Sahoo, R., Wan, D., Young, J., Dias Teixeira, K., Morisseau, C., Halperin, J., Hammock, B., Natarajan, A., Wang, P., Chorev, M. and Aktas, B. (2017). Development of 1-((1,4-trans)-4-aryloxycyclohexyl)-3-arylurea activators of heme-regulated inhibitor as selective activators of the eukaryotic initiation factor 2 Alpha (eIF2α) phosphorylation arm of the integrated endoplasmic reticulum stress response. *Journal of Medicinal Chemistry*, 60(13), pp.5392-5406.

Yoshida, H., Matsui, T., Yamamoto, A., Okada, T. and Mori, K. (2001). XBP1 mRNA Is induced by ATF6 and spliced by IRE1 in response to ER stress to produce a highly active transcription factor. *Cell*, 107(7), pp.881-891.

Yoo, J., Moyer, B., Bannykh, S., Yoo, H., Riordan, J. and Balch, W. (2002). Non-conventional Trafficking of the Cystic Fibrosis Transmembrane Conductance Regulator through the Early Secretory Pathway. *Journal of Biological Chemistry*, 277(13), pp.11401-11409.

Zaborske, J., Wu, X., Wek, R. and Pan, T. (2010). Selective control of amino acid metabolism by the GCN2 eIF2 kinase pathway in *Saccharomyces cerevisiae*. *BMC Biochemistry*, 11(1), p.29.

Zhan, K., Vattem, K., Bauer, B., Dever, T., Chen, J. and Wek, R. (2002). Phosphorylation of eukaryotic initiation factor 2 by heme-regulated inhibitor kinase-related protein kinases in *Schizosaccharomyces pombe* is important for resistance to environmental stresses. *Molecular and Cellular Biology*, 22(20), pp.7134-7146.

Zhang, L. and Wang, A. (2012). Virus-induced ER stress and the unfolded protein response. *Frontiers in Plant Science*, 3.

Zhang, P., McGrath, B., Reinert, J., Olsen, D., Lei, L., Gill, S., Wek, S., Vattem, K., Wek, R., Kimball, S., Jefferson, L. and Cavener, D. (2002). The GCN2 eIF2 kinase is required for adaptation to amino acid deprivation in mice. *Molecular and Cellular Biology*, 22(19), pp.6681-6688.

Zoll, W., Horton, L., Komar, A., Hensold, J. and Merrick, W. (2002). Characterization of Mammalian eIF2A and Identification of the Yeast Homolog. *Journal of Biological Chemistry*, 277(40), pp.37079-37087.

Zhou, C., Slaughter, B., Unruh, J., Guo, F., Yu, Z., Mickey, K., Narkar, A., Ross, R., McClain, M. and Li, R. (2014). Organelle-based aggregation and retention of damaged proteins in asymmetrically dividing cells. *Cell*, 159(3), pp.530-542.

Zubenko, G. and Jones, E. (1979). Catabolite inactivation of gluconeogenic enzymes in mutants of yeast deficient in proteinase B. *Proceedings of the National Academy of Sciences*, 76(9), pp.4581-4585.

Zundel, M., Basturea, G. and Deutscher, M. (2009). Initiation of ribosome degradation during starvation in *Escherichia coli*. *RNA*, 15(5), pp.977-983.

10. Appendices

10.1. Appendix 1. A

Minimal media

- 1% carbon source (glucose, unless otherwise stated)
- 20 ml Aspergillus Salts Solution
- pH adjusted with sodium hydroxide to pH 6.5
- For solid media granulated agar (Foremedium bacteriological grade agar) was added to either 1 or 3 % (w/v)

Regeneration media

- Minimal media + 1M sucrose

Aspergillus Salts Solution

• Potassium chloride	349 mM
• $MgSO_4$	216 mM
• Trace Elements	50 ml/L

Add 2ml chloroform to keep sterile

Aspergillus Trace Elements

• Sodium tetraborate decahydrate	104 µM
• Cupric sulphate	2.5 mM
• Iron phosphate	5.3 mM
• Manganese sulphate	5.3 mM
• Sodium molybdate	3.9 mM
• Zinc sulphate	49.5 mM

Transformation solution

• Polyethylene glycol 6000	60%
• Calcium cholride	10 mM
• Tris-Cl pH 7.5	20 mM

Supplements

• Ammonum tartrate	5.1 M
• Monosodium phosphate	0.67 M
• Para-aminobenzoic acid	3 mM
• Pyridoxine	307 µM
• Riboflavin	664 µM
• Sodium deoxycholate	192 mM

- Sodium nitrate 0.5 M
- Uridine 125 mM
- Uracil 125 mM

10.2. Appendix 1. B

RNA Loading Buffer

- Formamide 50 µl
- 37% formaldehyde (~ 2.2 M) 18 µl
- 10X MOPS buffer 10 µl
- 10X Dye Solution (50% glycerol, 0.3% Bromophenol Blue) 3 µl

10.3. Appendix 1. C

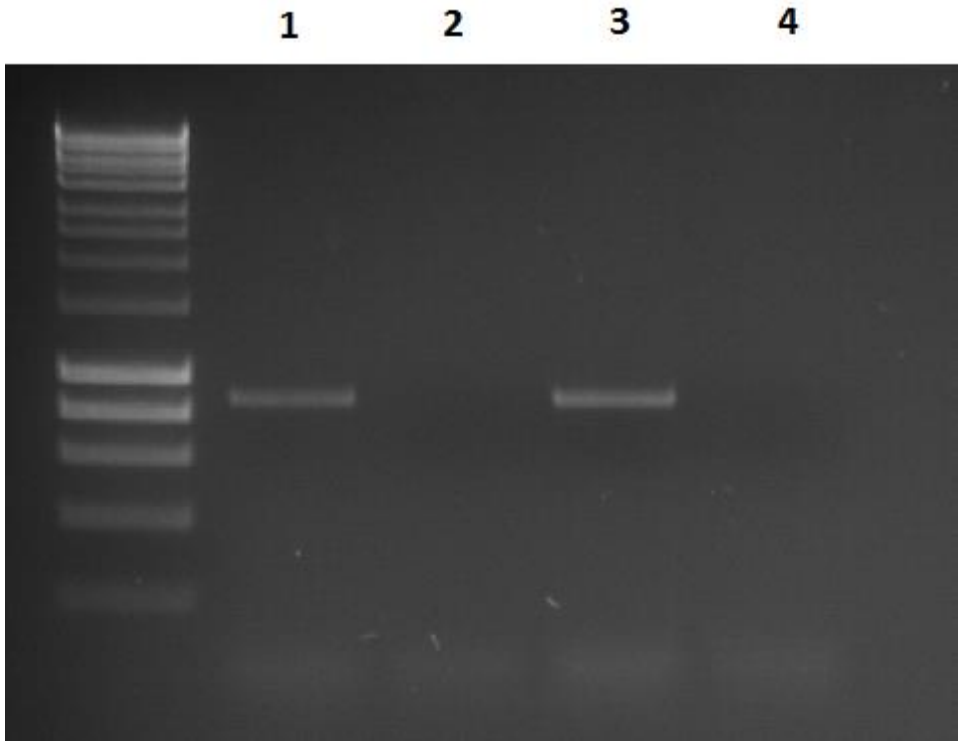

Figure 1. C – Gel image of PCR products produced with primers *hacA* F1 and *hacA* R2. Confirmation of re-insertion of intronless *hacA* into the *ΔhacA* strain. 1-4 are WT, *ΔhacA*, *hacA Δintron* and a blank. Ladder is Hyperladder 1KB. We can see re-insertion of the *hacA Δintron* back into the *hacA* locus was successful.

10.4. Appendix 1. D

See CD disc

10.5. Appendix 1. E

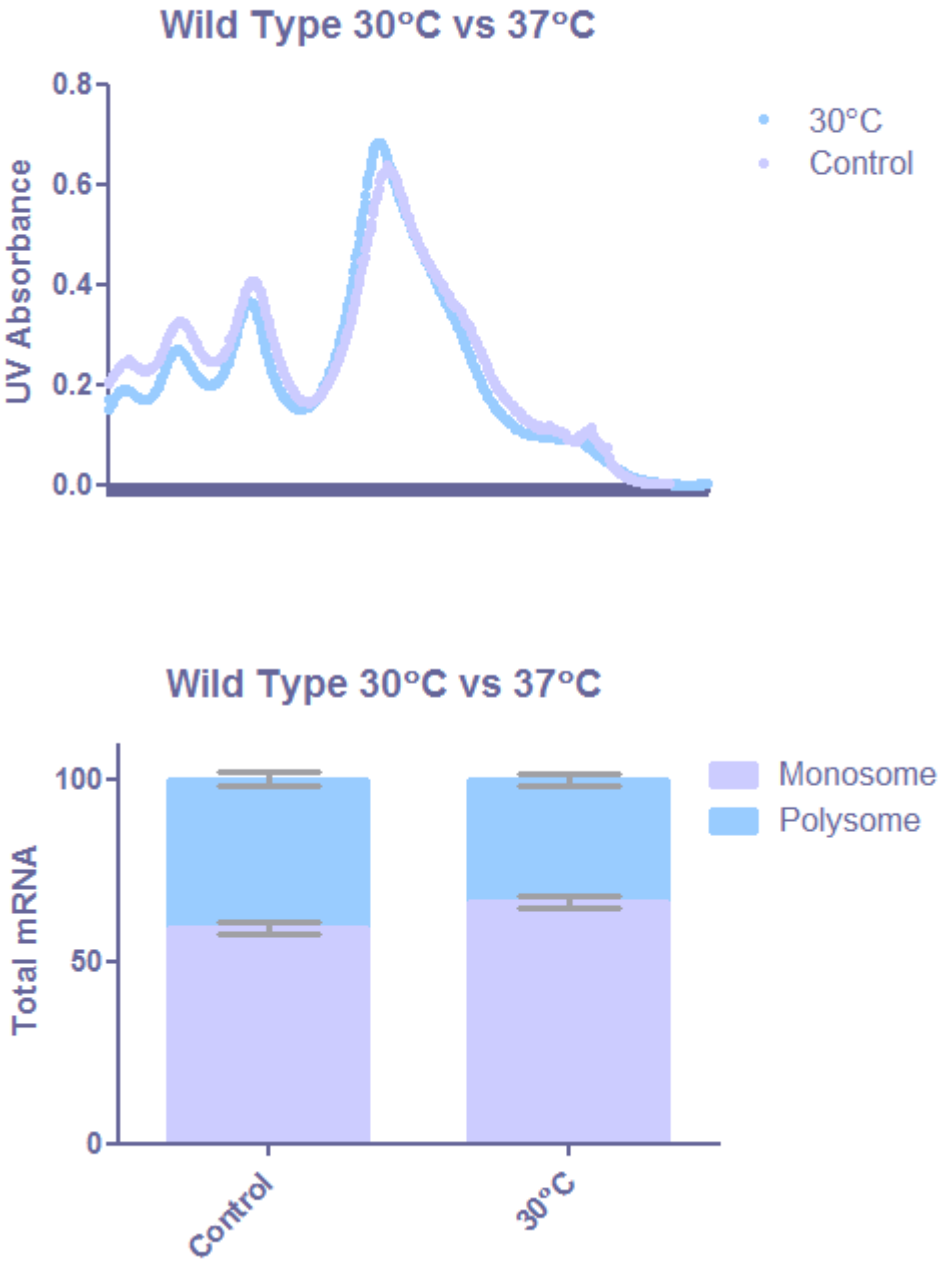

Comparison of polysome profiles of WT control conditions and growth at 30^{O}C. A shows the polysome profiles for the control (37^{O}C) and growth at 30^{O}C for WT. The control shows well defined polysomes and a larger monosome followed by slight peaks for the ribosomal subunits 60s and 40s. The cells grown at 30^{O}C display a very similar profile with marginally smaller polysome fractions. B shows ribosomal distribution as a percentage of polysomes to monosome/subunits. Polysomes decrease from ~41% to ~37% in cells grown at 30^{O}C. There is not a significant difference between the conditions (p=<0.086). Significance determined by Unpaired T-test N=3

10.6. Appendix 1. F

1- De Souza CP, et al. (2013)
2-Carvalho ND, et al. (2010)

3-Tanaka M, et al. (2015)
4-Valkonen, et al. (2003)
5- Mulder HJ, et al. (2004)
6- (YE and PAN, 2008)
7- Sims et al 2005
8-Kasuya T, et al. (1999)
9-(Jørgensen et al., 2009)
10 -Emri et al 2009
11- Katz ME, et al. (1994) I
12-Jarai G, et al. (1994)
13-(Tamano et al., 2008)
14-Fidel S, et al. (1988)
15-Meyer et al., 2008)
16-Marui J, et al. (2010)
17-(Gallwitz and Seidel, 1980)
18-(Nikawa and Yamashita, 1992)
19-**(**Mori et al., 1996**)**
20-(Lucchini et al., 1984)
21-(Donahue et al., 1988)
22-(Hampton, Gardner and Rine, 1996)
23-(Rose, Misra and Vogel, 1989)
24-(Zubenko and Jones, 1979)
25-(Welihinda, Tirasophon and Green, 1998
26-(Liou et al., 1990)
27-(Berlanga, Santoyo and de Haro, 1999)
28-(Hwang, Kim and Kim, 2000)
29-(Zoll et al., 2002)
30-(TING and LEE, 1988)
31-(Kaneko et al., 2002)
32-(Miwa and Kamada, 1990)